

UNIVERSITY of CALIFORNIA
Santa Barbara

Robust Hybrid Control Systems

A Dissertation submitted in partial satisfaction of the
requirements for the degree

Doctor of Philosophy

in

Electrical and Computer Engineering

by

Ricardo G. Sanfelice

Committee in charge:

Professor Andrew R. Teel, Chair

Professor Petar V. Kokotović

Professor João P. Hespanha

Professor Bassam Bamieh

September 2007

Robust Hybrid Control Systems

Copyright © 2007¹

by

Ricardo G. Sanfelice

¹Revised on January 2008.

To my mother Alicia, and my father Adolfo

Acknowledgements

I am deeply grateful to my advisor, mentor, and friend Andy Teel for having guided me through the challenges of academic life and for teaching me to strive for elegance and mathematical rigor in my research. He has continuously motivated me to think creatively and to always aim for high-quality research.

I would like to express my gratitude to my family and friends who have given me constant emotional and spiritual support and encouragement throughout my doctorate program. In particular, I want to thank my wife Christine who has been bold and remained supportive even in the busiest times of this journey.

I also want to thank the faculty in the Department of Electrical and Computer Engineering and in the Center of Control, Dynamics, and Computation who directly or indirectly have shaped my career. In particular, I want to thank Petar Kokotović and João Hespanha for their encouragement, advice, and friendship throughout the years. I thank all of the members of my doctoral committee for insightful discussions and useful suggestions made to improve this document.

I am grateful to my fellow graduate students, post-docs, and visitors who made graduate school an enjoyable experience and were always available for discussions. I offer special thanks to Rafal Goebel for his helpful comments, advice and friendship; and to Gene, Doca, Ryan, Emre, Dragan, Michael, Max, James, Cai, Sara, Prabir, Payam, Kavyesh, Diane, Chris, and Josh who have been my lab-mates and friends.

Finally, I am thankful for the help I have received from the Center for Control, Dynamical Systems' assistants during the last five years who have aided me very efficiently in the administrative paper work. I am also grateful for the financial support provided by the University of California Santa Barbara and the Office of International Students and Scholars, and through my advisor by the National Science Foundation, Air Force Office of Scientific Research, and Army Research Office.

Abstract

Robust Hybrid Control Systems

by

Ricardo G. Sanfelice

This thesis deals with systems exhibiting both continuous and discrete dynamics, perhaps due to intrinsic behavior or to the interaction of continuous-time and discrete-time dynamics emerging from its components and/or their interconnection. Such systems are called *hybrid systems* and permit the modeling of a wide range of engineering systems and scientific processes. In this thesis, hybrid systems are treated as dynamical systems: the interplay between continuous and discrete behavior is captured in a mathematical model given by differential equations/inclusions and difference equations/inclusions, which we simply call *hybrid equations*.

We develop tools for systematic analysis and robust design of hybrid systems, with an emphasis on systems that involve control algorithms, that is, *hybrid control systems*. To this effect, we identify mild conditions that hybrid equations need to satisfy so that their behavior captures the effect of arbitrarily small perturbations. This leads to novel concepts of generalized solutions that impart a deep understanding not only on the robustness properties of hybrid systems but also on the structural properties of their solutions. In turn, these conditions enable us to generate various tools for hybrid systems that resemble those in the stability theory of classical dynamical systems. These include general versions of Lyapunov and Krasovskii stability theorems, and LaSalle-type invariance principles. Additionally, we establish results on robustness of stability of hybrid control for general nonlinear systems. We also present a novel mathematical framework for numerical simulation of hybrid systems and its asymptotic stability properties.

The contributions of this thesis are not limited to the theory of hybrid systems as they have implications in the analysis and design of practically relevant engineering control systems. In this regard, we develop general control strategies for dynamical systems that are applicable, for example, to autonomous vehicles, multi-link pendulums, and juggling systems.

Notation

- \mathbb{R}^n denotes n -dimensional Euclidean space.
- \mathbb{R} denotes the real numbers.
- \mathbb{Z} denotes the integers.
- $\mathbb{R}_{\geq 0}$ denotes the nonnegative real numbers, i.e., $\mathbb{R}_{\geq 0} = [0, \infty)$.
- \mathbb{N} denotes the natural numbers including 0, i.e., $\mathbb{N} = \{0, 1, \dots\}$.
- \mathbb{B} denotes the open unit ball in Euclidean space.
- Given a set S , \overline{S} denotes its closure.
- Given a set S , $\text{co}S$ denotes the convex hull and $\overline{\text{co}S}$ the closure of the convex hull.
- Given a set $S \subset \mathbb{R}^n$ and a point $x \in \mathbb{R}^n$, $|x|_S := \inf_{y \in S} |x - y|$.
- Given sets $S_1, S_2 \subset \mathbb{R}^n$, $d_H(S_1, S_2)$ denotes the Hausdorff distance between S_1 and S_2 .
- Given sets S_1, S_2 subsets of \mathbb{R}^n , $S_1 + S_2 := \{x_1 + x_2 \mid x_1 \in S_1, x_2 \in S_2\}$.
- Given a vector $x \in \mathbb{R}^n$, $|x|$ denotes the Euclidean vector norm.
- The equivalent notation $[x^T \ y^T]^T$, $[x \ y]^T$, and (x, y) is used for vectors.
- The notation $f^{-1}(r)$ stands for the r -level set of f on $\text{dom } f$, the domain of definition of f , i.e., $f^{-1}(r) := \{z \in \text{dom } f \mid f(z) = r\}$.
- A function $\alpha : \mathbb{R}_{\geq 0} \rightarrow \mathbb{R}_{\geq 0}$ is said to belong to the class \mathcal{K} if it is continuous, zero at zero, and strictly increasing.
- A function $\alpha : \mathbb{R}_{\geq 0} \rightarrow \mathbb{R}_{\geq 0}$ is said to belong to the class \mathcal{K}_∞ if it belongs to the class \mathcal{K} and is unbounded.
- A function $\beta : \mathbb{R}_{\geq 0} \times \mathbb{R}_{\geq 0} \rightarrow \mathbb{R}_{\geq 0}$ is said to belong to class- \mathcal{KL} if it is continuous, nondecreasing in its first argument, nonincreasing in its second argument, and $\lim_{s \searrow 0} \beta(s, t) = \lim_{t \rightarrow \infty} \beta(s, t) = 0$.
- A function $\beta : \mathbb{R}_{\geq 0} \times \mathbb{R}_{\geq 0} \times \mathbb{R}_{\geq 0} \rightarrow \mathbb{R}_{\geq 0}$ is said to belong to class- \mathcal{KLL} if, for each $r \in \mathbb{R}_{\geq 0}$, the functions $\beta(\cdot, \cdot, r)$ and $\beta(\cdot, r, \cdot)$ belong to class- \mathcal{KL} .

Contents

- Acknowledgments** **iv**

- Abstract** **v**

- Notation** **vi**

- List of Figures** **xi**

- 1 Introduction** **1**
 - 1.1 Dynamical modeling from a robustness viewpoint 1
 - 1.2 Tools for systematic analysis and design 3
 - 1.3 Control strategies for robust stability 5
 - 1.4 Robustness of numerical simulations 6
 - 1.5 Notes 7

- 2 Mathematical Model and Solutions** **8**
 - 2.1 Preliminaries 8
 - 2.2 The model 9
 - 2.2.1 Examples 10
 - 2.2.2 Hysteresis in feedback control 13
 - 2.3 Time domains and arcs 16
 - 2.4 Solutions to hybrid systems 19
 - 2.5 Examples and further modeling 21
 - 2.5.1 Bouncing ball revisited 21
 - 2.5.2 Hybrid automaton 23
 - 2.6 Summary 23
 - 2.7 Notes and references 24

3	Generalized Solutions	26
3.1	Hybrid systems with state perturbations	26
3.2	Generalized solutions to hybrid systems	30
3.3	Measurement noise in feedback control	34
3.4	Regular hybrid systems	38
3.5	Summary	40
3.6	Notes and references	40
4	Stability and Invariance	42
4.1	Stability	42
4.1.1	Definitions	42
4.1.2	Lyapunov theorems	43
4.2	Invariance	45
4.2.1	Preliminaries	45
4.2.2	Properties of Ω -limits sets	46
4.2.3	Convergence via invariance principles	49
4.2.4	Connections to observability and detectability	54
4.3	Examples	56
4.4	Summary	64
4.5	Notes and references	64
5	Robustness of Hybrid Control	68
5.1	Hybrid control of nonlinear systems	68
5.2	Robustness to perturbations	71
5.2.1	Robustness via filtered measurements	71
5.2.2	Robustness to sensor and actuator dynamics	73
5.2.3	Robustness to sensor dynamics and smoothing	74
5.3	Robustness to digital implementation	76
5.3.1	Sample-and-hold model	76
5.3.2	Closed-loop system analysis	77
5.4	A benchmark problem: robust global swing-up of a pendulum on a cart	79
5.5	Summary	82
5.6	Notes and references	83
6	Hybrid Control Applications	85

6.1	Hysteresis-based control	85
6.1.1	A robustness motivation to hybrid control	85
6.1.2	A general robustness issue	87
6.1.3	Control design and analysis	90
6.1.4	Two numerical examples	94
6.2	Throw-and-catch control	97
6.2.1	An intuitive control strategy	97
6.2.2	Control design and analysis	98
6.2.3	Application: robust global pendubot swing-up control	104
6.3	Trajectory tracking control for a class of juggling systems	109
6.3.1	Introduction	109
6.3.2	Trajectory tracking approach to juggling control	110
6.3.3	Single-ball juggling	111
6.3.4	Multiple-balls juggling control	119
6.4	Summary	123
6.5	Notes and references	123
7	Simulation Theory	125
7.1	Introduction	125
7.2	Simulation model	126
7.3	From hybrid to discrete	127
7.4	Closeness and continuity properties	129
7.4.1	Numerical example	132
7.5	Summary	134
7.6	Notes and references	134
8	Conclusion	135
8.1	Summary	135
8.2	Future directions	136
A	Simulating Hybrid Systems in Matlab/Simulink	138
A.1	Simulink Model	138
A.2	Continuous dynamics	140
A.3	Jump Logic	140
A.4	Update Logic	142

A.5	Stop Logic	143
A.6	Examples	143
A.7	Notes	151
B	Proofs	155
B.1	Proofs of results in Chapter 3	155
B.1.1	Proof of Theorem 3.11 and Corollary 3.15	155
B.2	Proofs of results in Chapter 4	162
B.2.1	Proof of Theorem 4.3	162
B.2.2	Proof of Theorem 4.14	162
B.2.3	Proof of Corollary 4.15	162
B.2.4	Proof of Theorem 4.16	163
B.2.5	Proof of Theorem 4.17	163
B.2.6	Proof of Theorem 4.31	164
B.3	Proofs of results in Chapter 5	165
B.3.1	Proof of Theorem 5.12	165
B.4	Proofs of results in Chapter 6	173
B.4.1	Proof of Theorem 6.5	173
B.4.2	Proof of Corollary 6.7	175
B.4.3	Proof of Theorem 6.11	175
B.4.4	Proof of Theorem 6.12	177
B.4.5	Proof of Theorem 6.14	179
B.4.6	Proof of Theorem 6.15	180
	Bibliography	182

List of Figures

1.1	Solutions in continuous, discrete, and hybrid time domains.	3
1.2	Hybrid control of a nonlinear system under perturbations	6
2.1	Bouncing ball system	11
2.2	Bouncing ball data.	12
2.3	Digital control of a continuous-time nonlinear system with sample and hold devices.	12
2.4	Hysteresis behavior	14
2.5	General hysteresis.	14
2.6	Closed-loop system combining local and global controllers.	15
2.7	Hybrid controller data for combining local and global controllers.	16
2.8	Hybrid time domain.	17
2.9	Hybrid arc.	18
2.10	Hybrid arc types	19
2.11	A solution to a hybrid system \mathcal{H}	20
2.12	Bouncing ball solutions and domains.	22
2.13	A CADLAG solution x to \mathcal{H} (Example 2.8)	25
3.1	Flow and jump set for the hybrid system (Example 3.3).	28
3.2	The effect of state perturbations (Example 3.4).	28
3.3	Flow map and solutions (Example 3.5).	29
3.4	Jump map and solutions to Example 3.6.	30
3.5	Two hybrid arcs (τ, ε) -close.	31
3.6	Solutions to zero-crossing detection system in Example 3.12.	33
3.7	Robust feedback controller data (Example 3.13).	35
3.8	Steering a vehicle to its target.	38
3.9	Hybrid controller for steering a vehicle to its target with modified sets.	39

3.10	Convergence of solutions to the hybrid system (Example 3.20).	40
4.1	Solutions (Example 4.19)	51
4.2	Bouncing ball, Newton's cradle, and inverted pendulum on a cart.	57
4.3	A solution to the bouncing ball system.	58
5.1	Closed-loop system with noise and filtered measurements.	71
5.2	Closed-loop system with sensor and actuator dynamics.	73
5.3	Closed-loop system with sensor dynamics and control smoothing.	75
5.4	Sample-and-hold control of a nonlinear system.	76
5.5	Pendulum on a cart.	79
5.6	Solution to pendulum swing up with hybrid control including sensor and actuator dynamics: noise variance $\sigma = 0.1$.	80
5.7	Solution to pendulum swing up with hybrid control including sensor and actuator dynamics: noise variance $\sigma = 1$.	81
5.8	Control law and discrete mode for pendulum swing up with hybrid control including sensor and actuator dynamics: large noise case.	82
5.9	Solution of pendulum swing up with sample-and-hold implementation of hybrid control: variable timer constants.	83
5.10	Solution of pendulum swing up with sample-and-hold implementation of hybrid control: fixed sampling timer constant.	83
6.1	Global steering of an autonomous vehicle to different locations.	86
6.2	Global steering to a target with obstacle avoidance.	87
6.3	Sets for the problems in Section 6.1.1.	89
6.4	Closed-loop system data for the regulation to disconnected set of points problem.	94
6.5	Global stabilization of a robotic arm to two isolated destinations.	95
6.6	Global stabilization with obstacle avoidance.	96
6.7	Throw-and-catch control.	98
6.8	Swing up of a multi-link pendulum on a cart.	98
6.9	Control of autonomous vehicles with limited information.	99
6.10	General case of directed tree and j -th path.	100
6.11	Sets designed for the throw-and-catch strategy.	102
6.12	The pendubot system.	104
6.13	Equilibrium configurations of the pendubot.	105
6.14	Control strategy for robust global stabilization of the pendubot to the upright condition.	107
6.15	Simulation of the pendubot system with throw-and-catch hybrid control strategy.	108

6.16	One-degree of freedom juggler.	109
6.17	Ball height and reference trajectories on hybrid time domains.	110
6.18	Reference trajectory describing a periodic juggling pattern.	111
6.19	Ball and juggler position trajectories.	112
6.20	Main control idea for trajectory tracking of juggling systems.	113
6.21	Sequence of events during ball-robot impact.	114
6.22	Simulation (#1) of one-degree of freedom juggler: one ball case.	118
6.23	Simulation (#2) of one-degree of freedom juggler: one ball case.	119
6.24	One-degree of freedom juggler: multiple balls case.	120
6.25	Simulation of one-degree of freedom juggler: two balls case.	122
6.26	Simulation of one-degree of freedom juggler: two balls case, virtual states.	122
6.27	Simulation of one-degree of freedom juggler: three balls case.	123
7.1	Solution and simulation to the bouncing ball model.	127
7.2	Closeness of simulations to solutions to the bouncing ball.	133
7.3	Closeness of simulations to solutions to the bouncing ball (detail).	134
A.1	Matlab/Simulink implementation of a hybrid system.	139
A.2	Integrator.	140
A.3	Continuous dynamics.	141
A.4	Jump Logic.	142
A.5	Update Logic.	143
A.6	Stop Logic.	144
A.7	Solution to the bouncing ball example: height.	145
A.8	Solution to the bouncing ball example: velocity.	146
A.9	Hybrid arc corresponding to a solution to the bouncing ball example: height.	147
A.10	Solution to Example A.2 with forced jumps logic.	148
A.11	Solution to Example A.2 with forced flows logic.	149
A.12	Solution to Example A.2 with random logic for flowing/jumping.	150
A.13	Solution to Example A.2 with random logic for flowing/jumping.	151
A.14	Solution to Example A.2 with random logic for flowing/jumping. Zoomed version.	152
A.15	Solution to Example A.2 with forced jump logic and different O	153
A.16	Solution to Example A.2 with forced flow logic.	154

Chapter 1

Introduction

Driven by recent technological advances, most engineering systems combine analog and digital devices, interact through networks, conduct tasks collaboratively, and operate in environments filled with uncertainties. This ongoing trend has been one of the thrusts for research on modeling, stability analysis, control design, validation, verification, planning, and simulation of systems exhibiting both continuous and discrete behavior.

Because of their heterogeneous composition, the word *hybrid* is attached to these systems, where the presence of two different behaviors, continuous and discrete, is the cause of heterogeneity. *Hybrid systems* consist of a large class of systems that have been studied during the last few decades in several areas of engineering and science, and as a consequence, they adopt different names. These include *hybrid automata*, *embedded systems*, and *mixed-signal systems*, among others. Hybrid systems are prevalent as they permit the modeling of a wide range of engineering systems and scientific processes, they are sometimes induced by system design, and at other times, they appear as modeling abstractions.

This thesis takes a dynamical systems approach to hybrid systems in the sense that its continuous behavior is associated with the dynamics of a continuous-time system while its discrete behavior is related to the dynamics of a discrete-time system. The goal in treating hybrid systems as *hybrid dynamical systems* (which throughout this thesis will be referred to as simply *hybrid systems*) is to deeply understand their stability and robustness properties. The main purpose of this thesis is to provide tools for analysis, design, and simulation of hybrid systems where hybrid phenomena is not only intrinsic to the system but also induced by some external control mechanism. This broad class of hybrid systems is referred to as *hybrid control systems*.

1.1 Dynamical modeling from a robustness viewpoint

Over the last few decades, in research areas such as computer science, feedback control, and dynamical systems, researchers have given considerable attention to modeling and solution definitions for hybrid systems. Perhaps the earliest related reference is the work in [105] where a class of continuous-time systems with both continuous and discrete states (the state is referred to as *hybrid state*) exhibiting transitions was proposed in the context of optimal control. More recent contributions model hybrid phenomena as differential, hybrid, and automata [97, 74, 43, 14, 103, 67, 98]; impulsive systems and inclusions [11, 7, 40]; continuous-time systems with discrete events [4, 61]; among several others.

Even though these models, for the most part, differ from each other due to their structure and solution definition, they are similar in the sense that the continuous and discrete behavior are captured by one (or several) of their components which are active under certain conditions. In this thesis, such a modeling approach is made explicit as it appears naturally from a dynamical systems point of view. A hybrid system is denoted by \mathcal{H} with state denoted by x , possibly including both continuous and discrete state components, which takes value in a state space given by an open set $O \subset \mathbb{R}^n$. The continuous behavior or *flows* of a hybrid system is modeled by a differential equation $\dot{x} = f(x)$ (or inclusion $\dot{x} \in F(x)$), which is called *flow map*, while the discrete behavior or *jumps* is modeled by a difference equation $x^+ = g(x)$ (or inclusion $x^+ \in G(x)$), which is called *jump map*. The conditions that permit flows and/or jumps are given by the flow set C and the *jump set* D , respectively, subsets of the state space O . Then, a hybrid system \mathcal{H} is uniquely determined by these *five objects* and can be written as *hybrid equations* as follows

$$\mathcal{H}: \quad x \in O \quad \begin{cases} \dot{x} = f(x) & x \in C \\ x^+ = g(x) & x \in D \end{cases},$$

in the case of maps given by equations, or

$$\mathcal{H}: \quad x \in O \quad \begin{cases} \dot{x} \in F(x) & x \in C \\ x^+ \in G(x) & x \in D \end{cases},$$

in the case of maps given by inclusions. The compact representation above is suggestive for the solution concept adopted for these systems. In this thesis, solutions are given by functions parameterized by two time variables: ordinary time t and discrete time j . The variable t keeps track of the time that the system flows while the variable j counts the jumps. This solution concept not only captures the joint effect of continuous and discrete dynamics arising in hybrid systems, but also the behavior of purely continuous-time and purely discrete-time systems as special cases. Figure 1.1 depicts this combination of time variables which confers a specific structure to the time domain of a solution, which is called *hybrid time domain*. Hybrid time domains are similar to hybrid time trajectories in [66],[67], and [7], and to the concept of time evolution in [103], but give a more prominent role to the number of jumps. (This contrasts with the approaches in [105, 97, 11, 69, 25, 46, 98, 47, 37] where solutions are given by right-continuous functions parameterized only by ordinary time t , usually referred to as CADLAG functions, from the French “continue a droite, limite a gauche”.)

Chapter 2 makes the mathematical model for hybrid systems \mathcal{H} outlined above precise and rigorously introduces the solution concept. A key reason to insist on a modeling framework where the objects defining the continuous behavior (in the model above, the flow map and flow set) and the objects defining the discrete behavior (in the model above, the jump map and jump set) are clearly distinguished is so that good robustness and structural properties can be conferred to a hybrid system through regularity of these objects (such a task is certainly more challenging when considering, for example, the models in [67] and [37] defined by more than six objects). Chapter 3 addresses this topic from the point of view of robustness of hybrid systems with state perturbations by answering the question:

What are the properties that the state space, flow map, flow set, jump map, and jump set of a hybrid system \mathcal{H} need to satisfy so that its set of solutions is equal to the set of (converging) limiting solutions to \mathcal{H} under vanishing perturbations?

A clear understanding of the conditions required for the property in this question to hold is relevant in the analysis and design of robust hybrid control systems since, when such a property is not present, undesired behavior can arise in the control system due to arbitrarily small perturbations, such as measurement noise; see [88, 90]. Several examples throughout Chapter 3 demonstrate the importance of this property and motivate several conditions on the hybrid system \mathcal{H} . These are called hybrid basic conditions. Further motivation for the hybrid basic conditions, briefly mentioned in Chapter 3, has been given in [38] and [39] but from the point of view of the structural properties of solutions.

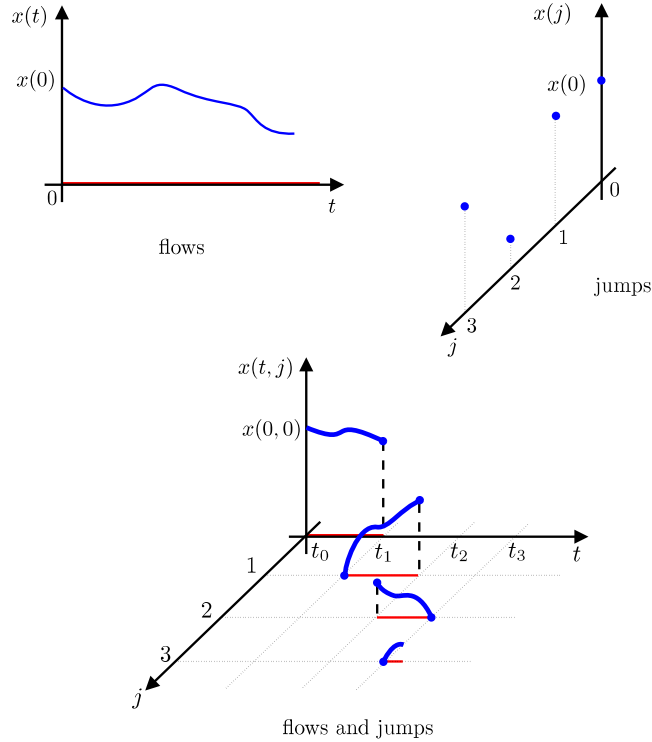


Figure 1.1. Continuous, discrete, and hybrid solutions parameterized by t , j , and both t and j , respectively. The latter corresponds to the solution concept for hybrid systems \mathcal{H} . Its domain is a *hybrid time domain*.

1.2 Tools for systematic analysis and design

The analysis and design tools for hybrid systems in Chapter 4 come in the form of Lyapunov stability theorems, LaSalle-like invariance principles, and their connections with observability and detectability [87, 89]. Systematic tools of this type are the foundation of the systems theory for purely continuous-time and discrete-time systems. Among similar tools available for hybrid systems before this thesis (for an overview of some other stability results for hybrid systems, see [70] and [32]), the tools presented in Chapter 4 generalize their classical versions for continuous-time and discrete-time systems to the hybrid setting by defining an equivalent notion of stability and providing intuitive extensions of the sufficient conditions for asymptotic stability as outlined below.

The standard notion of stability of a point or set for continuous-time and discrete-time systems: if a solution “starts close” then “it stays close” to the point or set, can be adopted as the notion of stability for hybrid systems \mathcal{H} : given a hybrid system \mathcal{H} , a compact set (or equilibrium point) $\mathcal{A} \subset O$ is *stable* if:

For every $\varepsilon > 0$ there exists $\delta > 0$ such that each solution to \mathcal{H} starting in a δ -neighborhood of \mathcal{A} stays in a ε -neighborhood of \mathcal{A} in its domain of definition.

Similarly, the notion of attractivity can also be extended: \mathcal{A} is *attractive* if ¹:

¹Note that these notions do not assume that solutions exist for arbitrarily long t and/or j . To denote this property, the prefix “pre” is added to these concepts when precisely defined in Chapter 4.

There exists a neighborhood of \mathcal{A} from which solutions stay in O and the ones that exist for arbitrarily long t and/or j converge to \mathcal{A} as $t + j$ goes unbounded.

With these definitions, and under the hybrid basic conditions, given a Lyapunov function V , continuously differentiable and positive definite with respect to \mathcal{A} , the checkable conditions that it needs to satisfy for \mathcal{A} to be stable and attractive, i.e., (locally) asymptotically stable, are simply

$$\begin{aligned} \langle \nabla V(x), f(x) \rangle &< 0 & \forall x \in C \setminus \mathcal{A}, \\ V(g(x)) - V(x) &< 0 & \forall x \in D \setminus \mathcal{A}, \quad V(g(x)) - V(x) \leq 0 & \forall x \in D, \end{aligned}$$

for the case of single-valued flow and jump maps, and

$$\begin{aligned} \max_{\xi \in F(x)} \langle \nabla V(x), \xi \rangle &< 0 & \forall x \in C \setminus \mathcal{A}, \\ \max_{\xi \in G(x)} \{V(\xi) - V(x)\} &< 0 & \forall x \in D \setminus \mathcal{A}, \quad \max_{\xi \in G(x)} \{V(\xi) - V(x)\} \leq 0 & \forall x \in D, \end{aligned}$$

for the case of set-valued flow and jump maps, where $\nabla V(x)$ is the gradient of V at x . Chapter 4 states this result for the case of locally Lipschitz V . It also presents special cases of it including a hybrid version of Krasovskii's stability theorem [54].

The second part of Chapter 4 includes general invariance principles for hybrid systems. These are applicable even in the cases when solutions are nonunique, depend semicontinuously with respect to initial conditions, and have multiple jumps at the same instant. These type of behaviors are common in robust hybrid control systems and current invariance principle results in the literature do not apply. (These include the invariance principles in [67] where uniqueness of solutions and continuity with respect to initial conditions is required, and in [25] where solutions with multiple jumps at an instant are not allowed and further quasi-continuity properties including uniqueness of solutions are imposed.)

The invariance principles in Chapter 4 include a result that parallels LaSalle's invariance principle², presented in [59, 60] for differential and difference equations. The notion of invariance is accommodated appropriately to allow for nonuniqueness of solutions. It is called *weak invariance* and is defined as follows:

Given a hybrid system \mathcal{H} , a set $\mathcal{M} \subset O$ is *weakly invariant* if it is both:

Weakly forward invariant: if for each point $\xi \in \mathcal{M}$ there exists at least one solution to \mathcal{H} starting from ξ that exist for arbitrarily long t and/or j and is contained in the set \mathcal{M} for all t and j in its domain of definition.

Weakly backward invariant: if for each point $\xi' \in \mathcal{M}$ and every positive number N there exists a point ξ from which there exists at least one solution to \mathcal{H} starting from ξ that is equal to ξ' for some t^*, j^* in its domain of definition with the property that $t^* + j^* \geq N$, and that remains in \mathcal{M} up to t^*, j^* .

Limiting this discussion to the case of single-valued flow and jump maps for simplicity, for a hybrid system \mathcal{H} satisfying the hybrid basic conditions, a continuously differentiable function $V : \mathbb{R}^n \rightarrow \mathbb{R}$, and a nonempty set $\mathcal{U} \subset \mathbb{R}^n$ such that

$$\begin{aligned} \langle \nabla V(x), f(x) \rangle &\leq 0 & \forall x \in C \cap \mathcal{U} \\ V(g(x)) - V(x) &\leq 0 & \forall x \in D \cap \mathcal{U}, \end{aligned}$$

²Also known as Barbashin-Krasovskii-LaSalle's invariance principle. Never intending to discredit any of the authors' contribution, for simplicity, this invariance principle is referred throughout this thesis as "LaSalle's invariance principle".

every solution x to \mathcal{H} that is bounded, exists for arbitrarily long t and/or j , and remains in \mathcal{U} is such that converges to the largest weakly invariant set contained in

$$\{\langle \nabla V(x), f(x) \rangle = 0\} \cup (\{V(g(x)) - V(x) = 0\} \cap g(\{V(g(x)) - V(x) = 0\})) \quad (1.1)$$

intersected with $V^{-1}(r) \cap \mathcal{U}$ for some constant $r \in V(\mathcal{U})$.

Expression (1.1) characterizes the set of points in which to search for an invariant set. The invariance notion, which involves both (weak) forward and backward invariance, reduces this set compared to results where only forward invariance is required. Note that the result automatically recovers the continuous-time and discrete-time versions of LaSalle’s invariance principle, which are obtained by omitting the terms to the right or to the left of the union symbol in (1.1), respectively. Even though the intersection in the term at its right does not improve the result when specialized to purely discrete-time systems, it does improve the result for the hybrid case. This is illustrated in an example in Chapter 4.

1.3 Control strategies for robust stability

Over the last fifteen years, researchers have begun to recognize the extra capabilities of hybrid control systems compared to classical continuous-time control systems. For example, it is now well-known that hysteresis switching control can stabilize large classes of nonholonomic systems even though stabilization is impossible using time-invariant continuous state feedback, and robust stabilization is impossible using time-invariant locally bounded feedback. See, for example, [49, 76]. Also, sample-and-hold control (a special type of hybrid feedback) can be used to achieve stabilization that is robust to measurement noise and fast sensor/actuator dynamics, even if such robustness is impossible using purely continuous-time feedback. See, for example, [95], [28], [53].

Despite these specific studies, a general investigation of the robustness of hybrid controllers to perturbations is absent from the literature. Research in these topics are relevant both from a theoretical and practical point of view. Chapter 5 answers the question of whether asymptotic stability of compact sets for closed-loop systems resulting from hybrid control of nonlinear systems is preserved when: a) small measurement error enters the plant state; b) fast unmodeled sensor and actuator dynamics are incorporated in the closed-loop system; c) the control law is “smoothed” by a fast filter; and d) the hybrid controller is digitally implemented with sample-and-hold devices. As the perturbations are explicitly added to the nominal closed-loop systems as independent subsystems given both by continuous-time models and hybrid models, these results are the first steps towards a general understanding of interconnections and singularly perturbed hybrid control systems. Figure 1.2 depicts some of the typical perturbations that arise in real-world scenarios [86, 83].

Hybrid control is a very powerful tool to solve control problems in a robust manner. For instance, it is a well-known fact in the nonlinear control literature that there are certain control problems for which it is impossible to use (possibly even discontinuous) pure state feedback to achieve asymptotic stability that is robust to arbitrarily small measurement noise. This is one of the motivations for the sample-and-hold state feedback laws proposed in [95] and [28]. It is the hybrid nature of these control laws that permits some level of robustness to measurement noise. In Chapter 6, general capabilities of hybrid control as a tool for robust stabilization are shown in three problems [82, 82, 85, 91]:

- A control strategy for the problem of stabilizing a nonlinear system to a disconnected set of points is proposed to accomplish global robust stabilization. An elementary proof of the fact that, for continuous-time systems, it is impossible to use (even discontinuous) pure state feedback to achieve this task when arbitrarily small measurement noise enters through the system state is given. A constructive, Lyapunov-based hybrid state feedback is developed for this purpose. This strategy has applications in the control of

unmanned autonomous vehicles in problems where topological constraints induce a partition of the state space where decisions need to be made, like in the case of obstacle avoidance and target acquisition.

- The problem of robustly globally asymptotically stabilizing a point or a set for a class of nonlinear systems is solved by combining local state feedback laws and open-loop control signals. A hybrid controller orchestrates the switching between these control laws to steer the trajectories toward the desired point from other particular points in the state space, and a “bootstrap” feedback controller that is capable of steering the trajectories to a neighborhood of one of these points. From there, the local feedback stabilizers and the open-loop controls can be used. A logic to select the control laws that is based on hysteresis and recover the system from failures of the open-loop controls is implemented in the hybrid controller using logic variables and logic rules. The main idea is illustrated in, but not limited to, the problem of global stabilization of the upright position of the pendubot.
- From a hybrid systems point of view, a modeling framework and a trajectory tracking control design methodology for a class of juggling systems is introduced. The main ideas and concepts are presented in a one degree-of-freedom juggling system with multiple impacting balls. A hybrid control strategy that, with only information of the state of the balls at impacts, controls the balls to track the reference inputs in finite time is designed.

1.4 Robustness of numerical simulations

Numerical simulation plays a very important role in the analysis of hybrid systems. In the literature of simulation of hybrid systems, special attention has been given to the definition of semantics for simulation, event detection, and numerical solvers, see e.g. [64, 73]. This has led to the generation of very powerful simulation tools for hybrid systems, which includes Modelica [34], Ptolemy [63], Charon [2], HYSDEL [100], and HyVisual [61], among others. Perhaps, the ultimate goal of a hybrid simulator is to reproduce with arbitrary precision the solutions to the system under simulation. In this setting, numerical simulation techniques have to account for both flows and jumps. As for continuous-time systems, the continuous-time dynamics of hybrid systems need to be discretized by a numerical integration method (perhaps using one-step integration methods like Euler and Runge-Kutta or more advanced multistep methods). However, even though this is intuitively true, rigorous results that parallel the well-known facts about simulation of continuous-time systems (see, for example, [96], [33]) are currently missing for the hybrid setting.

In Chapter 7, the following *hybrid simulation model* for \mathcal{H} , denoted by \mathcal{H}_s , based on discretization of the

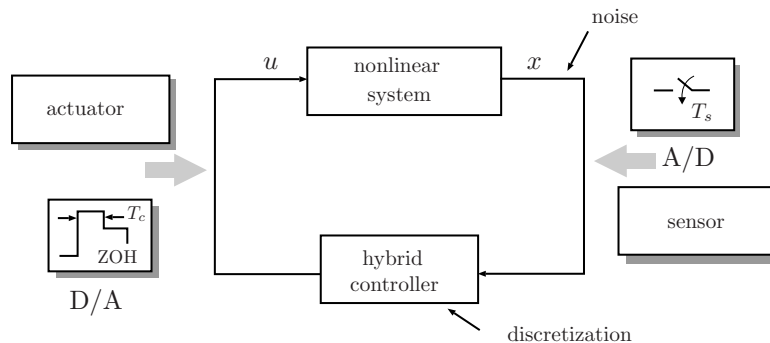


Figure 1.2. Hybrid control of a nonlinear system and some of the perturbations that arise in real-world scenarios.

dynamics is introduced:

$$\mathcal{H}_s : \quad x \in O \quad \begin{cases} x^+ \in F_s(x) & x \in C_s \\ x^+ \in G_s(x) & x \in D_s \end{cases}$$

where $s > 0$ is the integration step, F_s is the integration scheme for the flows, C_s is a subset of \mathbb{R}^n that indicates where in the state space the integration scheme F_s works, G_s is the discrete mapping that simulates the jumps, and D_s is a subset of \mathbb{R}^n that indicates where in the state space the mapping G_s for the simulation of jumps works. Note that the differential inclusion $\dot{x} \in F(x)$ was replaced by a difference inclusion. This corresponds to the discretization of the flows. In Chapter 7, the following question is addressed [84]:

What are the conditions on s , F_s , C_s , G_s , and D_s such that: 1) for a given simulation horizon, every simulation to a hybrid system is arbitrarily close to an actual solution to the hybrid system; 2) asymptotically stable compact sets for a hybrid system are semiglobally practically asymptotically stable compact sets for the hybrid simulator; 3) asymptotically stable compact sets for the hybrid simulator are continuous in the step size s ?

The required properties are obtained by treating the hybrid simulator \mathcal{H}_s as a perturbation of the hybrid system \mathcal{H} . The results make use of the recent results of asymptotic stability of compact sets for perturbed hybrid systems in [39].

1.5 Notes

The results outlined in the previous sections are given in the following chapters as indicated. More references and related material are included in the “Notes and references” section at the end of each of the following chapters.

Chapter 2

Mathematical Model and Solutions

In this chapter, a mathematical model is introduced as a framework for modeling, analyzing, and designing hybrid systems. The description of the model is exercised by some of the examples exhibiting hybrid phenomena discussed in Chapter 1. The concept of solution in this framework is given by functions, called *hybrid arcs*, in extended time domains, called *hybrid time domains*. These concepts are illustrated through several examples.

2.1 Preliminaries

A set-valued mapping from \mathbb{R}^m (or from a subset S of \mathbb{R}^m) to \mathbb{R}^n is understood to associate, with each point $x \in \mathbb{R}^m$ (or $x \in S$), a subset of \mathbb{R}^n . The notation $M : \mathbb{R}^m \rightrightarrows \mathbb{R}^n$ will distinguish a set-valued mapping M from a function.

Definition 2.1 (domain, range, graph)

Given a set-valued mapping $M : \mathbb{R}^m \rightrightarrows \mathbb{R}^n$,

- the domain of M is the set

$$\text{dom } M = \{x \in \mathbb{R}^m \mid M(x) \neq \emptyset\};$$

- the range of M is the set

$$\text{rge } M = \{y \in \mathbb{R}^n \mid \exists x \in \mathbb{R}^m \text{ such that } y \in M(x)\};$$

- the graph of M is the set

$$\text{gph } M = \{(x, y) \in \mathbb{R}^m \times \mathbb{R}^n \mid y \in M(x)\}.$$

A set-valued mapping M is fully determined by its graph, in the sense that

$$M(x) = \{y \mid (x, y) \in \text{gph } M\}.$$

A mapping M is empty-valued, single-valued, or multivalued at x if $M(x)$ is empty, a singleton, or a set containing more than one element. Every function defined on a set S is a set-valued mapping that is single-valued at each point of S .

Solutions to differential equations and differential inclusions will be understood in the *Carathéodory sense*. That is, given a function f or a set-valued mapping F , the classical and very restrictive condition that a solution

$z : [a, b] \rightarrow \mathbb{R}^n$ to $\dot{z}(t) = f(z(t))$ or $\dot{z}(t) \in F(z(t))$ be differentiable is replaced by requiring that it be absolutely continuous, and then $\dot{z}(t) = f(z(t))$ or $\dot{z}(t) \in F(z(t))$ are required to hold for almost all $t \in [a, b]$. (For an absolutely continuous $z : [a, b] \rightarrow \mathbb{R}^n$, the time derivative $\dot{z}(t) = \frac{d}{dt}z(t)$ need not exist for all $t \in [a, b]$ but is guaranteed to exist for all $t \in [a, b]$ except a set of measure zero.)

2.2 The model

In order to develop tools to analyze the behavior of hybrid systems, a mathematical model, one that can describe both the continuous evolution and the discontinuous evolution of the state variables, is needed. The approach taken in this thesis is from a dynamical systems point of view. A hybrid system has a state vector with dynamics governed by differential equations (or inclusions) and difference equations (or inclusions) in certain regions of a state space. More precisely, a hybrid system is described by five objects, which we refer to as the *data* of the hybrid system, that define what we call *hybrid equations*¹:

- The *state space*, i.e., the set to which the state of the hybrid system is restricted. The state space is denoted by O and is an open subset the Euclidean space \mathbb{R}^n , and often, the whole space itself. The state of the hybrid system is denoted by x .
- The *flow map* is either a function $f : O \rightarrow \mathbb{R}^n$ or, more generally, a set-valued mapping $F : O \rightrightarrows \mathbb{R}^n$ that describes, through a differential equation or a differential inclusion, the behavior of the state x when it evolves continuously. That is, during an interval of flow of x , either $\dot{x} = f(x)$ or $\dot{x} \in F(x)$ is satisfied. In the latter case, the velocity vector \dot{x} is restricted to be an element of the set $F(x)$.
- The *flow set* is a subset of the state space O that specifies where the continuous evolution can occur. It is denoted by C . Thus, only those solutions to a differential equation $\dot{x} = f(x)$ or inclusion $\dot{x} \in F(x)$ that satisfy the constraint $x \in C$, except possibly the times just before or just after a jump, will represent a possible behavior of the hybrid system.
- The *jump map* is either a function $g : O \rightarrow O$ or, more generally, a set-valued mapping $G : O \rightrightarrows O$ that describes, through a difference equation or a difference inclusion, the behavior of the state x when it jumps. That is, when a jump occurs, the value of the state after the jump, denoted x^+ , satisfies $x^+ = g(x)$ or $x^+ \in G(x)$ is satisfied. In the latter case, the state after the jump is restricted to be an element of the set $G(x)$ that depends on the state x before the jump.
- The *jump set* is a subset of the state space O that specifies from where the discontinuous evolution can occur. It will be denoted by D . Paralleling what was described for the flow, only those solutions to a difference equation $x^+ = g(x)$ or inclusion $x^+ \in G(x)$ that satisfy the constraint $x \in D$, i.e., the state x is in D before the jump, will represent a possible behavior of the hybrid system.

A shorthand notation for a hybrid system with the state space O , flow map f , flow set C , jump map g , and jump set D will be $\mathcal{H} = (O, f, C, g, D)$ or, in the case of set-valued mappings, $\mathcal{H} = (O, F, C, G, D)$. A representation that highlights the interplay between continuous and discrete dynamics by hybrid equations and suggests a concept of solution for hybrid systems \mathcal{H} is

$$\mathcal{H} : \quad x \in O \quad \begin{cases} \dot{x} &= f(x) & x \in C \\ x^+ &= g(x) & x \in D \end{cases},$$

¹In the general case, the data of a hybrid system will include set-valued mappings and the name *hybrid inclusions* would fit better, but for simplicity and uniformity, we simply use *hybrid equations*.

respectively

$$\mathcal{H} : \quad x \in O \quad \begin{cases} \dot{x} \in F(x) & x \in C \\ x^+ \in G(x) & x \in D . \end{cases} \quad (2.1)$$

The concept of solution will be rigorously stated in the next section, but the representation above suggests that

- solutions will stay in O ;
- solutions will only be allowed to flow when in C and will satisfy $\dot{x} = f(x)$ ($\dot{x} \in F(x)$ in the set-valued case);
- solutions will only be allowed to jump when in D and the value after the jump will satisfy $x^+ = g(x)$ (or $x^+ \in G(x)$ in the set-valued case);
- at points where C and D overlap, solutions could be nonunique, that is, they could either flow or jump;
- from points in C where flows are not possible solutions will not be able to evolve forward;
- from points in O that are not in $C \cup D$, and from points where solutions that initially flow do it outside of the set C , solutions will not exist.

An important property of the concept of solution used here that is worth it emphasizing is that solutions to \mathcal{H} could be nonunique not only due to the flow and jump dynamics given by inclusions, but also because it could be that from certain points in the state space, solutions could both flow and jump.

Since functions can be viewed as a special (single-valued) case of set-valued mappings, from now on, unless otherwise stated, set-valued mappings F and G as in (2.1) will be used in the symbolic description of hybrid systems. Note that this representation indicates that the proposed model for hybrid systems subsumes general models for continuous-time and discrete-time systems when the jump map and jump set are empty, i.e., when data is given by $(O, F, C, \emptyset, \emptyset)$, and when the flow map and flow set are empty, i.e., when data is given by $(O, \emptyset, \emptyset, G, D)$, respectively. This implies that the results in this thesis can be specialized, when appropriate, to these dynamical system subclasses.

The hybrid phenomena discussed in Section 1 will be revisited with an emphasis on describing possible choices for the corresponding data that comprise the mathematical model as described above.

2.2.1 Examples

As illustrated in the following examples, hybrid phenomena, i.e. the typical behavior in hybrid systems, can arise naturally or can be induced by interconnections and logic.

A bouncing ball

Consider a ball dropped from some height above the floor, as in Figure 2.1. A simplified way to model the ball's behavior is to assume that only gravity affects the ball when the ball is above the floor, and that the collision of the ball with the floor produces an instantaneous effect on the ball's velocity. In such a model, the velocity of the ball evolves continuously above the floor until a collision occurs. During a collision, the velocity undergoes a discontinuous change. More precisely, the velocity *jumps* as it changes sign and perhaps decreases in magnitude due to energy dissipation. After each collision, and so after each jump in the velocity, the ball position and velocity evolve continuously again, until the next collision with the floor.



Figure 2.1. Bouncing ball system: ball above the floor and gravity force g .

Denote the bouncing ball's height by h and its vertical velocity by \dot{h} . Take the state to be

$$x := \begin{bmatrix} h \\ \dot{h} \end{bmatrix} \in \mathbb{R}^2 .$$

The flow map for this system follows from the forces acting on the ball. For $x_1 > 0$, gravity acts on the ball generating the flow map

$$f(x) := \begin{bmatrix} x_2 \\ -g \end{bmatrix} \quad \text{if } x_1 > 0 ,$$

where g denotes the gravitational constant, according to Newton's laws of motion. Since flowing below the level of the floor will not be possible, the flow map does not need to be defined for $x_1 < 0$. Alternatively, one can view the flow map as a set-valued mapping with empty values for $x_1 < 0$. One may also consider defining the flow map for $x_1 = 0$. One possibility is to augment f with the additional definition

$$f(x) := \begin{bmatrix} x_2 \\ 0 \end{bmatrix} \quad \text{if } x_1 = 0 .$$

Another possibility is to augment f using the set-valued map

$$F(x) := \{f := [f_1 f_2]^T \in \mathbb{R}^2 \mid f_1 = x_2 , f_2 \in [-g, 0]\} \quad \text{if } x_1 = 0 .$$

The jump map can be taken to be

$$g(x) := \begin{bmatrix} x_1 \\ -\lambda x_2 \end{bmatrix}$$

where $\lambda \in [0, 1)$ quantifies the restitution factor for collisions between the ball and the floor.

Following the discussion above, the ball's velocity is allowed to jump when $x_1 = h = 0$ and $x_2 = \dot{h} < 0$. Thus, the jump set may be taken to be

$$D := \{x \in \mathbb{R}^2 \mid x_1 = 0 , x_2 < 0\} .$$

One may also consider choosing the jump set to be the closure of the set D given above. This would add the point $(x_1, x_2) = (0, 0)$ to the jump set, resulting in a closed set. The effect on solutions of closed jump sets will be discussed in the next chapter.

The state of the bouncing ball system changes continuously when the ball is above the floor. Thus, one may consider taking the flow set as

$$C := \{x \in \mathbb{R}^2 \mid x_1 > 0\} .$$

Figure 2.2 depicts the sets C and D defined above. It also shows the vector field f and the value of the jump map g for a particular point in its domain of definition.

Again, one may consider including some or all of the boundary points of C in the definition of the flow set. The effect on solutions will be discussed in the next chapter.

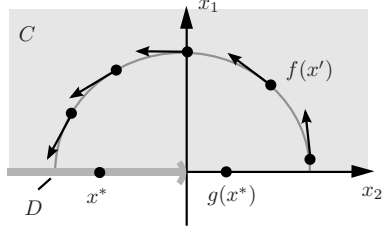


Figure 2.2. Bouncing ball data.

Sample-and-hold control systems

Digital computer systems have become the universal platform for the implementation of control algorithms for systems and processes. Typically, these digital controllers consist of microprocessors, digital signal processors, field-programmable gate arrays, etc., where the control algorithm is programmed in software. These constitute a large class of systems that is known as *sample-and-hold control systems* or *computer controlled systems*.

Consider the closed-loop system in Figure 2.3 resulting when digitally controlling a continuous-time nonlinear system with sample and hold devices. The basic operation of the digital controller is as follows. The output

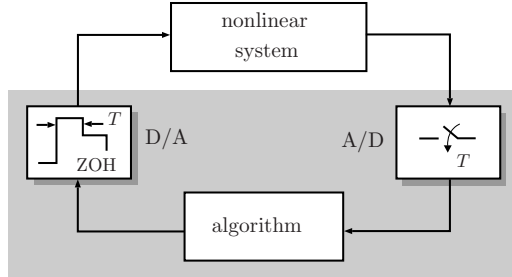


Figure 2.3. Digital control of a continuous-time nonlinear system with sample and hold devices.

of the nonlinear system is sampled by a sample device (this is the task of the *analog-to-digital converter* denoted as A/D) to obtain discrete values of the output to be processed by the control algorithm implemented in the digital controller. The result from the control algorithm computation is used to update the control input for the nonlinear system through the hold device (this is the task of the *digital-to-analog converter* denoted as D/A). For a periodic A/D sampler and a zero-order hold (ZOH) type of D/A, the output samples and control input updates occur at a fixed rate which is denoted by T . At every T units of time, there is a *jump* in the system which updates the outputs of these blocks and the time logic that synchronizes the devices. In between jumps, the system *flows*: the state of the nonlinear system evolves following its continuous-time dynamics under the effect of constant control input. The closed-loop system is a hybrid system with *jumps* at every T units of time, at which the digital controller obtains samples of the nonlinear system output and updates the control input, and *flows* in between those events.

Suppose that the nonlinear system to be controlled is given by

$$\dot{\xi} = \tilde{f}(\xi, u), \quad \xi \in \mathbb{R}^p, \quad u \in \mathbb{R}^m. \quad (2.2)$$

Let the control law to be implemented in the algorithm block in Figure 2.3 be the state-feedback law

$$\kappa : \mathbb{R}^p \rightarrow \mathbb{R}^m,$$

and suppose that the rate of D/A and A/D devices is $T > 0$, i.e., the sampling period. A timer variable τ is used to keep track of when the sampling period has elapsed. The held value of the control will be stored in the variable u in the ZOH device. This variable becomes part of the state of the closed-loop system, which is given by

$$x := \begin{bmatrix} \xi \\ u \\ \tau \end{bmatrix}$$

with state space \mathbb{R}^{p+m+1} . Since the variable u is held constant during flows, the timer variable τ keeps track of elapsed time, and the state x evolves with the dynamics in (2.2), the flow map is given by

$$f(x) := \begin{bmatrix} \tilde{f}(\xi, u) \\ 0 \\ 1 \end{bmatrix}.$$

Since, at the end of a sampling period, the variable u is updated by the feedback law κ (function of ξ), the timer should restart its count, and the state of the plant does not change, the jump map is given by

$$g(x) := \begin{bmatrix} \xi \\ \kappa(\xi) \\ 0 \end{bmatrix}.$$

The continuous evolution is allowed when the timer variable τ belongs to the interval $[0, T]$. In other words,

$$C := \{[\xi \ u \ \tau]^T \in \mathbb{R}^{p+m+1} \mid \tau \in [0, T]\}.$$

The jump evolution is allowed when the timer variable τ equals T , i.e.,

$$D := \{[\xi \ u \ \tau]^T \in \mathbb{R}^{p+m+1} \mid \tau = T\}.$$

2.2.2 Hysteresis in feedback control

Hysteresis is a property of a system that relates its input and output through a mechanism that keeps track of the previous input and output values, i.e. it has memory. It appears in nature and is exploited in many areas of technology.

Perhaps the most well-known hysteresis behavior is the one present in ferromagnetic materials. Figure 2.4(a) shows a typical relationship between the magnetic field intensity H and the magnetic flux density B in a ferromagnetic material. From an initial $B \approx 0$, B reaches a value close to one when $H \geq 1$, and from that condition, for B to reach a value close to zero, H needs to decrease below 0.1.

Hysteresis is usually incorporated into engineering systems by means of devices specially designed with such a characteristic. In particular, there exist electronic and mechanical devices where their input and output variables are related as shown in Figure 2.4(b), which we refer to as *relay-type hysteresis*. When the output of the device is zero, a transition to one is only possible when the input reaches the right threshold (denoted by u_2 in Figure 2.4(b)). From that condition, an output transition back to zero is only possible if the input reaches the left threshold (u_1).

Figure 2.5 shows a typical hysteresis input/output map. The two curves are defined for input values in the depicted overlapping input intervals. To model the input/output behavior, a logic variable can be associated to indicate the curve used to assign the output. The logic variable equal to one is assumed to indicate that the output is given by the lower curve, while equal to two indicates that the output is given by the upper curve. To be able to change from using the lower curve to the upper curve and vice versa, as hysteresis behavior requires,

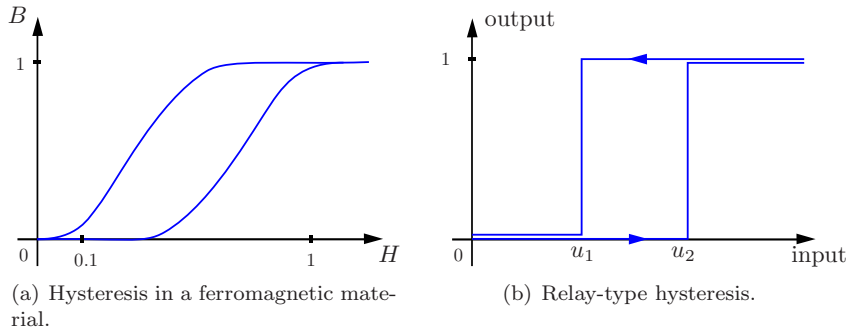


Figure 2.4. Examples of hysteresis behavior.

the logic variable has to jump. The update rule is as follows. When the logic variable is equal to one, indicating that the output is assigned through the lower curve, then a jump to two occurs when the input reaches the right end of the lower curve’s interval of definition. When the logic variable is equal to two, indicating that the output is assigned through the upper curve, then a *jump* to one occurs when the input reaches the left end of the upper curve’s interval of definition. When none of these *jump* events occur, the logic variable is constant. This corresponds to hybrid behavior.

Below, an application of hysteresis in control systems is presented.

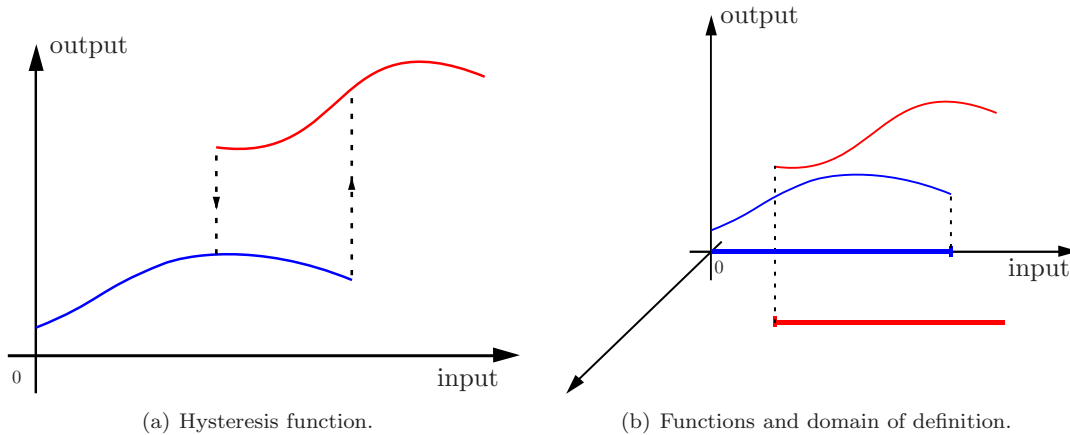


Figure 2.5. General hysteresis.

Combining local and global controllers

In several control applications, the design of a continuous-time feedback controller that performs a particular control task is not possible. For example, in the problem of globally stabilizing a multi-link pendulum to the upright position with actuation on the first link only, topological constraints rule out the existence of a continuous-time feedback controller that accomplishes this task globally and robustly. However, it is often possible to overcome such topological obstructions using hybrid feedback control to combine continuous-time feedback laws that achieve certain subtasks.

To illustrate this idea, consider the task of combining a high performance controller that only works near a

prescribed operating point with a controller that is able to steer every trajectory to the operating point but does not have as good a performance near that point. We refer to these as *local* and *global* controllers, respectively.

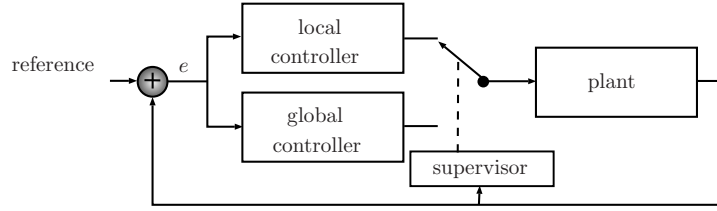


Figure 2.6. Closed-loop system combining local and global controllers.

Figure 2.6 depicts a block diagram of the control mechanism being described. Each controller measures the error signal given by the plant output and reference input. The controller selection is performed by the *supervisor*. By measuring the plant output, the supervisor decides whether to apply the local or global controller using a logic variable. This variable indicates the controller that is currently applied and is used in the selection rule as follows. If the logic variable indicates that the local controller is currently applied and the system output is far away from the region where the local controller works, then select the global controller and update the logic variable to indicate this. If the logic variable is such that the global controller is currently applied and the system output is in the region where the local controller works, then select the local controller and update the logic variable accordingly. If, with the logic variable indicating that the local controller is in the loop, the system output is in a small neighborhood of the region where the local controller works, then keep the current controller. However, if the system output is far away from that region where the local controller guarantees good performance, then select the global controller and update the logic variable as well. This switching rule introduces hysteresis. Note that the updates of the logic variable correspond to jumps, and that in between those, the closed-loop system flows. Hence, it is a hybrid system.

Suppose that two state feedback control laws $\kappa_1 : \mathbb{R}^p \rightarrow \mathbb{R}^m$, $\kappa_2 : \mathbb{R}^p \rightarrow \mathbb{R}^m$ have been designed to stabilize the origin of a nonlinear control system $\dot{\xi} = \tilde{f}(\xi, u)$. The feedback law κ_1 produces efficient transient responses, but only works near the origin. The feedback law κ_2 produces less efficient transients but works globally. The goal is to build a hybrid feedback law that globally asymptotically stabilizes the origin while using κ_1 near the origin and uses κ_2 far from the origin.

The controller will use a logic variable q , which here we assume to take values in the set $\{1, 2\}$, to keep track of which controller is currently being applied. Then, the state of the closed-loop system is given by

$$x := \begin{bmatrix} \xi \\ q \end{bmatrix} \in \mathbb{R}^{p+1} .$$

Since the logic variable does not change during flows, the flow map for the closed-loop system is given by

$$f(x) := \begin{bmatrix} \tilde{f}(\xi, \kappa_q(\xi)) \\ 0 \end{bmatrix} .$$

Hysteresis will be used as follows to determine when it is appropriate to switch between controllers. A jump should occur when $q = 2$ and the state ξ is close to the origin, say in a set D_2 , and a subsequent jump should not occur unless $q = 1$ and the state ξ attempts to leave a larger set C_1 . This behavior is generated by allowing flows when $q = 1$ and $\xi \in C_1$ or when $q = 2$ and $\xi \in \mathbb{R}^p \setminus D_2 =: C_2$, while allowing jumps when $q = 2$ and $\xi \in D_2$ or when $q = 1$ and $\xi \in \mathbb{R}^p \setminus C_1 =: D_1$. Thus, the flow set is taken to be

$$C := \{(\xi, q) \in \mathbb{R}^p \times \{1, 2\} \mid q \in \{1, 2\}, \xi \in C_q\} .$$

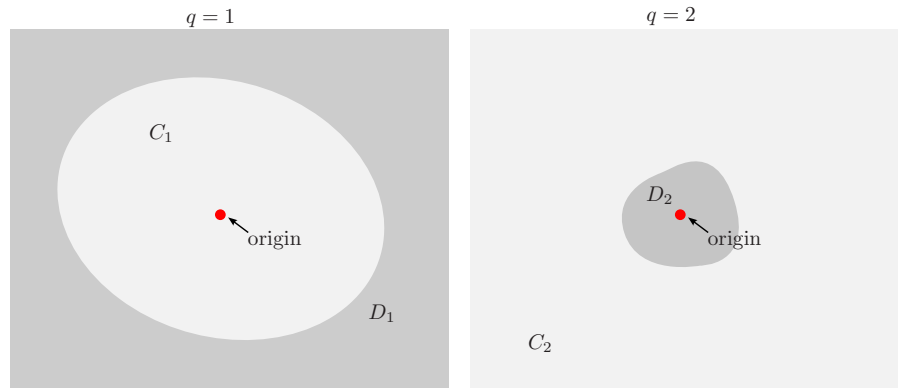


Figure 2.7. Sets for the hybrid controller combining control laws κ_1 and κ_2 .
 Sets for the hybrid controller combining control laws κ_1 and κ_2 .

The jump set is taken to be

$$D := \{(\xi, q) \in \mathbb{R}^p \times \{1, 2\} \mid q \in \{1, 2\} : \xi \in D_q\} .$$

These sets are depicted in Figure 2.7. Regarding the jump map, since the role of jump changes is to toggle the logic mode and since the state component ξ does not change during jumps, the jump map for the closed-loop system will be

$$g(x) := \begin{bmatrix} \xi \\ 3 - q \end{bmatrix} .$$

(Note that $3 - q = 2$ when $q = 1$ and $3 - q = 1$ when $q = 2$.)

Finally, in order for the hybrid feedback law to work as intended, there should be a relationship between D_2 and C_1 . In particular, if trajectories of

$$\dot{\xi} = \tilde{f}(\xi, \kappa_1(\xi))$$

start in D_2 they should remain in a closed set that is a strict subset of C_1 ; moreover any trajectory of this system that starts in C_1 and remains in C_1 should converge to the origin. Since the local controller is locally asymptotically stabilizing, both of these properties can be induced by first picking C_1 to be a sufficiently small neighborhood of the origin and then picking D_2 to be another sufficiently small neighborhood of the origin.

2.3 Time domains and arcs

Classical dynamical systems come in two main varieties: continuous-time systems, where solutions are parameterized by $t \in \mathbb{R}_{\geq 0}$, i.e., by time, and discrete-time systems, where solutions are parameterized by $j \in \mathbb{N}$, i.e., by the number of jumps. For general hybrid systems, which are a blend of continuous-time and discrete-time systems, it is natural to suggest that solutions be parameterized by both t , the amount of time passed, and j , the number of jumps that have occurred. Of course, it is impossible for a particular solution of a hybrid system to be defined for all $(t, j) \in \mathbb{R}_{\geq 0} \times \mathbb{N}$: for example, for a solution that jumps three times in the first two seconds of its evolution, it makes no sense to ask what is the state of this solution after four seconds and the first jump. More precisely, only certain subsets of $\mathbb{R}_{\geq 0} \times \mathbb{N}$ can correspond to evolutions of hybrid systems. Such sets are called *hybrid time domains*.

Definition 2.2 (hybrid time domains) A subset $E \subset \mathbb{R}_{\geq 0} \times \mathbb{N}$ is a compact hybrid time domain if

$$E = \bigcup_{j=0}^{J-1} ([t_j, t_{j+1}], j)$$

for some finite sequence of times $0 = t_0 \leq t_1 \leq t_2 \dots \leq t_J$. It is a hybrid time domain if for all $(T, J) \in E$, $E \cap ([0, T] \times \{0, 1, \dots, J\})$ is a compact hybrid domain.

Equivalently, E is a compact hybrid time domain if E is a union of a finite sequence of intervals $[t_j, t_{j+1}] \times \{j\}$, while E is a hybrid time domain if it is a union of a finite or infinite sequence of intervals $[t_j, t_{j+1}] \times \{j\}$, with the last interval, if the last one exists, possibly of the form $[t_j, T)$ with T finite or $T = \infty$.

Figure 2.8 shows an example of a hybrid time domain E given by the sequence of times $0 = t_0 < t_1 < t_2 = t_3 < t_4$. Note that for $(T, J) \in E$ in Figure 2.8, $E \cap ([0, T] \times \{0, 1, \dots, J\})$ is a compact hybrid domain. The figure suggests that for each hybrid time domain E , there is a natural (lexicographical) way of ordering its points: given $(t, j), (t', j') \in E$, $(t, j) \preceq (t', j')$ if $t < t'$ or $t = t'$ and $j \leq j'$. Equivalently (as long as the points are taken from the same time domain E) $(t, j) \preceq (t', j')$ if $t + j \leq t' + j'$. Points in two different hybrid time domains need not be comparable. For example, points $(1, 0)$ and $(0, 1)$ – which cannot belong to the same hybrid time domain – are not comparable: it is not the case that either $(1, 0) \preceq (0, 1)$ or $(1, 0) \succeq (0, 1)$.

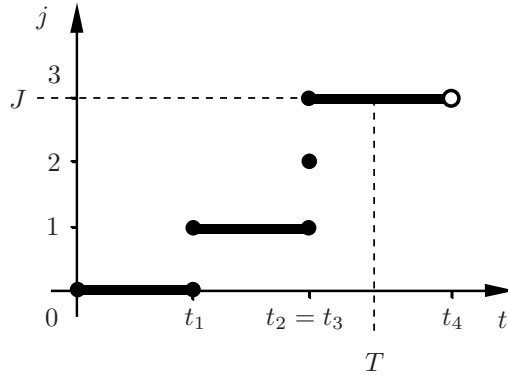


Figure 2.8. Hybrid time domain E .

Given a hybrid time domain E ,

$$\begin{aligned} \sup_t E &= \sup \{t \in \mathbb{R}_{\geq 0} \mid \exists j \in \mathbb{N} \text{ such that } (t, j) \in E\}, \\ \sup_j E &= \sup \{j \in \mathbb{N} \mid \exists t \in \mathbb{R}_{\geq 0} \text{ such that } (t, j) \in E\}. \end{aligned}$$

That is, the operations \sup_t and \sup_j on a hybrid time domain E return the supremum of the t and j coordinates, respectively, of points in E . Furthermore, $\sup E = (\sup_t E, \sup_j E)$, and finally, $\text{length}(E) = \sup_t E + \sup_j E$.

Definition 2.3 (hybrid arc) A function $x : E \rightarrow \mathbb{R}^n$ is a hybrid arc if E is a hybrid time domain and if for each $j \in \mathbb{N}$, the function $t \mapsto x(t, j)$ is locally absolutely continuous.

In the definition above, the absolute continuity requirement is only relevant for those intervals I^j , defined for each $j \in \mathbb{N}$ by $I^j \times \{j\} = E \cap (\mathbb{R}_{\geq 0} \times \{j\})$, that have nonempty interior. In general, such intervals may be empty or consist of just one point. On each I^j with nonempty interior, local absolute continuity of $t \mapsto x(t, j)$

means that $t \mapsto x(t, j)$ is absolutely continuous on each compact subinterval of I^j . Also, on each such I^j , $t \mapsto x(t, j)$ is differentiable almost everywhere, and $\dot{x}(t, j)$ will denote the time derivative of $x(t, j)$, whenever it exists. In short,

$$\dot{x}(t, j) = \frac{d}{dt}x(t, j).$$

Given a hybrid arc x , the notation $\text{dom } x$ represents its domain, which is a hybrid time domain. Such notation is consistent with the following “set-valued interpretation” of a hybrid arc. A hybrid arc x can be defined as a set-valued mapping $x : \mathbb{R}^2 \rightrightarrows \mathbb{R}^n$ that is single-valued on its domain $\text{dom } x$ (i.e., on the set of (t, j) on which $x(t, j) \neq \emptyset$, recall Definition 2.1) which is a hybrid time domain and for which $t \mapsto x(t, j)$ is locally absolutely continuous for each fixed $j \in \mathbb{N}$. Such interpretation makes it more natural to think that the hybrid time domain $\text{dom } x$ is determined by the arc x . This will be particularly relevant when talking about hybrid arcs that are solutions to a hybrid system. Then, it is certainly not appropriate to consider (an arbitrary) hybrid time domain E first, and then try to find a solution with E as a domain. Rather, it is necessary to find a solution x first, and say that its domain $\text{dom } x$ is determined by x . Furthermore, the “set-valued interpretation” above will help carry over some concepts of convergence and closeness of mappings from the set-valued realm to hybrid arcs and to solutions of hybrid systems, in later chapters.

Figure 2.9 illustrates a hybrid arc x with hybrid time domain $\text{dom } x$ that happens to coincide with the hybrid time domain in Figure 2.8.

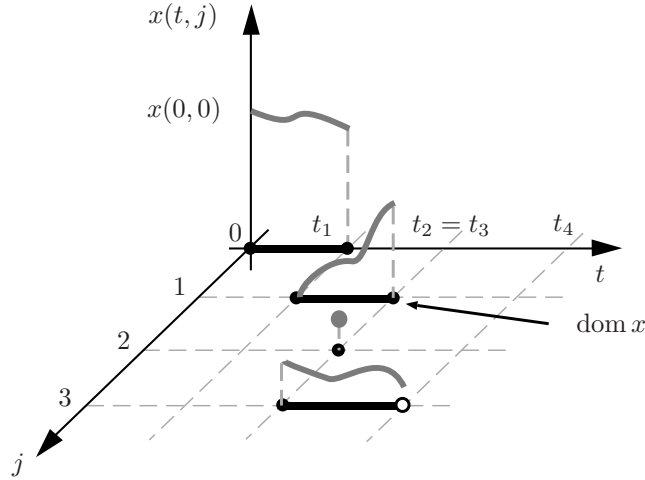


Figure 2.9. Hybrid arc x .

Certain classes of hybrid arcs can be defined based on the structure of their domains.

Definition 2.4 (types of hybrid arcs) *A hybrid arc x is called*

- *nontrivial* if $\text{dom } x$ contains at least two points;
- *complete* if $\text{dom } x$ is unbounded, i.e., if $\text{length}(E) = \infty$;
- *Zeno* if it is complete and $\sup_t \text{dom } x < \infty$;
- *eventually discrete* if $T = \sup_t \text{dom } x < \infty$ and $\text{dom } x \cap (\{T\} \times \mathbb{N})$ contains at least two points;
- *discrete* if nontrivial and $\text{dom } x \subset \{0\} \times \mathbb{N}$;

- eventually continuous if $J = \sup_j \text{dom } x < \infty$ and $\text{dom } x \cap (\mathbb{R}_{\geq 0} \times \{J\})$ contains at least two points;
- continuous if nontrivial and $\text{dom } x \subset \mathbb{R}_{\geq 0} \times \{0\}$.

The hybrid time domains associated with some of the classes defined above are shown in Figure 2.3.

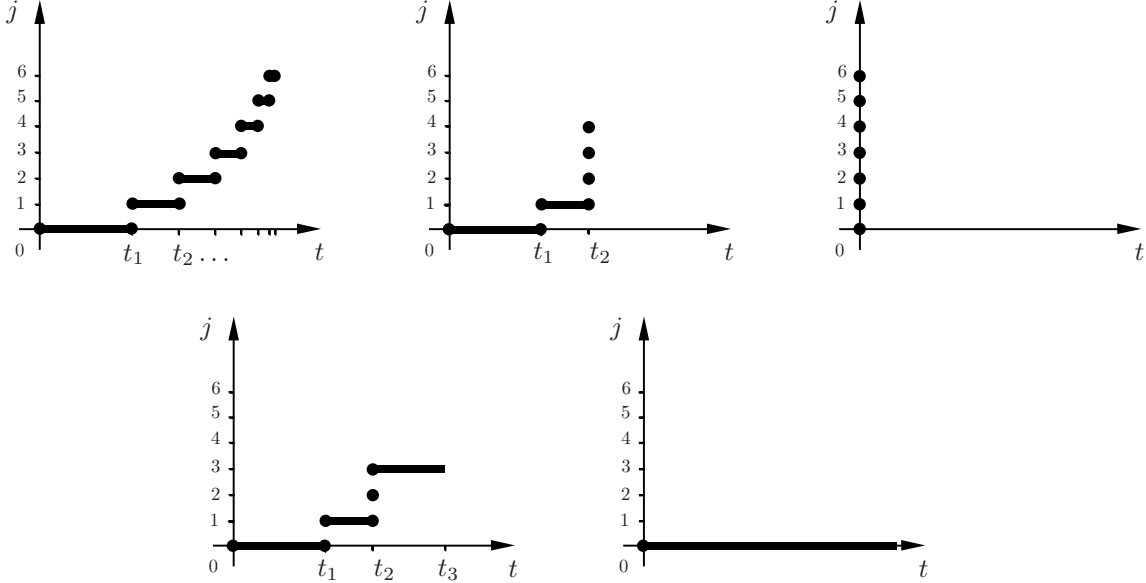


Figure 2.10. Hybrid time domains associated with various arc types: (a) Zeno, (b) eventually discrete, (c) discrete, (d) eventually continuous, and (e) continuous hybrid arcs.

2.4 Solutions to hybrid systems

Given a hybrid system \mathcal{H} , its solutions will be hybrid arcs x satisfying certain conditions determined by the data (O, F, C, G, D) of \mathcal{H} on hybrid time domains $\text{dom } x$. For each fixed j , the functions $t \mapsto x(t, j)$ will be required to satisfy conditions given by the flow set and the flow map, while for each fixed t , the functions $j \mapsto x(t, j)$ will be required to satisfy conditions given by the jump set and the jump map.

Definition 2.5 (solution to a hybrid system) *A hybrid arc x is a solution to the hybrid system \mathcal{H} if $x(0, 0) \in \overline{C} \cup D$, $x(t, j) \in O$ for all $(t, j) \in \text{dom } x$, and*

(S1) *for all $j \in \mathbb{N}$ such that I^j has nonempty interior, where $I^j \times \{j\} = \text{dom } x \cap ([0, \infty) \times \{j\})$,*

$$x(t, j) \in C \text{ for all } t \in \text{int } I^j, \quad \dot{x}(t, j) \in F(x(t, j)) \text{ for almost all } t \in I^j; \quad (2.3)$$

(S2) *for all $(t, j) \in \text{dom } x$ such that $(t, j + 1) \in \text{dom } x$,*

$$x(t, j) \in D, \quad x(t, j + 1) \in G(x(t, j)). \quad (2.4)$$

Figure 2.11 depicts a solution x to \mathcal{H} from $x(0,0)$. The solution flows in C to a point both in the flow and jump set where flow is no longer possible. This occurs at $(t,j) = (t_1,0)$ from where the solution jumps. After this jump, the solution jumps once more at $(t_1,1) = (t_2,1)$ and it flows in C with $j = 2$ for every t in the interior of $[t_2, t_3]$. At $(t_3,2)$, the solution jumps continuing its evolution.

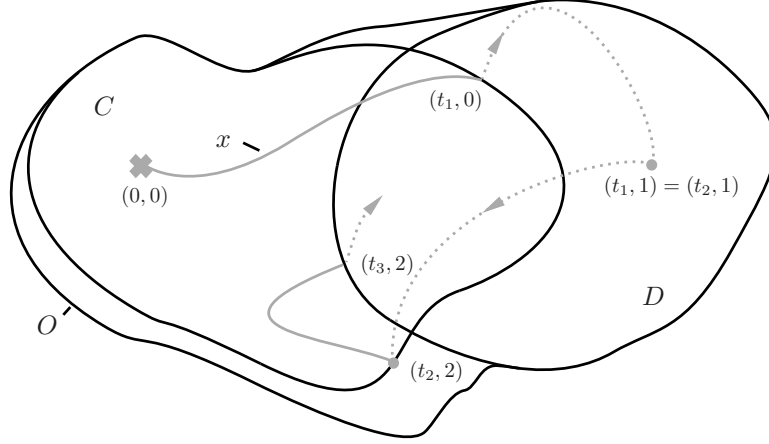


Figure 2.11. A solution to a hybrid system \mathcal{H} evolving in the state space O (The symbol \times denotes the initial condition. Dotted lines connect the solution values before the jump with the value after the jump.)

As in Definition 2.4, solutions to hybrid systems are classified based on their hybrid time domains as nontrivial, complete, Zeno, eventually discrete, discrete, eventually continuous, and continuous. Additionally, solutions that cannot be extended are said to be maximal.

Definition 2.6 (maximal solutions) *A solution x to \mathcal{H} is maximal if there does not exist another solution x' to \mathcal{H} such that $\text{dom } x$ is a proper subset of $\text{dom } x'$ and $x(t,j) = x'(t,j)$ for all $(t,j) \in \text{dom } x$.*

Throughout the thesis, $\mathcal{S}_{\mathcal{H}}(S)$ denotes the set of all maximal solutions x to \mathcal{H} with $x(0,0) \in S$. For example, given a point $\xi \in O$, writing $x \in \mathcal{S}_{\mathcal{H}}(\xi)$ means that x is a maximal solution to \mathcal{H} with $x(0,0) = \xi$. If no set S is mentioned, $x \in \mathcal{S}_{\mathcal{H}}$ means that x is a maximal solution to \mathcal{H} .

The following proposition gives natural conditions for the existence of nontrivial solutions to hybrid systems. Furthermore, it characterizes maximal solutions.

Proposition 2.7 (basic existence of solutions) *Consider a hybrid system $\mathcal{H} = (O, F, C, G, D)$. Let $\xi \in \overline{C} \cup D$. If $\xi \in D$ and $G(\xi) \neq \emptyset$ or*

(VC) *there exists $\varepsilon > 0$ and an absolutely continuous $z : [0, \varepsilon] \rightarrow \mathbb{R}^n$ such that $z(0) = \xi$, $\dot{z}(t) \in F(z(t))$ for almost all $t \in [0, \varepsilon]$, and $z(t) \in C$ for all $t \in (0, \varepsilon)$,*

then there exists a nontrivial solution x to \mathcal{H} with $x(0,0) = \xi$. If $G(\xi) \neq \emptyset$ for each $\xi \in D$ and (VC) holds for each $\xi \in \overline{C} \setminus D$, then there exists a nontrivial solution to \mathcal{H} from each point of $\overline{C} \cup D$, and each $x \in \mathcal{S}_{\mathcal{H}}$ satisfies exactly one of the following:

- (a) x is complete;
- (b) $\text{dom } x$ is bounded and, with $J = \sup_j \text{dom } x$, the interval I^J defined by $I^J \times \{J\} = \text{dom } x \cap (\mathbb{R}_{\geq 0} \times \{J\})$ has nonempty interior and $t \mapsto x(t, J)$ is a maximal solution to $\dot{z} \in F(z)$ on O ;

(c) $x(T, J) \notin \overline{C} \cup D$, where $(T, J) = \sup \text{dom } x$.

Furthermore, if $G(D) \subset \overline{C} \cup D$, then (c) above does not occur.

Proof. The first conclusion follows from the definition of a solution to \mathcal{H} . For the second, suppose that x is a maximal solution that is not complete, i.e., $\text{dom } x$ is bounded. Let $(T, J) = \sup \text{dom } x$. If $\text{dom } x$ is closed, in other words, if $(T, J) \in \text{dom } x$, then $x(T, J) \notin \overline{C} \cup D$. Indeed, if $x(T, J) \in D$, then x could be extended past (T, J) by a jump, if $x(T, J) \in \overline{C} \setminus D$, then x could be extended past (T, J) by flowing, and so x would not be maximal. If $\text{dom } x$ is not closed, then I^J defined by $I^J \times \{J\} = \text{dom } x \cap (\mathbb{R}_{\geq 0} \times \{J\})$ has nonempty interior and is open to the right, i.e., $I^J = [a, b)$ for some $b > a \geq 0$. Say $t \mapsto x(t, J)$ on I^J is not a maximal solution to $\dot{z} \in F(z)$ on O . Then $t \mapsto x(t, J)$ can be extended to a solution of $\dot{z} \in F(z)$ that remains in O on (at least) the interval $[a, b]$, and in such a way, one in fact obtains an extension of x that is a solution to \mathcal{H} on $\text{dom } x$. This contradicts the maximality of x . \square

2.5 Examples and further modeling

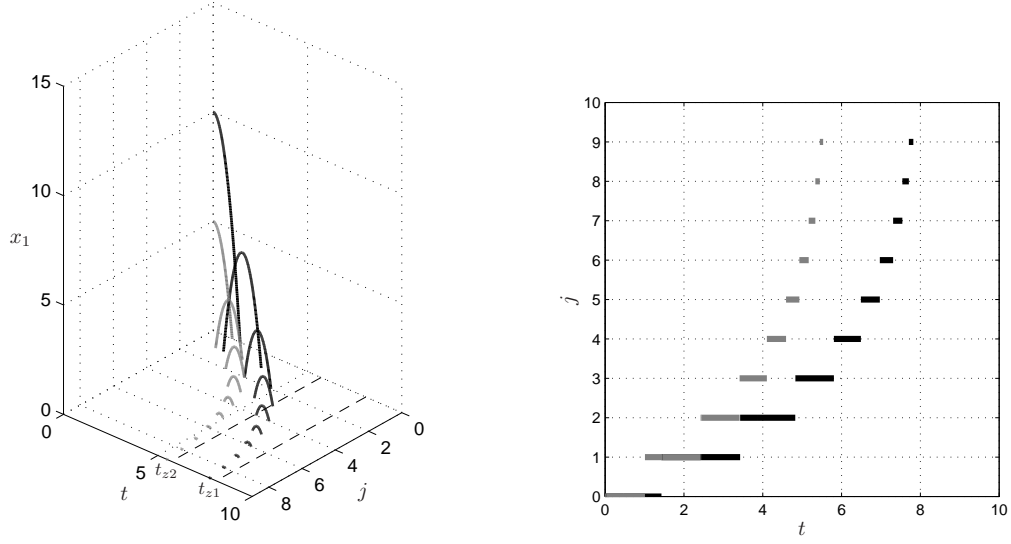
2.5.1 Bouncing ball revisited

The concept of a solution to hybrid system \mathcal{H} is now illustrated on the bouncing ball example from Section 2.2.1. First, the model summarized below is considered; later, effects of modifying this data on the solutions is addressed. Recall that x_1 represents the height and x_2 the velocity of the ball. Consider the data

$$\begin{aligned} O = \mathbb{R}^2, \quad f(x) &= \begin{bmatrix} x_2 \\ -g \end{bmatrix}, \quad C = \{x \in \mathbb{R}^2 \mid x_1 > 0\}, \\ g(x) &= \begin{bmatrix} x_1 \\ -\lambda x_2 \end{bmatrix}, \quad D = \{x \in \mathbb{R}^2 \mid x_1 = 0, x_2 < 0\}. \end{aligned}$$

Existence of nontrivial solutions is discussed first. From every initial state representing the ball above the floor, there exists a nontrivial solution that flows first. In technical terms, for every $\xi \in C$, there exists $\varepsilon > 0$ and a hybrid arc x satisfying $x(0, 0) = \xi$, $x(t, 0) \in C$ for all $t \in (0, \varepsilon)$ and $\dot{x}(t, 0) = f(x(t, 0))$ for almost all $t \in [0, \varepsilon]$, in fact for all $t \in [0, \varepsilon]$. This is true since C is open, and – because f is continuous – the very existence of solutions to the differential equation $\dot{z} = f(z)$ is not problematic. Similarly, there exists a nontrivial solution that flows first from each initial state ξ representing the ball at floor level and “moving up”, that is, from nonzero $\xi \in \overline{C} \setminus (C \cup D)$. This happens as f points into the set C from all points near ξ . From initial states ξ representing the ball at floor level and “moving down”, that is, from $\xi \in D$, there exists a nontrivial solution that jumps first. In technical terms, there exists a hybrid arc x with $x(0, 0) = \xi$, $x(0, 1) = g(\xi)$. This is possible as $g(\xi) \neq \emptyset$. However, there is no solution from the state representing the ball resting on the floor, that is, from $\xi = 0$. Indeed, the unique solution to $\dot{z}(t) = f(z(t))$ from the origin never enters C , while at the same time $0 \notin D$. In summary, there exists a nontrivial solution to \mathcal{H} from every initial point in $\overline{C} \setminus (C \cup D)$ except the origin.

Regarding maximal solutions to the bouncing ball model, it can be shown via Proposition 2.7, that maximal solutions from each nonzero initial state are complete. Indeed, $g(D) \subset C$, and option (c) from the conclusions of Proposition 2.7 can be excluded. Furthermore, any maximal solution to $\dot{z} = f(z)$ on O represents “the ball falling forever, as if there was no floor”. This cannot correspond to a solution to the hybrid system as required in (b) of Proposition 2.7, and so (b) can be excluded. This leaves completeness as the only option for maximal solutions. Now, the argument just given neglected the fact that the bouncing ball fails the assumptions of Proposition 2.7 at the origin. This can be overcome by noting that the origin is not reachable, in finite hybrid



(a) Solutions. (b) Hybrid time domains.

Figure 2.12. Bouncing ball solutions and domains.

time, from any nonzero initial state, and so does not affect the applicability of Proposition 2.7. In more technical terms, one can just apply the proposition to the bouncing ball with state space $\mathbb{R}^2 \setminus \{0\}$.

Each maximal, and so complete, solution from a nonzero initial state turns out to be Zeno. Given $\xi := [\xi_1 \ \xi_2]^T \in (\overline{C} \setminus D) \setminus \{0\}$, the time of the first bounce of the solution x from ξ is

$$t_1 = \frac{\xi_2 + \sqrt{\xi_2^2 + 2g\xi_1}}{g}. \quad (2.5)$$

(At that time, $x(t_1, 0) \in \overline{C} \cup D$, the flow is no longer possible, and a jump occurs.) Recursive use of (2.5) shows that the total amount of time before the first jump and in between all consecutive jumps (of which there is infinitely many) is

$$t_z = \frac{\xi_2 + \sqrt{\xi_2^2 + 2g\xi_1}}{g} + \frac{2\lambda\sqrt{\xi_2^2 + 2g\xi_1}}{g(1-\lambda)}. \quad (2.6)$$

If $\lambda < 1$, $t_z < \infty$ and the solution is Zeno. Figure 2.12 depicts two such solutions and corresponding hybrid time domains for different initial conditions.

Now, consider an augmented flow map f given by

$$f(x) = \begin{bmatrix} x_2 \\ 0 \end{bmatrix} \quad \text{if } x_1 = 0.$$

From $\xi = 0$, the hybrid arc x given by $x(t, j) = 0$ for all $(t, j) \in \text{dom } x = \mathbb{R}_{\geq 0} \times \{0\}$ satisfies $\dot{x}(t, j) \in f(x(t, j))$, $x(t, j) \in \overline{C}$ for all $(t, j) \in \text{dom } x$. However, this hybrid arc is not a solution to the bouncing ball system since it does not satisfy $x(t, j) \in C$ for all $t \in \text{int } I^0$, $I^0 = \mathbb{R}_{\geq 0}$. Clearly, replacing the jump set C by its closure causes this hybrid arc to be a solution. Since $\text{dom } x = \mathbb{R}_{\geq 0} \times \{0\}$, this solution is complete, and in contrast to the complete solutions present for the original mode, it is not Zeno.

Existence of a solution from the origin can be guaranteed if, instead, the point $\xi = 0$ is added to the jump set D . With this modification, a constant complete and discrete solution from ξ exists. Indeed, $g(D) \cap D = \{0\}$ and $x(0, j) = 0$ for all $j \in \mathbb{N}$ with $\text{dom } x = \{0\} \times \mathbb{N}$ is a solution. While allowing such a hybrid arc to be a solution of the bouncing ball model may seem counter intuitive, it can – and will be in later chapters – motivated by the pursuit of robustness of hybrid system models. Indeed, this solution reflects the nature of solutions from initial points in $\overline{C} \cup D$ arbitrarily close to 0 – all such solutions are Zeno.

2.5.2 Hybrid automaton

With appropriate choice of data, hybrid systems \mathcal{H} can model systems where the “discrete variable” q is explicitly mentioned. More specifically, consider

$$\mathcal{H} : \begin{cases} \dot{z} &= f_q(z) & z \in C_q \\ \begin{bmatrix} z^+ \\ q^+ \end{bmatrix} &\in G_q(z) & z \in D_q, \end{cases} \quad (2.7)$$

where Q is the set of “modes”, and for each $q \in Q$, $f_q : C_q \rightarrow \mathbb{R}^m$, $C_q \subset \mathbb{R}^m$, $G_q : D_q \rightrightarrows \mathbb{R}^m \times Q$, and $D_q \subset \mathbb{R}^m$. When Q can be identified with a subset of integers (and so a subset of \mathbb{R}), we can consider a system in the form (2.1) with the variable $x = [z \ q]^T \in \mathbb{R}^{m+1}$ and data

$$f(x) = \begin{bmatrix} f_q(z) \\ 0 \end{bmatrix}, \quad C = \bigcup_{q \in Q} (C_q \times \{q\}), \quad G(x) = G_q(z), \quad D = \bigcup_{q \in Q} (D_q \times \{q\}). \quad (2.8)$$

In turn, systems in the form (2.7) easily capture the commonly encountered hybrid automata where data is given in terms of domains, guards, edges, and resets. Let Q be the set of “modes”, for each $q \in Q$ let f_q be the flow map, let the mapping $\text{Domain} : Q \rightrightarrows \mathbb{R}^m$ give the domains of flow, let $\text{Edges} \subset Q \times Q$ be the set of edges, $\text{Guard} : \text{Edges} \rightrightarrows \mathbb{R}^m$ be the mapping giving the guards, and $\text{Reset} : \text{Edges} \times \mathbb{R}^m \rightrightarrows \mathbb{R}^m$ be the reset map. One then takes

$$C_q = \text{Domain}(q), \quad D_q = \bigcup_{e=(q,q') \in \text{Edges}} \text{Guard}(e), \quad (2.9)$$

$$G_q(x) = \bigcup_{\substack{e=(q,q') \text{ s.t.} \\ x \in \text{Guard}(e)}} \begin{bmatrix} \text{Reset}(e, x) \\ q' \end{bmatrix}. \quad (2.10)$$

Note that a set-valued mapping G_q will arise this way when two guard sets, $\text{Guard}(e')$ with $e' = (q, q')$ and $\text{Guard}(e'')$ with $e'' = (q, q'')$, overlap. This will even be the case when the resets $\text{Reset}(e', \cdot)$ and $\text{Reset}(e'', \cdot)$ are single valued. Solutions to the hybrid automaton by hybrid arcs are such that, for a fixed value of the discrete state q , the continuous state evolves with dynamics given by $\dot{z} = f_q(z)$, and once the jump set D is reached (given by D_q which corresponds to the current Guard), jumps are possible with the rule determined by the reset map Reset.

2.6 Summary

A modeling framework for hybrid systems has been introduced. Hybrid systems are given by *hybrid equations* with a state space O , a flow map given by a single-valued function f or a set-valued mapping F , a flow set $C \subset O$, a jump map given by a single-valued function g or a set-valued mapping G , and a jump set D . The

shorthand notation for a hybrid system is $\mathcal{H} = (O, f, C, g, D)$ or $\mathcal{H} = (O, F, C, G, D)$ in the set-valued case. Solutions are given by hybrid arcs and parameterized by (t, j) on hybrid time domains, which are subsets of $\mathbb{R}_{\geq 0} \times \mathbb{N}$. Depending on the hybrid time domain, solutions (or more generally, hybrid arcs) can be nontrivial, complete, Zeno, eventually discrete, discrete, eventually continuous, and continuous. Moreover, solutions that cannot be extended are called maximal. Several examples illustrated this modeling framework.

2.7 Notes and references

In what could be described as a “classical” approach to dynamical systems with jumps, the candidates for a solution are considered to be piecewise continuous functions of time that are right continuous and have left limits at each t in their domain of definition. This approach has been used in the early work by Witsenhausen [105] and Tavernini [97], and more recently in [11, 69, 25, 46, 98, 47, 37]. (Functions that are right continuous and have left limits are frequently referred to in the literature as CADLAG, from the French “continue a droite, limite a gauche”.)

More precisely, a *CADLAG solution* to $\mathcal{H} = (O, f, C, g, D)$ is a function $\xi : [0, T] \rightarrow \mathbb{R}^n$ or $\xi : [0, T] \rightarrow \mathbb{R}^n$ that is piecewise absolutely continuous (or piecewise differentiable), has a finite number of discontinuities in each compact subset of the interval on which it is defined, and that at every t it has left limits, is right continuous, and:

(D1) on each interval of continuity

$$\xi(t) \in C, \quad \dot{\xi}(t) = f(\xi(t));$$

(D2) at all points $\tau > 0$ of discontinuity satisfies

$$\xi^-(\tau) \in D, \quad \xi(\tau) \in g(\xi^-(\tau));$$

where $\xi^-(\tau) := \lim_{t \nearrow \tau} \xi(t)$. Whether $\dot{\xi}(t) = f(\xi(t))$ is to be understood as true for all t or for almost all t depends on whether one considers ξ 's that are differentiable on the intervals of continuity, or just absolutely continuous. By design, such a concept of a solution excludes multiple jumps at a single time instant. Furthermore, it makes it troublesome (or impossible) to discuss limits of solutions as the following example shows.

Example 2.8 (rotate and dissipate) Consider a hybrid system \mathcal{H} on \mathbb{R}^2 given by

$$\begin{aligned} \dot{x} &= f(x) := \begin{bmatrix} x_2 \\ -x_1 \end{bmatrix} & x \in C := \mathbb{R}^2, \\ x^+ &= g(x) := \frac{x}{2} & x \in D := (0, 1) \times \{0\}. \end{aligned}$$

For any point ξ with $0 < |\xi| < 1$ and $\xi \notin D$, a CADLAG solution from ξ exists. One such solution rotates clockwise around the origin for all time. (Such a solution will be excluded if D is considered to “force” jumps rather than “enable” them.) Another solution rotates clockwise until it hits D , then via a jump has its magnitude divided by 2, and then rotates again for 2π units of time until it hits D again at which point in time it jumps, and this cycle repeats for all time. Figure 2.13 depicts a solution of this type up to the second jump. Other solutions are created by rotating clockwise around the origin when not in D and permitting a jump whenever in D .

There are additional solutions that are admitted when using hybrid time domains that are not admitted when using CADLAG functions. In particular, the hybrid arc that corresponds to rotating clockwise around the origin until hitting D and then making an infinite number of jumps, each one cutting the magnitude of the solution in half, is a solution since each jump maps a point in D to another point in D . \square

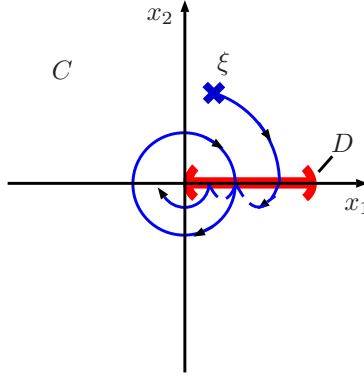


Figure 2.13. A CADLAG solution x to \mathcal{H} in Example 2.8 starting from ξ . When it reaches the D set, its magnitude is reduced by half. Flows continue after the jump until the solution hits the D set again.

We note that with each CADLAG solution, one can naturally associate a hybrid arc. More specifically, if t_j , $j = 1, 2, \dots, J$, is the time of the j -th jump of a CADLAG solution $\xi : [0, T] \rightarrow \mathbb{R}^n$, and $t_0 = 0$, $t_{J+1} = T$, one can associate with ξ a hybrid arc $\tilde{\xi}$ on a hybrid time domain given by $\bigcup_{j=1}^J ([t_j, t_{j+1}] \times \{j\})$, with $\tilde{\xi}(t, j) = \xi(t)$ for all $t \in [t_j, t_{j+1})$, $\tilde{\xi}(t_{j+1}, j) = \xi^-(t_{j+1})$ (recall that $\xi^-(t_{j+1}) = \lim_{t \nearrow t_{j+1}} \xi(t)$). Then $\tilde{\xi}$ is an *execution* of \mathcal{H} (another commonly used concept of a solution to hybrid systems; see for example [67]), in the sense that:

- (E1) $\tilde{\xi}(t, j) \in C$ for all $t \in [t_j, t_{j+1})$ while $\dot{\tilde{\xi}}(t, j) = f(\tilde{\xi}(t, j))$ for almost all $t \in [t_j, t_{j+1})$ (or for all $t \in [t_j, t_{j+1})$ if the original solution was piecewise differentiable);
- (E2) $\tilde{\xi}(t_{j+1}, j) \in D$, $\tilde{\xi}(t_{j+1}, j+1) \in g(\tilde{\xi}(t_{j+1}, j))$, for $j = 0, 1, \dots, J$.

Hybrid time domains are similar to hybrid time trajectories in [66],[67], and [7], and to the concept of time evolution in [103], but give a more prominent role to the number of jumps j (c.f. the definition of hybrid time set by Collins in [30]).

The hybrid automaton example in 2.5.2 follows the hybrid automaton modeling in [15, 18, 67].

Chapter 3

Generalized Solutions

This chapter discusses the effect of state perturbations on the solutions to a hybrid system. It is shown that state perturbations, of arbitrarily small size, can dramatically change the behavior of solutions. This behavior is related to the properties of the data of a hybrid system. A regularization procedure that results in a hybrid system with a set of “generalized solutions” that captures all limiting solutions with measurement noise converging to zero is proposed. This leads to and motivates the regularity conditions on the data of hybrid systems, called *hybrid basic conditions*, that will be required when deriving the results in the subsequent chapters.

3.1 Hybrid systems with state perturbations

A hybrid system $\mathcal{H} = (O, F, C, G, D)$ with a state perturbation e is denoted by \mathcal{H}_e , and following (2.1), will be written in the suggestive form:

$$\mathcal{H}_e : \quad x + e \in O \quad \begin{cases} \dot{x} & \in F(x + e) & x + e \in C \\ x^+ & \in G(x + e) & x + e \in D . \end{cases} \quad (3.1)$$

Before formally defining solutions to \mathcal{H}_e , a class of admissible state perturbation is specified.

Definition 3.1 (admissible state perturbation) *A mapping e is an admissible state perturbation if $\text{dom } e$ is a hybrid time domain and the function $t \rightarrow e(t, j)$ is measurable on $\text{dom } e \cap (\mathbb{R}_{\geq 0} \times \{j\})$ for each $j \in \mathbb{N}$.*

In several instances, the naturally arising state perturbation entering a hybrid system is dependent on time $t \in \mathbb{R}_{\geq 0}$ only, and not on j . For example, this is the case when a nonlinear control system is controlled by switching between several state-feedback laws, and the switching – which is what makes the closed-loop system hybrid – is not affected by the state perturbation. In such cases, any measurable signal $e' : \mathbb{R}_{\geq 0} \rightarrow \mathbb{R}^n$ corresponding to the state perturbation can be considered as given on an arbitrary hybrid time domain E , by setting

$$e(t, j) := e'(t) \quad (t, j) \in \text{dom } e := E . \quad (3.2)$$

A formal definition of solutions to \mathcal{H}_e with admissible state perturbation e follows.

Definition 3.2 (solution to a hybrid system with state perturbation) *A hybrid arc x is a solution to the hybrid system \mathcal{H}_e with admissible state perturbation e if $\text{dom } x = \text{dom } e$, $x(0, 0) + e(0, 0) \in \overline{C} \cup D$, $x(t, j) + e(t, j) \in O$ for all $(t, j) \in \text{dom } x$, and*

(S1_e) for all $j \in \mathbb{N}$ such that I^j has nonempty interior, where $I^j \times \{j\} := \text{dom } x \cap ([0, +\infty) \times \{j\})$,

$$\begin{aligned} x(t, j) + e(t, j) &\in C \quad \text{for all } t \in \text{int } I^j, \\ \dot{x}(t, j) &\in F(x(t, j) + e(t, j)) \quad \text{for almost all } t \in I^j; \end{aligned} \tag{3.3}$$

(S2_e) for all $(t, j) \in \text{dom } x$ such that $(t, j + 1) \in \text{dom } x$,

$$x(t, j) + e(t, j) \in D, \quad x(t, j + 1) \in G(x(t, j) + e(t, j)). \tag{3.4}$$

With some abuse of terminology, sometimes it will be said that a measurable $e' : \mathbb{R}_{\geq 0} \rightarrow \mathbb{R}^n$ leads to a solution x to \mathcal{H}_e if x with e given by $e(t, j) = e'(t)$ is a solution to \mathcal{H}_e in the sense of Definition 3.2. Similarly, the statement that $e' : \mathbb{R}_{\geq 0} \rightarrow \mathbb{R}^n$ leads to nonexistence of solutions to \mathcal{H}_e (possibly, with a specified initial point) will mean that there are no solutions x with e given by $e(t, j) = e'(t)$ for $(t, j) \in \text{dom } x$ to \mathcal{H}_e .

The behavior of solutions to \mathcal{H}_e can be dramatically different from that of solutions to \mathcal{H} . Even when the flow map and jump map are continuous functions and the state perturbations are very small, in which case state perturbations do not affect the flow and jump maps significantly, the flow set or the jump set not being closed can lead to \mathcal{H} being very sensitive to those perturbations. One simple consequence of this is that state perturbations can lead to solutions that “miss” the jump set. This means that it is possible that solutions that jump in the absence of state perturbations can flow forever when perturbations are present. Such phenomenon may be undesired in, say, hybrid feedback control, as stabilization may rely on certain variables jumping.

Example 3.3 (solutions miss the jump set) Consider the hybrid system \mathcal{H} on \mathbb{R}^2 with jump set D as in Figure 3.1, flow set $C = \mathbb{R}^2 \setminus D$, jump map $g(x) = 0$ for all $x \in D$, and flow map $f(x) = [1 \ 1]^T$ for all $x \in C$. The unique solution to \mathcal{H} from $\xi = 0$ is “periodic”: $x(t, j) = [t - j \ t - j]^T$ for $(t, j) \in \text{dom } x = \bigcup_{j \in \mathbb{N}} [j, j + 1] \times \{j\}$. (Note that the distance from the origin to D is unitary.) The unique solution to \mathcal{H}_e from $\xi = 0$ with $e(t, 0) = 0$ if $t \neq 1$ and $e(1, 0) \neq 0$ is continuous: $x_e(t, 0) = [t \ t]^T$ for $(t, 0) \in \text{dom } x_e = \mathbb{R}_{\geq 0} \times \{0\}$, and so, quite different from x ; in fact, different from all solutions to \mathcal{H} from initial points close to 0. Note though that x_e would be a solution to \mathcal{H} if the flow set was changed to be \mathbb{R} , that is, if one considered the closure of the original C . \square

With the effect of state perturbations so dramatic (for hybrid systems with data missing some regularity, for example, with the flow sets or the jump sets not closed), it can be expected that in some situations, asymptotic stability is not robust to perturbations. This is illustrated by the next example.

Example 3.4 (asymptotic stability without robustness) Consider a hybrid system with $f(x) = -x$ for all $x \in C := (-\infty, 1]$, and $g(x) = 1$ for all $x \in D := (1, \infty)$. Solutions starting from C (in particular, the unique solution starting from $\xi = 1$) converge to 0 exponentially. Solutions from D jump to $1 \in C$ instantly, and then converge to 0 exponentially. It can be easily verified that the system is globally uniformly asymptotically stable. However, the unique solution to \mathcal{H}_e from $\xi = 1$ with constant and equal to $\varepsilon > 0$ perturbation is given by $x_e(0, j) = 1$ for all $j \in \mathbb{N}$. Figure 3.2 illustrates this behavior. In particular, (arbitrarily small) state perturbation destroys asymptotic stability. Note that x_e corresponds to a solution to \mathcal{H} with D replaced by its closure. \square

When the flow map and/or jump maps are discontinuous, the effect of measurement noise can lead to unexpected behavior of the system. For instance, the presence of two opposite values of a discontinuous map

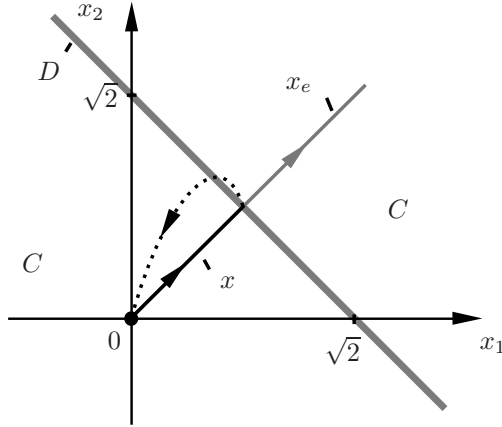


Figure 3.1. Flow and jump set for the hybrid system in Example 3.3. Solution x without measurement noise is periodic while solution x_e with measurement noise escapes to infinity.

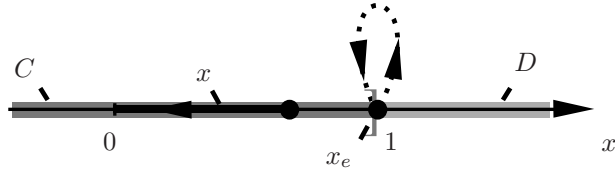


Figure 3.2. The effect of state perturbations in Example 3.4. x is a solution to \mathcal{H} and x_e is a solution to \mathcal{H}_e with admissible measurement noise e .

near an initial point can lead to a solution chattering around such a point. The following examples illustrate this, and more general behaviors resulting from state perturbations, for two extreme types of hybrid systems: purely continuous and purely discrete.

Example 3.5 (differential equation with discontinuous right-hand side) Consider the hybrid system on \mathbb{R}^2 with data $(O, f, C, \emptyset, \emptyset)$ where

$$f(z) = \begin{bmatrix} 1 \\ 0 \end{bmatrix} \text{ if } z_2 \geq 0, \quad f(z) = \begin{bmatrix} -1 \\ 0 \end{bmatrix} \text{ if } z_2 < 0$$

and $C = \mathbb{R}^2$. The unique solution from $\xi = 0$ is given by $z_1(t, 0) = t$, $z_2(t, 0) = 0$ for $t \in \mathbb{R}_{\geq 0}$. Now, given any $\varepsilon > 0$, consider $e : \mathbb{R}_{\geq 0} \times \{0\} \rightarrow \mathbb{R}^2$ given by $e_1(t, 0) = 0$, $e_2(t, 0) = \varepsilon \sin t$. The solution to $\dot{z}(t, 0) = f(z(t, 0) + e(t, 0))$, in the first variable, is a see-saw function z_{1e} oscillating between 0 and π as shown in Figure 3.3. This is significantly different than the original, unperturbed, solution.

More generally, given any $\varepsilon > 0$ and any $\lambda \in (0, 1)$, let $e : \mathbb{R}_{\geq 0} \times \{0\} \rightarrow \mathbb{R}^2$ be given by $e_1(t, 0) = 0$ for $t \in \mathbb{R}_{\geq 0}$ and by e_2 that is periodic, with period ε , and defined on $[0, \varepsilon)$ by $e_2(t, 0) = \varepsilon$ for $t \in [0, \lambda\varepsilon)$, $e_2(t, 0) = -\varepsilon$ for $t \in [\lambda\varepsilon, \varepsilon)$. The resulting solution, from $\xi = 0$, displays a “see-saw like” function in the first variable. The average rate of growth of that function, over $[0, k\varepsilon)$ for any $k \in \mathbb{N}$, is $\lambda(1) + (1 - \lambda)(-1) = 2\lambda - 1$. The limit (uniform on compact intervals, and in fact uniform), as $\varepsilon \rightarrow 0$, of such “see-saw like” functions is $z_1(t, 0) = (2\lambda - 1)t$ for $t \in \mathbb{R}_{\geq 0}$. Together with $z_2(t, 0) = 0$ for $t \in \mathbb{R}_{\geq 0}$, such limit is in fact a solution to the

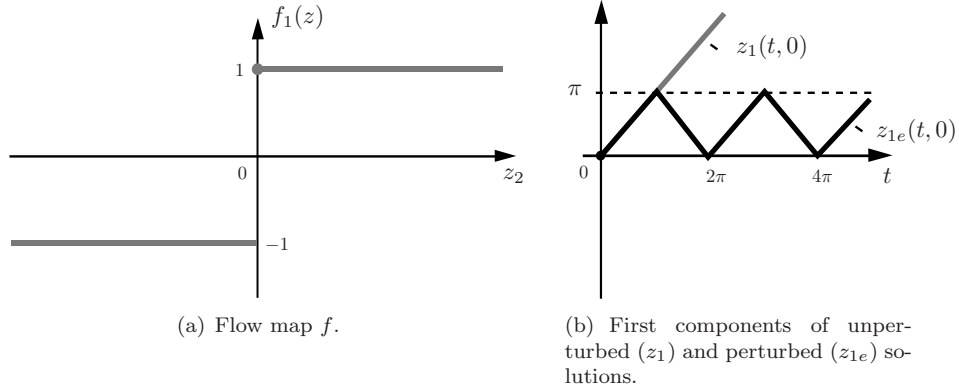


Figure 3.3. Flow map and solutions to Example 3.5.

differential inclusion $\dot{z} \in F(z)$, where

$$F(z) = \begin{bmatrix} 1 \\ 0 \end{bmatrix} \quad \text{if } z_2 > 0, \quad F(z) = \begin{bmatrix} -1 \\ 0 \end{bmatrix} \quad \text{if } z_2 < 0, \quad F(z) = \begin{bmatrix} [-1, 1] \\ 0 \end{bmatrix} \quad \text{if } z_2 = 0.$$

In particular, at the points of discontinuity of f , the set-valued mapping F is given by the convex set containing the values of f from nearby points. \square

The example suggests that the effect of state perturbations on solutions to a hybrid system with discontinuous flow map may be reflected by solutions to the hybrid system with flow map $F(z)$ with F being a “convex closure” of f . This will be made formal later.

Example 3.6 (difference equation with discontinuous right-hand side) Consider the hybrid system on \mathbb{R} with data $(O, \emptyset, \emptyset, g, D)$ where g is given as in Figure 3.4(a) and $D = \mathbb{R}$. For every $\xi \in \mathbb{R}$, solutions converge to zero in finite steps (or jumps). In fact, the number of jumps for solutions to converge to zero is equal to $\text{floor}(\xi) + 1$ if $\xi \notin \mathbb{Z}$, and equal to ξ otherwise, where $\text{floor}(\xi)$ is the smallest closest integer to ξ . Given any $\varepsilon > 0$, consider $e : \{0\} \times \mathbb{N} \rightarrow \mathbb{R}$ given by $e(0, j) := \varepsilon$ for each $j \in \mathbb{N}$. The solution to $z^+ = g(z + e)$ from $\xi' \in \mathbb{R}$ is a constant function $z(0, j) = \text{floor}(\xi' + \varepsilon)$ for all $j \in \mathbb{N}$. Then, the limit of such solution as $\varepsilon \rightarrow 0$ is $z(0, j) = \xi'$ for all $j \in \mathbb{N}$. This limiting solution is a solution to the differential inclusion $z^+ \in G(z)$ where G is given as in Figure 3.4(b). At the points of discontinuity, the set-valued map G is given by all of the limiting points of g from nearby points. \square

A different phenomenon is also possible: for some hybrid systems, even with quite regular data, some state perturbations can lead to nonexistence of solutions. This is certainly possible for initial conditions ξ that are on the boundary of $C \cup D$, independently of regularity of the data (in fact, C, D can be closed in \mathbb{R}^n , f, g continuous, and the necessary conditions for existence of solutions, as in Proposition 2.7 can be assumed). Indeed, for such ξ , there exists an arbitrarily small $\Delta \in \mathbb{R}^n$ such that $\xi + \Delta \notin \overline{C \cup D}$. Then, there are no nontrivial solutions to \mathcal{H}_e with $e(t) = \Delta, t \geq 0$. In fact, when ξ is in the intersection of the boundaries of C and of D (but is possibly in the interior of $C \cup D$), existence may still be problematic for some perturbations. For such ξ , there exists (arbitrarily small) Δ_1 such that $\xi + \Delta_1 \notin D$ and Δ_2 such that $\xi + \Delta_2 \notin \overline{C}$. Taking noise defined by $e(0) = \Delta_1, e(t) = \Delta_2$ for $t > 0$, results in no solutions to \mathcal{H}_e from ξ . Indeed, any solution to \mathcal{H}_e from ξ would either satisfy $x(0, 0) + \Delta_1 \in D$, which does not hold, or $x(t, 0) + \Delta_2 \in C$ for small enough t , which also does not hold (this follows since $x(0, 0) + \Delta_2 \notin \overline{C}$, the complement of \overline{C} is open, and $x(t, 0)$ is close to $x(0, 0)$ for small t).

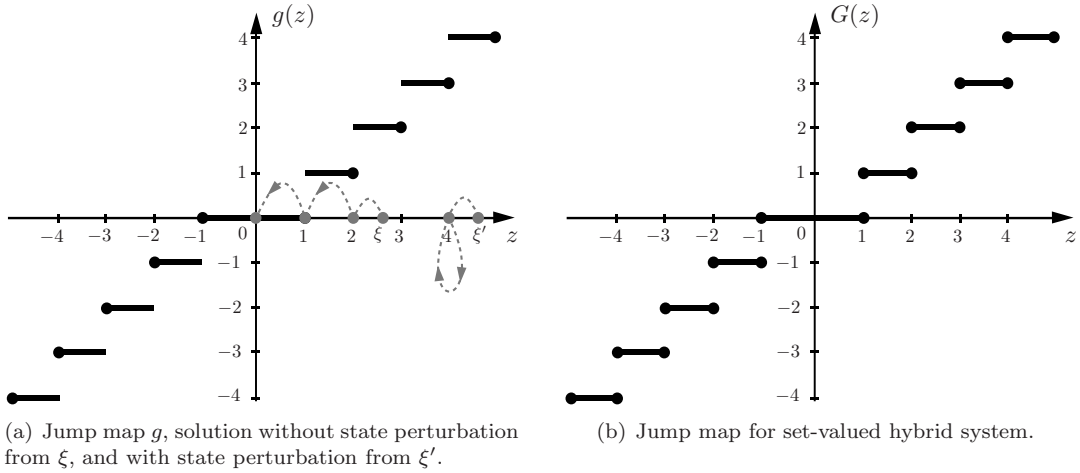


Figure 3.4. Jump map and solutions to Example 3.6.

Proposition 3.7 (basic existence with state perturbations) *Consider a hybrid system $\mathcal{H} = (O, F, C, G, D)$. Let $\xi \in \overline{C} \cup D$. If there exists $\delta > 0$ such that either $\xi + \delta\mathbb{B} \subset D$ and $G(\xi') \neq \emptyset$ for all $\xi' \in \xi + \delta\mathbb{B}$ or*

(VC_e) $\xi + \delta\mathbb{B} \subset C$ and for every measurable $e' : \mathbb{R}_{\geq 0} \rightarrow \mathbb{R}^n$ with $e'(t) \in \delta\mathbb{B}$ for all $t \in \mathbb{R}_{\geq 0}$ there exists $\varepsilon > 0$ and an absolutely continuous $z_{e'} : [0, \varepsilon] \rightarrow \mathbb{R}^n$ such that $z_{e'} = \xi$, $\dot{z}_{e'}(t) \in F(z_{e'}(t) + e'(t))$ for almost all $t \in [0, \varepsilon]$, and $z_{e'}(t) + e'(t) \in C$ for all $t \in (0, \varepsilon)$,

then there exists a nontrivial solution x to \mathcal{H}_e with $x(0, 0) = \xi$ for any admissible state perturbation e with $e(t, j) \in \delta\mathbb{B}$ for all $(t, j) \in \text{dom } e$.

Proof. Suppose first that ξ is such that for some $\delta > 0$, $\xi + \delta\mathbb{B} \subset D$ and $G(\xi') \neq \emptyset$ for all $\xi' \in \xi + \delta\mathbb{B}$. Then, for any admissible state perturbation $e : \{(0, 0), (0, 1)\} \rightarrow \mathbb{R}^n$ with $e(0, 0) \in \delta\mathbb{B}$, $e(0, 1) \in \mathbb{R}^n$, it follows that $\xi + e(0, 0) \in D$. Then, the hybrid arc $x : \{(0, 0), (0, 1)\} \rightarrow \mathbb{R}^n$ with $x(0, 0) = \xi$ and $x(0, 1) \in G(x(0, 0) + e(0, 0))$ is a nontrivial solution to \mathcal{H}_e with admissible measurement noise e . Suppose instead that (VC_e) holds. Let $e(t, 0) = e'(t)$ for all $t \in [0, \varepsilon]$. Then, the hybrid arc $x : [0, \varepsilon] \rightarrow \mathbb{R}^n$ with $x(t, 0) = z_{e'}(t)$ for all $t \in [0, \varepsilon]$ is nontrivial solution to \mathcal{H}_e with admissible measurement noise e . \square

Limits of solutions to hybrid systems, as the perturbations vanish, are discussed in the next section.

3.2 Generalized solutions to hybrid systems

The previous sections illustrated that the effect of state perturbations on the solutions to a hybrid systems can be quite significant. In this section, the effect of (arbitrarily small) state perturbations is related to an operation that regularizes the data of the hybrid system. Briefly speaking, an appropriately understood limit of a sequence of solutions to a hybrid system, generated with state perturbation decreasing in magnitude, turns out to be a solution to a regularized hybrid system. Conversely, any solution to the regularized system can be approximated, with arbitrary precision, with solutions to the original system generated with state perturbations.

To make these statements precise, a way to measure whether two hybrid arcs are close to one another is needed. Certainly, as two different hybrid arcs need not have the same domains, relying on the uniform metric

is impossible. The (τ, ε) -closeness defined below is related to the distance between the graphs of hybrid arcs as Figure 3.5 shows.

Definition 3.8 ((τ, ε) -closeness) *Given $\tau \geq 0$ and $\varepsilon > 0$, two hybrid arcs x_1 and x_2 are (τ, ε) -close if*

(a) *for all $(t, j) \in \text{dom } x_1$ with $t + j \leq \tau$ there exists s such that $(s, j) \in \text{dom } x_2$, $|t - s| < \varepsilon$, and*

$$|x_1(t, j) - x_2(s, j)| < \varepsilon,$$

(b) *for all $(t, j) \in \text{dom } x_2$ with $t + j \leq \tau$ there exists s such that $(s, j) \in \text{dom } x_1$, $|t - s| < \varepsilon$, and*

$$|x_2(t, j) - x_1(s, j)| < \varepsilon.$$

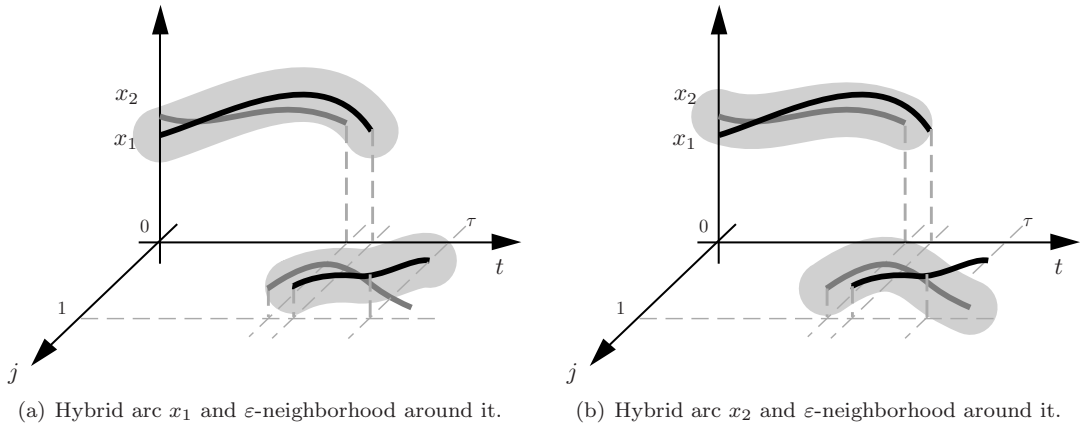


Figure 3.5. Two hybrid arcs (τ, ε) -close.

Accounting for state perturbations, or regularizing the data of a hybrid system, will lead to two concepts of generalized solutions to a hybrid system. The terminology used for these concepts, Hermes solutions and Krasovskii solutions, is borrowed from what was established for differential equations.

Definition 3.9 (Hermes solutions to hybrid systems) *A compact hybrid arc x is a compact Hermes solution to \mathcal{H} if there exist a sequence $\{x_i\}_{i=1}^{\infty}$ of hybrid arcs and a sequence $\{e_i\}_{i=1}^{\infty}$ of admissible state perturbations such that*

- x_i is a solution to \mathcal{H}_e with state perturbation e_i for each $i \in \mathbb{N}$;
- for each $\varepsilon > 0$ there exists i_0 such that for all $i > i_0$, x_i and x are (τ, ε) -close, where $\tau = \text{length}(x)$;
- the sequence of $\sup_{(t,j) \in \text{dom } e_i} |e_i(t, j)|$ converges to 0.

A hybrid arc x is a Hermes solution to \mathcal{H} if the restriction of x to each compact subset of $\text{dom } x$ that is a hybrid time domain is a compact Hermes solution to \mathcal{H} .

Definition 3.10 (Krasovskii solutions to hybrid systems) *A hybrid arc x is a Krasovskii solution to $\mathcal{H} = (O, F, C, G, D)$ if x is a solution to the regularized hybrid system*

$$\widehat{\mathcal{H}}: \quad x \in O \quad \begin{cases} \dot{x} \in \widehat{F}(x) & x \in \widehat{C} \\ x^+ \in \widehat{G}(x) & x \in \widehat{D} \end{cases} \quad (3.5)$$

where $\widehat{C} := \overline{C} \cap O$, $\widehat{D} := \overline{D} \cap O$, and

$$\begin{aligned} \forall x \in \widehat{C} \quad \widehat{F}(x) &:= \bigcap_{\delta > 0} \overline{\text{co}F((x + \delta\mathbb{B}) \cap C)}, \\ \forall x \in \widehat{D} \quad \widehat{G}(x) &:= \bigcap_{\delta > 0} \overline{G((x + \delta\mathbb{B}) \cap D)}. \end{aligned}$$

For the hybrid system \mathcal{H} in Example 3.3, the regularized hybrid system $\widehat{\mathcal{H}}$ has the same jump set, flow map, and jump map as the original \mathcal{H} . The only change is in the flow set, with $\widehat{C} = \mathbb{R}$. This leads to nonuniqueness of solutions to $\widehat{\mathcal{H}}$ from $\xi = 0$. One solution is the solution already present for \mathcal{H} (and unique for \mathcal{H}). Another solution, that reflects what was exhibited by \mathcal{H} under perturbations, is continuous, and flows through D (while remaining in C). Of course, other solutions are also present.

Regarding Example 3.4, the only difference between \mathcal{H} and $\widehat{\mathcal{H}}$ is the jump set which, for $\widehat{\mathcal{H}}$, is given by $\widehat{D} = \overline{D} = [1, \infty)$. Solutions from $\xi = 1$ are no longer unique: the solution that (exponentially) converges to the origin is still present while the discrete solution that is always equal to 1 is new. The new solution is the Krasovskii solution to \mathcal{H} that does not converge to the origin as discussed in Example 3.4.

All of the interesting behavior of solutions to hybrid systems discussed in Section 3.1 and the equivalences between Hermes and Krasovskii solutions in the examples discussed above are true even when f and g are single valued. Recall that motivation for considering set-valued jump maps was given by the general model of a hybrid automaton in Section 2.5.2. Further motivation comes from decision-making control algorithms which, in some applications, as it will be shown in Chapter 6, it is the case that the controller has multiple options to choose from. The following equivalence result between Hermes and Krasovskii solutions covers this large class of hybrid systems.

Below, given an open set O , a function $\phi : S \rightarrow \mathbb{R}^n$ (or a set-valued mapping $\phi : S \rightrightarrows \mathbb{R}^n$) defined on a subset $S \subset \mathbb{R}^n$ is said to be locally bounded on O if for each compact set $K \subset O$ there exists a compact set $K' \subset \mathbb{R}^n$ such that $\phi(K) \subset K'$. It is locally bounded with respect to O on O if $K' \subset O$.

Theorem 3.11 (Hermes and Krasovskii solutions to hybrid systems) *Let $\mathcal{H} = (O, f, C, G, D)$ be a hybrid system with set $O \subset \mathbb{R}^n$ open, sets C and D subsets of O , function $f : C \rightarrow \mathbb{R}^n$ locally bounded on O , and set-valued mapping $G : D \rightrightarrows \mathbb{R}^n$ locally bounded with respect to O on O . Then, a hybrid arc x is a Hermes solution to \mathcal{H} if and only if it is a Krasovskii solution to \mathcal{H} .*

The following example illustrates a situation where a hybrid system with data coinciding with the data of its regularized version can be easily and intuitively derived.

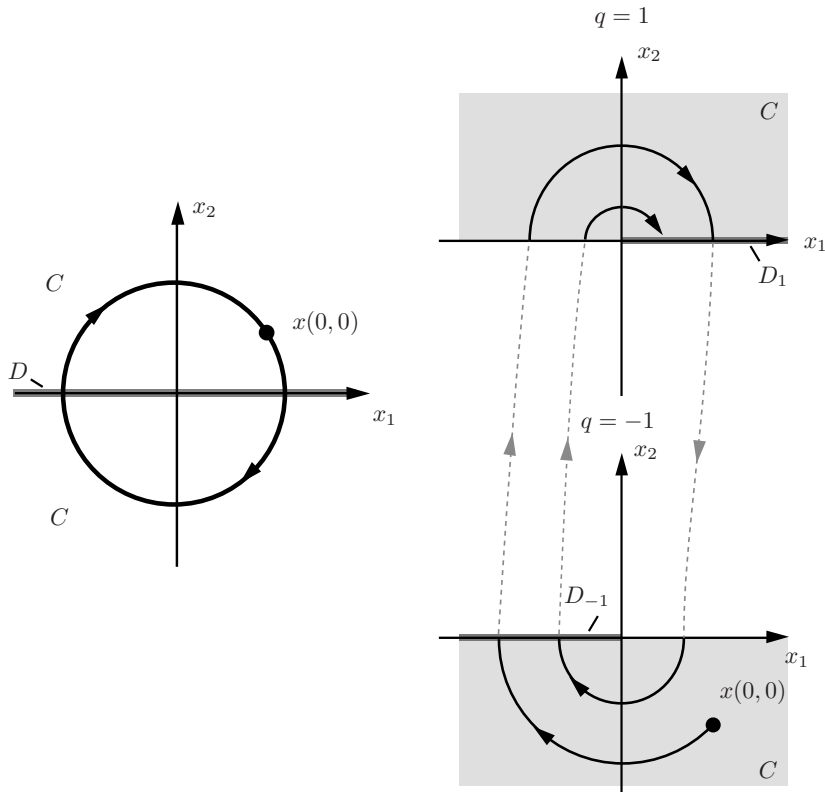
Example 3.12 (robust zero-crossing detection) The effect of state perturbations illustrated in Example 3.3 can arise in general when decisions are made at a surface or “thin” jump set D . In the problem of counting the number of times that the trajectories of the planar nonlinear system $\dot{x} = [x_2 \ -x_1]^T$, cross the x_1 -axis, the crossing detection algorithm determines the effect of state perturbations in the counts. Suppose that the crossing algorithm is designed so that every time that the x_1 component of the solution is equal to zero, a counter is incremented and that the resulting hybrid system \mathcal{H} is simulated numerically. The hybrid system \mathcal{H} has state given by $[x \ p]^T$, where $p \in \mathbb{N}$, flow map $f(x, p) = [x_2 \ -x_1 \ 0]^T$, jump map $g(x, p) = [x \ p + 1]^T$, jump set $D = \{x \in \mathbb{R}^2 \mid x_1 = 0\} \times \mathbb{N}$, and flow set given by $C := (\mathbb{R}^2 \setminus \{x \in \mathbb{R}^2 \mid x_1 = 0\}) \times \mathbb{N}$. Following the discussion in Example 3.3, the presence of arbitrarily small state perturbation can cause the hybrid system from missing the jump, and consequently, miss a count. In fact, in numerical simulations, state perturbations appear, among other things, due to the approximation of the value of the system state. However, it is likely that such pathology is not actually observed since in general, commercial numerical simulators, by default, use zero-crossing detection algorithms when performing computations. These algorithms usually include a memory

variable that keeps track of the side of the decision boundary in which the state is located. Such an algorithm can be modeled with the following hybrid system with the state space $O = \mathbb{R}^4$:

$$f(x, p, q) := \begin{bmatrix} x_2 \\ -x_1 \\ 0 \\ 0 \end{bmatrix}, C := \{(x, p, q) \in \mathbb{R}^2 \times \mathbb{N} \times \{-1, 1\} \mid x_1 q \geq 0\}$$

$$g(x, p, q) := \begin{bmatrix} x \\ p + 1 \\ -\text{sign}(x_1) \end{bmatrix}, D := \cup_{q \in \{-1, 1\}} (D_q \times \mathbb{N} \times \{q\})$$

where $\text{sign}(r) = -1$ if $r < 0$, 1 if $r > 0$, and $\{-1, 1\}$ if $r = 0$; $D_1 := \{x \in \mathbb{R}^2 \mid x_1 \geq 0, x_2 = 0\}$; and $D_{-1} := \{x \in \mathbb{R}^2 \mid x_1 \leq 0, x_2 = 0\}$. It follows that this hybrid system and its regularization coincide. Then, state perturbations do not affect the number of crosses of the x_1 -axis. Figure 3.6 illustrates solutions to \mathcal{H} and this hybrid system with state perturbations. \square



(a) Solutions with state perturbations may miss counts when state perturbations are present.

(b) Solutions with robust zero-crossing detection: flows are not possible any longer once the jump set is crossed, which forces q to jump and register a count.

Figure 3.6. Solutions to zero-crossing detection system in Example 3.12.

3.3 Measurement noise in feedback control

In general feedback control systems, hybrid or not, *measurement noise* enters the system not as a state perturbation affecting every occurrence of the state in the equations of motion, but only through feedback. More specifically, given a general nonlinear control system $\dot{z} = \phi(z, u)$ and a feedback mapping $u = \kappa(z)$ (certain control objectives require the use of discontinuous feedback κ), measurement noise enters the closed loop $\dot{z} = \phi(z, \kappa(z))$ through the feedback, leading to differential equations like $\dot{z} = \phi(z, \kappa(z + e))$. When the feedback is hybrid, or when the control system is hybrid to begin with, the measurement error can also interplay with the flow sets, jump sets, and the jump map. Some of this is illustrated in the following example.

Example 3.13 (robust stabilization and measurement noise) Consider a simple control system $\dot{z} = u$ with $z \in \mathbb{R}$, $u \in [-1, 1]$. The goal is to robustly stabilize the set consisting of two points: $\mathcal{A} = \{0, 6\}$ via feedback. Let $\text{sat} : \mathbb{R} \rightarrow [-1, 1]$ be the standard saturation function, that is

$$\text{sat}(u) = -1 \text{ if } u < -1, \quad \text{sat}(u) = u \text{ if } u \in [-1, 1], \quad \text{sat}(u) = 1 \text{ if } u > 1.$$

A nonhybrid feedback that results in asymptotic stability of \mathcal{A} for the closed loop $\dot{z} = k(z)$, and that closed-loop system are described below:

$$\dot{z} = k(z) := \begin{cases} -\text{sat}(z) & \text{if } z \leq 3 \\ -\text{sat}(z - 6) & \text{if } z > 3 \end{cases}.$$

Note that this k is discontinuous at $z = 3$, and because of this, the resulting asymptotic stability is not robust to measurement noise. Indeed, for arbitrarily small $\varepsilon > 0$, the unique solution from 3 to $\dot{z} = k(z + e)$ with $e(t) := \varepsilon \cos(\pi t / \varepsilon)$ is a see-saw function oscillating between $3 - \varepsilon$ and $3 + \varepsilon$ with period 2ε . The uniform limit of such see-saw functions is a constant function $z(t) = 3$ for all $t \in \mathbb{R}_{\geq 0}$. Of course, the nonrobustness of asymptotic stability can be detected by looking for Krasovskii solutions to $\dot{z} = k(z)$. These are the solutions to the differential inclusion $\dot{z} \in K(z)$, where K differs from k only at the point of discontinuity of k , that is, $K(3) = [-1, 1]$. Obviously, 3 is an equilibrium of $\dot{z} \in K(z)$. (And so the constant function $z(t) = 3$ is a Krasovskii solution to $\dot{z} = f(z)$, and equivalently, a Hermes solution. That the constant function is a Hermes solution can be seen directly, as it is the uniform limit, as $\varepsilon \searrow 0$, of the see-saw functions constructed above.)

Asymptotic stability of \mathcal{A} that is robust to measurement noise can be accomplished by hybrid feedback. One possible approach is based on hysteresis, with the hybrid feedback involving an additional logic variable $q \in \{1, 2\}$. To make an analogy with the nonhybrid feedback analyzed above, the logic variable will, in a sense, keep track of whether $z \leq 3$ or $z > 3$, and will prohibit switching between these two instances too often. More specifically, the hybrid feedback will set $u = -\text{sat}(z)$ if the logic variable q equals 1 and $z \leq 4$, and will set $u = -\text{sat}(z - 6)$ if $q = 2$ and $z \geq 2$. If neither of the conditions is met, the logic variable q will be toggled. In closed loop, this leads to a hybrid system \mathcal{H} in \mathbb{R}^2 with the flow and jump sets

$$C = (-\infty, 4] \times \{1\} \cup [2, \infty) \times \{2\}, \quad D = (4, \infty) \times \{1\} \cup (-\infty, 2) \times \{2\},$$

and the flow and jump equations given by

$$\dot{z} = f(z, q) := \begin{cases} -\text{sat}(z) & \text{if } (z, 1) \in C \\ -\text{sat}(z - 6) & \text{if } (z, 2) \in C \end{cases}, \quad q^+ = g(q) = 3 - q.$$

The logic variable q remains constant during flow, and the state z remains constant during jumps. Figure 3.7 depicts the flow and jump sets and two solutions. It is easy to verify that solutions $x = (z, q)$ to \mathcal{H} jump at most once, the maximal ones are complete, and the set $\mathcal{A} \times \{1, 2\}$ is globally uniformly asymptotically stable. The solutions are also unique for any initial condition. The uniqueness would no longer be true if the jump set D was replaced by its closure. Indeed, then a solution from $(4, 1)$ could only flow (with z converging to 0) or jump first (with q changing from 1 to 2) and then flow (with z converging to 6). Similar nonuniqueness would also occur from $(2, 2)$. Still, such nonuniqueness does not affect asymptotic stability.

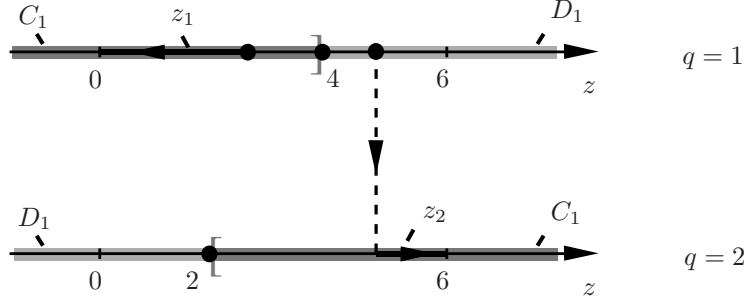


Figure 3.7. Sets $C := (C_1 \times \{1\}) \cup (C_2 \times \{2\})$, $D := (D_1 \times \{1\}) \cup (D_2 \times \{2\})$ for the robust feedback controller in Example 3.13.

For robustness analysis of \mathcal{H} , it is natural to only consider measurement noise affecting z and not q . This suggests considering (c.f. (3.1)) the following system:

$$\begin{cases} \dot{z} = f(z + e) & (z + e, q) \in C \\ q^+ = g(q) & (z + e, q) \in D. \end{cases} \quad (3.6)$$

It can be verified that if $e : \mathbb{R}_{\geq 0} \rightarrow [-\varepsilon, \varepsilon]$ with $\varepsilon < 2$, solutions to (3.6) converge to the set $[-\varepsilon, \varepsilon] \times \{1, 2\}$ and a bound as required by global asymptotic stability also exists. (Solutions to (3.6) may either only flow, instantly jump from the initial state and then only flow – these two behaviors are the same as for the system without noise – or flow for at most ε amount of time before jumping and then flowing forever.) Considering arbitrarily small ε suggests that practical stability of $\mathcal{A} \times \{1, 2\}$ is preserved. Certainly, the behavior that appeared when measurement noise affected the nonhybrid feedback – a constant solution remaining at the initial state 3 – is not possible for the proposed hybrid feedback.

However, the very existence of solutions to (3.6) may still be an issue, as alluded to above Proposition 3.7. Indeed, for the initial condition $(4, 1)$ and measurement noise $e(0) = -\varepsilon$, $e(t) = \varepsilon$ for $t > 0$, there are no solutions to (3.6). Following Proposition 3.7, robust existence can be guaranteed by altering the data so that the flow set and the jump set overlap. This can be done without affecting the asymptotic stability and its robustness. For example, it is sufficient to alter the jump set to be

$$C = (-\infty, 5] \times \{1\} \cup [1, \infty) \times \{2\}.$$

This introduces nonuniqueness, even in the absence of measurement noise: from any point in $(4, 5] \times \{1\} \cup [1, 2) \times \{2\}$ there exists a solution that only flows and a solution that jumps first. However, asymptotic stability is preserved, it is robust to measurement noise as discussed above, and existence of solutions to (3.6) is guaranteed for $e : \mathbb{R}_{\geq 0} \rightarrow [-\varepsilon, \varepsilon]$ with $\varepsilon < 1$. \square

In general, application of hybrid feedback to a nonlinear control system $\dot{z} = \phi(z, u)$ can lead, in the closed loop, to a hybrid system of the kind

$$\mathcal{H}^c : \quad x \in O \quad \begin{cases} \dot{x} \in F(x, \kappa_c(x)) & x \in C \\ x^+ \in G(x, \kappa_d(x)) & x \in D, \end{cases}$$

with the state x including the original state z and other variables as well, for example a discrete variable q as it was the case in Example 3.13, or a timer variable, as it is the case in sample-and-hold control. For such a system, it may be natural to consider F and G quite regular, but allow discontinuous “feedbacks” κ_c, κ_d .

Assuming that the measurement error enters \mathcal{H}^c through the mappings κ_c, κ_d and also affects the flow and the jump sets, leads to the system

$$\mathcal{H}_e^c : \quad x + e \in O \quad \begin{cases} \dot{x} & \in F(x, \kappa_c(x + e)) & x + e \in C \\ x^+ & \in G(x, \kappa_d(x + e)) & x + e \in D . \end{cases}$$

Two notions of generalized solutions to \mathcal{H}^c above can be considered, paralleling the notions of Hermes solutions and Krasovskii solutions in Definitions 3.9 and 3.10. *Control Hermes solutions* can be defined as limits of sequences of solutions to \mathcal{H}_e^c generated with sequences of measurement noise vanishing in the limit.

Definition 3.14 (Control Hermes solutions to hybrid systems) *A compact hybrid arc x is a compact control Hermes solution to \mathcal{H} if there exist a sequence $\{x_i\}_{i=1}^\infty$ of hybrid arcs and a sequence $\{e_i\}_{i=1}^\infty$ of admissible state perturbations such that*

- x_i is a solution to \mathcal{H}_{e_i} (with flow map condition $F(x, \kappa_c(x + e))$ and jump map condition $G(x, \kappa_d(x + e))$) with state perturbation e_i for each $i \in \mathbb{N}$;
- for each $\varepsilon > 0$ there exists i_0 such that for all $i > i_0$, x_i and x are (τ, ε) -close, where $\tau = \text{length}(x)$;
- the sequence of $\sup_{(t,j) \in \text{dom } e_i} |e_i(t, j)|$ converges to 0.

A hybrid arc x is a control Hermes solution to \mathcal{H} if the restriction of x to each compact subset of $\text{dom } x$ that is a hybrid time domain is a compact control Hermes solution to \mathcal{H} .

Control Krasovskii solutions can be defined as just Krasovskii solutions, as in Definition 3.9. (While a seemingly different approach would be to consider $\dot{x} \in \cap_{\delta > 0} \overline{\text{co}}F(x, \kappa_c((x + \delta\mathbb{B}) \cap C))$ and a similarly defined jump equation, mild regularity – including continuity – of F and just local boundedness – but not continuity – of κ_c make such an approach lead to Krasovskii solutions.) Equivalences between control Hermes and Krasovskii solutions to \mathcal{H}^c as in Theorem 3.11 can be also shown. This is stated below.

Corollary 3.15 (control Hermes and Krasovskii solutions to hybrid systems) *Let $\mathcal{H} = (O, f, C, g, D)$ be a hybrid system with set $O \subset \mathbb{R}^n$ open; sets C and D subsets of O ; function $f : O \times \mathbb{R}^{m_c} \rightarrow \mathbb{R}^n$ locally Lipschitz continuous in the first argument, locally uniformly in the second argument¹. ; function $g : O \times \mathbb{R}^{m_d} \rightarrow O$ continuous in the first argument, locally uniformly in the second argument; and functions $\kappa_c : C \rightarrow \mathbb{R}^{m_c}$, $\kappa_d : D \rightarrow \mathbb{R}^{m_d}$ locally bounded on O . Then a hybrid arc x is a control Hermes solution to \mathcal{H}^c if and only if it is a Krasovskii solution to \mathcal{H}^c .*

The following feedback control examples illustrate the relevance of generalized solutions in robust stabilization.

Example 3.16 (impulsive and reset control systems) State-dependent impulsive systems are dynamical systems with states that jump when a condition of the state is satisfied, and flow otherwise. State-dependent impulsive systems are generally modeled as

$$\begin{aligned} \dot{x} &= f(x) := f_c(x) & x \notin \mathcal{M} \\ x^+ &= g(x) := x + f_d(x) & x \in \mathcal{M} \end{aligned}$$

¹A function $h : O \times \mathbb{R}^m \rightarrow \mathbb{R}^n$ is continuous (locally Lipschitz continuous) in the first argument, locally uniformly in the second argument if for each $z \in O$, each compact $U \subset \mathbb{R}^m$, and each $\varepsilon > 0$ there exists $\delta > 0$ ($K > 0$) such that $|x - z| < \delta$ implies $|h(x, u) - h(z, u)| < \varepsilon$ ($x, y \in (z + \varepsilon\mathbb{B}) \cap O$ implies $|h(x, u) - h(y, u)| \leq K|x - y|$) for all $u \in U$.

where the function f_c defines the continuous dynamics, the function f_d defines the discrete dynamics, and \mathcal{M} is the reset set. In most applications, the reset set \mathcal{M} defines a surface in \mathbb{R}^n . A particular case of a state-dependent impulsive system is reset control systems. A reset controller is a linear system with the property that has its output reset to zero whenever its input and output satisfy certain algebraic condition.

Among several models for reset control systems, the following model has been widely used

$$\dot{x} = f(x) := A_{cl}x + B_{cl}d \quad x \notin \mathcal{M} \quad (3.7)$$

$$x^+ = g(x) := A_R x \quad x \in \mathcal{M} \quad (3.8)$$

where $\mathcal{M} := \{x \in \mathbb{R}^n \mid C_{cl}x = 0, (I - A_R)x \neq 0\}$; A_{cl}, B_{cl}, C_{cl} are the closed-loop system matrices; A_R is the reset control matrix; x is the state of the system; and d is an exogenous signal.

State-dependent impulsive systems, and in particular, reset control systems, are hybrid systems that can be modeled with data (O, f, C, g, D) where the jump set is given by $D := \mathcal{M}$ and the flow set is given by $C := \mathbb{R}^n \setminus D$. It follows from the definition of \mathcal{M} that the flow set corresponds to almost every point in the state space. Given a state-dependent impulsive system \mathcal{H} , its Krasovskii regularization $\widehat{\mathcal{H}} = (O, \widehat{F}, \widehat{C}, \widehat{G}, \widehat{D})$ with $O = \mathbb{R}^n$ has $\widehat{F} \equiv f$, $\widehat{G} \equiv g$, $\widehat{C} = \mathbb{R}^n$, and $\widehat{D} = D$. Since the flow set is the entire state space, there exist Krasovskii solutions to \mathcal{H} that never jump. It follows by Theorem 3.11 that there exist Hermes solutions to \mathcal{H} that never jump. In fact, it is easy to construct a convergent sequence of solutions to \mathcal{H} with vanishing measurement noise that never hits D . Such a limiting solution, a Hermes solution to \mathcal{H} , is indeed captured in the Krasovskii regularization of \mathcal{H} above.

Generally, the reset control system in (3.7)-(3.8) is implemented and simulated with a zero-cross detection (ZCD) algorithm (like the one in Example 3.12) that does not miss the jumps in the presence of noise (for example, in Matlab/Simulink, one usually uses special blocks like ‘‘Compare to zero’’, ‘‘Hit crossing’’, etc.). An alternative approach, which does not involve extending the state space, corresponds to thickening the jump set in order to obtain robustness. (Cf. Example 3.17.) \square

Example 3.17 (switching on surfaces) In many robotics applications, navigation algorithms for mobile robots are designed by switching between several feedback laws when the state of the system hits a switching surface. For example, consider the scenario where it is desired to steer a vehicle in the plane from its initial location to a target while avoiding an obstacle. The following hysteresis-type switching scheme is proposed. As depicted in Figure 3.8, the basic idea is to define two sets given by circles, D_0 and D_1 , and design control laws, κ_0 and κ_1 , so that when κ_0 is applied, the vehicle approaches the target, while when κ_1 is applied, the vehicle is driven away from the obstacle.

Without changing the control strategy described above, we write the closed-loop system as a hybrid system, let $q \in Q := \{0, 1\}$ be a set of modes, $z \in \mathbb{R}^2$ the position of the vehicle, and $\dot{z} = f'(z, u)$ the dynamics of the vehicle with input $u \in \mathbb{R}^2$. Let x be the vector resulting from stacking z and q . The closed-loop hybrid system is given by

$$\begin{aligned} \dot{x} &= f(x) := \begin{bmatrix} f'(z, \kappa_q(z)) \\ 0 \end{bmatrix} & x \notin D_q \times \{q\} \\ x^+ &= g(x) := \begin{bmatrix} z \\ 1 - q \end{bmatrix} & x \in D_q \times \{q\} . \end{aligned}$$

Denote this hybrid system by $\mathcal{H} = (O, f, C, g, D)$ where $C := \cup_{q \in Q} (\mathbb{R}^2 \setminus D_q) \times \{q\}$, $D := \cup_{q \in Q} (D_q \times \{q\})$, and $O := \mathbb{R}^3$. It follows that the Krasovskii regularization of \mathcal{H} , denoted by $\widehat{\mathcal{H}} = (O, \widehat{F}, \widehat{C}, \widehat{G}, \widehat{D})$, has data given by $\widehat{f} \equiv f$, $\widehat{g} \equiv g$, $\widehat{C} = \mathbb{R}^2 \times Q$, and $\widehat{D} = D$. Since for each $q \in Q$, the set \widehat{C} allows flows for every $z \in \mathbb{R}^2$, there exist Krasovskii solutions to \mathcal{H} that never jump. Then, Theorem 3.15 and the definition of control Hermes solutions imply that there exist solutions influenced by arbitrarily small measurement noise that either crash into the

obstacle or miss the target. For example, suppose that initially the controller is in mode $q = 0$ and consequently, it is driven towards the target. If it gets close to the set D_0 , (arbitrarily small) noise in the measurement of the position of the robot can prevent the controller from detecting that D_0 was hit and cause the vehicle to crash into the obstacle. A similar argument shows that under (arbitrarily small) measurement noise, the controller can miss the jump at the set D_1 , and thus, cause the vehicle to miss the target. All of the possible control Hermes/Krasovskii solutions, including the one that actually reaches the target with two jumps, are depicted in Figure 3.8.

Note that the nonrobustness phenomenon in this example is not due to the existence of an obstacle itself; it is due to the fact that the control strategy switches when the state z belongs to either of the surfaces D_0 and D_1 , switching condition that is vulnerable to small measurement noise in z . A possible modification of \mathcal{H} to accomplish the task robustly is to replace D_0 by the closed disk that it defines and D_1 by its (closed) complement, and take $C := \cup_{q \in Q} (C_q \times \{q\})$, $C_q = (\mathbb{R}^2 \setminus D_q)$ for each $q \in Q$, as shown in Figure 3.9. This implementation is an alternative to the zero-crossing detection used in Example 3.12. It has the features that no extra states are introduced, solutions exist from every initial condition (except those starting on the obstacle), and the data meets the regularity requirements.

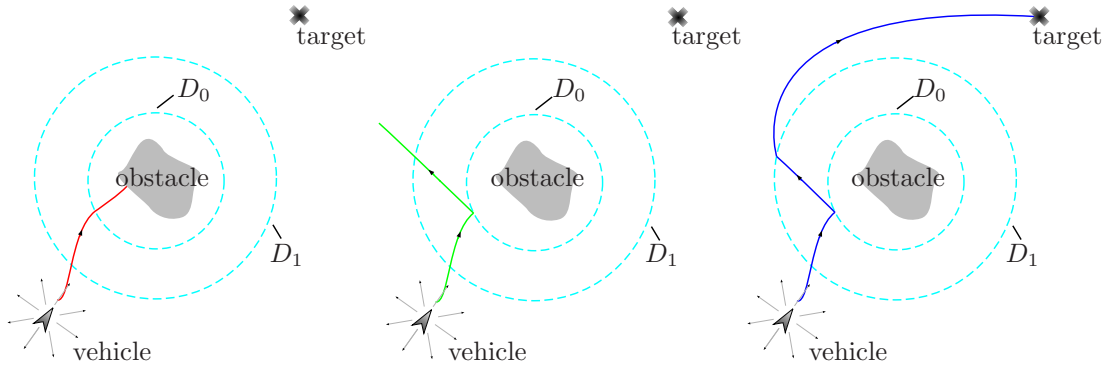


Figure 3.8. Steering a vehicle to its target; a hybrid closed-loop system with logic variables. The circles represent the switching surfaces for the control strategy. The three different control Hermes/Krasovskii solutions in Example 3.17 are depicted: 1) the vehicle crashes into the obstacle; 2) the vehicle avoids the obstacle but does not acquire the target; 3) the vehicle avoids the obstacle and acquires the target.

□

3.4 Regular hybrid systems

The examples in Section 3.1, 3.2, and 3.3 show the effect of the properties of the data in the set of solutions to hybrid systems. Theorem 3.11 (and Corollary 3.15 for the feedback control case) shows that the set of solutions to $\hat{\mathcal{H}}$ contains the limiting solutions obtained with vanishing state perturbations to \mathcal{H} . Such a result is only possible due to the properties of the data $(O, \hat{F}, \hat{C}, \hat{G}, \hat{D})$ of the regularized hybrid system $\hat{\mathcal{H}}$. In general, given a hybrid system, if its data satisfy the same regularity properties as the data of $\hat{\mathcal{H}}$ does, then it is said that \mathcal{H} satisfies the *hybrid basic conditions* introduced below.

Before that, the following concepts should be introduced. The set S , subset of an open set $O \subset \mathbb{R}^n$, is closed relative to O if $S = \bar{S} \cap O$. A set-valued mapping $\phi : S \rightrightarrows \mathbb{R}^n$, where $S \subset O$, is outer semicontinuous relative to S if for any $x \in S$ and any sequence $\{x_i\}_{i=1}^{\infty}$ with $x_i \in S$, $\lim_{i \rightarrow \infty} x_i = x$ and any sequence $\{y_i\}_{i=1}^{\infty}$ with $y_i \in \phi(x_i)$ and $\lim_{i \rightarrow \infty} y_i = y$ we have $y \in \phi(x)$.

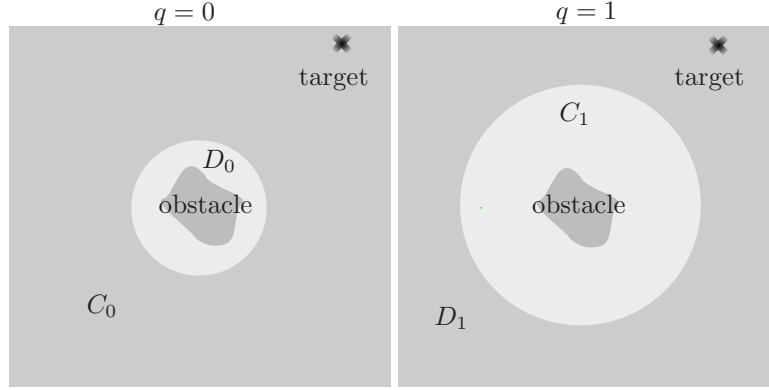


Figure 3.9. Modified flow and jump sets in Example 3.17 for $q = 0$ and $q = 1$. The jumps are enforced when the trajectories leave the set C_q for the current $q \in \{0, 1\}$. Solutions starting away from the obstacle converge to the target even in the presence of small measurement noise.

Definition 3.18 (hybrid basic conditions) *A hybrid system $\mathcal{H} = (O, F, C, G, D)$ satisfies the hybrid basic conditions if*

- (A0) $O \subset \mathbb{R}^n$ is an open set.
- (A1) C and D are relatively closed sets in O .
- (A2) $F : O \rightrightarrows \mathbb{R}^n$ is outer semicontinuous relative to C and locally bounded on O , and for all $x \in C$, $F(x)$ is nonempty and convex.
- (A3) $G : O \rightrightarrows O$ is outer semicontinuous relative to D and locally bounded on O , and for all $x \in D$, $G(x)$ is nonempty.

When a hybrid system does not satisfy the hybrid basic conditions, then the Krasovskii regularization in Definition 3.10 results in a hybrid system that satisfies them. (Note that this follows by construction.) When regularizing a la Krasovskii, the regularized maps \widehat{F}, \widehat{G} are “minimal” among all set-valued mappings possessing the properties in (A2), (A3) and such that $F(x) \in \widehat{F}(x)$ for all $x \in C$, $G(x) \subset \widehat{G}(x)$ for all $x \in D$. Similarly, \widehat{C}, \widehat{D} are the smallest relatively closed subsets of O containing $C \cap O, D \cap O$, respectively.

A different motivation to hybrid systems satisfying the hybrid basic conditions comes from the point of view of the properties of solutions. In particular, a structural property needed to extend classical stability analysis tools to the hybrid setting, like the stability theorems and invariance principles in the next chapter, is the following: for every given sequence of bounded solutions, there exists a subsequence that converges to a solution. For hybrid systems, such a property only holds when the hybrid basic conditions are satisfied. The result below, extracted from the literature², states such a property for solutions to hybrid systems.

A sequence $\{x_i\}_{i=1}^{\infty}$ of solutions is *locally eventually bounded* with respect to O if for any $m > 0$, there exists $i_0 > 0$ and a compact set $K \subset O$ such that for all $i > i_0$, all $(t, j) \in \text{dom } x_i$ with $t + j < m$, $x_i(t, j) \in K$.

Theorem 3.19 (sequential compactness) *Given a hybrid system \mathcal{H} satisfying the hybrid basic conditions, let $x_i : \text{dom } x \rightarrow O$, $i = 1, 2, \dots$, be a locally eventually bounded (with respect to O) sequence of solutions to \mathcal{H} . Then there exists a subsequence of solutions $\{x_i\}_{i=0}^{\infty}$ which as graphs (with the graphic metric in Definition 3.8), converges to a solution to \mathcal{H} .*

²See Theorem 4.4 in [39].

3.5 Summary

The concept of solution to hybrid systems with admissible state perturbations was introduced. Several examples illustrated the effect of this perturbation in the system behavior. Solutions obtained as the limit of solutions with admissible state perturbation with size converging to zero were defined as Hermes solutions. It was shown that these solutions are captured by the solutions to a regularized hybrid system, denoted by $\widehat{\mathcal{H}}$, with data regularized through a “closure” operation. This regularization and the solutions to the resulting system are called Krasovskii. Furthermore, it is shown that every Krasovskii solutions is a Hermes solution. A similar result holds for a general hybrid feedback control case. Finally, the hybrid basic conditions for the data of hybrid systems were introduced after their motivation from a robustness to state perturbations such as measurement noise.

3.6 Notes and references

The effect of measurement noise when solutions are taken as CADLAG solutions or executions (see Section 2.7) is more notorious. This is due to these concepts of solutions not behaving well under graphical convergence.

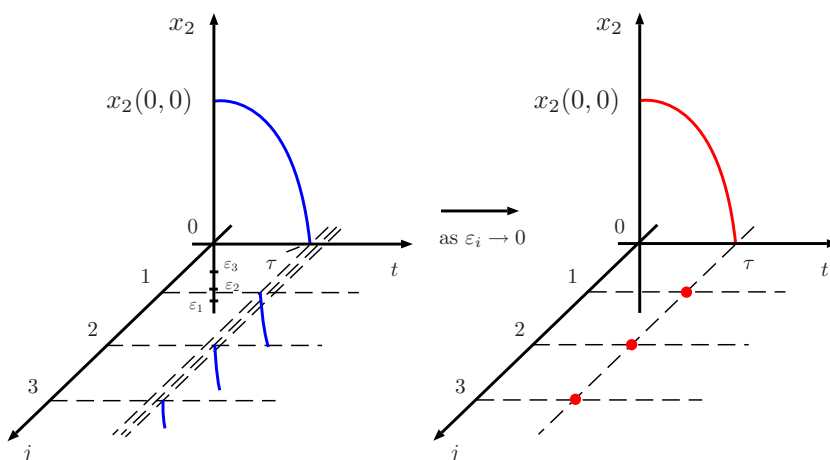


Figure 3.10. Convergence of solutions to the hybrid system in Example 3.20 when the noise approaches zero. The value of the noise e at the i -th jump is given by $(0, \varepsilon_i)$ where $\varepsilon_i \rightarrow 0$ as $i \rightarrow \infty$. The limiting function is not a CADLAG solution.

Example 3.20 (rotate and dissipate, revisited) Consider the system \mathcal{H} from Example 2.8. Let x be a CADLAG solution from ξ with $0 < |\xi| < 1$ and $\xi \notin D$. Let τ be the first time when $x(\tau) \in D$ and consider the noise $e(t) = (0, 0)$ if $t \leq \tau$, $e(t) = (0, \varepsilon)$ for $t > \tau$. Then, one CADLAG solution x to $\dot{x} = f(x + e)$, $x + e \in C$ with jumps governed by $x^+ = g(x^- + e^-)$, $x^- + e^- \in D$ will jump at τ and then again when $x_2 = -\varepsilon$ since by definition of e , after the first jump at τ there exists $\tau' > \tau$ at which $x(\tau') + e(\tau') \in D$. This way, one can generate sequences of hybrid arcs x_i from ξ and noise signals e_i such that x_i is a solution to \mathcal{H}_{e_i} with admissible measurement noise e_i , such that x_i that rotates to D , and then jumps infinitely many times, with jumps separated by less than $1/i$ amount of time. The graphical limit x of such x_i 's flows to D and then jumps infinitely many times. Figure 3.10 illustrates this limiting process. Of course, such x does not correspond to a CADLAG solution. It is an execution, though. However, if one considers a sequence of x_i 's as above, but with initial points on the line $x_1 = x_2$ and converging to $(0, 0)$, the graphical limit is a discrete solution: it jumps

infinitely many times from $(0, 0)$ to $(0, 0)$ with no intervals of flow. While such limit is a hybrid arc, it is not an execution of \mathcal{H} since $(0, 0) \notin D$. By definition, it is a Hermes solution. \square

The following example connects the regularization of the hybrid systems introduced in this chapter with Example 2.8 and the example above.

Example 3.21 (rotate and dissipate, re-revisited) Consider the system \mathcal{H} from Example 2.8. The regularized hybrid system $\widehat{\mathcal{H}}$ with $O = \mathbb{R}^2$ has data given by $\widehat{C} = \mathbb{R}^2$, $\widehat{D} = [0, 1] \times \{0\}$, while $\widehat{f} \equiv f$, $\widehat{g} \equiv g$. In particular, there exists a discrete Krasovskii solution given by $x(0, j) = [0 \ 0]^T$ for all $j \in \mathbb{N}$. As we noted in Example 3.20, this is also a Hermes solution to \mathcal{H} , but is not an execution of \mathcal{H} . Another way that Krasovskii solutions differ from executions is that there are Krasovskii solutions from initial points ξ with $|\xi| = 1$ that flow and then jump (as $[1 \ 0]^T \in \widehat{D}$) while the unique execution from ξ only flows. \square

The regularization for F follows the Krasovskii regularization for discontinuous right-hand sides introduced in [55] (see also [42]). It differs from the Filippov’s regularization [36] as this ignores the behavior of the right-hand side on sets of measure zero. Such a regularization technique proves to be unsuitable for hybrid systems (and even for constrained differential equations). Indeed, for example, a set C with zero measure leads to an “empty” regularization. For further details on the relationship of regularized to unregularized right-hand sides see [36], [44], [55], and [42]. Regarding G , the regularization follows the one used in [52] for single-valued right-hand sides; due to the nature of discrete time, the convexification is not needed.

Theorem 3.11 and Corollary 3.15 are generalizations to the hybrid setting of a result for differential equations initially reported by Hermes in [44] and expanded upon by Hájek in [42] and a result by Coron and Rosier [31] given in the context of robust stabilization of nonlinear control systems (with non-hybrid feedback), respectively. As a special case, they subsume analogous results for difference equations. These generalizations are enabled both by the novel concept of solution to hybrid systems and the use of graphical convergence, rather than pointwise, of sequences of solutions.

To be consistent with what is encountered in hybrid feedback control design, the equivalence result in Corollary 3.15 did not allow for the control functions κ_c and κ_d to be set valued. However, this can be easily adjusted to account for a set-valued version of this functions. Similarly, Theorem 3.11 can be adjusted to allow for a set-valued flow map.

One of the earliest references dealing with impulsive systems as in Example 3.16 is the work by Bainov and Simeonov [11]. The general model in that example follows the model in [25]. Regarding reset control systems, the first reset integrator was introduced in [29] in order to improve the performance of linear systems. Subsequent efforts in studying the stability properties of reset control include [56], [12], [106]. The particular model for reset control systems in Example 3.16 follows the model in [12].

Example 3.6 is borrowed from [52]. Example 3.13 was suggested by Rafal Goebel.

The robotic problem and hysteresis control strategy in Example 3.17 was taken from [13, Section 3].

Theorem 3.19 appeared as Theorem 4.4 in [39]. The proofs of Theorem 3.11 and Corollary 3.15 can be found in Section B.1.

Chapter 4

Stability and Invariance

In this chapter, stability theorems and invariance principles for hybrid systems are developed. These results provide a methodical procedure to establish stability and asymptotic stability of compact sets, and to obtain information about the convergence properties of solutions to hybrid systems. Examples throughout the chapter illustrate the concepts and results.

4.1 Stability

4.1.1 Definitions

The concept of stability for hybrid systems \mathcal{H} is now introduced. They parallel the standard notions for continuous and discrete-time systems. The prefix “pre” in the definitions below is used to indicate that maximal solutions, that is, the elements in $\mathcal{S}_{\mathcal{H}}$, are not necessarily complete. In fact, in the case that every maximal solution is complete, the prefix “pre” can be dropped. For instance, this is the case when in addition to (A0)-(A4), it is true that (VC) (see Proposition 2.7) and

(VD) for each $\xi \in D$, $G(\xi) \subset C \cup D$

hold. (Under conditions (VC) and (VD), any maximal solution to \mathcal{H} is either complete or eventually leaves any compact subset of O .)

Definition 4.1 (stability) *For a hybrid system \mathcal{H} , given a compact set \mathcal{A} , subset of the state space O ,*

- \mathcal{A} is pre-stable for \mathcal{H} if for each $\varepsilon > 0$ there exists $\delta > 0$ such that any solution x to \mathcal{H} with $|x(0, 0)|_{\mathcal{A}} \leq \delta$ satisfies $|x(t, j)|_{\mathcal{A}} \leq \varepsilon$ for all $(t, j) \in \text{dom } x$;
- \mathcal{A} is pre-attractive for \mathcal{H} if there exists $\delta > 0$ such that any solution x to \mathcal{H} with $|x(0, 0)|_{\mathcal{A}} \leq \delta$ is bounded with respect to O and if it is complete then $x(t, j) \rightarrow \mathcal{A}$ as $t + j \rightarrow \infty$;
- \mathcal{A} is pre-asymptotically stable if it is both pre-stable and pre-attractive;
- \mathcal{A} is asymptotically stable if it is pre-asymptotically stable and there exists $\delta > 0$ such that any maximal solution x to \mathcal{H} with $|x(0, 0)|_{\mathcal{A}} \leq \delta$ is complete.

The set of all $x \in C \cup D$ from which all solutions are bounded with respect to O and the complete ones converge to \mathcal{A} is called the *pre-basin of attraction* of \mathcal{A} . This set is denoted by $\mathcal{B}_{\mathcal{A}}^p$. At times, the stability properties defined above will hold relative to a subset K of the state space, that is, they will hold when the solutions to \mathcal{H} stay in that set, i.e., $\text{rge } x \subset K$.

4.1.2 Lyapunov theorems

Throughout this chapter, it is assumed that hybrid systems \mathcal{H} satisfy the hybrid basic conditions.

Sufficient conditions for pre-asymptotic stability are given in terms of functions V , which will be called *Lyapunov functions*, satisfying certain conditions. Let $V : O \rightarrow \mathbb{R}$ be continuous on O and locally Lipschitz on a neighborhood of C . Let x be any solution to the hybrid system \mathcal{H} , and let $(\underline{t}, \underline{j}), (\bar{t}, \bar{j}) \in \text{dom } x$ be such that $(\underline{t}, \underline{j}) \preceq (\bar{t}, \bar{j})$. Let $t(j)$ denote the least time t such that $(t, j) \in \text{dom } x$, and $j(t)$ denote the least index j such that $(t, j) \in \text{dom } x$. The increment $V(x(\bar{t}, \bar{j})) - V(x(\underline{t}, \underline{j}))$ is given by

$$\int_{\underline{t}}^{\bar{t}} \frac{d}{dt} V(x(t, j(t))) dt + \sum_{j=\underline{j}+1}^{\bar{j}} [V(x(t(j), j)) - V(x(t(j), j-1))] . \quad (4.1)$$

This expression takes into account the “continuous increment” due to the integration of the time derivative of $V(x(t, j))$ and the “discrete increment” due to the difference in V before and after the jump. The integral above expresses the desired quantity since $t \mapsto V(x(t, j(t)))$ is locally Lipschitz and absolutely continuous on every interval on which $t \mapsto j(t)$ is constant.

Conditions for stability of compact sets will be given in terms of functions $u_C(x)$ and $u_D(x)$ constructed from V . The function u_C will bound the “derivative” of V at x in directions belonging to $F(x)$, while the function u_D will bound the difference between V at x and at points belonging to $G(x)$.

The function $u_C : O \rightarrow [-\infty, \infty)$ is given by

$$u_C(x) := \begin{cases} \max_{v \in F(x)} \max_{\zeta \in \partial V(x)} \langle \zeta, v \rangle & x \in C \\ -\infty & \text{otherwise} \end{cases} \quad (4.2)$$

where $\partial V(x)$ is the generalized gradient (in the sense of Clarke) of V at $x \in C$. It is a closed, convex, and nonempty set equal to the convex hull of all limits of sequences $\nabla V(x_i)$ where x_i is any sequence converging to x while avoiding an arbitrary set of measure zero containing all the points at which V is not differentiable (as V is locally Lipschitz, ∇V exists almost everywhere).

This function can be used to bound the increase of V along solutions to the hybrid system. In fact, for any solution to the hybrid system, and any t where $\frac{d}{dt} V(x(t, j(t)))$ exists, it follows that

$$\frac{d}{dt} V(x(t, j(t))) \leq u_C(x(t, j(t))).$$

This follows by the fact that u_C is equal to the (Clarke) generalized directional derivative of V at x in the direction of v (One of its basic properties is that for any solution $z(\cdot)$ to $\dot{z}(t) \in F(z(t))$, $\frac{d}{dt} V(z(t)) \leq V^\circ(z(t), \dot{z}(t))$ for almost all t . Note that as V is locally Lipschitz, the derivative on the left above can be understood in the standard sense.)

To bound the “discrete increment” of V , the following quantity will be used:

$$u_D(x) := \begin{cases} \max_{\zeta \in G(x)} \{V(\zeta) - V(x)\} & x \in D \\ -\infty & \text{otherwise.} \end{cases} \quad (4.3)$$

Even without any regularity on V , one gets the bound

$$V(x(t_{j+1}, j+1)) - V(x(t_{j+1}, j)) \leq u_D(x(t_{j+1}, j))$$

for any solution to the hybrid system.

The following result corresponds to the main stability theorem.

Theorem 4.2 (hybrid Lyapunov theorem) *For a hybrid system \mathcal{H} , suppose that*

- (\star) $\mathcal{A} \subset O$ is compact, $\mathcal{U} \subset O$ is a neighborhood of \mathcal{A} , $V : O \rightarrow \mathbb{R}$ is continuous on O , locally Lipschitz on a neighborhood of C , and positive definite on $C \cup D$ with respect to \mathcal{A} , and u_C and u_D satisfy $u_C(z) \leq 0$, $u_D(z) \leq 0$ for all $z \in \mathcal{U}$.

Then \mathcal{A} is pre-stable. Suppose additionally that

$$u_C(z) < 0 \text{ and } u_D(z) < 0 \text{ for all } z \in \mathcal{U} \setminus \mathcal{A} .$$

Then \mathcal{A} is pre-attractive, and hence pre-asymptotically stable.

Note that this result recovers the classical Lyapunov stability theorem for purely continuous-time (discrete-time) systems when \mathcal{H} has only continuous (discrete) dynamics since there is no need to check the condition on u_D (u_C).

The following result states that when u_C (respectively, u_D) is negative in points near a compact set and discrete solutions (respectively, continuous solutions) converge to the compact set, then it is pre-asymptotically stable.

Theorem 4.3 (special case of Lyapunov theorem) *For the hybrid system \mathcal{H} , suppose that (\star) of Theorem 4.2 holds. Suppose that either*

- (a) $u_C(z) < 0$ for each $z \in \mathcal{U} \setminus \mathcal{A}$,
(b) any discrete solution x to \mathcal{H} with $\text{rge } x \subset \mathcal{U}$ converges to \mathcal{A} ;

or

- (a') $u_D(z) < 0$ for each $z \in \mathcal{U} \setminus \mathcal{A}$,
(b') any continuous solution x to \mathcal{H} with $\text{rge } x \subset \mathcal{U}$ converges to \mathcal{A} .

Then \mathcal{A} is pre-asymptotically stable.

The results above actually hold for any functions u_c, u_d such that

$$V(x(\bar{t}, \bar{j})) - V(x(\underline{t}, \underline{j})) \leq \int_{\underline{t}}^{\bar{t}} u_c(x(t, j(t))) dt + \sum_{j=\underline{j}+1}^{\bar{j}} u_d(x(t(j), j-1)) \quad (4.4)$$

holds along solutions x to \mathcal{H} for every $(\underline{t}, \underline{j}), (\bar{t}, \bar{j}) \in \text{dom } x$ such that $(\underline{t}, \underline{j}) \preceq (\bar{t}, \bar{j})$. Such generality, but in the context of invariance principles, is pursued in the next section.

4.2 Invariance

4.2.1 Preliminaries

The concept of invariance for hybrid systems is defined below. The prefix “weak” is used to indicate that the invariance notion involves only a particular solution to satisfy the invariance property, while the prefix “strong” is used to indicate that all solutions (from the set under analysis) need to satisfy the invariance property.

Definition 4.4 (invariance) *Given a hybrid system \mathcal{H} , the set $\mathcal{M} \subset O$ is said to be*

- *weakly forward invariant if for each $\xi \in \mathcal{M}$, there exists at least one complete solution $x \in \mathcal{S}_{\mathcal{H}}(\xi)$ with $x(t, j) \in \mathcal{M}$ for all $(t, j) \in \text{dom } x$;*
- *weakly backward invariant if for each $q \in \mathcal{M}$, $N > 0$, there exist $\xi \in \mathcal{M}$ and at least one solution $x \in \mathcal{S}_{\mathcal{H}}(\xi)$ such that for some $(t^*, j^*) \in \text{dom } x$, $t^* + j^* \geq N$, the solution satisfies $x(t^*, j^*) = q$ and $x(t, j) \in \mathcal{M}$ for all $(t, j) \preceq (t^*, j^*)$, $(t, j) \in \text{dom } x$;*
- *weakly invariant if it is both weakly forward invariant and weakly backward invariant;*
- *strong pre-forward invariant if for each $\xi \in \mathcal{M}$ and each $x \in \mathcal{S}_{\mathcal{H}}(\xi)$, it holds that $x(t, j) \in \mathcal{M}$ for all $(t, j) \in \text{dom } x$.*
- *strong forward invariant if it is strongly pre-forward invariant and each maximal solution starting in \mathcal{M} is complete.*

Definition 4.5 (Ω -limit set of a set) *Given a set $\mathcal{X} \subset O$, the Ω -limit set of \mathcal{X} for \mathcal{H} is given by*

$$\Omega_{\mathcal{H}}(\mathcal{X}) := \{y \in \mathbb{R}^n \mid y = \lim_{i \rightarrow \infty} x_i(t_i, j_i), x_i \in \mathcal{S}_{\mathcal{H}}(\mathcal{X}), (t_i, j_i) \in \text{dom } x_i, t_i + j_i \rightarrow \infty\} .$$

Ω -limit sets capture the asymptotic behavior of solutions to a dynamical system from an initial set.

Define, for each $i \in \mathbb{N}$,

$$\mathcal{R}_{\mathcal{H}}^i(\mathcal{X}) := \{y \in O \mid y = x(t, j), x \in \mathcal{S}_{\mathcal{H}}(\mathcal{X}), (t, j) \in \text{dom } x, t + j \geq i\} .$$

Note that if $i' > i$ then $\mathcal{R}_{\mathcal{H}}^{i'}(\mathcal{X}) \subset \mathcal{R}_{\mathcal{H}}^i(\mathcal{X})$. Because of this, a sequence of sets $\mathcal{R}_{\mathcal{H}}^i(\mathcal{X})$ is said to be *nested*. $\mathcal{R}_{\mathcal{H}}^i(\mathcal{X})$ corresponds to the reachable set of \mathcal{H} from \mathcal{X} for all $t + j \geq i$. It is related to $\Omega_{\mathcal{H}}(\mathcal{X})$ in the following lemma.

Lemma 4.6 ($\Omega_{\mathcal{H}}(\mathcal{X})$ characterization) *Let $\mathcal{X} \subset O$. Then¹*

$$\Omega_{\mathcal{H}}(\mathcal{X}) = \lim_{i \rightarrow \infty} \mathcal{R}_{\mathcal{H}}^i(\mathcal{X}) = \bigcap_i \overline{\mathcal{R}_{\mathcal{H}}^i(\mathcal{X})} . \quad (4.5)$$

Equivalently, for each $\varepsilon > 0$ and $\rho > 0$ there exists i^ such that for all $i \geq i^*$*

1. $\Omega_{\mathcal{H}}(\mathcal{X}) \cap \rho \overline{\mathbb{B}} \subset \mathcal{R}_{\mathcal{H}}^i(\mathcal{X}) + \varepsilon \overline{\mathbb{B}}$
2. $\mathcal{R}_{\mathcal{H}}^i(\mathcal{X}) \cap \rho \overline{\mathbb{B}} \subset \Omega_{\mathcal{H}}(\mathcal{X}) + \varepsilon \overline{\mathbb{B}}$.

¹A sequence of sets $S_i \subset \mathbb{R}^n$ converges to $S \subset \mathbb{R}^n$ (i.e. $\lim_{i \rightarrow \infty} S_i = S$) if for all $x \in S$ there exists a convergent sequence of $x_i \in S_i$ such that $\lim_{i \rightarrow \infty} x_i = x$ and, for any sequence of $x_i \in S_i$ and any convergent subsequence x_{i_k} , $\lim_{k \rightarrow \infty} x_{i_k} \in S$.

Proof. From the very definition of the outer limit of a sequence of sets, $\Omega_{\mathcal{H}}(\mathcal{X}) = \limsup_{i \rightarrow \infty} \mathcal{R}_{\mathcal{H}}^i(\mathcal{X})$. As the sequence $\mathcal{R}_{\mathcal{H}}^i(\mathcal{X})$ is nested, [79, Exercise 4.3] implies that the limit $\lim_{i \rightarrow \infty} \mathcal{R}_{\mathcal{H}}^i(\mathcal{X})$ exists, and by its definition, it equals

$$\limsup_{i \rightarrow \infty} \mathcal{R}_{\mathcal{H}}^i(\mathcal{X}) = \Omega_{\mathcal{H}}(\mathcal{X}) .$$

By Exercise 4.3b in [79], it follows that $\lim_{i \rightarrow \infty} \mathcal{R}_{\mathcal{H}}^i(\mathcal{X})$ is equal to $\bigcap_i \overline{\mathcal{R}_{\mathcal{H}}^i(\mathcal{X})}$. Theorem 4.10 in [79] implies the equivalent characterization of convergence of $\mathcal{R}_{\mathcal{H}}^i(\mathcal{X})$ to $\Omega_{\mathcal{H}}(\mathcal{X})$. \square

A concept that captures the asymptotic behavior of a particular complete solution is the Ω -limit set of the solution x .

Definition 4.7 (Ω -limit set of a solution) *Given a complete solution $x \in \mathcal{S}_{\mathcal{H}}$, its Ω -limit set, denoted $\Omega(x)$, is the set of all ω -limit points, that is, points $x^* \in O$ for which there exists an increasing and unbounded sequence $\{(t_i, j_i)\}_{i=1}^{\infty}$ in $\text{dom } x$ so that $\lim_{i \rightarrow \infty} x(t_i, j_i) = x^*$.*

Clearly, there are connections between Ω -limit sets of sets and ω -limit sets of solutions to hybrid systems. Such connections are not pursued here, but it is observed that

$$\bigcup_{\xi \in \mathcal{X}, x \in \mathcal{S}_{\mathcal{H}}(\xi)} \Omega(x) \subset \Omega_{\mathcal{H}}(\mathcal{X})$$

The opposite set containment does not necessarily hold.

The following type of solutions will be used in the invariance principles.

Definition 4.8 (precompact solutions) *A solution x to \mathcal{H} is precompact if it is both complete and bounded.*

The following result for precompact solutions, which characterizes the time elapsed between jumps under a condition on the jump map and jump set, will be combined with some of the special cases of the hybrid LaSalle's invariance principle in Section 4.2.3.

Lemma 4.9 (uniform bound on time between jumps) *Suppose that \mathcal{H} has data such that $D \cap G(D) = \emptyset$. Then, for any precompact $x \in \mathcal{S}_{\mathcal{H}}$ there exists $\gamma > 0$ such that $t_{j+1} - t_j \geq \gamma$ for all $j \geq 1$, $(t_j, j), (t_{j+1}, j) \in \text{dom } x$ (i.e. the elapsed time between jumps is uniformly bounded below by a positive constant).*

Proof. By local boundedness of F and precompactness of x , $F(\text{rge } x)$ is bounded, and thus for some $\delta > 0$, $|\dot{x}(t, j)| < \delta$ for all $(t, j) \in \text{dom } x$. Let $E := \bigcup_{j=0}^{J-1} (t_{j+1}, j)$ be the set of all points in $\text{dom } x$ at which a jump occurs (J can be finite or infinite). By precompactness of x , $\overline{x(E)} \subset O$ is compact. We have $x(E) \subset D$, and by (relative) closedness of D in O , $\overline{x(E)} \subset D$. By outer semicontinuity of G , $\overline{G(x(E))} \subset G(D)$ is closed, and since $\overline{x(E)} \cap \overline{G(x(E))} = \emptyset$, the distance between $\overline{x(E)}$ and $\overline{G(x(E))}$ is positive, say $\epsilon > 0$. In particular, for $j = 0, 1, 2, \dots, J-1$, the time interval between t_j and t_{j+1} is at least ϵ/δ (as the distance between $x(t_j, j)$ and $x(t_{j+1}, j)$ is at least ϵ). \square

4.2.2 Properties of Ω -limits sets

In what follows, various properties of $\Omega_{\mathcal{H}}(\mathcal{X})$ are shown. The assumption that the sets $\mathcal{R}_{\mathcal{H}}^i(\mathcal{X})$ are uniformly bounded with respect to O for large i will be used in some of the results below:

Assumption 4.10 ($\mathcal{R}_{\mathcal{H}}^i(\mathcal{X})$ assumption) *The set $\mathcal{X} \subset O$ is such that the hybrid system \mathcal{H} is eventually uniformly bounded from \mathcal{X} , i.e., there exist a compact set $K \subset O$ and a nonnegative integer i^* such that $\mathcal{R}_{\mathcal{H}}^i(\mathcal{X}) \subset K$ for all $i \geq i^*$.*

The next theorem asserts that, under Assumption 4.10, the properties of weak backward invariance and uniform attractivity from \mathcal{X} are generic for $\Omega_{\mathcal{H}}(\mathcal{X})$.

Theorem 4.11 (invariance property of $\Omega_{\mathcal{H}}(\mathcal{X})$) *Under Assumption 4.10, the set $\Omega_{\mathcal{H}}(\mathcal{X})$ is contained in O , compact, weakly backward invariant, and for each $\varepsilon > 0$ there exists i^* such that, for all $i \geq i^*$, $\Omega_{\mathcal{H}}(\mathcal{X}) \subset \mathcal{R}_{\mathcal{H}}^i(\mathcal{X}) + \varepsilon\overline{\mathbb{B}}$ and $\mathcal{R}_{\mathcal{H}}^i(\mathcal{X}) \subset \Omega_{\mathcal{H}}(\mathcal{X}) + \varepsilon\overline{\mathbb{B}}$. If, in addition, $\Omega_{\mathcal{H}}(\mathcal{X}) \subset \mathcal{R}_{\mathcal{H}}^0(\mathcal{X}) \cup \mathcal{X}$ then $\Omega_{\mathcal{H}}(\mathcal{X})$ is strongly pre-forward invariant.*

Proof. Since the sequence of sets $\mathcal{R}_{\mathcal{H}}^i(\mathcal{X})$ is nested, its limit exists and is given by (4.5). Then, $\Omega_{\mathcal{H}}(\mathcal{X})$ is closed. By Assumption 4.10, $\Omega_{\mathcal{H}}(\mathcal{X})$ is bounded with respect to O . Then, it follows that $\Omega_{\mathcal{H}}(\mathcal{X})$ is compact and a subset of O . By Assumption 4.10, using Theorem 4.10 in [79], for each $\varepsilon > 0$ there exists i^* such that, for all $i \geq i^*$, $\Omega_{\mathcal{H}}(\mathcal{X}) \subset \mathcal{R}_{\mathcal{H}}^i(\mathcal{X}) + \varepsilon\overline{\mathbb{B}}$ and $\mathcal{R}_{\mathcal{H}}^i(\mathcal{X}) \subset \Omega_{\mathcal{H}}(\mathcal{X}) + \varepsilon\overline{\mathbb{B}}$.

To show that $\Omega_{\mathcal{H}}(\mathcal{X})$ is weakly backward invariant, let $x^* \in \Omega_{\mathcal{H}}(\mathcal{X})$ be arbitrary (note that when $\Omega_{\mathcal{H}}(\mathcal{X}) = \emptyset$ there is nothing to check). By Assumption 4.10, there exists a compact set $K \subset O$ and a nonnegative index i^* such that $\mathcal{R}_{\mathcal{H}}^i(\mathcal{X}) \subset K$ for all $i \geq i^*$. We will not relabel this sequence and assume that $\mathcal{R}_{\mathcal{H}}^i(\mathcal{X}) \subset K$ for all $i > 0$. Then, with the definition of $\Omega_{\mathcal{H}}(\mathcal{X})$ in (4.5), there exists a sequence $x_i \in \mathcal{R}_{\mathcal{H}}^i(\mathcal{X})$ with $x_i \rightarrow x^*$ as $i \rightarrow \infty$. Let $N > 0$ be arbitrary. Then, for each $l = i - N$, $i > N$, there exists a sequence of solutions $\phi_l \in \mathcal{S}_{\mathcal{H}}(\mathcal{X})$ such that $\phi_l(t_i, j_i) = x_i$ with $t_i + j_i \geq i$. From ϕ_l , generate another sequence of solutions, which we will not relabel, by truncating the hybrid time domain of each solution so that $\phi_l(t, j) \in \mathcal{R}_{\mathcal{H}}^l(\mathcal{X})$ for all $(t, j) \in \text{dom } \phi_l$. Note that ϕ_l is nontrivial for every l . Note also that by the construction above, the sequence $\{\phi_l\}_{l=1}^{\infty}$ is a uniformly bounded sequence of solutions; in particular, it is locally eventually bounded. By Theorem 3.19, there exists a graphically convergent subsequence, that we will not relabel, converging to a solution $\phi \in \mathcal{S}_{\mathcal{H}}(\mathcal{X})$. By construction, ϕ has the property that for some $(t^*, j^*) \in \text{dom } \phi$ such that $t^* + j^* \geq N$, $\phi(t^*, j^*) = x^*$ and $\phi(t, j) \in \Omega_{\mathcal{H}}(\mathcal{X})$ for all $(t, j) \in \text{dom } \phi$ satisfying $(0, 0) \preceq (t, j) \preceq (t^*, j^*)$. Weak backward invariance of $\Omega_{\mathcal{H}}(\mathcal{X})$ is shown since this holds for every point in $\Omega_{\mathcal{H}}(\mathcal{X})$ and every $N > 0$.

We now show that under the assumption that $\Omega_{\mathcal{H}}(\mathcal{X}) \subset \mathcal{R}_{\mathcal{H}}^0(\mathcal{X}) \cup \mathcal{X}$, $\Omega_{\mathcal{H}}(\mathcal{X})$ is strongly pre-forward invariant. By contradiction, suppose that there exist $q \in \Omega_{\mathcal{H}}(\mathcal{X})$ and $\bar{\phi} \in \mathcal{S}_{\mathcal{H}}(q)$ so that for some $(\bar{t}, \bar{j}) \in \text{dom } \bar{\phi}$, $\bar{z} = \bar{\phi}(\bar{t}, \bar{j}) \notin \Omega_{\mathcal{H}}(\mathcal{X})$. By weak backward invariance of $\Omega_{\mathcal{H}}(\mathcal{X})$, for each $N > 0$ there exists $\phi'(0, 0) \in \Omega_{\mathcal{H}}(\mathcal{X})$ and $\phi' \in \mathcal{S}_{\mathcal{H}}(\phi'(0, 0))$ such that for some $(t', j') \in \text{dom } \phi'$, $t' + j' \geq N$, we have $\phi'(t', j') = q$ and $\phi'(t, j) \in \Omega_{\mathcal{H}}(\mathcal{X})$ for all $(t, j) \preceq (t', j')$, $(t, j) \in \text{dom } \phi'$. Define $\phi(t, j) := \phi'(t, j)$ for each $(t, j) \in \text{dom } \phi'$, $(t, j) \prec (t', j')$, and $\phi(t, j) := \bar{\phi}(t, j)$ for each (t, j) such that $(t - t', j - j') \in \text{dom } \bar{\phi}$, $(t - t', j - j') \preceq (\bar{t}, \bar{j})$. Let $t^* = t' + \bar{t}$, $j^* = j' + \bar{j}$ and note that $\phi(t^*, j^*) = \bar{z}$. By construction, ϕ is bounded. Construct in this way a sequence of bounded solutions ϕ_i with $\phi_i(0, 0) \in \Omega_{\mathcal{H}}(\mathcal{X})$ and $\phi_i(t_i^*, j_i^*) = \bar{z}$ where $t_i^* + j_i^* \geq i$ for each i . By construction, $\lim_{i \rightarrow \infty} \phi_i(t_i^*, j_i^*) = \bar{z}$. Let $x^0 = \lim_{i \rightarrow \infty} \phi_i(0, 0)$. By compactness of $\Omega_{\mathcal{H}}(\mathcal{X})$, $x^0 \in \Omega_{\mathcal{H}}(\mathcal{X})$. Then, by assumption, $x^0 \in \mathcal{R}_{\mathcal{H}}^0(\mathcal{X}) \cup \mathcal{X}$. Suppose that $x^0 \in \mathcal{X}$. By definition of $\Omega_{\mathcal{H}}(\mathcal{X})$, $\bar{z} \in \Omega_{\mathcal{H}}(\mathcal{X})$ which is a contradiction. Suppose instead that $x^0 \in \mathcal{R}_{\mathcal{H}}^0(\mathcal{X})$. By definition of $\mathcal{R}_{\mathcal{H}}^0(\mathcal{X})$ there exists $\tilde{x}^0 \in \mathcal{X}$ and $\tilde{\phi} \in \mathcal{S}_{\mathcal{H}}(\tilde{x}^0)$ such that $\tilde{\phi}(\tilde{t}, \tilde{j}) = x^0$ for some $(\tilde{t}, \tilde{j}) \in \text{dom } \tilde{\phi}$. Define $\phi_i''(t, j) := \tilde{\phi}(t, j)$ for each $(t, j) \in \text{dom } \tilde{\phi}$, $(t, j) \prec (\tilde{t}, \tilde{j})$, and $\phi_i''(t, j) := \phi_i(t - \tilde{t}, j - \tilde{j})$ for each $(t - \tilde{t}, j - \tilde{j}) \in \text{dom } \phi_i$, $(t, j) \succeq (\tilde{t}, \tilde{j})$, $(t - \tilde{t}, j - \tilde{j}) \in \text{dom } \phi_i$. By construction, $\tilde{x}^0 \in \mathcal{X}$ and $\lim_{i \rightarrow \infty} \phi_i''(t_i^* + \tilde{t}, j_i^* + \tilde{j}) = \bar{z}$. Then $\bar{z} \in \Omega_{\mathcal{H}}(\mathcal{X})$ which is also a contradiction. \square

In order to guarantee weak forward invariance of $\Omega_{\mathcal{H}}(\mathcal{X})$, it is assumed that the hybrid system \mathcal{H} is *eventually complete from \mathcal{X}* , i.e., there exists a nonnegative integer i^* such that, for all $i \geq i^*$, every maximal solution starting in $\mathcal{R}_{\mathcal{H}}^i(\mathcal{X})$ has an unbounded hybrid time domain. (Note: this still doesn't guarantee that $\mathcal{R}_{\mathcal{H}}^i(\mathcal{X})$ is nonempty for all i and thus still doesn't guarantee that $\Omega_{\mathcal{H}}(\mathcal{X})$ is nonempty.) Since the sequence of sets $\mathcal{R}_{\mathcal{H}}^i(\mathcal{X})$ is nested, it is enough to verify this property for solutions starting in $\mathcal{R}_{\mathcal{H}}^{i^*}(\mathcal{X})$ for some nonnegative integer

i^* . Eventual completeness combined with the condition for strong pre-forward invariance in Theorem 4.11 guarantees strong pre-forward invariance with complete solutions. Additionally, the next theorem establishes weak forward invariance under Assumption 4.10 and the assumption that the system \mathcal{H} is eventually complete from \mathcal{X} .

Theorem 4.12 (invariance property of $\Omega_{\mathcal{H}}(\mathcal{X})$) *Under Assumption 4.10, if the hybrid system \mathcal{H} is eventually complete from \mathcal{X} then $\Omega_{\mathcal{H}}(\mathcal{X})$ is weakly forward invariant. If, in addition, $\Omega_{\mathcal{H}}(\mathcal{X}) \subset \mathcal{R}_{\mathcal{H}}^0(\mathcal{X}) \cup \mathcal{X}$ then $\Omega_{\mathcal{H}}(\mathcal{X})$ is strongly forward invariant.*

Proof. Let $x^* \in \Omega_{\mathcal{H}}(\mathcal{X})$ be arbitrary. By definition of the limit and the assumptions, there exists a sequence $x_{i_k} \in \mathcal{R}_{\mathcal{H}}^{i_k}(\mathcal{X})$, $k = 1, 2, \dots$, with $x_{i_k} \rightarrow x^*$ as $k \rightarrow \infty$, complete solutions $\phi_{i_k} \in \mathcal{S}_{\mathcal{H}}(x_{i_k})$ satisfying $\text{rge } \phi_{i_k} \subset \mathcal{R}_{\mathcal{H}}^{i_k}(\mathcal{X})$ for each k , and a compact set $K \subset O$ such that $\mathcal{R}_{\mathcal{H}}^{i_k}(\mathcal{X}) \subset K$ for each k . Then, the sequence of solutions $\{\phi_{i_k}\}_{k=1}^{\infty}$ is a uniformly bounded sequence of solutions; in particular, it is locally eventually bounded. By Theorem 3.19, there exists a graphically convergent subsequence, that we will not relabel, converging to a complete solution $\phi \in \mathcal{S}_{\mathcal{H}}(x^*)$. Let $(\tilde{t}, \tilde{j}) \in \text{dom } \phi$ be arbitrary. By the graphical convergence of ϕ_{i_k} to ϕ , there exists a sequence $(\tilde{t}_{i_k}, \tilde{j}_{i_k}) \in \text{dom } \phi_{i_k}$, $(\tilde{t}_{i_k}, \tilde{j}_{i_k}) \rightarrow (\tilde{t}, \tilde{j})$ such that $\phi_{i_k}(\tilde{t}_{i_k}, \tilde{j}_{i_k}) \rightarrow \phi(\tilde{t}, \tilde{j})$ as $k \rightarrow \infty$. By construction, $\lim_{k \rightarrow \infty} \phi_{i_k}(\tilde{t}_{i_k}, \tilde{j}_{i_k}) \in \Omega_{\mathcal{H}}(\mathcal{X})$. Therefore, for every $(\tilde{t}, \tilde{j}) \in \text{dom } \phi$, $\phi(\tilde{t}, \tilde{j})$ is in $\Omega_{\mathcal{H}}(\mathcal{X})$. Thus $\Omega_{\mathcal{H}}(\mathcal{X})$ is weakly forward invariant.

Strong forward invariance of $\Omega_{\mathcal{H}}(\mathcal{X})$ with the additional assumption $\Omega_{\mathcal{H}}(\mathcal{X}) \subset \mathcal{R}_{\mathcal{H}}^0(\mathcal{X}) \cup \mathcal{X}$ follows from Theorem 4.11 and the eventually completeness assumption. \square

Theorem 4.11 combined with Theorem 4.12 parallel the following result for $\Omega(x)$.

Lemma 4.13 (invariance property of $\Omega(x)$) *If $x \in \mathcal{S}_{\mathcal{H}}$ is a precompact solution to \mathcal{H} then its ω -limit set $\Omega(x)$ is nonempty, compact, and weakly invariant. Moreover, the solution x approaches $\Omega(x)$, which is the smallest closed set approached by x . That is, for all $\epsilon > 0$ there exists $(\bar{t}, \bar{j}) \in \text{dom } x$ such that for all (t, j) satisfying $(t, j) \succeq (\bar{t}, \bar{j})$, $(t, j) \in \text{dom } x$, $x(t, j) \in \Omega(x) + \epsilon \mathbb{B}$.*

Proof. As x is precompact, it is complete and bounded. For any increasing and unbounded sequence (t_i, j_i) , $x(t_i, j_i)$'s are bounded and have a convergent subsequence. Thus $\Omega(x) \neq \emptyset$. Boundedness of x implies that of $\Omega(x)$. To prove that $\Omega(x)$ is closed, pick $x_k^* \in \Omega(x)$ with $x_k^* \rightarrow x^*$. By the definition of $\Omega(x)$, for each k there exists an increasing and unbounded sequence (t_k^i, j_k^i) such that $x_k(t_k^i, j_k^i) \rightarrow x_k^*$ as $i \rightarrow \infty$. Let \bar{i}_k be such that $|x_k(t_k^i, j_k^i) - x_k^*| \leq k^{-1}$ for all k , all $i \geq \bar{i}_k$. Now, pick i_k 's so that for each k , $i_k \geq \bar{i}_k$ and $(t_k^{i_k}, j_k^{i_k}) \prec (t_k^{i_{k+1}}, j_k^{i_{k+1}})$. As $x_k^* \rightarrow x^*$, we must have $x_k(t_k^{n_{i_k}}, j_k^{n_{i_k}}) \rightarrow x^*$ as $k \rightarrow \infty$. Thus $x^* \in \Omega(x)$, and $\Omega(x)$ is closed.

Now we show weak invariance, dealing with forward invariance first. Let $x^* \in \Omega(x)$ be arbitrary and let (t_i, j_i) be an increasing and unbounded sequence such that $x(t_i, j_i) \rightarrow x^*$ as $i \rightarrow \infty$. Consider $\bar{x}_i \in \mathcal{S}_{\mathcal{H}}(x(t_i, j_i))$ defined by $\bar{x}_i(t, j) := x(t + t_i, j + j_i)$, $(t, j) \in \text{dom } \bar{x}_i$. As x is bounded with respect to O and \bar{x}_i are truncations of x , $\{\bar{x}_i\}_{i=0}^{\infty}$ is locally eventually bounded with respect to O . Then, by the hybrid basic conditions, there exists a subsequence $\{\bar{x}_{i_k}\}_{k=0}^{\infty}$ of $\{\bar{x}_i\}_{i=0}^{\infty}$, graphically converging to another complete hybrid trajectory of $\tilde{x} \in \mathcal{S}_{\mathcal{H}}$ starting at x^* (since $\bar{x}_i(0, 0) \rightarrow x^*$ as $i \rightarrow \infty$ so does $\bar{x}_{i_k}(0, 0)$), i.e. $\bar{x}_{i_k} \rightarrow \tilde{x} \in \mathcal{S}_{\mathcal{H}}(x^*)$ as $k \rightarrow \infty$, where $x^* \in \Omega(x)$. Let $(\tilde{t}, \tilde{j}) \in \text{dom } \tilde{x}$ be arbitrary. By the graphical convergence of \bar{x}_{i_k} to \tilde{x} , there exists a sequence $(\tilde{t}_{i_k}, \tilde{j}_{i_k}) \in \text{dom } \bar{x}_{i_k}$, $(\tilde{t}_{i_k}, \tilde{j}_{i_k}) \rightarrow (\tilde{t}, \tilde{j})$ such that $\bar{x}_{i_k}(\tilde{t}_{i_k}, \tilde{j}_{i_k}) \rightarrow \tilde{x}(\tilde{t}, \tilde{j})$ as $k \rightarrow \infty$. By construction, $\bar{x}_{i_k}(\tilde{t}_{i_k}, \tilde{j}_{i_k}) = x(\tilde{t}_{i_k} + t_{i_k}, \tilde{j}_{i_k} + j_{i_k})$ where (t_{i_k}, j_{i_k}) is increasing and unbounded by properties of (t_i, j_i) . Therefore, for every $(\tilde{t}, \tilde{j}) \in \text{dom } \tilde{x}$, $\tilde{x}(\tilde{t}, \tilde{j})$ is an ω -limit point of x . Thus $\Omega(x)$ is weakly forward invariant.

To show weak backward invariance, let $x^{**} \in \Omega(x)$ and $N > 0$ be arbitrary. Let (t_i, j_i) be an increasing and unbounded sequence such that $x(t_i, j_i) \rightarrow x^{**}$ as $i \rightarrow \infty$. Pick $\underline{t}_i, \underline{j}_i$ such that $t_i + j_i - (N+1) \leq \underline{t}_i + \underline{j}_i \leq t_i + j_i - N$ and let $\bar{x}_i(t, j) = x(t + \underline{t}_i, j + \underline{j}_i)$ for all $(t, j) \in \text{dom } \bar{x}_i$. Since x is bounded and \bar{x}_i are truncations of x for each i , $\{\bar{x}_i\}_{i=0}^{\infty}$ is locally eventually bounded with respect to O . Then, by the hybrid basic conditions, there exists

a subsequence $\{\bar{x}_{i_k}\}_{k=0}^\infty$ of $\{\bar{x}_i\}_{i=0}^\infty$, graphically converging to another hybrid trajectory of $\tilde{x} \in \mathcal{S}_{\mathcal{H}}$ starting at some $x^* \in \Omega(x)$ (since $(\underline{t}_i, \underline{j}_i)$ is unbounded and increasing), i.e. $\bar{x}_{i_k} \rightarrow \tilde{x} \in \mathcal{S}_{\mathcal{H}}(x^*)$ as $k \rightarrow \infty$. For $\bar{t}_i = t_i - \underline{t}_i$ and $\bar{j}_i = j_i - \underline{j}_i$, since $(\bar{t}_i, \bar{j}_i) \in \text{dom } \bar{x}_i$, $\bar{x}_i(\bar{t}_i, \bar{j}_i) = x(t_i, j_i) \rightarrow x^{**}$ as $i \rightarrow \infty$. Since $\bar{x}_i(\bar{t}_i, \bar{j}_i)$ converge, there exists $(t^*, j^*) \in \text{dom } \tilde{x}$, such that $(t_i - \underline{t}_i, j_i - \underline{j}_i) \rightarrow (t^*, j^*)$ as $i \rightarrow \infty$ that satisfies $\tilde{x}(t^*, j^*) = x^{**}$. Note that (t^*, j^*) satisfies $N \leq t^* + j^* \leq N + 1$. That $\tilde{x}(t, j) \in \Omega(x)$ for all $t + j \leq t^* + j^*$, $(t, j) \in \text{dom } \tilde{x}$ follows by the same argument used at the end of the paragraph above.

Finally, we show convergence of x to its ω -limit set. Suppose that for some $\epsilon > 0$ there exists an increasing and unbounded sequence $(t_i, j_i) \in \text{dom } x$ such that $x(t_i, j_i) \notin \Omega(x) + \epsilon\mathbb{B}$ for $i = 1, 2, \dots$. By precompactness of x , there exists a convergent subsequence of $x(t_i, j_i)$'s. Its limit is, by definition, in $\Omega(x)$. This is a contradiction. \square

Lemma 4.13 is a key result needed when showing the invariance principles in the next section.

4.2.3 Convergence via invariance principles

In this section, invariance principles for hybrid systems are introduced. First, invariance principles that involve conditions given by Lyapunov functions are introduced. These are followed by invariance principles that use more general functions, both involving conditions about several solutions and a single solution.

Invariance principles with Lyapunov functions

When the conditions on the functions u_C and u_D in Theorem 4.2 are not satisfied with strict inequality, even though stability of the compact set under analysis is established, convergence to that set is not guaranteed by Theorem 4.2. However, with additional knowledge of the behavior of the solutions, information about convergence of solutions can be obtained as stated in the following result.

Theorem 4.14 (hybrid LaSalle's invariance principle) *Given a hybrid system \mathcal{H} , let $V : O \rightarrow \mathbb{R}$ be continuous on O and locally Lipschitz on a neighborhood of C . Suppose that $\mathcal{U} \subset O$ is nonempty, and that $x \in \mathcal{S}_{\mathcal{H}}$ is precompact with $\overline{\text{rge } x} \subset \mathcal{U}$. If*

$$u_C(z) \leq 0 \text{ and } u_D(z) \leq 0 \text{ for all } z \in \mathcal{U}$$

then for some constant $r \in V(\mathcal{U})$, x approaches the largest weakly invariant set in

$$V^{-1}(r) \cap \mathcal{U} \cap (u_C^{-1}(0) \cup (u_D^{-1}(0) \cap G(u_D^{-1}(0)))) . \quad (4.6)$$

When it is known that solutions are either Zeno or the time between jumps can be upper bounded from below by a positive constant, the set in (4.6) where invariance is to be checked becomes smaller. This is stated in the following result.

Corollary 4.15 (special case of hybrid LaSalle's invariance principle) *Under the assumptions of Theorem 4.14,*

(a) *if x is Zeno, then, for some $r \in V(\mathcal{U})$, it approaches the largest weakly invariant subset of*

$$V^{-1}(r) \cap \mathcal{U} \cap u_D^{-1}(0) \cap G(u_D^{-1}(0)); \quad (4.7)$$

(b) *if x is s.t., for some $\gamma > 0$, $J \in \mathbb{N}$, and all $j \geq J$, $t_{j+1} - t_j \geq \gamma$ (i.e. the elapsed time between jumps is eventually bounded below by γ), then, for some $r \in V(\mathcal{U})$, x approaches the largest weakly invariant subset of*

$$V^{-1}(r) \cap \mathcal{U} \cap \overline{u_C^{-1}(0)}. \quad (4.8)$$

The invariance principle in Theorem 4.14 can be used to show the following stability result that parallels Krasovskii stability theorem. Note that instead of requiring an strict inequality to hold for the conditions involving u_C and u_D , an invariance condition is in place.

Theorem 4.16 (hybrid Krasovskii) *Given a hybrid system \mathcal{H} , suppose that*

- (\star) $\mathcal{A} \subset O$ is compact, $\mathcal{U} \subset O$ is a neighborhood of \mathcal{A} , $V : O \rightarrow \mathbb{R}$ is continuous on O , locally Lipschitz on a neighborhood of C , and positive definite on $C \cup D$ with respect to \mathcal{A} , and u_C and u_D satisfy $u_C(z) \leq 0$, $u_D(z) \leq 0$ for all $z \in \mathcal{U}$.

Then \mathcal{A} is pre-stable. Suppose additionally that

- ($\star\star$) there exists $r^* > 0$ such that for all $r \in (0, r^*)$ the largest weakly invariant subset in

$$V^{-1}(r) \cap \mathcal{U} \cap [u_C^{-1}(0) \cup (u_D^{-1}(0) \cap G(u_D^{-1}(0)))] . \quad (4.9)$$

is empty.

Then \mathcal{A} is pre-asymptotically stable.

Examples where these results are applied are given in Section 4.3.

Invariance principles with general functions

Versions of the results above for general functions u_c and u_d , instead of u_C and u_D , satisfying the condition in (4.4) are possible. The following theorem states an equivalent result to Theorem 4.14.

Theorem 4.17 (general invariance principle) *Suppose that there exist a continuous function $V : O \rightarrow \mathbb{R}$, a set $\mathcal{U} \subset O$, and functions $u_c, u_d : O \rightarrow [-\infty, \infty]$ such that for any solution $\xi \in \mathcal{S}_{\mathcal{H}}$ with $\text{rge } \xi \subset \mathcal{U}$,*

$$u_c(\xi(t, j)) \leq 0, \quad u_d(\xi(t, j)) \leq 0$$

for all $(t, j) \in \text{dom } \xi$ and (4.4) holds for any $(t, j), (t', j') \in \text{dom } \xi$ such that $(t, j) \preceq (t', j')$.

Let $x \in \mathcal{S}_{\mathcal{H}}$ be a precompact solution such that

$$\overline{\{x(t, j) \mid (t, j) \in \text{dom } x, (T, J) \preceq (t, j)\}} \subset \mathcal{U},$$

for some $(T, J) \in \text{dom } x$, which holds when $\overline{\text{rge } x} \subset \mathcal{U}$. Then, for some $r \in V(\mathcal{U})$, x approaches the largest weakly invariant subset of

$$V^{-1}(r) \cap \mathcal{U} \cap \left(\overline{u_c^{-1}(0)} \cup (u_d^{-1}(0) \cap G(u_d^{-1}(0))) \right) . \quad (4.10)$$

The following results parallels Corollary 4.15

Corollary 4.18 (special case of general invariance principle) *Under the assumptions of Theorem 4.17,*

- (a) if x is Zeno, then, for some $r \in V(\mathcal{U})$, it approaches the largest weakly invariant subset of

$$V^{-1}(r) \cap \mathcal{U} \cap u_d^{-1}(0) \cap G(u_d^{-1}(0)); \quad (4.11)$$

(b) if x is such that, for some $\gamma > 0$, $J \in \mathbb{N}$, and all $j \geq J$, $t_{j+1} - t_j \geq \gamma$ (i.e. the elapsed time between jumps is eventually bounded below by a positive γ), then, for some $r \in V(\mathcal{U})$, x approaches the largest weakly invariant subset of

$$V^{-1}(r) \cap \mathcal{U} \cap \overline{u_c^{-1}(0)}. \quad (4.12)$$

Corollary 4.15 relies on the character of the solutions verifying the weak invariance of $\Omega(x)$, rather than on whether x jumps infinitely many times or whether x is not Zeno. The example below illustrates this, among other things.

Example 4.19 (linear oscillator with reset) Consider the hybrid system on $O = \mathbb{R}^2$ given by

$$\dot{x} = \begin{bmatrix} -x_2 \\ x_1 \end{bmatrix} \quad x \in C := \mathbb{R} \times [0, \infty), \quad x^+ = \begin{bmatrix} -x_2 \\ x_1 \end{bmatrix} \quad x \in D := \mathbb{R} \times (-\infty, 0].$$

Any solution to this system satisfies (4.4) with $V(x) = |x|$. Let $u_c(x) = 0$ if $x_2 \geq 0$, $u_c(x) = -\infty$ if $x_2 < 0$, and $u_d(x) = 0$ if $x_2 \leq 0$, $u_d(x) = -\infty$ if $x_2 > 0$. Functions u_c, u_d are the natural bounds on the decrease of V , see (4.2) and (4.3). For these functions, $\overline{u_c^{-1}(0)}$ is the (closed) upper half plane, $u_d^{-1}(0)$ is the (closed) lower half plane, and $G(u_d^{-1}(0))$ is the (closed) right half plane. For the periodic solution given by $x(t, j) = (\cos t, \sin t)$ for $t \in [0, \pi]$, $x(\pi, 1) = (0, -1)$, and $x(t, j) = x(t - \pi, j - 2)$ for $t \geq \pi$, $j \geq 2$, the Ω -limit set is just $\text{rge } x$: the (closed) upper half of the unit circle and $(0, -1)$. Note that the domain of this solution is unbounded in both t and j directions. For this solution, $V(x(t, j)) = 1$ for all $(t, j) \in \text{dom } x$. Suppose that Corollary 4.15 were applicable. Taking $r = 1$ and $\mathcal{U} = \mathbb{R}^2$, the set (4.7) would be the unit circle in the closed fourth quadrant and the set (4.8) would be the unit circle in the (closed) upper half plane. In particular, x does not approach either of these two sets even though $\text{dom } x$ is unbounded in both t and j directions, and therefore, it will not approach an invariant set included in those sets. Of course, x approaches the largest weakly invariant set contained in the union of the sets (4.7) and (4.8) (as dictated by Theorem 4.17). This set turns out to be $\text{rge } x$; see Figure 4.1. Note that if $G(u_d^{-1}(0))$ is not used in Theorem 4.17 then one must search for the largest weakly invariant subset

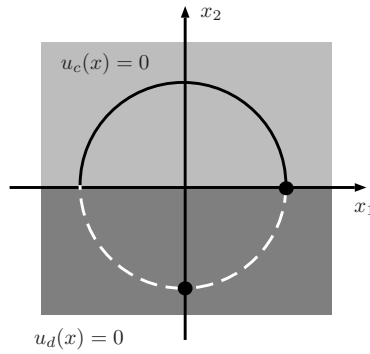


Figure 4.1. Solutions to the hybrid system in Example 4.19 converge to the solid line and to points where jumps occur, denoted with dots.

of $V^{-1}(1) \cap \mathcal{U} \cap (\overline{u_c^{-1}(0)} \cup u_d^{-1}(0))$. This turns out to be the unit circle, which is larger than $\text{rge } x$. \square

Note that the strong conclusion in the example above relies both on the strong (forward and backward) invariance notion and the set $G(u_d^{-1}(0))$ in (4.7).

Note that when applying Theorem 4.17, as a difference to Theorem 4.14, a condition “for all solutions in a set \mathcal{U} ” has to be checked. A follow-up question is whether conditions that involve a single solution, or in general, a *hybrid trajectory* (if no data is associated to it) can be stated to obtain information about its convergence. The following lemma states the conditions that two functions need to satisfy along a single hybrid trajectory in order to characterize the point(s) to which it converges. The results that follow in this section are also stated for a single hybrid trajectory.

Below, a function $f : \mathbb{R}_{\geq 0} \rightarrow \mathbb{R}$ is *weakly meagre* if $\lim_{n \rightarrow \infty} (\inf_{t \in I_n} |f(t)|) = 0$ for every family $\{I_n \mid n \in \mathbb{N}\}$ of nonempty and pairwise disjoint closed intervals I_n in $\mathbb{R}_{\geq 0}$ with $\inf_{n \in \mathbb{N}} \mu(I_n) > 0$. Here, μ stands for the Lebesgue measure. Moreover, f is weakly meagre if for some $\tau > 0$,

$$\lim_{M \rightarrow \infty} \int_M^{M+\tau} |f(t)| dt = 0. \quad (4.13)$$

In particular, any L^1 function is weakly meagre.

Lemma 4.20 (meagre-limsup conditions) *Let x be a complete hybrid trajectory such that*

- (*) *For each $z \in \Omega(x)$ and $\epsilon > 0$ there exist $\delta > 0$ and $T > 0$ such that, if $x(t, j) \in z + \delta\mathbb{B}$ for some $(t, j) \in \text{dom } x$ then $x(t', j) \in z + \epsilon\mathbb{B}$ for all $t' \in [t - T, t + T]$ such that $(t', j) \in \text{dom } x$.*

Furthermore, suppose that for some set $\mathcal{U} \subset O$ with $\text{rge } x \subset \mathcal{U}$ there exist functions $\ell_c, \ell_d : \mathcal{U} \rightarrow [0, \infty]$ that, for the hybrid trajectory x , satisfy the meagre-limsup conditions given by

- (a) *if the projection of $\text{dom } x$ onto $\mathbb{R}_{\geq 0}$ is unbounded then $t \mapsto \ell_c(x(t, j(t)))$ is weakly meagre,*
 (b) *if the projection of $\text{dom } x$ onto \mathbb{N} is unbounded then for all large enough j there exists $t_j^* \in [t(j), t(j+1)]$ such that $\limsup_{j \rightarrow \infty} \ell_d(x(t_j^*, j)) = 0$.*

Then $\Omega(x) \subset E_{x, \ell_c} \cup E_{x, \ell_d}$, where E_{x, ℓ_c} and E_{x, ℓ_d} are respectively defined by

$$\begin{aligned} \{z \in \overline{\text{rge } x} \mid \exists z_i \rightarrow z, z_i \in \text{rge } x, \liminf_{i \rightarrow \infty} \ell_c(z_i) = 0\}, \\ \{z \in \overline{\text{rge } x} \mid \exists z_i \rightarrow z, z_i \in \text{rge } x, \liminf_{i \rightarrow \infty} \ell_d(z_i) = 0\}. \end{aligned}$$

Proof. Suppose otherwise, that for some $x^* \in \Omega(x)$ and $\epsilon, \gamma > 0$,

$$\ell(z) := \min\{\ell_c(z), \ell_d(z)\} \geq \gamma$$

for all $z \in x^* + \epsilon\mathbb{B}$, $z \in \text{rge } x$. By definition of ω -limit point, there is an increasing and unbounded sequence $(t_i, j_i) \in \text{dom } x$ with $x(t_i, j_i) \rightarrow x^*$ as $i \rightarrow \infty$. We can assume that for all i , $t_i + j_i + 1 \leq t_{i+1} + j_{i+1}$. Let $\delta, T > 0$ be related to x^* , ϵ as in condition (*) and, without loss of generality, suppose that $T < 1$. Ignoring initial terms if necessary, we have $x(t_i, j_i) \in x^* + \delta\mathbb{B}$ for all $i \in \mathbb{N}$. Consequently, $x(t, j_i) \in x^* + \delta\mathbb{B}$ for all $t \in [t_i - T, t_i + T]$, $(t, j_i) \in \text{dom } x$. For each i , either of the two conditions holds:

- (1') either $t(j_i) \leq t_i - T$ or $t(j_i + 1) \geq t_i + T$ (x flows for time T either before t_i or after t_i)
 (2') $t(j_i) > t_i - T$ and $t(j_i + 1) < t_i + T$ (x jumps within time T before and after t_i)

Either (1') or (2') has to occur for infinitely many i 's. Suppose it is (1') and that $t(j_i) \leq t_i - T$ for such i 's (the other case is treated similarly). Then, $\text{dom } x$ must be unbounded in the t -direction. The fact that $\ell(x(t, j(t))) > \gamma$ for any $t \in [t_i - T, t_i]$ for infinitely many i 's contradicts weak meagreness of $t \mapsto \ell_c(x(t, j(t)))$

(note that intervals $[t_i - T, t_i]$ are disjoint). If (2') holds for infinitely many i 's, then $\text{dom } x$ is unbounded in the j -direction, and for infinitely many i 's and all $t \in [t(j_i), t(j_i + 1)]$ we have $\ell_d(x(t, j_i)) > \gamma$. This contradicts (b). \square

The condition (*) above can be viewed as a sort of continuity of $x(t, j)$ in t , uniform “near each point of $\Omega(x)$ ”. The condition automatically holds if x is a solution to a hybrid system that satisfies (S1) and (S2) and the hybrid basic conditions. In fact, since F is locally bounded, $x(t, j)$ is Lipschitz in t , locally “near each point of $\Omega(x)$ ”.

In Lemma 4.20, $E_{x, \ell_c} \subset \{z \in \overline{\text{rge } x} \mid \underline{\ell}_c(z) = 0\}$, where $\underline{\ell}_c$ is the lower semicontinuous closure of ℓ_c . (Given a set \mathcal{U} and a function $\ell : \mathcal{U} \rightarrow [-\infty, \infty]$, its *lower semicontinuous closure* $\underline{\ell} : \overline{\mathcal{U}} \rightarrow [-\infty, \infty]$, is the greatest lower semicontinuous function defined on $\overline{\mathcal{U}}$, bounded above by ℓ on \mathcal{U} . Equivalently, for any $x \in \overline{\mathcal{U}}$, $\underline{\ell}(x) = \liminf_{x_i \rightarrow x} \ell(x_i)$. In this terminology, $E_{x, \ell}$ is the zero-level set of the lower semicontinuous closure of the function ℓ truncated to $\text{rge } x$.) In particular, if both ℓ_c and ℓ_d are lower semicontinuous, and $\overline{\text{rge } x} \subset \mathcal{U}$, then the conclusion of Lemma 4.20 implies that $\Omega(x)$ is a subset of

$$\{z \in \overline{\text{rge } x} \mid \ell_c(z) = 0\} \cup \{z \in \overline{\text{rge } x} \mid \ell_d(z) = 0\}.$$

However, if the assumption that ℓ_c, ℓ_d are nonnegative was weakened to say that they are nonnegative only on $\text{rge } x$, the last conclusion above may fail.

The following result corresponds to an invariance principle involving the meagre-limsup conditions which automatically follows from Lemma 4.20.

Theorem 4.21 (meagre-limsup invariance principle) *Let x be a precompact hybrid trajectory. Suppose that for $\mathcal{U} \subset O$, $\text{rge } x \subset \mathcal{U}$, there exist functions $\ell_c, \ell_d : \mathcal{U} \rightarrow [0, \infty]$ for which the meagre-limsup conditions hold. Then x converges to the largest weakly invariant subset of*

$$\{z \in \overline{\mathcal{U}} \mid \underline{\ell}_c(z) = 0\} \cup \{z \in \overline{\mathcal{U}} \mid \underline{\ell}_d(z) = 0\}.$$

If $\overline{\text{rge } x} \subset \mathcal{U}$ and ℓ_c, ℓ_d are lower semicontinuous, then all the closure operations above can be removed.

Let x be a precompact hybrid trajectory for which there exist functions $u_c, u_d : O \rightarrow [-\infty, 0]$ and $V : O \rightarrow \mathbb{R}$ such that (4.4) holds for the hybrid trajectory x for all $(t, j), (t', j') \in \text{dom } x$ such that $(t, j) \preceq (t', j')$. Then $\ell_c = -u_c, \ell_d = -u_d$ satisfy conditions (a) and (b) of Theorem 4.20. In fact, there exists a constant $M > 0$ for which

$$\int_0^T \ell_c(x(t, j(t))) dt < M, \quad \sum_{j=0}^J \ell_d(x(t(j+1), j)) < M,$$

for any $(T, J) \in \text{dom } x$ (this shows that $\ell_c(t, j(t))$ is integrable on $[0, \infty)$ and thus weakly meagre, while to satisfy (b), one can take $t_j^* = t(j+1)$).

Based on the previous discussion, the next result shows that, when a function V with the right properties exists, the conditions (a) and (b) of Lemma 4.20 are guaranteed.

Corollary 4.22 (meagre-limsup conditions with a V) *Let x be a precompact hybrid trajectory. Suppose that there exists a continuous function $V : O \rightarrow \mathbb{R}$, and functions $u_c, u_d : O \rightarrow [-\infty, \infty]$ such that for some $(T, J) \in \text{dom } x$,*

$$u_c(x(t, j)) \leq 0, \quad u_d(x(t, j)) \leq 0$$

for all $(t, j) \in \text{dom } x$ with $(T, J) \preceq (t, j)$, and (4.4) holds for the hybrid trajectory x for all $(t, j), (t', j') \in \text{dom } x$ such that $(T, J) \preceq (t, j) \preceq (t', j')$. Then $\Omega(x) \subset E^{x, u_c} \cup E^{x, u_d}$, where E^{x, u_c} and E^{x, u_d} are respectively defined by

$$\{z \in \overline{\text{rge } x} \mid \exists z_i \rightarrow z, z_i \in \text{rge } x, \limsup_{i \rightarrow \infty} u_c(z_i) = 0\},$$

$$\{z \in \overline{\text{rge } x} \mid \exists z_i \rightarrow z, z_i \in \text{rge } x, \limsup_{i \rightarrow \infty} u_d(z_i) = 0\}.$$

More precise results can be obtained if the hybrid time domain of the hybrid trajectory is bounded in either the t or j direction.

Corollary 4.23 (special cases for meagre-limsup conditions) *Let x be a complete hybrid trajectory for which (*) holds.*

- (a) *If the projection of $\text{dom } x$ onto \mathbb{N} is bounded and there exists a function $\ell_c : \text{rge } x \rightarrow [0, \infty]$ such that $t \mapsto \ell_c(x(t, j(t)))$ is weakly meagre, then $\Omega(x) \subset E_{x, \ell_c}$.*
- (b) *If the projection of $\text{dom } x$ onto $\mathbb{R}_{\geq 0}$ is bounded and there exists a function $\ell_d : \text{rge } x \rightarrow [0, \infty]$ such that, for all large enough j , there exists $t_j^* \in [t(j), t(j+1)]$ such that $\limsup_{j \rightarrow \infty} \ell_d(x(t_j^*, j)) = 0$, then $\Omega(x) \subset E_{x, \ell_d}$.*

If, for a hybrid trajectory, the elapsed time between jumps is uniformly positive then only (a) of the meagre-limsup conditions needs to be checked to draw the conclusion of Lemma 4.20.

Corollary 4.24 (meagre-limsup invariance with uniformly bounded time between jumps) *Let x be a complete hybrid trajectory such that (*) holds and $t_{j+1} - t_j \geq \gamma > 0$ for all $j = 1, 2, \dots$. If there exists a function $\ell_c : \text{rge } x \rightarrow [0, \infty]$ such that condition (a) of the meagre-limsup conditions holds, then $\Omega(x) \subset E_{x, \ell_c}$.*

Proof. In the proof of Lemma 4.20, T can be chosen arbitrarily small. Picking $T < \frac{\gamma}{2}$ shows that (2') in the proof of Lemma 4.20 cannot hold; hence (1') has to hold for infinitely many times. The proof follows that of Lemma 4.20. \square

If multiple instantaneous jumps can occur “only on the zero level set of ℓ_d ” (for a hybrid system \mathcal{H} , this is equivalent to $\ell_d(G(D) \cap D) = 0$) and x is precompact, then only (a) of the meagre-limsup conditions needs to be checked to draw the conclusion of Lemma 4.20. This is because under such an assumption on the jumps, on each compact set away from the zero level set of ℓ_d , the elapsed time between jumps is uniformly bounded below by a positive constant.

Corollary 4.25 (case of multiple instantaneous jumps) *Given the function $\ell_d : O \mapsto \mathbb{R}_{\geq 0}$, assume that for all $\tilde{x} \in \mathcal{S}_{\mathcal{H}}$, if $(t, j-1), (t, j), (t, j+1) \in \text{dom } \tilde{x}$, then $\ell_d(\tilde{x}(t, j)) = 0$. Let $x \in \mathcal{S}_{\mathcal{H}}$ be a precompact solution. Suppose that there exists a function $\ell_c : \text{rge } x \rightarrow [0, \infty]$ such that condition (a) of the meagre-limsup conditions holds. Then the conclusion of Lemma 4.20 is true.*

4.2.4 Connections to observability and detectability

Classically, (zero-state) observability means that if the output of a system is held to zero, the state is identically zero. The following definition extends this concept to hybrid systems.

Definition 4.26 (observability) *Given sets $\mathcal{A}, K \subset O$, the distance to \mathcal{A} is observable relative to K for the hybrid system \mathcal{H} if for every nontrivial solution x satisfying $\text{rge } x \subset K$ then $|x(t, j)|_{\mathcal{A}} = 0$ for all $(t, j) \in \text{dom } x$.*

If, for a certain (output) function $h : O \rightarrow \mathbb{R}^k$, $K = h^{-1}(0)$, then it is said that the distance to \mathcal{A} is observable through (the output) h .

Basic properties based on observability are stated below, under the assumption that \mathcal{A} and K are compact subsets of O and the distance to \mathcal{A} is observable relative to K .

Theorem 4.27 (observability and the invariance principle) *Let $\mathcal{A}, K \subset O$ be compact, and suppose that \mathcal{A} is stable relative to K for the hybrid system \mathcal{H} . Then the following statements are equivalent:*

1. *The distance to \mathcal{A} is observable relative to K .*
2. *The largest weakly invariant set in K is a subset of \mathcal{A} .*

In differential equations, detectability is the property that when the output is held to zero, complete solutions x satisfy $\lim_{t \rightarrow \infty} |x(t)|_{\mathcal{A}} = 0$. Below, this notion is generalized.

Definition 4.28 (detectability) *Given sets $\mathcal{A}, K \subset O$, the distance to \mathcal{A} is detectable relative to K for \mathcal{H} if for every complete solution $x \in \mathcal{S}_{\mathcal{H}}$ satisfying $\text{rge } x \subset K$ then $\liminf_{t+j \rightarrow \infty} |x(t, j)|_{\mathcal{A}} = 0$.*

This detectability notion above can be understood as x having an ω -limit point at \mathcal{A} . As for observability relative to $K := h^{-1}(0)$ for some function $h : O \rightarrow \mathbb{R}^k$, it is said that the distance to \mathcal{A} is detectable through h .

When detectability (as in Definition 4.28) is combined with relative stability, the usual detectability is recovered.

Lemma 4.29 (detectability and relative stability) *Let $\mathcal{A}, K \subset O$ be compact. If the distance to \mathcal{A} is detectable relative to K and \mathcal{A} is stable relative to K , then each complete solution $x \in \mathcal{S}_{\mathcal{H}}$ with $\text{rge } x \subset K$ converges to \mathcal{A} .*

Example 4.30 (hybrid system with linear dynamics) For $x \in \mathbb{R}^n$, $A_1, A_2 \in \mathbb{R}^{n \times n}$, and closed $C, D \subset \mathbb{R}^n$, consider the hybrid system \mathcal{H} given by

$$\dot{x} = A_1 x \text{ when } x \in C, \quad x^+ = A_2 x \text{ when } x \in D.$$

For simplicity, assume that $C \cup D = \mathbb{R}^n$. The motivation for this type of systems comes from many applications, like sample-data control, reset systems, etc. Suppose that:

(o) Let $\tilde{C} \in \mathbb{R}^{m \times n}$ be such that there exists matrices L_1, L_2 , and $P = P^T > 0$ that satisfy

$$\begin{aligned} x^T \left(\left(A_1 + L_1 \tilde{C} \right)^T P + P \left(A_1 + L_1 \tilde{C} \right) \right) x &< 0, \\ x^T \left(\left(A_2 + L_2 \tilde{C} \right)^T P \left(A_2 + L_2 \tilde{C} \right) - P \right) x &< 0, \end{aligned}$$

where the first inequality is for all $x \in C \setminus \{0\}$ and the second one for all $x \in D \setminus \{0\}$.

This assumption holds in particular when the pairs (\tilde{C}, A_1) and (\tilde{C}, A_2) are detectable (in the linear sense) and the detectability of both pairs can be verified with a common Lyapunov function (which is quadratic and given by P).

Let K be any subset of $\left\{ z \in \mathbb{R}^n \mid \tilde{C}z = 0 \right\}$ and $\mathcal{A} = \{0\} \subset \mathbb{R}^n$. By definition of K , solutions that remain in K are also solutions of the output injected hybrid system \mathcal{H}_O defined as

$$\dot{x} = (A_1 + L_1 \tilde{C})x \quad x \in C, \quad x^+ = (A_2 + L_2 \tilde{C})x \quad x \in D.$$

Stability of \mathcal{A} (for the system above, and hence for \mathcal{H} relative to K) can be easily verified with the use of the common quadratic Lyapunov function $V(x) = x^T P x$. Moreover, by Corollary 4.14 with $\mathcal{U} = \mathbb{R}^n$ and $V(x)$,

every solution that stays in K converges to \mathcal{A} . Hence, the distance to \mathcal{A} is detectable relative to K for \mathcal{H} . However, (o) is not a necessary condition for detectability of \mathcal{H} relative to K , it is only sufficient.

Note that for LTI systems, the concepts of relative stability and detectability introduced above reduces to the standard concept in the literature. For instance, for the continuous-time LTI system $\dot{x} = Ax$ with output $y = \tilde{C}x$, detectability of the pair (\tilde{C}, A) is equivalent to the distance to $\mathcal{A} := \{0\}$ being detectable relative to subsets of $\left\{z \in \mathbb{R}^n \mid \tilde{C}z = 0\right\}$. \square

Theorem 4.31 (detectability and invariance principle) *Let $\mathcal{A}, K \subset O$ be compact, and suppose that \mathcal{A} is stable relative to K for the hybrid system \mathcal{H} . Then the following statements are equivalent:*

1. *The distance to \mathcal{A} is detectable relative to K .*
2. *The largest weakly invariant set in K is a subset of \mathcal{A} .*

Corollary 4.32 (connection with meagre-limsup invariance principles) *Let \mathcal{A}, K be compact subsets of O , with \mathcal{A} stable relative to K and with the distance to \mathcal{A} detectable on K , and let $\omega : O \rightarrow \mathbb{R}_{\geq 0}$ be a continuous and positive definite function with respect to K . If $x \in \mathcal{S}_{\mathcal{H}}$ is precompact and the meagre-limsup conditions hold for x with ℓ_c, ℓ_d replaced by ω , then x converges to \mathcal{A} .*

Stability and detectability of the distance to a compact set \mathcal{A} relative to a compact set K leads to uniform convergence.

Theorem 4.33 (uniform convergence) *Let $\mathcal{A}, K \subset O$ be compact. Suppose that \mathcal{A} is stable relative to K and the distance to \mathcal{A} is detectable relative to K . Then, for each $\epsilon > 0$, there exists $M > 0$ such that for each complete solution $x \in \mathcal{S}_{\mathcal{H}}$ with $\text{rge } x \subset K$ implies $|x(t, j)|_{\mathcal{A}} \leq \epsilon$ for all $(t, j) \in \text{dom } x, t + j \geq M$.*

Proof. Suppose otherwise. Then, for some $\epsilon > 0$, there exist a sequence of complete trajectories $x_i \in \mathcal{S}_{\mathcal{H}}$ such that $\text{rge } x_i \subset K$ and a sequence $(t_i, j_i) \in \text{dom } x_i$ with $t_i + j_i \geq i$ such that $|x_i(t_i, j_i)|_{\mathcal{A}} > \epsilon$. By relative stability of \mathcal{A} , there exists $\delta > 0$ such that for each $i = 1, 2, \dots$, $|x_i(t, j)|_{\mathcal{A}} > \delta$ for all $t + j \leq i, (t, j) \in \text{dom } x_i$. Since K is compact, the sequence $\{x_i\}_{i=1}^{\infty}$ is locally eventually bounded, and, by the hybrid basic conditions, it has a graphically convergent subsequence. Its limit, let us call it x , is complete (since each x_i is complete; see [39, Lemma 3.5]) and such that $\text{rge } x \subset K$. Furthermore, for all $(t, j) \in \text{dom } x, |x(t, j)|_{\mathcal{A}} \geq \delta$. This contradicts the detectability assumption. \square

4.3 Examples

The stability theorems, the invariance principles, and their connections to observability and detectability presented above are applied to hybrid systems with purely hybrid dynamics, set-valued dynamics, nonuniqueness of solutions, and solutions with multiple jumps at the same instant. Figure 4.2 depicts the hybrid systems for the first three examples. The last example corresponds to the problem of disturbance rejection for a class of hybrid control systems.

Example 4.34 (bouncing ball) Consider the bouncing ball example in Section 2.2.1 with regular data given by

$$O := \mathbb{R}^2, f(x) := \begin{bmatrix} x_2 \\ -g \end{bmatrix}, C := \{x \in \mathbb{R}^2 \mid x_1 \geq 0\} \quad (4.14)$$

$$g(x) := \begin{bmatrix} x_1 \\ -\lambda x_2 \end{bmatrix}, D := \{x \in \mathbb{R}^2 \mid x_1 = 0, x_2 \leq 0\} \quad (4.15)$$

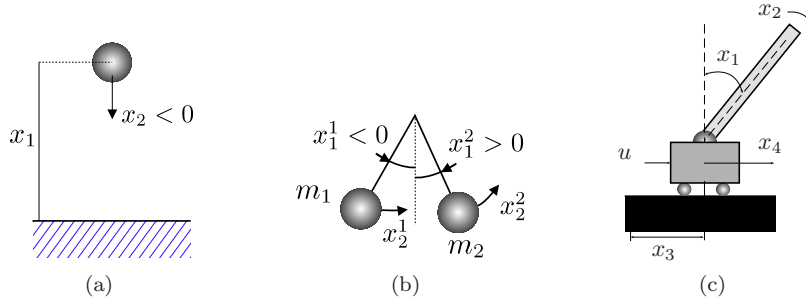


Figure 4.2. Examples: (a) bouncing ball, (b) simplified Newton's cradle, and (c) inverted pendulum on a cart.

where $g > 0$ is the gravity constant and $\lambda \in [0, 1)$ is the restitution coefficient.

Consider the continuously differentiable function $V(x) = \frac{1}{2}x_2^2 + \gamma x_1$. To apply hybrid LaSalle's invariance principle, we compute the function $u_C : O \rightarrow [-\infty, \infty)$ given by equation (4.2), which amounts to computing $\langle \nabla V(x), f(x) \rangle$ for all $x \in C$. Then

$$\langle \nabla V(x), f(x) \rangle = 0 \quad \text{for all } x \in C. \quad (4.16)$$

The increment of the energy at jumps is given by

$$V(g(x)) - V(x) = -\frac{1}{2}(1 - e^2)x_2^2 - \gamma x_1 \leq 0$$

for all $x \in D$. From (4.3),

$$u_D(x) = -\frac{1}{2}(1 - e^2)x_2^2 - \gamma x_1$$

for each $x \in D$. Since u_C and u_D are never positive, $\mathcal{U} = \mathbb{R}^2$ satisfies the conditions in Theorem 4.14. Therefore, every precompact solution to the bouncing ball system converges to the largest weakly invariant set in (4.6) for some $r \in V(\mathcal{U})$ (with $G = g$). Note that

$$u_C^{-1}(0) = C, \quad g(u_D^{-1}(0)) = u_D^{-1}(0) = \{x \in O \mid x = 0\}.$$

Suppose $r > 0$ and consider solutions starting in the set (4.6). Such solutions will hit $x_1 = 0$ and then jump. Since $u_D(x)$ is strictly negative away from the origin, V needs to decrease after the jump. This shows that with positive r there is no invariant set in (4.6). The only invariant set is for $r = 0$ and it is given by $\{x \in O \mid x = 0\}$; see Figure 4.3. Thus, precompact solutions to the bouncing ball converge to the origin.

The same conclusion follows from Corollary 4.15 by noting that solutions to the bouncing ball are Zeno. Our invariance principles involving functions satisfying the meagre-limsup conditions in Lemma 4.20 are also applicable, in particular, Corollary 4.23(b) with $\ell_d(x) = |x_1|$, $j > 1$, and $t_j^* = t(j + 1)$. Moreover, it follows with our hybrid Krasovskii theorem (Theorem 4.16) that \mathcal{A} is asymptotically stable with basin of attraction $C \cup D$. \square

Example 4.35 (Newton's cradle) Consider a simplified model of the Newton's cradle consisting of a pair of pendulums with mass m_1, m_2 as shown in Figure 4.2(b). Denote by x_1^1 and x_1^2 the angular position of each pendulum, and by x_2^1 and x_2^2 their tangential velocity defining the state $x = [x_1^1 \ x_1^2 \ x_2^1 \ x_2^2]^T$. Viscous friction for the circular motion and elastic collisions are considered. Moreover, it is assumed that the pendulums remain ordered with angles in $(-\pi, \pi)$ along solutions ("ordered" means that the pendulum with mass m_1 stays to the

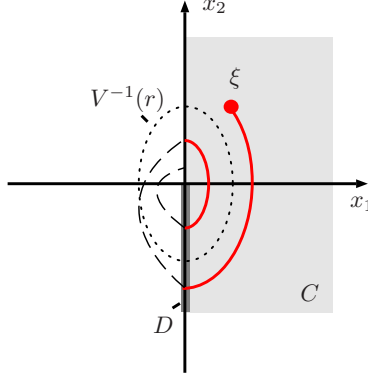


Figure 4.3. A solution to the bouncing ball system in the $x_1 - x_2$ plane and a level set of V (dashed). Solutions escape a level set with $r > 0$ in finite time.

left of the pendulum with mass m_2 along solutions). More general models allowing the pendulums to change their order can be derived but for simplicity, they are not pursued here. Let $O = (-\pi, \pi) \times (-\pi, \pi) \times \mathbb{R}^2$.

The equations of motion for the pendulums in between collisions are given by Newton's laws

$$\dot{x}_1^i = x_2^i, \quad \dot{x}_2^i = -\frac{\gamma}{l} \sin(x_1^i) - b_i x_2^i, \quad (4.17)$$

when either $x_1^1 \leq x_1^2$ (pendulums in the right order) or $x_2^1 \leq x_2^2$ (pendulums moving in the right direction), where $i = 1, 2$, $b_i > 0$, $\gamma > 0$ is the gravity constant, and $l > 0$ is the length of the pendulums. Jumps are assumed to happen when $x_1^1 \geq x_1^2$ and $x_2^1 \geq x_2^2$. When this holds, the state is updated by

$$x_1^+ = \begin{bmatrix} 1 \\ 1 \end{bmatrix} \arg \min_{s \in \{x_1^1, x_1^2\}} \{1 - \cos(s)\}, \quad x_2^+ = M x_2, \quad (4.18)$$

where $x_1 = [x_1^1 \ x_1^2]^T$, $x_2 = [x_2^1 \ x_2^2]^T$, and the matrix M characterizes the exchange of kinetic energy at impacts. Note that the angular positions are mapped to the minimal potential energy configuration (typically, collisions between the pendulums occur when $x_1^1 = x_1^2$). When the usual impact rule with conservation of momentum is used, the jump mapping for velocities is

$$\begin{aligned} (x_2^1)^+ - (x_2^2)^+ &= -e (x_2^1 - x_2^2), \\ m_1(x_2^1)^+ + m_2(x_2^2)^+ &= m_1 x_2^1 + m_2 x_2^2, \end{aligned}$$

where $e \in [0, 1]$ is the restitution coefficient. In this case

$$M = \begin{bmatrix} \lambda - (1 - \lambda)e & (1 - \lambda)(1 + e) \\ \lambda(1 + e) & 1 - \lambda - \lambda e \end{bmatrix}, \quad (4.19)$$

where $\lambda = \frac{m_1}{m_1 + m_2} \in (0, 1)$. For the following analysis, it is assumed that M is given as in (4.19).

The continuous dynamics of the Newton's cradle system are given by $f(x)$ which is the vector function resulting from stacking the vector fields given in (4.17) for $i = 1, 2$. The flow and jump sets are given by

$$C := \{x \in O \mid x_1^1 \leq x_1^2 \text{ or } x_2^1 \leq x_2^2\}, \quad D := \{x \in O \mid x_1^1 \geq x_1^2, x_2^1 \geq x_2^2\}.$$

The jump mapping on D is given by $g(x)$, the vector function constructed by stacking the mappings in (4.18).

Let $\mathcal{J} = \begin{bmatrix} \lambda & 0 \\ 0 & 1 - \lambda \end{bmatrix}$. It is easy to show that $M^T \mathcal{J} M - \mathcal{J} \leq 0$. Moreover, the data of the Newton's cradle system satisfies the hybrid basic conditions.

Let V be the energy of the system normalized by $m_1 + m_2$:

$$V(x) = \frac{1}{2} l^2 x_2^T \mathcal{J} x_2 + \gamma \lambda l (1 - \cos(x_1^1)) + \gamma (1 - \lambda) l (1 - \cos(x_1^2)) . \quad (4.20)$$

It turns out that for all $x \in C$

$$\langle \nabla V(x), f(x) \rangle = -\lambda b_1 l^2 (x_2^1)^2 - (1 - \lambda) b_2 l^2 (x_2^2)^2 \leq 0 .$$

Thus, with (4.2), $u_C(x) = -\lambda b_1 l^2 (x_2^1)^2 - (1 - \lambda) b_2 l^2 (x_2^2)^2$ for all $x \in C$. At jumps, $V(g(x)) - V(x)$ is given by

$$\frac{l^2}{2} x_2^T (M^T \mathcal{J} M - \mathcal{J}) x_2 + \gamma l (1 - \cos(s^*)) - \gamma \lambda l (1 - \cos(x_1^1)) - \gamma (1 - \lambda) l (1 - \cos(x_1^2)) ,$$

where $s^* = \arg \min_{s \in \{x_1^1, x_1^2\}} \{1 - \cos(s)\}$. It follows that $V(g(x)) - V(x) \leq 0$, and for each point in D , defines u_D .

To apply hybrid LaSalle's invariance principle, compute

$$u_C^{-1}(0) = \{x \in O \mid x_2^1 = x_2^2 = 0\} ,$$

$$u_D^{-1}(0) = \{x \in O \mid x_1^1 = x_1^2, x_2^T (M^T \mathcal{J} M - \mathcal{J}) x_2 = 0\} .$$

The set $u_C^{-1}(0)$ follows from the definition of C and u_C above. To find $u_D^{-1}(0)$ note that points $x \in D$ with $x_1^1 = x_1^2$ are such that $s^* = x_1^1 = x_1^2$, and consequently, u_D is zero only if $x_2^T (M^T \mathcal{J} M - \mathcal{J}) x_2 = 0$. The remaining points in D are such that $x_1^1 \neq x_1^2$. Since the first term of u_D is nonpositive and the remaining terms are strictly negative for $x_1^1 \neq x_1^2$, points with $x_1^1 \neq x_1^2$ are not in $u_D^{-1}(0)$. When g acts on $u_D^{-1}(0)$, the angles are mapped to their same value and the velocities are mapped to $(x_2^1)^+, (x_2^2)^+$ with $(x_2^1)^+ \leq (x_2^2)^+$. Using the jump rule (4.18) and the properties of M and \mathcal{J}

$$u_D^{-1}(0) \cap g(u_D^{-1}(0)) = \{x \in O \mid x_1^1 = x_1^2, x_2^1 = x_2^2\} .$$

By Theorem 4.14 with $\mathcal{U} = O$, every precompact solution converges to the largest weakly invariant set in (4.6) for some $r \in V(\mathcal{U})$ (with $G = g$). Solutions starting in $u_C^{-1}(0)$ and staying in the largest weakly invariant subset of (4.6) need to have same angles. Therefore, only points with $x_1^1 = x_1^2$ in $u_C^{-1}(0)$ qualify for the invariance property. It follows that

$$u_C^{-1}(0) \cup (u_D^{-1}(0) \cap g(u_D^{-1}(0))) = \{x \in O \mid x_1^1 = x_1^2, x_2^1 = x_2^2\} .$$

For every ξ in this set, there exists one discrete solution that stays in it. Then, precompact solutions approach

$$V^{-1}(r) \cap \{x \in O \mid x_1^1 = x_1^2, x_2^1 = x_2^2\}$$

for some $r = V(\mathcal{U})$. Note that the same conclusion holds when the jump map for the angles is the identity and the inequality condition for the angles in D is replaced by equality.

The invariance principle shows that solutions to the Newton's cradle system approach points with equal angles and velocities. The reason for this is that with the jump map considered above, the kinetic energy of the balls remains constant when the pendulums collide with equal velocity. This generates solutions that after such a collision, jump for all time (discrete solutions). This undesirable behavior can be removed by including the "spring effect" at collisions (or when the balls are touching). (Another option is to redefine the collision rule,

this is not pursue this here.) To model the “spring effect” we add temporal regularization by means of a timer τ with continuous dynamics $\dot{\tau} = 1 - \tau$, jump map $\tau^+ = 0$, and temporal regularization constant $\delta \in (0, 1)$.

The hybrid system for the model of the Newton’s cradle with temporal regularization has state $x = [x_1^1 \ x_1^2 \ x_2^1 \ x_2^2 \ \tau]^T$ and state space given by $O^\tau = \mathbb{R}^5$. The flow and jump sets under temporal regularization are given by

$$C^\tau := \{x \in O^\tau \mid x_1^1 \leq x_1^2 \text{ or } x_2^1 \leq x_2^2 \text{ or } \tau \in [0, \delta]\},$$

$$D^\tau := \{x \in O^\tau \mid x_1^1 \geq x_1^2, x_2^1 \geq x_2^2, \tau \geq \delta\}.$$

The continuous dynamics are given by $f^\tau(x)$ which is the vector function resulting from stacking the vector field $f(x)$ and the timer dynamics defined above. The jump mapping is given by $g^\tau(x)$, the vector function constructed by stacking the mapping $g(x)$ and the jump mapping for the timer.

For the energy function given by equation (4.20), the functions u_C and u_D , and their zero-level sets turn out to be the same as above but with the addition of the timer state τ .

By Theorem 4.14 with $\mathcal{U} = O^\tau$, every precompact solution converges to the largest weakly invariant set in (4.6) for some $r \in V(\mathcal{U})$ (with $G = g^\tau$). Note that in this case, $u_D^{-1}(0) \cap g^\tau(u_D^{-1}(0)) = \emptyset$. Then by Lemma 4.9 and Corollary 4.15(b) with $\mathcal{U} = O^\tau$, precompact solutions converge to the largest weakly invariant subset in

$$V^{-1}(r) \cap \mathcal{U} \cap u_C^{-1}(0) = V^{-1}(r) \cap \{x \in O^\tau \mid x_2^1 = x_2^2 = 0\}$$

for some $r \in V(\mathcal{U})$. From the continuous dynamics of the system, that largest weakly invariant subset is given for $r = 0$ and is equal to

$$\mathcal{A} := \{x \in O \mid x_1^i = x_2^i = 0, i = 1, 2, \tau \in [0, \delta]\}.$$

Hence, precompact solutions that stay in \mathcal{U} are such that the pendulums converge to the resting position. Local asymptotic stability of \mathcal{A} follows from Theorem 4.16. \square

Example 4.36 (pendulum swing-up with hybrid control) Consider an inverted pendulum on a cart controlled by an external input force \tilde{u} as shown in Figure 4.2(c). The variable x_1 is the pendulum angle ($x_1 = 0$ is the vertical upright position), x_2 is the angular velocity, x_3 is the cart position, and x_4 is the cart velocity. After a preliminary input feedback transformation of the form $\tilde{u} = \psi(x) + \phi(x)u$, a hybrid model of the resulting system can be written as

$$\dot{x} = f(x, u) \quad x \in C_\pi, \quad x^+ = g(x) \quad x \in D_\pi,$$

where

$$f(x, u) := [x_2 \quad \frac{\gamma}{l} \sin(x_1) - \frac{1}{l} \cos(x_1)u \quad x_4 \quad u]^T,$$

$$g(x) := [(x_1 - 2\pi\mathbb{Z}) \cap [-\pi, \pi] \quad x_2 \quad x_3 \quad x_4]^T,$$

$$C_\pi := \{x \in \mathbb{R}^4 \mid |x_1| \leq \pi + \mu\},$$

$$D_\pi := \{x \in \mathbb{R}^4 \mid |x_1| \geq \pi + \mu\}.$$

where μ is a positive constant, $\gamma > 0$ is the gravity constant, and $l > 0$ the length of the pendulum. The purpose of the jump mapping g is to keep the angle x_1 bounded (g remaps x_1 to the set $[-\pi, \pi]$ at every jump.)

The proposed hybrid swing-up strategy chooses the appropriate feedback control law depending on the location of the pendulum. When the pendulum is in the region i , the control law is given by $k(\cdot, i)$, $i \in Q := \{1, 2, 3\}$. Let $W(x)$ be the energy of the pendulum and c_1, c_2 be constants that are sufficiently close to but larger than $\min_{x \in \mathbb{R}^4} W(x)$ and satisfy $c_1 > c_2$. Take U_{3a} and U_{3b} , $U_{3a} \subset U_{3b}$, to be closed neighborhoods of the origin in \mathbb{R}^2 contained in $[-\pi, \pi] \times \mathbb{R}$, such that for the system $\dot{x} = f(x, u)$, the control law $k(\cdot, 3)$ renders the

origin (in \mathbb{R}^4) locally asymptotically stable with basin of attraction containing $U_{3b} \times \mathbb{R}^2$ and such that solutions starting in $U_{3a} \times \mathbb{R}^2$ do not reach the boundary of $U_{3b} \times \mathbb{R}^2$.

Define three regions by the sets Ω_i and C_i ($\Omega_i \subset C_i$), $i \in Q$, as follows

$$\begin{aligned}\Omega_1 &= C_1 = \{x \in \mathbb{R}^4 \mid W(x) \leq c_1\} \\ \Omega_3 &= U_{3a} \times \mathbb{R}^2, C_3 = U_{3b} \times \mathbb{R}^2 \\ \Omega_2 &= \left\{x \in \overline{\mathbb{R}^2 \setminus U_{3a}} \times \mathbb{R}^2 \mid W(x) \geq c_1\right\} \\ C_2 &= \left\{x \in \overline{\mathbb{R}^2 \setminus U_{3a}} \times \mathbb{R}^2 \mid W(x) \geq c_2\right\}\end{aligned}$$

As previously stated, the control law in the set C_3 is given by $k(\cdot, 3)$. In the region defined by C_2 , the control $k(\cdot, 2)$ is designed to inject enough energy into the system so that U_{3a} is reached. The control law for the set C_1 is given by $k(\cdot, 1)$ which is designed to drive the system away from the resting condition (e.g. $k(x, 1) = 1$).

The state of the closed-loop system is denoted by (x, q) where $x \in \mathbb{R}^4$ and $q \in Q$. Define the state space $O := \mathbb{R}^5$. For each $i \in Q$, $D_i := \overline{\mathbb{R}^4 \setminus C_i} \cap C_\pi$, $D := \{(x, q) \in \mathbb{R}^4 \times Q \mid x \in D_q\} \cup D_\pi$, $C := \{(x, q) \in \mathbb{R}^4 \times Q \mid x \in C_q \cap C_\pi\}$, and $\Psi(q) := \cup_{p < q, p \in Q} \Omega_p$. The closed-loop system defines a hybrid system \mathcal{H}_I that can be written as

$$\begin{aligned}\dot{x} &= f(x, k(x, q)), \quad \dot{q} = 0 \quad (x, q) \in C, \\ \begin{bmatrix} x \\ q \end{bmatrix}^+ &= G(x, q) \quad (x, q) \in D,\end{aligned}$$

where $G(x, q)$ is defined by

$$\begin{cases} \begin{bmatrix} g(x) \\ q \end{bmatrix} & x \in D_\pi \setminus D_q \\ G_1(x, q) & x \in (D_q \cap \Psi(q)) \setminus D_\pi \\ G_2(x, q) & x \in D_q \setminus (\Psi(q) \cup D_\pi) \\ \left\{ \begin{bmatrix} g(x) \\ q \end{bmatrix}, G_1(x, q) \right\} & x \in D_q \cap \Psi(q) \cap D_\pi \\ \left\{ \begin{bmatrix} g(x) \\ q \end{bmatrix}, G_2(x, q) \right\} & x \in (D_q \setminus \Psi(q)) \cap D_\pi \end{cases}$$

where

$$\begin{aligned}G_1(x, q) &:= \left[\begin{array}{c} x \\ \{p \in Q \mid x \in \Omega_p\} \end{array} \right], \\ G_2(x, q) &:= \left[\begin{array}{c} x \\ \{p \in Q \mid p > q, x \in \Omega_p\} \end{array} \right].\end{aligned}$$

Note that the hybrid system \mathcal{H}_I satisfies (A0)-(A3). Note that there exists initial conditions for which solutions are nonunique. For instance, there exist $(\xi, 1) \in (\Omega_1 \cap \Omega_2) \times Q$ such that either q immediately jumps to 2 and then flows according to $\dot{x} = f(x, k(x, 2))$ or else flows according to $\dot{x} = f(x, k(x, 1))$ while remaining in Ω_1 until flows are not longer possible and then q jumps to 2.

To show that solutions converge to the compact set $\mathcal{A} := \{0\} \times \{3\} \subset O$. Consider the continuously differentiable function $V(x, q) = 1/q$. Since the continuous dynamics of q are such that $q(t, j)$ remains constant during flows, V does not increase along flows and u_C is identically zero. The design of the controller guarantees that solutions starting with initial x and q in $\Omega_1 \times \{1\}$ will sequentially transition from region 1 to region 2 and

finally to region 3. Solutions starting with arbitrary initial conditions will be mapped after the first jump to $\mathcal{U} := \cup_{i=1}^3 \Omega_i \times \{i\}$ and from there on will follow the transition rule. Then

$$u_D(x, q) = \frac{1}{\eta} - \frac{1}{q} < 0$$

where $\eta \in Q$, $\eta > q$, $(x, q) \in \mathcal{U}$. By Theorem 4.14, precompact solutions that stay in \mathcal{U} approach the largest weakly invariant set in (4.6) for some $r \in V(\mathcal{U})$. From the previous definitions, $u_C^{-1}(0) = C$, $u_D^{-1}(0) = \emptyset$. Then the set (4.6) is given by $V^{-1}(r) \cap \mathcal{U} \cap C$. By construction of the controller, the largest weakly invariant set contained in this set is for $r = \frac{1}{3}$ and is equal to \mathcal{A} . Thus, by Theorem 4.14, precompact solutions to \mathcal{H}_I converge to \mathcal{A} , i.e. pendulum in the straight-up position and zero position and velocity of the cart.

The same result can be obtained by means of detectability. Let $K = C_3 \times \{3\}$. Every solution (x, q) satisfying $\text{rge}(x, q) \subset K$ has $q(t, j) = 3$ for all $(t, j) \in \text{dom}(x, q)$. Since the control law in C_3 is the local stabilizer for the origin (in \mathbb{R}^4), the compact set \mathcal{A} is stable relative to K and the distance to \mathcal{A} is detectable relative to K for \mathcal{H}_I . Given a precompact solution (x, q) to \mathcal{H}_I , let $K' = K \cap \text{rge}(x, q)$. Detectability and stability of \mathcal{A} relative to K' automatically holds since $K' \subset K$. Then, by Corollary 4.32, with ω being the distance to K , precompact solutions x to \mathcal{H}_I converge to \mathcal{A} . Note that the meagre-limsup conditions hold for ω since, by design of the controller, for each solution (x, q) there exists T^* such that $(x(t, j), q(t, j)) \in K'$ for all $t + j \geq T^*$, $(t, j) \in \text{dom}(x, q)$. \square

Example 4.37 (disturbance rejection) Consider the control of a nonlinear system $\dot{x} = f(x, u, d)$ with state x , control input u , and disturbance input d , by a hybrid controller \mathcal{H}_c with state x_c . Let the closed-loop hybrid system \mathcal{H}_{cl} be

$$\dot{\xi} = f_{cl}(\xi, d) \quad \xi \in C_{cl}, \quad \xi^+ = g_{cl}(\xi) \quad \xi \in D_{cl},$$

with output $y = h_{cl}(\xi)$, where $\xi := [x, x_c]^T \in \mathbb{R}^{n_c}$, $f_{cl} : \mathbb{R}^{n_c} \times \mathbb{R}^m \rightarrow \mathbb{R}^{n_c}$, $g_{cl} : \mathbb{R}^{n_c} \rightarrow \mathbb{R}^{n_c}$, and $h_{cl} : \mathbb{R}^{n_c} \rightarrow \mathbb{R}^{m_c}$ are continuous. Suppose that the following holds for \mathcal{H}_{cl} .

Assumption 4.38 (\mathcal{H}_{cl} conditions 1)

1. There exists a continuously differentiable, positive definite, radially unbounded function $V_{cl} : \mathbb{R}^{n_c} \rightarrow \mathbb{R}_{\geq 0}$ and $\gamma_{cl} \geq 0$ such that

$$\langle \nabla V_{cl}(\xi), f_{cl}(\xi, u_{cl}) \rangle \leq -|h_{cl}(\xi)|^2 + \gamma_{cl}^2 |u_{cl}|^2$$

$$\forall \xi \in C_{cl}, u_{cl} \in \mathbb{R}^m; \text{ and } V_{cl}(g_{cl}(\xi)) \leq V_{cl}(\xi) \quad \forall \xi \in D_{cl}.$$

2. The hybrid closed-loop system \mathcal{H}_{cl} with $d \equiv 0$ is such that the distance of the state ξ to the origin (in \mathbb{R}^{n_c}) is detectable relative to the set $K_{cl} := \{\xi \in \mathbb{R}^{n_c} \mid h_{cl}(\xi) = 0\}$.

Let $\dot{x}_d = f_d(x_d, u_d)$ with output $y_d = h_d(x_d)$ be the model for the disturbance d where $x_d \in \mathbb{R}^n$; $f_d : \mathbb{R}^n \times \mathbb{R}^{m_c} \rightarrow \mathbb{R}^n$, $h_d : \mathbb{R}^n \rightarrow \mathbb{R}^{m_c}$ are continuous. Below, $\|\cdot\|_2$ denotes the \mathcal{L}_2 -norm and $\|\cdot\|_\infty$ denotes the \mathcal{L}_∞ -norm.

Assumption 4.39 (disturbance model conditions) The disturbance model satisfies

1. There exist $\gamma_d \geq 0$ and $\rho_d \in \mathcal{K}_\infty$ s.t. $\|y_d\|_2 \leq \gamma_d \|u_d\|_2 + \rho_d(|x_d(0)|)$, $\|x_d\|_\infty \leq \rho_d(\|y_d\|_2 + \|u_d\|_2 + |x_d(0)|)$ $\forall u_d \in \mathcal{L}_2, x_d(0) \in \mathbb{R}^n$.
2. When $u_d \equiv 0$, the distance of the state x_d to the origin (in \mathbb{R}^n) is detectable relative to the set $K_d := \{x_d \in \mathbb{R}^n \mid h_d(x_d) = 0\}$.

Under the following additional assumptions:

Assumption 4.40 (\mathcal{H}_{cl} conditions 2) C_{cl}, D_{cl} are relatively closed in \mathbb{R}^{n_c} , $C_{cl} \cup D_{cl} = \mathbb{R}^{n_c}$, and $g_{cl}(D_{cl}) \cap D_{cl} = \emptyset$;

Assumption 4.41 (gain condition) $\gamma_d \gamma_{cl} < 1$;

the origin of the closed-loop system, denoted by \mathcal{H} , resulting of interconnecting \mathcal{H}_{cl} with the disturbance model is globally asymptotically stable.

To show the claim, let $\zeta = [\xi^T, x_d^T]^T$ be a maximal solution to \mathcal{H} and let $E := \text{dom } \zeta \cap ([0, T] \times \{0, \dots, J\})$ be a compact subset of $\text{dom } \zeta$ (Recall that it is possible to write $E = \cup_{i=0}^J [t_i, t_{i+1}] \times \{i\}$ where $t_0 = 0$ and $t_{J+1} = T$.) By Assumption 4.38.1, it follows that

$$\int_0^T |h_{cl}(\xi(t, j(t)))|^2 dt \leq \gamma_{cl}^2 \int_0^T |h_d(x_d(t, j(t)))|^2 dt + \sum_{i=0}^J [-V_{cl}(\xi(t_{i+1}, j(t_i))) + V_{cl}(\xi(t_i, j(t_i)))] .$$

Note that by Assumption 4.40 and Lemma 4.9, for every $0 \leq i \leq J$, the intervals $[t_i, t_{i+1}] \subset [0, T]$ have non-zero length, and therefore, contribute to the integrals above. Using Assumption 4.38.1 and positive definiteness of V_{cl}

$$(\|h_{cl}(\xi)\|_2^S)^2 \leq V_{cl}(\xi(0, 0)) + \gamma_{cl}^2 (\|h_d(x_d)\|_2^S)^2 ,$$

where $\|h_d(x_d)\|_2^S$ denotes $\sqrt{\int_0^T |h_d(x_d(t, j(t)))|^2 dt}$.

Let $u_d(t) = h_{cl}(\xi(t, j(t)))$ for all $t \in [0, T]$, $u_d(t) = 0$ for all $t > T$. For each $t \in [0, T]$, u_d generates $y_d(t) = h_d(x_d(t, j(t)))$. Then, using u_d, y_d in Assumption 4.39.1, the bound on the norm of $h_{cl}(\xi)$ and $h_d(x_d)$ are

$$\begin{aligned} \|h_{cl}(\xi)\|_2^S &\leq \frac{1}{1 - \gamma_d \gamma_{cl}} \left(\sqrt{V_{cl}(\xi(0, 0))} + \gamma_{cl} \rho_d(|x_d(0, 0)|) \right) , \\ \|h_d(x_d)\|_2^S &\leq \frac{1}{1 - \gamma_d \gamma_{cl}} \left(\gamma_d \sqrt{V_{cl}(\xi(0, 0))} + \rho_d(|x_d(0, 0)|) \right) . \end{aligned}$$

By Assumption 4.41, $\frac{1}{1 - \gamma_d \gamma_{cl}} \in (0, \infty)$. Integrating the flow condition in Assumption 4.38.1 along $\xi(t, j)$ from 0 to some t , $(t, j(t)) \in \text{dom } \zeta$, $(t, j(t)) \preceq (T, J)$, yields

$$\int_0^t \frac{d}{d\tau} V_{cl}(\xi(\tau, j(\tau))) d\tau \leq \gamma_{cl}^2 (\|h_d(x_d)\|_2^S)^2 .$$

Using the nonincreasing condition at jumps gives

$$V_{cl}(\xi(t, j(t))) \leq \gamma_{cl}^2 (\|h_d(x_d)\|_2^S)^2 + V_{cl}(\xi(0, 0)) .$$

Since V_{cl} is radially unbounded, there exists $\alpha \in \mathcal{K}_\infty$ that satisfies $\alpha(|z|) \leq V_{cl}(z)$ for all $z \in \mathbb{R}^{n_c}$. It follows that

$$\begin{aligned} \|\xi\|_\infty^S &\leq \alpha^{-1} \left(V_{cl}(\xi^0) + \gamma_1 \left(\gamma_d \sqrt{V_{cl}(\xi^0)} + \rho_d(|x_d^0|) \right)^2 \right) \\ \|x_d\|_\infty^S &\leq \rho_d \left(\gamma_2 \sqrt{V_{cl}(\xi^0)} + \gamma_3 \rho_d(|x_d^0|) + |x_d^0| \right) \end{aligned}$$

where $\|\xi\|_\infty^S$ means $\sup_{(t,j) \in S} |\xi(t, j)|$, $\gamma_1 := \frac{\gamma_{cl}^2}{(1 - \gamma_d \gamma_{cl})^2}$, $\gamma_2 := \frac{1 + \gamma_d}{1 - \gamma_d \gamma_{cl}}$, $\gamma_3 := \frac{1 + \gamma_{cl}}{1 - \gamma_d \gamma_{cl}}$, $\xi^0 = \xi(0, 0)$, and $x_d^0 = x_d(0, 0)$. Note that the bounds for the norm of the states ξ , x_d and the outputs $h_{cl}(\xi)$, $h_d(x_d)$ are independent of the compact hybrid time domain S . Therefore those bounds can be extended to the entire domain $\text{dom } \zeta$.

Since ζ is maximal and bounded, and since $C_{cl} \cup D_{cl} = \mathbb{R}^{n_c}$, by Proposition 2.1 in [39], ζ must be complete, i.e. ζ is precompact. Thus, the origin (in $\mathbb{R}^{n_c} \times \mathbb{R}^n$) is stable.

Let $\ell(\zeta) = |h_{cl}(\xi)|^2 + |h_d(x_d)|^2$. By Assumption 4.40 and Lemma 4.9, the elapsed time between jumps is uniformly bounded below by a positive constant. Since ζ is complete, the projection of $\text{dom } \zeta$ on $\mathbb{R}_{\geq 0}$ is unbounded and only condition (a) of the meagre-limsup conditions needs to be checked. Since the integral of $|h_{cl}(\xi)|^2$ and $|h_d(x_d)|^2$ over the domain of ζ are finite, $t \mapsto \ell(\zeta(t, j(t)))$ is weakly meagre. Define $K := K_{cl} \times K_d$ and $\mathcal{A} := \{0\} \subset \mathbb{R}^{n_{cl}} \times \mathbb{R}^{n_d}$. Then, using Assumption 4.39.2 and Assumption 4.38.2, \mathcal{A} is stable relative to K and the distance to \mathcal{A} is detectable on K . By Corollary 4.32 with $\omega = \ell$, ζ converges to \mathcal{A} . Since this holds for every solution ζ to \mathcal{H} , \mathcal{A} is globally asymptotically stable. \square

4.4 Summary

Concepts of stability and invariance for hybrid system were introduced. The main new stability and convergence tools for hybrid systems \mathcal{H} were presented: hybrid Lyapunov theorem and hybrid LaSalle's invariance principle. Special cases of these results and more general invariance principles were derived. In particular, invariance principles involving functions not necessarily obtained from Lyapunov functions were stated, and versions of these involving several trajectories and a single trajectory were proposed. Connections of the invariance principles to observability and detectability were given. Finally, the results were exercised in four examples involving hybrid systems exhibiting different types of behavior.

4.5 Notes and references

For more details about Clarke's generalized derivative see [27].

Theorem 4.14 implies the original invariance principle of LaSalle, [59, Theorem 1], by considering $F = f$, $C = O$, and $D = \emptyset$. Taking $C = O$ and $D = \emptyset$ but letting F be a set-valued map satisfying (A2) reduces Theorem 4.14 to the invariance principle in [81, Theorem 2.11]. Theorem 4.17 implies the invariance principle as stated by LaSalle in [60, Chapter 2, Theorem 6.4] — the general notion of a derivative used in [60, Chapter 2, Theorem 6.4] can take the place of u_c in inequality (4.4); see [60, Chapter 2, Lemma 6.2] and the comment following it. Theorem 4.17 also implies [9, Proposition 3], by using the nonpathological derivative of the Lyapunov function as u_c in (4.4) and relying on the solutions closure property, [9, Definition 5], to satisfy our hybrid basic conditions.

Considering $C = \emptyset$, $G = g$ where g is a function, and $D = O$ reduces Theorem 4.14 to a discrete-time systems invariance principle as stated in [60, Theorem 6.3, Chapter 1]. Indeed, the term $G(u_D^{-1}(0))$ in (4.6) becomes irrelevant for purely discrete-time systems. (But is important in truly hybrid systems; recall Example 4.19.)

Theorems 4.17, 4.14 and their corollaries can also be used to deduce convergence of trajectories of switched systems. This is possible because these results can be stated for a larger (and rather more abstract) class of hybrid systems given by only hybrid trajectories satisfying certain properties, which are referred as *sets of hybrid trajectories* in [89]. The conditions that the elements in the sets of hybrid trajectories need to satisfy are summarized in the following assumption.

Assumption 4.42 (sets of hybrid trajectories conditions) *Given a set of hybrid trajectories $\mathcal{S}_{\mathcal{H}}$ (without data associated):*

(B1) *$\text{rge } x \subset O$ for all $x \in \mathcal{S}_{\mathcal{H}}$,*

(B2) *for any $x \in \mathcal{S}_{\mathcal{H}}$ and any $(\bar{t}, \bar{j}) \in \text{dom } x$ we have $\bar{x} \in \mathcal{S}_{\mathcal{H}}$, where $\text{dom } \bar{x} = \{(t, j) \mid (t + \bar{t}, j + \bar{j}) \in \text{dom } x\}$ and $\bar{x}(t, j) = x(t + \bar{t}, j + \bar{j})$ for all $(t, j) \in \text{dom } \bar{x}$,*

(B3) for any locally eventually bounded (with respect to O) sequence $\{x_i\}_{i=1}^{\infty}$ of elements of $\mathcal{S}_{\mathcal{H}}$ that converges graphically, the limit is an element of $\mathcal{S}_{\mathcal{H}}$.

Assumption (B1) identifies O as the state space of the system. (B2) says that tails of trajectories in $\mathcal{S}_{\mathcal{H}}$ are also in $\mathcal{S}_{\mathcal{H}}$, and reduces to the standard semi-group property under further existence and uniqueness conditions. (B3) guarantees a kind of semicontinuous dependence of trajectories on initial conditions. More specifically, given a sequence of $x_i \in \mathcal{S}_{\mathcal{H}}$ with $x_i(0,0)$ convergent to some point x^* , a general property of set convergence (see [79, Theorem 4.18] or Section III in [39]) implies that one can pick a subsequence of x_i 's that converge graphically. Under the eventual local boundedness assumption, (B3) guarantees that the graphical limit of that subsequence, say x , is an element of $\mathcal{S}_{\mathcal{H}}$. As from the very definition of graphical convergence it also follows that $x(0,0) = x^*$, this essentially means that a limit of graphically convergent trajectories with initial points convergent to x^* is a trajectory with initial point x^* . (However, this does not mean that every trajectory from x^* is a limit of some trajectories with initial points different from, but convergent to x^* .) It follows from the results in [39] that the solution set of a hybrid system \mathcal{H} satisfying the hybrid basic conditions automatically satisfies Assumption 4.42.

Various subsets of $\mathcal{S}_{\mathcal{H}}$ also satisfy Assumption 4.42. A general result is stated first followed by examples.

Corollary 4.43 (a subset of a set of hybrid trajectories satisfying Assumption 4.42) *Suppose that \mathcal{H} satisfies the hybrid basic conditions. Let $\phi : \mathbb{R}_{\geq 0} \times \mathbb{N} \times \mathbb{R}_{\geq 0} \times \mathbb{N} \rightarrow [-\infty, \infty]$ be a lower semicontinuous function. Then the subset of $\mathcal{S}_{\mathcal{H}}$ consisting of all solutions x to \mathcal{H} such that*

$$(\diamond) \phi(s, i, t, j) \leq 0 \text{ for all } (s, i), (t, j) \in \text{dom } x,$$

satisfies (B3) of Assumption 4.42. If furthermore ϕ is such that for some function Φ , $\phi(s, i, t, j) = \Phi(t - s, j - i)$ for all $(s, i, t, j) \in \mathbb{R}_{\geq 0} \times \mathbb{N} \times \mathbb{R}_{\geq 0} \times \mathbb{N}$, then the subset of solutions satisfies (B2) of Assumption 4.42.

Proof. If $\{x_k\}_{k=1}^{\infty}$ is a locally eventually bounded and a graphically convergent sequence of elements of $\mathcal{S}_{\mathcal{H}}$, then by Lemma 4.3 in [38], the limit, which is denoted by x , is a solution to \mathcal{H} . Moreover, the sets $\text{dom } x_k$ converge (in the sense of set convergence) to $\text{dom } x$; see the proof of Lemma 4.3 in [39]. In particular, given any $(s, i), (t, j) \in \text{dom } x$, there exist $(s_k, i_k), (t_k, j_k) \in \text{dom } x_k$ for all large enough k 's, so that $(s_k, i_k) \rightarrow (s, i)$ and $(t_k, j_k) \rightarrow (t, j)$. If each of x_k 's satisfies (\diamond) , then by lower semicontinuity of ϕ , so does x . This shows the first claim of the corollary. Now, suppose that $x \in \mathcal{S}_{\mathcal{H}}$ satisfies (\diamond) and that $\phi(s, i, t, j) = \Phi(t - s, j - i)$ for all (s, i, t, j) . For any $(T, J) \in \text{dom } x$, let $\bar{x}(t, j) := x(t + T, j + J)$. Then, for any $(s, i), (t, j) \in \text{dom } \bar{x}$, $\phi(s, i, t, j)$ equals

$$\Phi(t - s, j - i) = \Phi((t + T) - (s + T), (j + J) - (i + J)) = \phi(s + T, i + J, t + T, j + J) \leq 0$$

since $(s + T, i + J), (t + T, j + J) \in \text{dom } x$. This shows the second claim. \square

To illustrate Corollary 4.43, consider

$$\phi(s, i, t, j) = \begin{cases} a(j - i) - b(t - s) - c & i < j \\ -\infty & i \geq j. \end{cases}$$

Note that for such ϕ , $\phi(s, i, t, j) = \Phi(t - s, j - i)$ with $\Phi(\tau, \iota) = a\iota - b\tau - c$ if $\iota > 0$, $\Phi(\tau, \iota) = -\infty$ if $\iota \leq 0$. When $a = c = 1$ and $b = 1/\tau_D > 0$, then (\diamond) reduces to $(j - i - 1)\delta \leq t - s$ when $i < j$, which requires that the jumps be separated by at least τ_D amount of ‘‘dwell-time’’. This class of solutions is known as dwell-time solutions. Bounds of the type $j - i \leq b(t - s) + c$ for $i < j$ describe solutions with bounded average dwell time. See [46] and [48].

An invariance principle for switched systems is now stated. Let $\dot{x}(t) = f_{q(t)}(x(t))$, $q(t) \in Q := \{1, 2, \dots, m\}$ be a switched system and \mathcal{H} be a corresponding hybrid system with data $(\dot{x}, \dot{q}) = (f_q(x), 0)$, $(x^+, q^+) \in (x, Q)$, $C = D = O \times Q$. Let $\mathcal{S}_{\mathcal{H}}(\tau_D)$ be the set of all solutions to this hybrid system with dwell-time τ_D .

Proposition 4.44 (invariance principle for switched systems under dwell-time switching) *For each $q \in Q$ let $f_q : \mathbb{R}^n \rightarrow \mathbb{R}^n$ be a continuous function and $V_q : \mathbb{R}^n \rightarrow \mathbb{R}_{\geq 0}$ be a continuously differentiable function such that $\nabla V_q(x) \cdot f_q(x) \leq 0$ for all $x \in \mathbb{R}^n$. Let $\mathcal{S}_{\mathcal{H}}^* \subset \mathcal{S}_{\mathcal{H}}(\tau_D)$ for some $\tau_D > 0$ be such that Assumption 4.42 holds for $\mathcal{S}_{\mathcal{H}}^*$ and $V_{q(t,j+1)}(x(t,j+1)) \leq V_{q(t,j)}(x(t,j))$ for all solutions $(x,q) \in \mathcal{S}_{\mathcal{H}}^*$. Then each precompact solution $(x,q) \in \mathcal{S}_{\mathcal{H}}^*$ approaches the largest subset K of $\bigcup_{q=1}^m \{\nabla V_q(x) \cdot f_q(x) = 0\}$ that is invariant in the following sense: for each $\xi \in K$ there exists $\varepsilon > 0$ and: i) $q \in Q$ and a solution x to $\dot{x}(t) = f_q(x(t))$ such that $x(0) = \xi$ and $x(t) \in K$ for all t in $[0, \varepsilon]$; ii) $q \in Q$ and a solution x to $\dot{x}(t) = f_q(x(t))$ such that $x(0) = \xi$ and $x(t) \in K$ for all t in $(-\varepsilon, 0]$.*

Proof. The bound (4.4) holds for each $(x,q) \in \mathcal{S}_{\mathcal{H}}^*$ with $u_c(x,q) = \nabla V_q(x) \cdot f_q(x)$ and $u_d(x,q) = 0$ for all $(x,q) \in \mathbb{R}^n \times Q$. Corollary 4.15 implies that (x,q) approaches L , the largest weakly invariant (with respect to $\mathcal{S}_{\mathcal{H}}^*$, and thus with respect to the larger set $\mathcal{S}_{\mathcal{H}}(\tau_D)$) subset of $\bigcup_{q \in Q} \{\nabla V_q(x) \cdot f_q(x) = 0\} \times \{q\}$. Thus x approaches the projection L' of L onto \mathbb{R}^n . It remains to show that this projection is invariant in the sense stated in the proposition. Pick any $x^0 \in L'$ and a corresponding $(x^0, q^0) \in L$. By weak forward invariance of L , there exists a complete $(x,q) \in \mathcal{S}_{\mathcal{H}}(\tau_D)$ with $(x(0,0), q(0,0)) = (x^0, q^0)$ and $(x(t,j), q(t,j)) \in L$ for all $(t,j) \in \text{dom}(x,q)$. As $(x,q) \in \mathcal{S}_{\mathcal{H}}(\tau_D)$, either $(t,0) \in \text{dom}(x,q)$ and $q(t,0) = q^0$ for some $\varepsilon > 0$ and all $t \in [0, \varepsilon]$, in which case $\dot{x}(t,0) \in f_{q^0}(x(t,0))$ and $x(t,0) \in L'$ for $t \in [0, \varepsilon]$, or $(0,1) \in \text{dom}(x,q)$ in which case $\dot{x}(t,1) \in f_{q(0,1)}(x(t,1))$ and $x(t,1) \in L'$ for $t \in [0, \tau_D]$. Either $x(\cdot, 0)$ or $x(\cdot, 1)$, with the corresponding values of q , provide the needed (forward) solutions. Arguments involving backward invariance are similar. \square

When the functions V_1, V_2, \dots, V_m are identical, the decrease condition $V_{q(t,j+1)}(x(t,j+1)) \leq V_{q(t,j)}(x(t,j))$ is trivially satisfied for any solution of the switched system. Thus, the result above implies that any solution with a positive dwell-time (i.e., an element of $\mathcal{S}_{\mathcal{H}}(\tau_D)$ for some $\tau_D > 0$) approaches the set K . This is essentially the invariance principle for switched systems as stated in [10, Theorem 1]; our result is actually stronger as the concept of invariance in Proposition 4.44 involves both forward and backward parts, and not forward or backward, as in [10]. For related results involving multiple Lyapunov functions, see [46].

Regarding truly hybrid systems, a result most closely related to our work, in particular to Theorem 4.14, is [67, Theorem IV.1]. The first difference is in the assumptions. [67, Theorem IV.1] assumes continuous dependence of solutions on initial conditions, properties quite hard to verify by looking at the data (see [18] and [21] for some results in that direction). Theorem 4.14 of this paper relies on semicontinuous dependence, both weaker and easier to verify (given by the hybrid basic conditions). Another difference is the sharper notion of invariance (which includes backward invariance) used in Theorem 4.14 and the presence of the term $G(u_D^{-1}(0))$ in (4.6) which leads to a tighter characterization of the set to which trajectories converge. For instance, Example 4.19 can be used to compare the invariance principles in Section 4.2.3 with the one in [67]. For that particular example, the invariance principle in [67] only concludes that the solutions converge to the unit circle, while the invariance principle in Corollary 4.15 concludes that the convergence set is the solution itself.

Weak meagreness was used previously by Logemann et al. in [65] to formulate extensions of the Barbatal's lemma and resulting invariance principles. A reduction of the invariance principles involving the meagre-limsup conditions in Section 4.2.3 to continuous-time systems is possible. Lemma 4.20 implies [81, Theorem 2.10] (which in turn implies the result of [20]) because condition (*) of Lemma 4.20 is satisfied for solutions of differential inclusions discussed in [81] and the set E_{x,ℓ_c} is exactly $\{z \in \overline{\text{rge } x} \mid \ell_c(z) = 0\}$ when ℓ_c is lower semicontinuous, as assumed in [81, Theorem 2.10].

As discussed in [62], the detectability concept in Definition 4.28 can be understood as x having an ω -limit point in \mathcal{A} .

The jump map for the Newton's cradle system in Example 4.35 is as the one in Section 2.2.6 of [103]. The "spring effect" at collisions missing from the initial model of the Newton's cradle is discussed by Herrmann and Seitz in [45].

For a possible design of the control law $k(\cdot, 3)$ in Example 4.36, see [99].

Finally, the proof of Theorem 4.2 follows from the proof of Theorem 4.16 in Section B.2. For the proof of Theorem 4.27 see the proof of Theorem 4.31 in Section B.2. Corollary 4.22 and Corollary 4.23 follow from combining Lemma 4.20, Theorem 4.17 and Corollary 4.18. The remainder proofs associated to the results in this chapter can be found in Section B.2.

Chapter 5

Robustness of Hybrid Control

In this chapter, robustness properties of asymptotic stability of compact sets for closed-loop system resulting from hybrid control of nonlinear systems are presented. Constructive models for the resulting closed-loop systems are proposed for a class of perturbations that arise in real-world implementations of hybrid control systems.

5.1 Hybrid control of nonlinear systems

Over the last fifteen years, researchers have begun to recognize the extra capabilities of hybrid control systems compared to classical continuous-time control systems. For example, it is now well-known that hysteresis switching control can stabilize large classes of nonholonomic systems even though stabilization is impossible using time-invariant continuous state feedback, and robust stabilization is impossible using time-invariant locally bounded feedback. Also, sample and hold control (a special type of hybrid feedback) can be used to achieve stabilization that is robust to measurement noise and fast sensor/actuator dynamics, even if such robustness is impossible using purely continuous-time feedback.

For nonlinear control systems

$$\dot{x} = f_p(x, u) \quad (5.1)$$

where the state x of (5.1) takes value in \mathbb{R}^{n_p} and the function f_p is defined as a map from $\mathbb{R}^{n_p} \times \mathbb{R}^m$ to \mathbb{R}^{n_p} , robustness of hybrid control to perturbations is characterized. It is assumed that the nonlinear system in (5.1) satisfies the following mild assumption.

Assumption 5.1 (regularity properties of controlled nonlinear system)

The function $f_p : \mathbb{R}^{n_p} \times \mathbb{R}^m \rightarrow \mathbb{R}^{n_p}$ is continuous.

Hybrid controllers for (5.1) are denoted by \mathcal{H}_c , have a state given by x_c taking value in \mathbb{R}^{n_c} , and have continuous and discrete dynamics modeled by a flow map f_c , a flow set C_c , a jump map G_c , and a jump set D_c . The state space is given by $O := \mathbb{R}^{n_p} \times \mathbb{R}^{n_c}$. Note that x_c can contain both continuous and discrete states.

As in (2.1), the hybrid controller \mathcal{H}_c is represented in the suggestive form

$$\mathcal{H}_c : \quad \begin{cases} \dot{x}_c &= f_c(x, x_c) & (x, x_c) \in C_c \\ x_c^+ &\in G_c(x, x_c) & (x, x_c) \in D_c . \end{cases} \quad (5.2)$$

The output of \mathcal{H}_c , i.e., the input u of (5.1), is a function of x and x_c given by $\kappa : \mathbb{R}^{n_p} \times \mathbb{R}^{n_c} \rightarrow \mathbb{R}^m$. A shorthand notation for a hybrid controller \mathcal{H}_c will be $\mathcal{H}_c = (O, f_c, C_c, G_c, D_c, \kappa)$.

The closed-loop system resulting from controlling the nonlinear system (5.1) with the hybrid controller \mathcal{H}_c in (5.2) is a hybrid system which is denoted by \mathcal{H}_{cl} , its state is $\zeta := [x \ x_c]^T$, and it can be written as

$$\mathcal{H}_{cl} : \quad \zeta \in O \quad \begin{cases} \dot{\zeta} &= f(\zeta) & \zeta \in C_c \\ \zeta^+ &\in G(\zeta) & \zeta \in D_c \end{cases} \quad (5.3)$$

where

$$f(\zeta) := \begin{bmatrix} f_p(x, \kappa(x, x_c)) \\ f_c(x, x_c) \end{bmatrix}, \quad G(\zeta) := \begin{bmatrix} x \\ G_c(x, x_c) \end{bmatrix}. \quad (5.4)$$

The hybrid controller \mathcal{H}_c is assumed to satisfy the following mild regularity conditions.

Assumption 5.2 (regularity properties of \mathcal{H}_c) *The following conditions hold for \mathcal{H}_c :*

1. *The sets C_c and D_c are closed subsets of O .*
2. *The functions $\kappa : O \rightarrow \mathbb{R}^m$ and $f_c : \mathbb{R}^{n_p} \times \mathbb{R}^{n_c} \rightarrow \mathbb{R}^{n_c}$ are continuous.*
3. *The set-valued mapping $G_c : O \rightrightarrows \mathbb{R}^{n_c}$ is outer semicontinuous and G_c is nonempty for all $\zeta \in D_c$.*

This conditions guarantee that the closed-loop system \mathcal{H}_{cl} satisfies the hybrid basic conditions.

Since the focus of this chapter is the robustness properties of asymptotic stability of hybrid control systems, the following asymptotic stability assumption is in place for the closed-loop system \mathcal{H}_{cl} .

Assumption 5.3 (nominal global asymptotic stability) *The compact set \mathcal{A} , subset of O , is globally asymptotically stable for the closed-loop hybrid system \mathcal{H}_{cl} .*

Following Definition 4.1, globally asymptotic stability of the compact set \mathcal{A} means that solutions starting from $C_c \cup D_c$ exist, are complete, and that \mathcal{A} is stable and attractive with $\mathcal{B}_{\mathcal{A}} = C_c \cup D_c$. Note that \mathcal{A} is a subset of the state space, and consequently, involves the controller's state.

Perhaps the most intuitive hybrid control strategy consists of, given a pool of static feedback laws with certain stabilizing properties, appropriately switching between these control laws based on the measurements of the system state x to stabilize to the origin. Suppose that the controller state is given by q which is a logic state taking value in a finite set $Q \subset \mathbb{N}$, and that there exist two families of sets, $\{\Omega_q\}_{q \in Q}$ and $\{C_q\}_{q \in Q}$, and a family of feedback laws $\{\kappa_c(\cdot, q)\}_{q \in Q}$ designed so that, for each $q \in Q$, the trajectories $x(t)$ of $\dot{x} = f_p(x, \kappa(x, q))$ starting in C_q have the following properties:

- (C1) When a trajectory hits the boundary of the current C_q set and may be able to flow with larger q , it does not belong to Ω_α with α smaller than the current mode q , i.e., if $x(0) \in \Omega_q$ and $x(t) \in \partial C_q \setminus \{0\}$ for some $t \geq 0$ then $x(t) \notin \Omega_\alpha$ for any $\alpha < q$;
- (C2) Trajectories that never switch converge to the origin, i.e., if $x(t) \in C_q$ for all t in its domain and x is maximal, then x is complete and $\lim_{t \rightarrow \infty} x(t) = 0$ (maximal and complete solutions to differential equations are defined similarly as for hybrid systems in Definition 2.4 and 2.6);
- (C3) The trajectories do not go unbounded;

(C4) Every control law corresponding to a q such that $0 \in C_q$ renders the origin of the closed loop stable, i.e., for each $\varepsilon_q > 0$ there exists $\delta_q > 0$ such that $|x(0)| \leq \delta_q$ implies $|x(t)| \leq \varepsilon_q$ for all t where $x(\cdot)$ is defined. (Notice that if $0 \notin C_q$ then, since C_q is closed, there is nothing to check.)

Moreover, suppose that $\cup_{q \in Q} \Omega_q = \mathbb{R}^{n_p}$, for each $q \in Q$, Ω_q and C_q are closed and satisfy $\Omega_q \subset C_q$, the map $\kappa_q : \mathbb{R}^{n_p} \rightarrow \mathbb{R}^m$, defined by $x \mapsto \kappa_c(x, q)$ is continuous.

For each $q \in Q$, define $D_q := \overline{\mathbb{R}^{n_p} \setminus C_q}$. Then, define

$$D_c := \{(x, q) \in \mathbb{R}^{n_p} \times Q \mid x \in D_q\}$$

and

$$C_c := \{(x, q) \in \mathbb{R}^{n_p} \times Q \mid x \in C_q\}$$

and note that $C_c \cup D_c = \mathbb{R}^{n_p} \times Q$. Then the closed loop system \mathcal{H}_{cl} obtained from connecting this particular controller \mathcal{H}_c with the nonlinear system (5.1) is given by

$$\begin{aligned} \dot{x} &= f_p(x, \kappa(x, q)) & (x, q) \in C_c \\ q^+ &\in Q_c(x, q) & (x, q) \in D_c \end{aligned} \quad (5.5)$$

where

$$Q_c(x, q) := \begin{cases} \{\alpha \in Q \mid \alpha > q, x \in \Omega_\alpha\} & \text{if } x \in D_q \setminus (\cup_{\alpha < q} \Omega_\alpha) \\ \{\alpha \in Q \mid x \in \Omega_\alpha\} & \text{if } x \in D_q \cap (\cup_{\alpha < q} \Omega_\alpha) \end{cases}.$$

It follows from the fact that $\cup_{\alpha < q} \Omega_\alpha$ is closed that Q_c is outer semicontinuous. It also follows that Q_c is nonempty on D_c . Indeed, if $x \in D_q$ then, since the sets Ω_α are closed and $\Omega_q \subset C_q$ and $D_q = \overline{\mathbb{R}^n \setminus C_q}$, we have $x \in \cup_{\alpha \neq q} \Omega_\alpha$. Thus $x \in D_q \setminus (\cup_{\alpha < q} \Omega_\alpha)$ implies $x \in \cup_{\alpha > q} \Omega_\alpha$.

Theorem 5.4 (global asymptotic stability) *With the construction above, the closed-loop system (5.5) has the set $\{0\} \times Q$ globally asymptotically stable.*

The stability property in Theorem 5.4 follows by construction. Given $\varepsilon > 0$, to construct δ , denoting by m the number of elements in Q and letting q_m be the maximum element of Q , take $\varepsilon_{q_m} = \varepsilon$ and let this generate δ_{q_m} according to (C4). Note that $0 < \delta_{q_m} \leq \varepsilon_{q_m}$. Then, let q_{m-1} be the second largest element in Q and take $\varepsilon_{q_{m-1}} = \delta_{q_m}$ and let this generate $\delta_{q_{m-1}}$. Continuing in this way to the smallest element q_0 of Q , we take $\delta = \delta_{q_0}$. If a solution has no jumps, q is constant and the x component of the solution remains in $C_{q(0,0)}$ for all time. By (C2) and (C4), $|x(t, 0)| \leq \varepsilon$ for all $t \geq 0$ and $\lim_{t \rightarrow \infty} |x(t, j)| = 0$. Otherwise, when the solution jumps, note that since, by the assumption and the controller construction, the variable q evolves monotonically increasing, if x reaches the origin then it remains there forever, due to the stability assumption on each controller. If it does not reach the origin, then it stays in some C_q set for all (t, j) with large enough t and j in the domain of the solution. Then, by (C2) and taking the tail of the solution, it converges to the origin.

In control systems, like the one in the example above, several perturbations can arise and potentially destroy the good behavior for which the controller was designed for. For example, noise in the measurements of the state taken by the controller arises in every implemented system. It is also common that when a controller is designed, only a simplified model of the system to control exhibiting the most important dynamics is considered. This usually simplifies the control design. However, sensors/actuators dynamics that remain unmodeled can substantially affect the behavior of the system when in the loop. Additionally, in almost every application, the control of nonlinear systems is accomplished by implementing the controller in a digital device (e.g. computer, microcontroller, digital signal processor, etc.). In this setting, the output of the plant is usually sampled by an analog-to-digital (A/D) converter and the sample is passed to the digital controller which computes the control law and actuates on the nonlinear system through a digital-to-analog (D/A) converter. In these scenarios, it is desired that the hybrid controller provides a certain degree of robustness to such perturbations. In the following sections, general statements are made to that extent.

5.2 Robustness to perturbations

5.2.1 Robustness via filtered measurements

In this section, the case of noise in the measurements of the state of the nonlinear system is considered. As discussed in Section 3.3, measurement noise in hybrid systems can lead to nonexistence of solutions. This situation can be remedied, at least for small measurement noise, if under global existence of solutions, C_c and D_c always “overlap” while guaranteeing that the stability properties still hold. The “overlap” means that for every $\zeta \in O$, either $\zeta + e \in C_c$ or $\zeta + e \in D_c$ for all small e ; see also Proposition 3.7. In general, there always exist inflations of C and D that preserve semiglobal practical asymptotic stability; however, they only guarantee existence of solutions for small measurement noise. Alternatively, solutions are guaranteed to exist locally for any locally bounded measurement noise if the measurement noise does not appear in the flow and jump sets. This can be achieved by filtering the measurements. Figure 5.1 depicts this scenario. The state x is corrupted with noise e and the hybrid controller \mathcal{H}_c measures a filtered version of $x + e$.

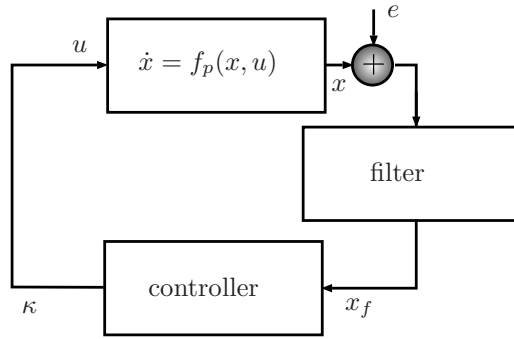


Figure 5.1. Closed-loop system with noise and filtered measurements.

The filter used for the noisy output $y = x + e$ is taken to be linear and defined by the matrices A_f , B_f , and L_f , and an additional parameter $\varepsilon_f > 0$. It is designed to be asymptotically stable. Its state is denoted by x_f which takes value in \mathbb{R}^{n_f} . At jumps, x_f is reset to the current value of y . Then, the filter has flows given by

$$\varepsilon_f \dot{x}_f = A_f x_f + B_f y, \quad (5.6)$$

and jumps given by

$$x_f^+ = A_f^{-1} B_f x_f + B_f y. \quad (5.7)$$

Assumption 5.5 (filter properties) *The matrices $A_f \in \mathbb{R}^{n_f} \times \mathbb{R}^{n_f}$, $B_f \in \mathbb{R}^{n_f} \times \mathbb{R}^{n_p}$, $L_f \in \mathbb{R}^{n_p} \times \mathbb{R}^{n_f}$ are such that A_f is Hurwitz and $-L_f A_f^{-1} B_f = I$.*

The output of the filter replaces the state x in the feedback law κ and in the flow and jump conditions in (5.3)-(5.4), thereby guaranteeing local existence of solutions. The resulting closed-loop system can be interpreted

as a family of hybrid systems that depends on the parameter ε_f . It is denoted by $\mathcal{H}_{cl}^{\varepsilon_f}$ and is given by

$$\mathcal{H}_{cl}^{\varepsilon_f} : \left\{ \begin{array}{l} \dot{x} = f_p(x, \kappa(L_f x_f, x_c)) \\ \dot{x}_c = f_c(L_f x_f, x_c) \\ \varepsilon_f \dot{x}_f = A_f x_f + B_f(x + e) \\ x^+ = x \\ x_c^+ \in G_c(L_f x_f, x_c) \\ x_f^+ = -A_f^{-1} B_f(x + e) \end{array} \right\} \begin{array}{l} (L_f x_f, x_c) \in C_c \\ (L_f x_f, x_c) \in D_c \end{array} \quad (5.8)$$

Solutions to $\mathcal{H}_{cl}^{\varepsilon_f}$ are defined as in Definition 3.2 for a certain admissible state perturbation e (in this case, a measurement noise signal) with the difference that the noise enters through the plant state x rather than the closed-loop system state ζ .

It can be shown that for every compact set of initial conditions and positive number ν , the solutions to the family of hybrid systems $\mathcal{H}_{cl}^{\varepsilon_f}$ with a small enough parameter ε_f satisfy a \mathcal{KLL} bound with an offset given by ν . The proofs of the following statement uses results from [39] (see Appendix B.3).

Theorem 5.6 (semiglobal practical stability with filtered measurements) *Under Assumptions 5.1, 5.2, 5.3, and 5.5, there exists $\beta \in \mathcal{KLL}$ and for each $\mu > 0$ and $\nu > 0$, there exist $\varepsilon_f^* > 0$ and $\delta > 0$ such that, for all $\varepsilon_f \in (0, \varepsilon_f^*]$, the solutions (ζ, x_f) to $\mathcal{H}_{cl}^{\varepsilon_f}$ with admissible measurement noise with a magnitude no larger than δ are bounded and the ζ component satisfy*

$$|\zeta(t, j)|_{\mathcal{A}} \leq \beta(|\zeta(0, 0)|_{\mathcal{A}}, t, j) + \nu$$

for all initial conditions $(\zeta(0, 0), x_f(0, 0)) \in \mathbb{R}^{n_p} \times \mathbb{R}^{n_c} \times \mathbb{R}^{n_f}$ with $|\zeta(0, 0)|_{\mathcal{A}} \leq \mu$ and $|x_f(0, 0)| \leq \mu$.

Proof. First, note that at every jump of $\mathcal{H}_{cl}^{\varepsilon_f}$, $x_f^+ = -A_f^{-1} B_f(x + e)$ and that with Assumption 5.5, the value of $L_f x_f$ after the jump is given by

$$L_f x_f^+ = -L_f A_f^{-1} B_f(x + e) = x + e .$$

Combining this with the properties of A_f in Assumption 5.5, given $\tilde{\delta} > 0$, $\mu > 0$, and $T > 0$, there exist $\varepsilon_f^* > 0$ and $\delta > 0$ such that each solution (ζ, x_f) to $\mathcal{H}_{cl}^{\varepsilon_f}$, $\varepsilon_f \in (0, \varepsilon_f^*]$, with admissible measurement noise e with a magnitude no larger than δ and with $|\zeta(0, 0)|_{\mathcal{A}} \leq \mu$, $|x_f(0, 0)|_{\mathcal{A}} \leq \mu$, satisfies

$$|x(t, j) - L_f x_f(t, j)| \leq \tilde{\delta} \quad \forall (t, j) \succeq T, (t, j) \in \text{dom}(\zeta, x_f) .$$

(Recall that $\zeta = [x \ x_c]^T$.) Then $L_f x_f(t, j) \in \zeta(t, j) + \tilde{\delta}\mathbb{B}$ for all $(t, j) \succeq T$, $(t, j) \in \text{dom}(\zeta, x_f)$. It follows that solutions to $\mathcal{H}_{cl}^{\varepsilon_f}$, $\varepsilon_f \in (0, \varepsilon_f^*]$, with admissible measurement noise e with a magnitude no larger than δ , and with $|\zeta(0, 0)|_{\mathcal{A}} \leq \mu$, $|x_f(0, 0)|_{\mathcal{A}} \leq \mu$, are contained in the set of solutions to the perturbed hybrid system

$$\left. \begin{array}{l} \dot{x} \in f_p(x, \kappa(x + \tilde{\delta}\mathbb{B})) \\ \dot{x}_c \in f_c(x + \tilde{\delta}\mathbb{B}, x_c) \end{array} \right\} (x + \tilde{\delta}\mathbb{B}, x_c) \cap C_c \neq \emptyset$$

$$\left. \begin{array}{l} x^+ = x \\ x_c^+ \in G_c(x + \tilde{\delta}\mathbb{B}, x_c) \end{array} \right\} (x + \tilde{\delta}\mathbb{B}, x_c) \cap D_c \neq \emptyset .$$

With Assumptions 5.1, 5.2, and 5.3, and Theorem B.14, the claim follows directly from an application of Theorem B.15 to the auxiliary system above. \square

5.2.2 Robustness to sensor and actuator dynamics

This section addresses the robustness properties of the closed-loop \mathcal{H}_{cl} when additional dynamics, coming from sensors and actuators, are incorporated. Figure 5.2 shows the closed-loop \mathcal{H}_{cl} with two additional blocks: a model for the sensor and a model for the actuator. In general, to simplify the controller design procedure, these dynamics are usually not included in the model of the nonlinear system (5.1) when the hybrid controller \mathcal{H}_c is designed. Therefore, it is important to know whether the stability properties of the closed-loop system are preserved, at least semiglobally and practically, when those dynamics are incorporated in the closed loop.

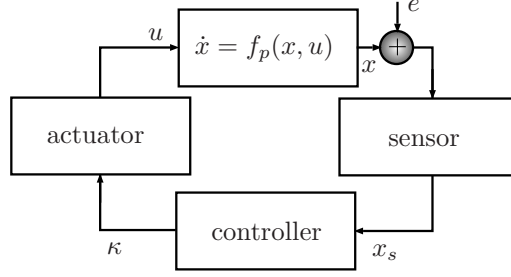


Figure 5.2. Closed-loop system with sensor and actuator dynamics.

The sensor and actuator dynamics are modeled as stable filters. The state of the filter that models the sensor dynamics is given by $x_s \in \mathbb{R}^{n_s}$ with matrices (A_s, B_s, L_s) and the state of the filter that models the actuator dynamics by $x_a \in \mathbb{R}^{n_a}$ with matrices (A_a, B_a, L_a) . The parameter $\varepsilon_d > 0$ is common to both filters.

Assumption 5.7 (sensor and actuator properties) *The matrices (A_s, B_s, L_s) and (A_a, B_a, L_a) are such that A_s and A_a are Hurwitz, $-L_s A_s^{-1} B_s = I$ and $-L_a A_a^{-1} B_a = I$.*

Assumption 5.7 states that the filters are stable and have unitary DC gain. Note that since the filters are not internal components of the hybrid controller, their state cannot be reset at jumps to an arbitrary value given by the controller (cf. the filter in Section 5.2.1). This physical impossibility can cause that when the sensor and actuator dynamics are incorporated into the system, new Zeno solutions are added to the closed-loop system.

To prevent from adding new Zeno solutions that do not converge to \mathcal{A} , temporal regularization is added to the closed-loop system. Let $\tau \in \mathbb{R}$ be the timer state and $\bar{\tau} > 0$ be the timer parameter for the temporal regularization.

Augmenting \mathcal{H}_{cl} by adding filters and temporal regularization leads to a family $\mathcal{H}_{cl}^{\varepsilon_d}$ given as follows

$$\mathcal{H}_{cl}^{\varepsilon_d} : \left\{ \begin{array}{l} \dot{x} = f_p(x, L_a x_a) \\ \dot{x}_c = f_c(L_s x_s, x_c) \\ \dot{\tau} = -\tau + \tau^* \\ \varepsilon_d \dot{x}_s = A_s x_s + B_s(x + e) \\ \varepsilon_d \dot{x}_a = A_a x_a + B_a \kappa(L_s x_s, x_c) \\ x^+ = x \\ x_c^+ \in G_c(L_s x_s, x_c) \\ x_s^+ = x_s \\ x_a^+ = x_a \\ \tau^+ = 0 \end{array} \right. \left\{ \begin{array}{l} (L_s x_s, x_c) \in C_c \\ \text{or } \tau \leq \bar{\tau} \\ \\ (L_s x_s, x_c) \in D_c \\ \text{and } \tau \geq \bar{\tau} \end{array} \right. \quad (5.9)$$

where τ^* is a constant satisfying $\tau^* > \bar{\tau}$. The following result states that for fast enough sensors and actuators, and small enough temporal regularization parameter, the compact set \mathcal{A} is semiglobally practically asymptotically stable.

Theorem 5.8 (semiglobal practical stability with sensor and actuator dynamics) *Under Assumptions 5.1, 5.2, 5.3, and 5.7, there exists $\beta \in \mathcal{K}\mathcal{L}\mathcal{L}$, for each $\mu > 0$ and $\nu > 0$ there exist $\bar{\tau}^* > 0$ and $\delta > 0$, and for each $\bar{\tau} \in (0, \bar{\tau}^*]$ there exist $\varepsilon_d^* > 0$ such that, for each $\bar{\tau} \in (0, \bar{\tau}^*]$, each $\varepsilon_d \in (0, \varepsilon_d^*]$, the solutions (ζ, x_s, x_a, τ) to $\mathcal{H}_{cl}^{\varepsilon_d}$ with admissible measurement noise with a magnitude no larger than δ are bounded and the ζ component satisfy*

$$|\zeta(t, j)|_{\mathcal{A}} \leq \beta(|\zeta(0, 0)|_{\mathcal{A}}, t, j) + \nu$$

for all initial conditions $(\zeta(0, 0), x_s(0, 0), x_a(0, 0), \tau(0, 0)) \in \mathbb{R}^{n_p} \times \mathbb{R}^{n_c} \times \mathbb{R}^{n_s} \times \mathbb{R}^{n_a} \times \mathbb{R}$ with $|\zeta(0, 0)|_{\mathcal{A}} \leq \mu$, $|x_s(0, 0)| \leq \mu$, and $|x_a(0, 0)| \leq \mu$.

Proof. Consider the auxiliary system

$$\left. \begin{aligned} \dot{x} &= f_p(x, \kappa(x, x_c)) \\ \dot{x}_c &= f_c(x, x_c) \\ \dot{\tau} &= -\tau + \tau^* \\ x^+ &= x \\ x_c^+ &\in G_c(x, x_c) \\ \tau^+ &= 0 \end{aligned} \right\} \begin{aligned} &(x, x_c) \in C_c \text{ or } \tau \leq \bar{\tau} \\ &(x, x_c) \in D_c \text{ and } \tau \geq \bar{\tau} . \end{aligned}$$

By Assumption 5.5, [39, Example 5.3], and Theorem B.14 there exists $\beta \in \mathcal{K}\mathcal{L}\mathcal{L}$ and for each $\mu > 0$ and $\nu > 0$ there exists $\bar{\tau}^* > 0$ such that, for the auxiliary system, the trajectories satisfy

$$|z(t, j)|_{\mathcal{A}} \leq \beta(|z(0, 0)|_{\mathcal{A}}, t, j) + \frac{\nu}{2} .$$

Moreover, for each solution and each $j \geq 1$ in the domain of the solution, the length of the j -th interval is at least $\bar{\tau}$. Then $\varepsilon_d^* > 0$ can be chosen so that, on an arbitrarily large part of such an interval, $L_s x_s$ is arbitrarily close to x and $L_a x_a$ is arbitrarily close to $\kappa(x, x_c)$. The proof is finished continuing as in the proof of Theorem 5.6. \square

In Theorem 5.8, the parameter ε_d^* , the maximum value for ε_d , depends on the size of the compact set of initial conditions, determined by μ , and on the desired level of closeness ν to \mathcal{A} for the solutions to $\mathcal{H}_{cl}^{\varepsilon_d}$. The smaller the parameter ε_d^* resulting from this result, the faster the filters modeling the sensor and actuator dynamics have to be.

5.2.3 Robustness to sensor dynamics and smoothing

In several hybrid control applications, the state of the controller is explicitly given as a continuous state ξ and a discrete state $q \in Q := \{1, \dots, n\}$, that is, $x_c := [\xi \ q]^T$. When such is the case and the discrete state q chooses a different control law to be applied to the system for different values of q , then the control law generated by the hybrid controller \mathcal{H}_c can have jumps when q changes. In many scenarios, it is not possible for the actuator to switch between control laws instantaneously. Moreover, especially when the control law $\kappa(\cdot, \cdot, q)$ is continuous for each $q \in Q$, it is desired to have a smooth transition between them when q changes.

Figure 5.3 shows the closed-loop system, denoted as $\mathcal{H}_{cl}^{\varepsilon_u}$, resulting from adding a block that performs the smooth transition between control laws indexed by q and denoted by κ^q . The smoothing control block is modeled as a linear filter for the variable q . It is defined by the matrices (A_u, B_u, L_u) and the parameter ε_u . The output of the control smoothing block is given by

$$\alpha(x, x_c, L_u x_u) = \sum_{q \in Q} \lambda_q(L_u x_u) \kappa(x, x_c, q)$$

where for each $q \in Q$, $\lambda_q : \mathbb{R} \rightarrow [0, 1]$ is continuous and $\lambda_q(q) = 1$. Note that the output is such that the control laws are smoothly “blended” by the function λ_q .

Assumption 5.9 (actuator smoothing properties) *The matrices (A_u, B_u, L_u) are such that A_u is Hurwitz, $-L_u A_u^{-1} B_u = I$.*

The smoothing block is considered to be part of the actuator, and for that reason, it is not possible to reset its state at jumps. In addition to this block, a filter modeling the sensor dynamics is also incorporated as in Section 5.2.2. The closed loop $\mathcal{H}_{cl}^{\varepsilon_u}$ can be written as

$$\mathcal{H}_{cl}^{\varepsilon_u} : \left\{ \begin{array}{l} \dot{x} = f_p(x, \alpha(x, x_c, L_u x_u)) \\ \dot{\xi} = f_c(L_s x_s, x_c) \\ \dot{q} = 0 \\ \dot{\tau} = -\tau + \bar{\tau}^* \\ \varepsilon_u \dot{x}_s = A_s x_s + B_s(x) \\ \varepsilon_u \dot{x}_u = A_u x_u + B_u q \\ x^+ = x \\ \begin{bmatrix} \xi^+ \\ q^+ \end{bmatrix} \in G_c(L_s x_s, x_c) \\ x_s^+ = x_s \\ x_u^+ = x_u \\ \tau^+ = 0 \end{array} \right\} \begin{array}{l} (L_s x_s, x_c) \in C_c \text{ or } \tau \leq \bar{\tau} \\ (L_s x_s, x_c) \in D_c \\ \text{and } \tau \geq \bar{\tau} . \end{array} \quad (5.10)$$

Theorem 5.10 (semiglobal practical stability with actuator smoothing) *Under Assumptions 5.1, 5.2, 5.3, and 5.9, there exists $\beta \in \mathcal{K}\mathcal{L}\mathcal{L}$, for each $\mu > 0$ and $\nu > 0$ there exist $\bar{\tau}^* > 0$, and for each $\bar{\tau} \in (0, \bar{\tau}^*]$ there exist $\varepsilon_u^* > 0$ such that, for each $\bar{\tau} \in (0, \bar{\tau}^*]$, each $\varepsilon_u \in (0, \varepsilon_u^*]$, the solutions (ζ, x_s, x_u, τ) to $\mathcal{H}_{cl}^{\varepsilon_u}$ are bounded and the ζ component satisfy*

$$|\zeta(t, j)|_{\mathcal{A}} \leq \beta(|\zeta(0, 0)|_{\mathcal{A}}, t, j) + \nu$$

for all initial conditions $(\zeta(0, 0), x_s(0, 0), x_u(0, 0), \tau(0, 0)) \in \mathbb{R}^{n_p} \times \mathbb{R}^{n_c} \times \mathbb{R}^{n_a} \times \mathbb{R}$ with $|\zeta(0, 0)|_{\mathcal{A}} \leq \mu$, and $|x_u(0, 0)| \leq \mu$.

A corollary to Theorem 5.10 establishing robustness to noise in the state x (as in Theorem 5.6) also holds for the closed-loop system with control smoothing $\mathcal{H}_{cl}^{\varepsilon_u}$.

In Section 5.4, we add fast sensor dynamics and control smoothing to the problem of swinging up a pendulum on a cart.

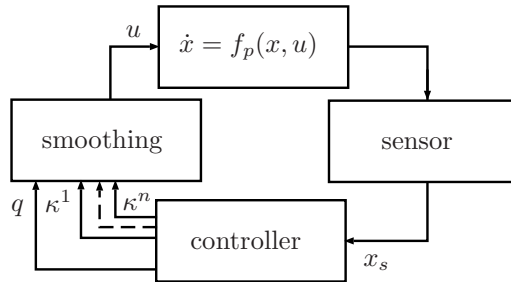


Figure 5.3. Closed-loop system with sensor dynamics and control smoothing.

5.3 Robustness to digital implementation

A hybrid controller like the one in (5.2) is frequently implemented in a *digital device*, e.g. computer, microcontroller, digital signal processor, etc. In such a scenario as that depicted in Figure 5.4, the controller is usually interfaced with sample-and-hold devices. The sample-and-hold device that samples the state x of the plant is referred to as *sampling device* (or analog-to-digital (A/D) converter), while the sample-and-hold device that stores the output of the controller in between computations is referred to as *hold device* (or digital-to-analog (D/A) converter) which is assumed to be of zero-order type, that is, a zero-order hold (ZOH).

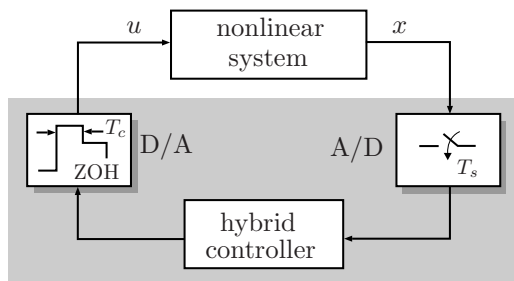


Figure 5.4. Sample-and-hold control of a nonlinear system.

In contrast to purely continuous-time and discrete-time systems, hybrid systems can experience jumps in their variables at any rate, even without flows between consecutive jumps. A challenge in the sample-and-hold implementation of hybrid control systems is that the sampling task and the update of the control law need to be performed fast enough in order to reproduce the jumps that were designed to accomplish a particular stabilization task. Therefore, it is important to know, in a practical sense, for which values of the parameters of the sample-and-hold devices the stability properties of the closed-loop system are preserved when these devices are incorporated in the closed-loop system. The bounds on these parameters obtained from such a result are useful in choosing the sampling time, computation rate, and rate of the control law for the devices used in the implementation.

In the next sections, a detailed description of the models for each of the components in Figure 5.4 is given. Note that the models for the sampling device and for the controller and ZOH device are themselves hybrid. In this way, the resulting closed-loop system consists of an interconnection of hybrid systems. Following this section, a general stability result for closed-loop systems with sample-and-hold implementation of hybrid controllers is given.

5.3.1 Sample-and-hold model

The main function of the sampling device is to sample the state x of the nonlinear system (5.1) and to transfer this sample to the digital device so that the control law is computed. To model this system, define $\tau_s \in \mathbb{R}$ to be the timer for the samples and $z_s \in \mathbb{R}^{n_p}$ to be the state of the sampling device that stores the last sample. For simplicity, only the case of periodic sampling x at every $T_s \in \mathbb{R}_{>0}$ units of time is considered. Then, the sampling device can be modeled as the following hybrid system

$$\left. \begin{aligned} \dot{\tau}_s &= 1 \\ \dot{z}_s &= 0 \end{aligned} \right\} \tau_s \in [0, T_s]$$

$$\left. \begin{aligned} \tau_s^+ &= 0 \\ z_s^+ &= x \end{aligned} \right\} \tau_s = T_s,$$

where the continuous dynamics are such that the timer counts the time elapsed from the last jump and the sampling state z_s is kept constant as long as $\tau_s \in [0, T_s]$. When $\tau_s = T_s$, flows are no longer possible, jumps are forced, and are such that the timer is updated to zero, and the sampling state is updated to the current value of the state x .

The digital controller performs the actual computation of the control algorithm in \mathcal{H}_c and updates the state of the ZOH device, which are denoted by $z_c \in \mathbb{R}^{n_c}$. These are modeled as a single hybrid system \mathcal{H}_{h-c} . Synchrony between this system and the sampling device is not assumed, i.e., the computation of the algorithm and the update of the ZOH are governed by an independent clock, which in general, has a different sampling time than the sampling device. The model for \mathcal{H}_{h-c} is given in terms of the ZOH state $z_c \in \mathbb{R}^{n_c}$ which stores the computation resulting from the controller \mathcal{H}_c , a timer state $\tau_c \in \mathbb{R}$ which after every $T_c \in \mathbb{R}_{>0}$ units of time, triggers the computation of the control algorithm and updates the ZOH. Since there is no synchronization with the sampling device and no relationship between the constants τ_s and τ_c a priori, it could be the case that the sampling device is updated in between computations. To accommodate to this situation, a memory state $z_m \in \mathbb{R}^{n_p}$ is added to the model in order to store the samples provided by the sampling device. With these definitions, the model of \mathcal{H}_{h-c} , that is, the digital controller with the hold device, is given by

$$\left. \begin{array}{l} \dot{\tau}_c = 1 \\ \dot{z}_c = 0 \\ \dot{z}_m = 0 \end{array} \right\} \tau_c \in [0, T_c]$$

$$\left. \begin{array}{l} \tau_c^+ = 0 \\ z_c^+ \in g_{\mathcal{H}_c}(z_m, z_c) \\ z_m^+ = z_s \end{array} \right\} \tau_c = T_c$$

where $g_{\mathcal{H}_c}$ is defined below.

These dynamics are such that when $\tau_c \in [0, T_c]$, the timer τ_c counts the elapsed time and the states z_c and z_m remain constant. When $\tau_c = T_c$ then the timer is reset to zero, the output of the ZOH device z_c is updated, and the memory state z_m is updated to the last sample z_s . The update law for z_c is given by

$$g_{\mathcal{H}_c}(z_m, z_c) := \begin{cases} g_{f_c}(z_m, z_c) & (z_m, z_c) \in C_c \setminus D_c \\ G_c(z_m, z_c) & (z_m, z_c) \in D_c \setminus C_c \\ \{g_{f_c}(z_m, z_c), G_c(z_m, z_c)\} & (z_m, z_c) \in C_c \cap D_c \end{cases} \quad (5.11)$$

where g_{f_c} is an approximation of the flow equation of \mathcal{H}_c , and G_c is the same jump mapping as for \mathcal{H}_c .

5.3.2 Closed-loop system analysis

The closed-loop system with the models for the nonlinear system, sampling device, and digital controller and ZOH device given in Section 5.3.1 is denoted by $\mathcal{H}_{cl}^{S/H}$; has states $x, z_c, z_s, \tau_s, \tau_c, z_m$; has continuous dynamics given by

$$\left. \begin{array}{l} \dot{x} = f_p(x, \kappa(z_s, z_c)) \\ \dot{z}_c = 0 \\ \dot{z}_s = 0 \\ \dot{\tau}_s = 1 \\ \dot{\tau}_c = 1 \\ \dot{z}_m = 0 \end{array} \right\} \tau_s \in [0, T_s] \text{ and } \tau_c \in [0, T_c];$$

and discrete dynamics given by

$$\begin{bmatrix} x^+ \\ z_c^+ \\ z_s^+ \\ \tau_s^+ \\ \tau_c^+ \\ z_m^+ \end{bmatrix} = \begin{bmatrix} x \\ z_c \\ x \\ 0 \\ \tau_c \\ z_m \end{bmatrix} =: \tilde{g}_1(x, z_c, z_s, \tau_s, \tau_c, z_m)$$

when $\tau_s = T_s$ and $\tau_c \in [0, T_c)$,

$$\begin{bmatrix} x^+ \\ z_c^+ \\ z_s^+ \\ \tau_s^+ \\ \tau_c^+ \\ z_m^+ \end{bmatrix} \in \begin{bmatrix} x \\ g_{\mathcal{H}_c}(z_m, z_c) \\ z_s \\ \tau_s \\ 0 \\ z_s \end{bmatrix} =: \tilde{g}_2(x, z_c, z_s, \tau_s, \tau_c, z_m)$$

when $\tau_s \in [0, T_s)$ and $\tau_c = T_c$, and

$$\begin{bmatrix} x^+ \\ z_c^+ \\ z_s^+ \\ \tau_s^+ \\ \tau_c^+ \\ z_m^+ \end{bmatrix} \in \{\tilde{g}_1(x, z_c, z_s, \tau_s, \tau_c, z_m), \tilde{g}_2(x, z_c, z_s, \tau_s, \tau_c, z_m)\}$$

when $\tau_c = T_c$ and $\tau_s \in T_s$. The flows of the closed loop are governed by the flow equation of each subsystem. The jump mappings are combined so that only the states of the original jump mapping are updated. For instance, when $\tau_s = T_s$ and $\tau_c \in [0, T_c)$, only the states z_s and τ_s are updated to new values (as discussed in Section 5.3.1) while the other states are mapped back to their current values. Moreover, note that the data of $\mathcal{H}_{cl}^{S/H}$ satisfy the hybrid basic conditions.

It is expected that, in order to establish any type of stability result for $\mathcal{H}_{cl}^{S/H}$ inherited from the stability properties of \mathcal{H}_{cl} , the value of the flows of \mathcal{H}_c and the value of g_{f_c} in the controller's jump mapping $g_{\mathcal{H}_c}$ have to be "close" at jumps. The consistency property defined below is one way to guarantee such closeness.

Given two positive real numbers δ and Δ satisfying $0 < \delta \leq \Delta < \infty$ and a compact set $\mathcal{A} \subset \mathbb{R}^{n_p + n_c}$, define

$$\Omega_{\mathcal{A}}(\delta, \Delta) := \{(x, x_c) \in \mathbb{R}^{n_p} \times \mathbb{R}^{n_c} \mid \delta \leq |(x, x_c)|_{\mathcal{A}} \leq \Delta\} .$$

Definition 5.11 (consistency of flow map of \mathcal{H}_c) *Let \mathcal{A} be a compact subset of $\mathbb{R}^{n_p} \times \mathbb{R}^{n_c}$. The integration scheme g_{f_c} is said to be consistent with respect to f_c if for each positive number Δ_s there exists $\rho \in \mathcal{K}_{\infty}$ and $T'_c > 0$ such that for each $(x^0, x_c^0) \in \Omega_{\mathcal{A}}(0, \Delta_s)$ and each $T_c \in (0, T'_c)$ there exists a solution $\varphi(t)$ to $\dot{\varphi} = f_c(x, \varphi)$, $\varphi(0) = x_c^0$, with $x(t)$ satisfying $\dot{x} = f_p(x, \kappa(x^0, \varphi(0)))$, $x(0) = x^0$, such that*

$$|g_{f_c}(x(0), \varphi(0)) - \varphi(T_c)| \leq T_c \rho(T_c) . \quad (5.12)$$

Theorem 5.12 (semiglobal practical stability) *Let Assumption 5.1, 5.2, and 5.3 hold. Let the integration scheme g_{f_c} in \mathcal{H}_{cl} be consistent with respect to f_c . Then, the set \mathcal{A} is semiglobally practically asymptotically stable for $\mathcal{H}_{cl}^{S/H}$, i.e. there exists $\beta \in \mathcal{KLL}$, for every compact set $K \subset \mathbb{R}^{n_p} \times \mathbb{R}^{n_c}$ and every $\varepsilon > 0$ there*

exists $T_s^*, T_c^* > 0$ such that for each $T_s \in (0, T_s^*)$, $T_c \in (0, T_c^*)$, solutions $(x, z_c, z_s, \tau_s, \tau_c, z_m)$ to $\mathcal{H}_{cl}^{S/H}$ with $(x(0, 0), z_c(0, 0)) \in K$ are bounded and the x and z_c components satisfy

$$|(x(t, j), z_c(t, j))|_{\mathcal{A}} \leq \beta(|(x(0, 0), z_c(0, 0))|_{\mathcal{A}}, t, j) + \varepsilon \quad (5.13)$$

for all $(t, j) \in \text{dom}(x, z_c)$.

5.4 A benchmark problem: robust global swing-up of a pendulum on a cart

Consider the problem of swinging a pendulum on a cart to the upright position by acting on the cart, as shown in Figure 5.5, and simultaneously stabilizing the cart to the neutral position. The inverted pendulum on a cart

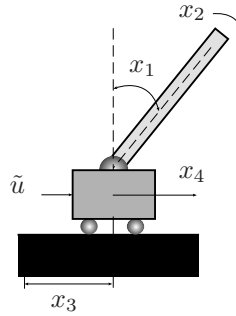


Figure 5.5. Pendulum on a cart.

system, after a preliminary state feedback of the form¹ $\tilde{u} = \psi(x) + \phi(x)u$, is given by

$$\begin{aligned} \dot{x}_1 &= x_2, \\ \dot{x}_2 &= \sin(x_1) + \cos(x_1)u, \\ \dot{x}_3 &= x_4, \\ \dot{x}_4 &= u \end{aligned} \quad (5.14)$$

where x_1 represents the angle of the pendulum from the up vertical position, x_2 is the angular velocity, x_3 is the cart position and x_4 is the cart velocity. Note that for simplicity, the constants have been normalized.

Consider the hybrid swing-up strategy that chooses the appropriate feedback control law depending on the location of the pendulum. Let W be the energy of the pendulum, $W(x) = \frac{1}{2}x_2^2 + \cos(x_1)$, and let c_1, c_2 be constants that are sufficiently close to but larger than $\min_{x \in \mathbb{R}^4} W(x)$ and satisfy $c_1 > c_2$. Take U_{3a} and U_{3b} , $U_{3a} \subset U_{3b}$, to be closed neighborhoods of the origin in \mathbb{R}^2 such that for the system $\dot{x} = f(x, u)$, there exists a state feedback law $\tilde{\kappa}$ that renders the origin (in \mathbb{R}^4) locally asymptotically stable with basin of attraction containing $U_{3b} \times \mathbb{R}^2$ and such that solutions starting in $U_{3a} \times \mathbb{R}^2$ do not reach the boundary of $U_{3b} \times \mathbb{R}^2$. Then, for each $q \in Q := \{1, 2, 3\}$, define sets Ω_q and C_q ($\Omega_q \subset C_q$) as follows

$$\begin{aligned} \Omega_1 &= C_1 = \{x \in \mathbb{R}^4 \mid W(x) \leq c_1\}, \\ \Omega_3 &= U_{3a} \times \mathbb{R}^2, \quad C_3 = U_{3b} \times \mathbb{R}^2, \\ \Omega_2 &= \left\{x \in \overline{\mathbb{R}^2 \setminus U_{3a}} \times \mathbb{R}^2 \mid W(x) \geq c_1\right\}, \\ C_2 &= \left\{x \in \overline{\mathbb{R}^2 \setminus U_{3a}} \times \mathbb{R}^2 \mid W(x) \geq c_2\right\}. \end{aligned}$$

¹This state feedback is also subject to measurement noise, but the effect of measurement noise at this location is as in standard ordinary differential equations. For simplicity, this subtlety will be ignored.

When the pendulum is in the region q , the control law is given by $\kappa_c(\cdot, q)$, $q \in Q$. The control law for C_1 is given by κ_1 which drives the system away from the resting condition. One can simply choose $\kappa_1 \equiv 1$. In C_2 , the control law should inject enough energy into the system so that U_{3a} is reached. For that purpose, we let κ_2 be a feedback law that stabilizes W to the value one, e.g. $\kappa_2(x) = -x_2 \cos(x_1)(W(x) - 1)$. Design the control law for region $q = 3$ so that it satisfies the properties of $\tilde{\kappa}$ above. This control law can be constructed by feedback linearizing the system (5.14), computing the basin of attraction with a quadratic Lyapunov function, and extending the linearized controller so that the cart position and velocity are stabilized to the origin:

$$\begin{aligned} \kappa_3(x) &= \frac{\sin(x_1) + x_1 + x_2}{\cos(x_1)} + \text{sat}_{\lambda_1} \{z_4 + \text{sat}_{\frac{\lambda_1}{2}} \{z_3 + z_4\}\} \\ U_{3a} &= \left\{ x \in \mathbb{R}^4 \mid \frac{1}{2}(x_1^2 + x_2^2) \leq c_3 \right\} \\ U_{3b} &= \left\{ x \in \mathbb{R}^4 \mid \frac{1}{2}(x_1^2 + x_2^2) \leq c_4 \right\}, \end{aligned}$$

where $z_4 = x_4 + 2x_2 + x_1$, $z_3 = x_3 + x_4 + x_2 + 2x_1$, and $c_4 > c_3 > 0$. Finally, define $\kappa_c(\cdot, q) = \kappa_q(\cdot)$.

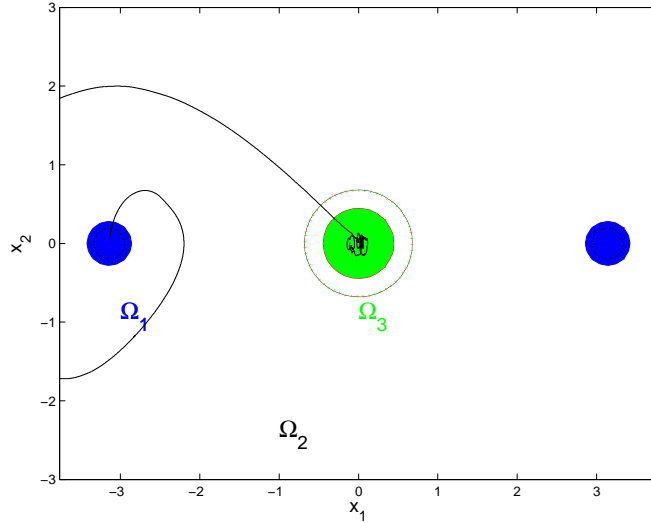


Figure 5.6. Solution with normally distributed measurement noise with variance $\sigma = 0.1$ starts in Ω_1 , the mode switches when the solution hits the boundary of C_1 and C_2 and then stays in Ω_3 (and also inside C_3 which is the depicted set contained in Ω_3). The noise is not able to keep the system away from a neighborhood of the upright condition.

Note that this construction meets the specifications of the controller proposed at the end of Section 5.1.

The closed-loop system including fast sensor dynamics and control smoothing as discussed in Section 5.2.3 is implemented. Since there are three different modes, the control smoothing is modeled as

$$u = u_s(x, x_u) := \sum_{q=1}^3 \lambda_q(L_u x_u) u_q(x)$$

where the selection functions $\lambda_q : \mathbb{R} \rightarrow [0, 1]$, for each $q \in Q$, are continuous and $\lambda_q(q) = 1$.

Finally, the parameters for the simulations are

$$A_u = \begin{bmatrix} 0 & 1 & 0 \\ 0 & 0 & 1 \\ -1 & -2 & -1 \end{bmatrix}, B_u = \begin{bmatrix} 0 \\ 0 \\ 2 \end{bmatrix}, L_u = [1 \ 0 \ 0]$$

$$\varepsilon_u = 0.01, \bar{\tau} = 0.001, \tau^* = 0.0005 \ A_s = -I, B_s = I, L_s = I,$$

$$c_1 = -0.96, c_2 = -0.98, c_3 = 0.1, c_4 = 0.23, \lambda_1 = 0.5.$$

Figure 5.6 shows a closed-loop solution in the (x_1, x_2) plane starting at $x^0 = [-\pi \ 0 \ 0 \ 0]^T$, $q^0 = 1$, $x_u^0 = [0 \ 0 \ 0]^T$, and with normally distributed noise on each measurement with $\sigma = 0.1$. In the same figure, the sets Ω_q in solid and the sets C_q with dashes lines are also plotted.

To highlight the robustness property to measurement noise, the magnitude of the noise was increased by setting $\sigma = 1$. The results are shown in Figure 5.7 and 5.8. When the noise is able to kick the solution, for example, outside the set C_3 , the controller reaction is to switch the mode from $q = 3$ to $q = 2$. Then, it drives the solution back to Ω_3 by switching the mode back to $q = 3$. The time between switches in Figure 5.8 shows that the controller reacts relatively fast.

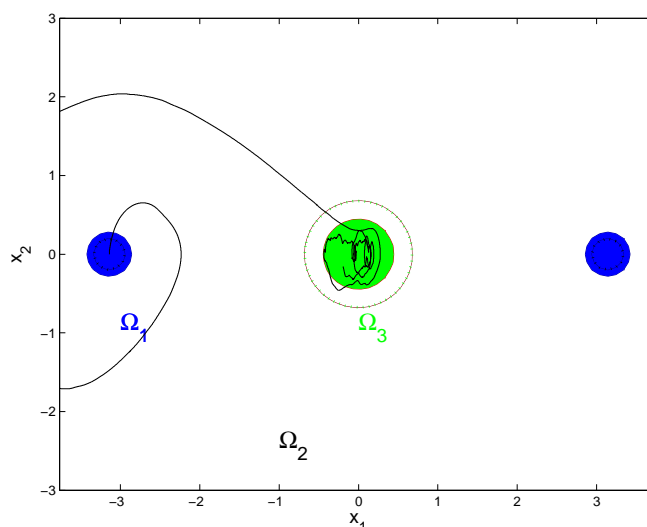


Figure 5.7. Solution starting with the same initial conditions as before but with ten times larger measurement noise. The noise is able to cause the state to leave C_3 and therefore, perturb the pendulum from the straight-up position, but the hybrid controller reacts and steers it back in.

The hybrid controller designed above is now implemented with sample and hold devices as in Section 5.3.1. Note that Assumption 5.2 and 5.3 are both satisfied. A numerical analysis of the margin of robustness of \mathcal{H}_{cl} to sample and hold devices was performed with results shown in Figure 5.9 and Figure 5.10. In these figures, along with the regions Ω_q , $q \in Q$, of the controller, the position x_1 and the velocity x_2 of the pendulum for different values of timer constants T_s and T_c are depicted.

Figure 5.9 shows the nominal trajectory (no sample and hold devices) as well as closed-loop trajectories resulting from periodic sample and digital controller/ZOH device in the loop for timer constants $T_s = T_c$ (for simplicity, both devices were considered to be synchronized) and initial condition $x^0 = [-\pi, 0, 0, 0]$. The effect

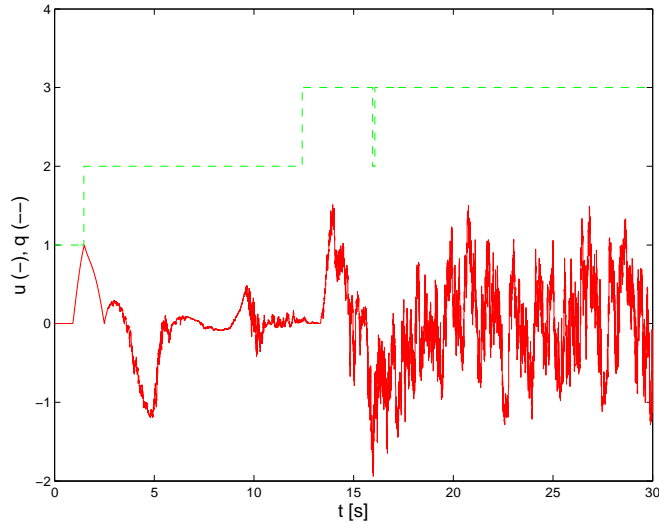


Figure 5.8. Control law and discrete mode for large noise. The mode changes rapidly between $q = 3$ and $q = 2$ when the noise causes the state to leave the set C_3 (see Figure 5.7).

of the sample and digital controller/ZOH device in the loop becomes noticeable for timer constants of 2/10 seconds. This indicates that, as predicted by Theorem 5.12, the closed-loop system \mathcal{H}_{cl} has some robustness properties to sample and digital controller/ZOH device since typical rates for commercial devices of this type are around the order of milliseconds. (For example, academic control systems kits manufactured by Quanser provide sample/ZOH rates that can be set below $0.005sec$.) Figure 5.9 shows that as the sample/hold rate increases, the trajectories approach the upright position after performing more swings. We detected by simulations that for $T_s = T_c > 0.6sec$, more than one swing is required to stabilize the pendulum to the upright position, and that for $T_s = T_c > 0.85sec$, the rate of failure to accomplish the task increases. Figure 5.10 presents trajectories with constant sampling rate $T_s = 0.01sec$ and different values of the timer constant T_c for the digital controller/ZOH device. In this situation, as in Figure 5.9, a large timer constant T_c causes similar effect, requiring more than one swing to stabilize the pendulum to the upright position and to stabilize the cart to zero position and zero velocity, in this case for T_c larger than $0.48sec$. Again, as T_c approaches $0.85sec$ the rate of failure increases. When the timer constant T_c for the digital controller/ZOH device is fixed to $0.01sec$ and the timer constant T_s varies, the results obtained line up with the ones depicted in Figure 5.9. This suggests that for this particular system both the sampling and digital controller/ZOH device introduce similar effects.

5.5 Summary

Robustness of asymptotic stability of closed-loop systems resulting from hybrid control was characterized for several perturbations: measurement noise, unmodeled sensor and actuator dynamics, control smoothing, and sample-and-hold implementation. The results guarantee that when this perturbations are small enough, the compact set (which is nominally asymptotically stable) is semiglobally practically asymptotically stable. The global stabilization of one-link pendulum on a cart to the upright condition was used as a benchmark problem to test the robustness properties of hybrid control guaranteed by the results presented.

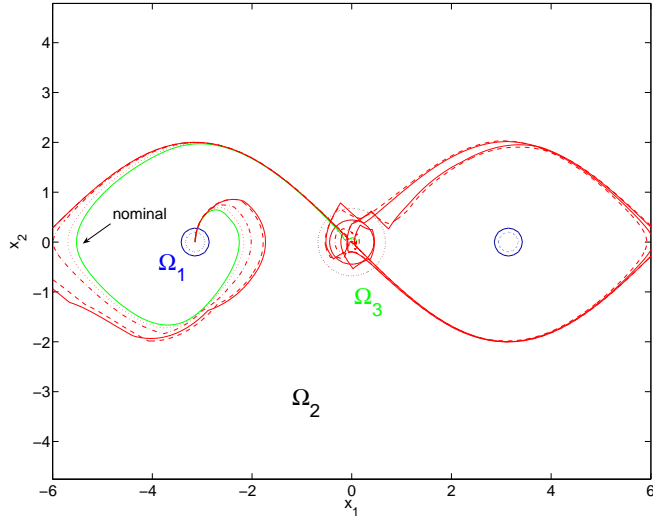


Figure 5.9. Closed-loop trajectories for the nominal case (no sample and hold devices) and for timer constants: $T_s = T_c = 0.2\text{sec}$ (:), $T_s = T_c = 0.6\text{sec}$ (-.), $T_s = T_c = 0.8\text{sec}$ (---), $T_s = T_c = 0.85\text{sec}$ (solid).

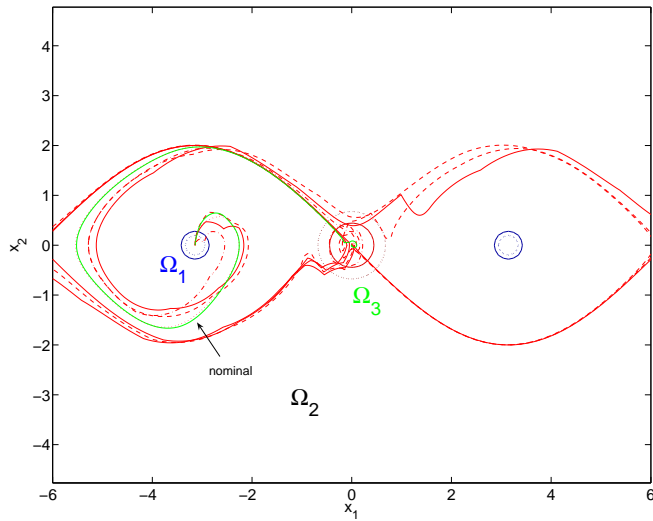


Figure 5.10. Closed-loop trajectories for the nominal case (solid) and for (fixed) timer constant of the sampler $T_s = 0.01\text{sec}$ and for timer constants of the digital controller/ZOH device: $T_c = 0.2\text{sec}$ (:), $T_c = 0.48\text{sec}$ (-.), $T_c = 0.8\text{sec}$ (---), $T_c = 0.85\text{sec}$ (solid).

5.6 Notes and references

For references showing that it is impossible to stabilize nonholonomic using time-invariant continuous state feedback and robust stabilization is impossible using time-invariant locally bounded feedback see, for example,

[49, 76].

The robustness properties inherited when sample and hold control is used in stabilization is discussed in [95, 28, 53].

Consistency properties have been considered for numerical integration schemes in the numerical analysis literature (see e.g. [96, 5]) and in the construction of approximate models for discrete-time systems (see e.g. [75]).

The ideas in the particular hybrid controller at the end of Section 5.1 are similar to the ones in [77].

For swing up of a pendulum on a cart control algorithms related to the one in Section 5.4 see, for example, [6, 102, 26].

The preliminary state feedback and the construction of $\tilde{\kappa}$ in Section 5.4 are, for example, given in [99] .

The proof of 5.12 is given in Section B.3.

Chapter 6

Hybrid Control Applications

In this chapter, relying on the tools developed in the previous chapters three general hybrid control strategies to accomplish tasks that are recast as asymptotic stabilization problems are presented. The need of hybrid control and the strategies themselves are motivated, explained, and illustrated by several engineering problems. The hybrid controller implementing each control strategy will be designed so that the resulting hybrid closed-loop system satisfies the hybrid basic conditions, and consequently, the results in the previous chapters are applicable.

6.1 Hysteresis-based control

6.1.1 A robustness motivation to hybrid control

The problem of designing feedback systems for nonlinear systems to accomplish a particular stabilization task in the presence of noise in the measurements is relevant in most industrial applications. The reason for this is that measurements are usually taken from sensors which are frequently corrupted by noise. When the control strategy involves switching between different controllers, it is crucial to guarantee that the decision making algorithm is not fragile to measurement noise. In some engineering applications, like the ones described below, the presence of measurement noise in the closed loop may lead to undesired behavior of the system.

Suppose that two different locations are given, denoted by the points (or sets) \mathcal{A}_1 and \mathcal{A}_2 in Figure 6.1(a), and that it is desired to steer an autonomous vehicle to either one of these points using position feedback. Let the dynamics of the autonomous vehicle be given by $\dot{x} = u$ where $x, u \in \mathbb{R}^2$. One possible design technique to accomplish the task is to design a feedback controller that globally asymptotically stabilizes the closed-loop trajectories to the set $\mathcal{A} := \mathcal{A}_1 \cup \mathcal{A}_2$. To that end, one can easily construct functions V_1 and V_2 that are quadratic, positive definite with respect to \mathcal{A}_1 and \mathcal{A}_2 , respectively, and design a state-dependent switching law between the steepest descent control laws

$$\kappa_1(x) = -\nabla V_1(x) \quad \text{and} \quad \kappa_2(x) = -\nabla V_2(x) .$$

To render the set \mathcal{A} globally asymptotically stable, trajectories starting near \mathcal{A}_1 (\mathcal{A}_2) should approach \mathcal{A}_1 (\mathcal{A}_2) and starting far from them, should approach one of them.

Consequently, a line, like the one depicted in Figure 6.1(b) denoted by \mathcal{M} , arises partitioning the state space in a way that for initial conditions on one side of it, trajectories approach \mathcal{A}_1 , while for initial condition at the other side, trajectories approach \mathcal{A}_2 . Such a control strategy renders the set \mathcal{A} globally asymptotically stable, that is, steers the vehicle to one of the locations for each initial condition. However, issues may arise in the

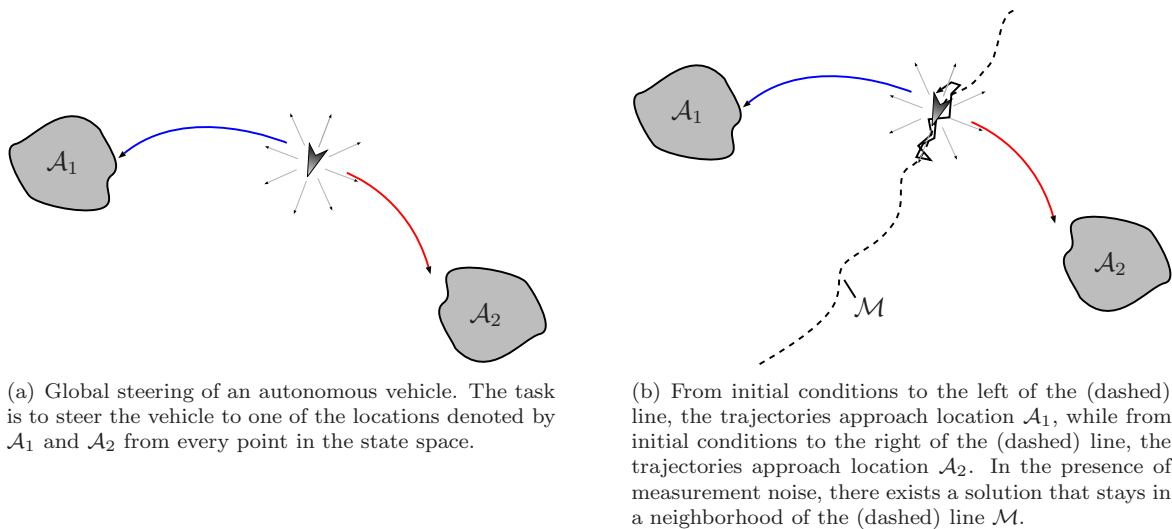


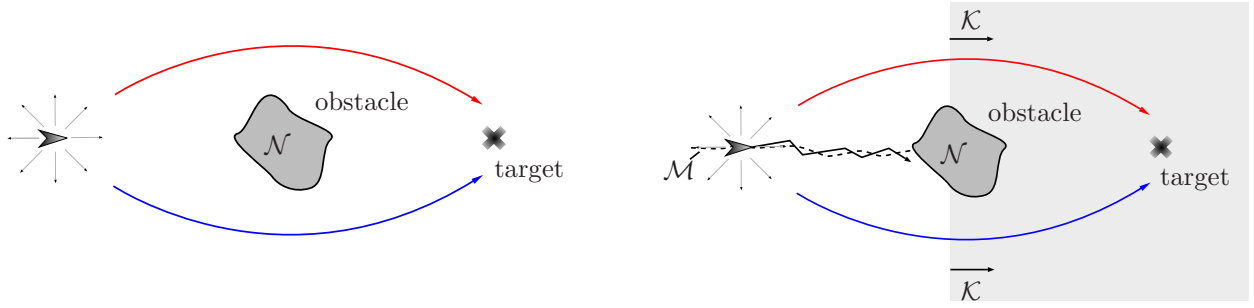
Figure 6.1. Global steering of an autonomous vehicle to different locations.

presence of noise in measurement of the vehicle position (even when this noise is arbitrarily small). To illustrate this, consider an initial condition that is close to the line \mathcal{M} . There exists a measurement noise signal e such that x and $x + e$ are at opposite sides of \mathcal{M} . Then, the control strategy just described will steer the vehicle over the line towards the opposite side. Since e can change at any time instant, it can change as soon as the vehicle has crossed the line and report that the vehicle is now in the opposite side of \mathcal{M} . This can occur repetitively, preventing the autonomous vehicle from reaching \mathcal{A} as illustrated in Figure 6.1(b). In fact, as it is shown later, there exists arbitrarily small measurement noise that causes the vehicle trajectories to stay arbitrarily close to \mathcal{M} .

Another scenario where a similar phenomenon can arise under perturbations is the problem of driving a vehicle from its initial position to a specific target while avoiding an obstacle. Figure 6.2(a) depicts an autonomous vehicle to be steered to a target \times while avoiding the obstacle \mathcal{N} . Suppose that there exists a feedback law that achieves stability and “global” convergence to the target (in the sense that for every point not in \mathcal{N} , trajectories approach the target) and, for simplicity of the exposition, suppose that the trajectories are unique and once they reach some set \mathcal{K} , like the one depicted in Figure 6.2(a), they converge to the target.

Due to the topological properties of the problem, as shown in Figure 6.2(b), there exists a line \mathcal{M} such that for initial conditions at each side of it, trajectories approach the set \mathcal{K} either from above the obstacle or from below it. It follows that, for initial conditions arbitrarily close to the line \mathcal{M} , there exists a noise signal e for the measurements of the vehicle position such that there exist closed-loop trajectories that stay in a neighborhood of the line \mathcal{M} . Eventually, if the forward velocity of the vehicle is positive, such trajectories could indicate that the vehicle crashes onto the obstacle. This is depicted in Figure 6.2(b).

A similar type of behavior arises in other applications, including multiple agent control of autonomous vehicles, control of robotic manipulators, etc. This lack of robustness appears in general when the control task is such that the state space is partitioned generating a similar topological structure as in the examples above. The following section formalizes these issues for a large class of nonlinear systems.



(a) Global steering of an autonomous vehicle to a target with obstacle avoidance. The task is to control the vehicle so that it avoids the obstacle \mathcal{N} and approaches the target \times .

(b) From initial conditions above the (dashed) line, the trajectories approach the set \mathcal{K} , and from there they approach the target from above the obstacle, while from initial conditions below the (dashed) line, the trajectories approach the set \mathcal{K} and then the target from below the obstacle. In the presence of measurement noise, a trajectory could stay in a neighborhood of the (dashed) line, potentially causing the vehicle to crash into the obstacle.

Figure 6.2. Global steering to a target with obstacle avoidance.

6.1.2 A general robustness issue

Consider the nonlinear system

$$\dot{x} = f_p(x) \tag{6.1}$$

where x is the state, $O \subset \mathbb{R}^n$ is an open state space, and $f_p : O \rightarrow \mathbb{R}^n$. Solutions to (6.1) are in the sense of Carathéodory.

Definition 6.1 (Carathéodory solution) *A Carathéodory solution to system (6.1) on an interval $I \subset \mathbb{R}_{\geq 0}$ is an absolutely continuous function $x : I \rightarrow \mathbb{R}^n$ that satisfies $\dot{x}(t) = f(x(t))$ almost everywhere on I ; equivalently, for every $t_0 \in I$, $x(t)$ satisfies*

$$x(t) = x(t_0) + \int_{t_0}^t f_p(x(\tau)) d\tau$$

for all $t \in I$, $t \geq t_0$.

A Carathéodory solution is said to be *maximal* if there is no proper right extension which is also a solution to (6.1), and it is said to be *complete* if its domain is equal to $\mathbb{R}_{\geq 0}$ (cf. Definition 2.6 and 2.4).

Assumption 6.2 (existence of solutions) *The function f_p is locally bounded and for every initial condition $x(t_0) = x^0 \in O$ at least one Carathéodory solution to (6.1) exists and all solutions are complete.*

Note that this assumption is reasonable since the goal is to make a point about robust stability rather than about existence of solutions. Carathéodory solutions to (6.1) in the presence of measurement noise¹ are defined as follows.

¹Measurement noise arises in control scenarios where perturbations enter the state measurements when computing a control law. Even though a control law has not been defined explicitly yet, the term “measurement noise” will be still used when referring to general state perturbations, like the ones in Definition 6.3.

Definition 6.3 (Carathéodory solutions with measurement noise) *Given an interval $I \subset \mathbb{R}_{\geq 0}$ and a measurable function $e : I \rightarrow \mathbb{R}^n$, a Carathéodory solution to the system $\dot{x} = f_p(x + e)$ on I is an absolutely continuous function $x : I \rightarrow O$ that satisfies $\dot{x}(t) = f_p(x(t) + e(t))$ almost everywhere on I ; equivalently, for every $t_0 \in I$, $x(t)$ satisfies*

$$x(t) = x(t_0) + \int_{t_0}^t f_p(x(\tau) + e(\tau)) d\tau$$

for all $t \in I$.

A general result about vulnerability to measurement noise for a class of nonlinear systems is stated below. Let $\mathcal{B} \subset O$ be open and let $\mathcal{M}_i \subset O$, $i \in \{1, \dots, m\}$, $m \in \mathbb{N}_{\geq 2}$, be disjoint sets satisfying $\bigcup_{i=1}^m \mathcal{M}_i = \mathcal{B}$. Let

$$\mathcal{M} := \bigcup_{i,j \in \{1, \dots, m\}, i \neq j} \overline{\mathcal{M}_i} \cap \overline{\mathcal{M}_j}.$$

Assumption 6.4 (state partition) *Suppose that there exists $T > 0$ such that for each $x \in \mathcal{M}$ and each $\rho > 0$, there exist points $z_i, z_j \in \{x\} + \rho\mathbb{B}$, $i, j \in \{1, \dots, m\}$, $i \neq j$, for which there exist Carathéodory solutions x_i and x_j to system (6.1) starting from z_i and z_j , respectively, satisfying $x_i(t) \in \mathcal{M}_i \setminus \mathcal{M}$ and $x_j(t) \in \mathcal{M}_j \setminus \mathcal{M}$ for all $t \in [0, T]$.*

Theorem 6.5 (nonrobustness to measurement noise) *Let Assumptions 6.2 and 6.4 hold. For every positive constants ε , ρ' , and ρ'' , and every $x^0 \in \mathcal{M} + \varepsilon\mathbb{B}$ such that $x^0 + \rho'\mathbb{B} \subset O$ and $x^0 + \rho''\mathbb{B} \subset \mathcal{B}$ there exist a piecewise constant function $e : \text{dom } e \rightarrow \varepsilon\mathbb{B}$ and a maximal Carathéodory solution $x : \text{dom } x \rightarrow O$ to $\dot{x} = f_p(x + e)$ with $x(0) = x^0$ such that $x(t) \in (\mathcal{M} + \varepsilon\mathbb{B}) \cap \mathcal{B} \cap (x^0 + \rho'\mathbb{B})$ for all $t \in [0, T']$ for some $T' \in (T^*, \infty]$, where $\text{dom } x = \text{dom } e$, $T^* = \frac{\min\{\rho', \rho''\}}{m}$, and $m := \sup \{1 + |f(\eta)| \mid \eta \in x^0 + \max\{\rho', \rho''\}\mathbb{B}\}$. If T' is finite, then $\lim_{t \rightarrow T'} x(t) \notin \mathcal{B} \cup (x^0 + \rho'\mathbb{B})$.*

Theorem 6.5 states that for nonlinear systems with the topological properties in Assumption 6.4, there exists a set of points of the state space (the set \mathcal{M}) such that from every point x^0 arbitrarily close to it, there exists an arbitrarily small noise signal e and a solution x to $\dot{x} = f_p(x + e)$ starting from x^0 that stays close to an arbitrarily small neighborhood of \mathcal{M} (intersected with a ball around x^0). Moreover, if the solution ever leaves such set then either it does it through the boundary of \mathcal{B} or through the boundary of $x^0 + \rho'\mathbb{B}$.

Note that Assumption 6.4 states in general the scenario that arises, for example, in the stabilization problems in Section 6.1.1. For the problem of stabilizing a disconnected set of points, the regions on each side of the line define the sets \mathcal{M}_1 and \mathcal{M}_2 , respectively. Note that by global asymptotic stability, the union of $\overline{\mathcal{M}_1}$ and $\overline{\mathcal{M}_2}$ covers the state space. Then, the open set \mathcal{B} is equal to $O = \mathbb{R}^n$. The set \mathcal{M} is given by $\mathcal{M} := \overline{\mathcal{M}_1} \cap \overline{\mathcal{M}_2}$ as depicted in Figure 6.3(a) (it corresponds to the dashed line in Figure 6.1(b)). For the obstacle avoidance problem in Section 6.1.1, the state space is given by $O = \mathbb{R}^n \setminus \mathcal{N}$ where \mathcal{N} is a closed subset of \mathbb{R}^n . The set of points from which at least one trajectory converges to \mathcal{K} by crossing into the set \mathcal{K} from below the obstacle defines the set \mathcal{M}_1 while the set of points from above the obstacle define the set \mathcal{M}_2 . By “global” convergence, $\mathcal{M}_1 \cup \mathcal{M}_2$ covers every point of the state space except the obstacle \mathcal{N} and the set \mathcal{K} . By stability and attractivity, those sets are nonempty. Then, the set \mathcal{M} is defined as the intersection of the closures of the sets \mathcal{M}_1 and \mathcal{M}_2 . The set \mathcal{B} is given by the union of the sets \mathcal{M}_i , $i = 1, 2$, and \mathcal{K} is such that $O = \mathcal{B} \cup \mathcal{K}$. Figure 6.3(b) depicts these sets.

Under further assumptions, a version of Theorem 6.5 also holds in the state feedback case, that is, for nonlinear systems of the form

$$\dot{x} = \tilde{f}(x, \kappa(x)) \tag{6.2}$$

where x is the state, $O \subset \mathbb{R}^n$ is the open state space, $\kappa : O \rightarrow \mathbb{R}^m$, and $\tilde{f} : O \times \mathbb{R}^m \rightarrow \mathbb{R}^n$.

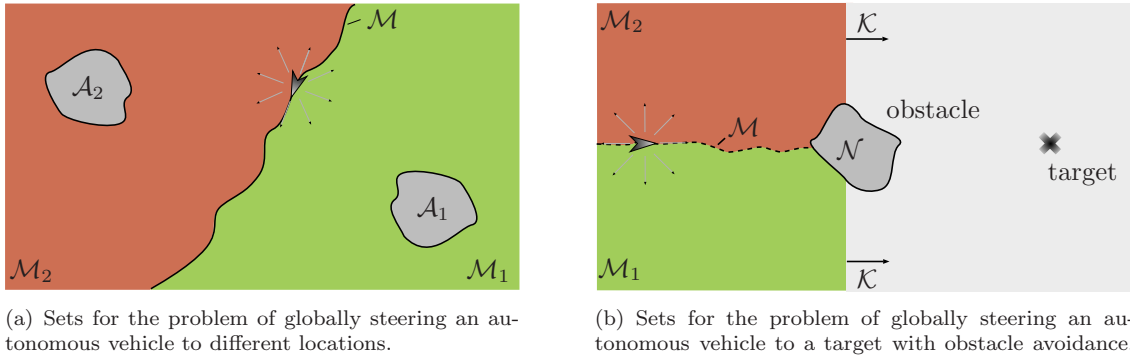


Figure 6.3. Sets for the problems in Section 6.1.1.

Assumption 6.6 (regularity conditions for state feedback case) *The function \tilde{f} is locally Lipschitz continuous in the first argument, locally uniformly in the second argument²; the function κ is locally bounded; and for every $x^0 \in O$ at least one Carathéodory solution to (6.2) exists and all solutions from O are complete.*

The function κ usually corresponds to a static control law designed to accomplish some control task. In this scenario, a Carathéodory solution to (6.2) with measurement noise is as in Definition 6.3 but with measurement noise entering through κ only, that is, $x(t)$ satisfies

$$x(t) = x(t_0) + \int_{t_0}^t f_p(x(\tau), \kappa(x(\tau) + e(\tau))) d\tau .$$

In this way, κ models the case of closed-loop systems where not every state component is perturbed by measurement noise because some of its components come from the natural dynamics. The assumption on f in Assumption 6.6 holds in many cases since the nonlinearities of the natural dynamics are Lipschitz continuous. For example, in the problem of regulating a double integrator to two different points of zero velocity by means of state feedback, measurement noise does not enter the natural dynamics of the system (note that the natural dynamics are linear in this case); it only enters through the feedback law.

Under Assumption 6.4, it follows that measurement noise entering the system through κ may prevent the trajectories to approach the set \mathcal{A} . This is stated in the next corollary.

Corollary 6.7 (state feedback case of general nonrobustness) *Let Assumptions 6.4 and 6.6 hold. For every $\varepsilon > 0$ and every $z \in \mathcal{M} \cap \mathcal{B}$ there exists $\delta > 0$ such that for each $x^0 \in (z + \delta\mathbb{B}) \cap \mathcal{B}$ there exist a measurable function $e : \text{dom } e \rightarrow \varepsilon\mathbb{B}$ and a maximal Carathéodory solution $x : \text{dom } x \rightarrow O$ to $\dot{x} = f_p(x, \kappa(x + e))$ with $x(0) = x^0$ such that $x(t) \in (\mathcal{M} + \varepsilon\mathbb{B}) \cap \mathcal{B}$ for all $t \in [0, T')$ for some $T' \in (0, \infty]$. If T' is finite, then $\lim_{t \rightarrow T'} x(t) \notin \mathcal{B}$.*

As in Theorem 6.5, Corollary 6.7 states that under the stated assumptions, solutions can stay arbitrarily close to the set \mathcal{M} under the presence of arbitrarily small measurement noise. The proof of this result uses the fact that Theorem 6.5 implies the existence of a maximal Krasovskii solution to (6.1) that stays in \mathcal{M} (cf. [31, Proposition 1.4]). Then, a solution and measurement noise signal for (6.2) is constructed to “track” the Krasovskii solution with arbitrary precision.

²A function $h : O \times \mathbb{R}^m \rightarrow \mathbb{R}^n$ is continuous (locally Lipschitz continuous) in the first argument, locally uniformly in the second argument if for each $z \in O$, each compact $U \subset \mathbb{R}^m$, and each $\varepsilon > 0$ there exists $\delta > 0$ ($K > 0$) such that $|x - z| < \delta$ implies $|h(x, u) - h(z, u)| < \varepsilon$ ($x, y \in (z + \varepsilon\mathbb{B}) \cap O$ implies $|h(x, u) - h(y, u)| \leq K|x - y|$) for all $u \in U$.

6.1.3 Control design and analysis

In this section, nonlinear control systems of the following form are considered:

$$\dot{x} = f_p(x, u) \quad (6.3)$$

where x is the state, $O \subset \mathbb{R}^n$ is an open state space, $u \in \mathbb{R}^m$ is the control input, and $f_p : O \times \mathbb{R}^m \rightarrow \mathbb{R}^n$.

Assumption 6.8 (regularity of f_p) *The function f_p is continuous.*

Let $\mathcal{A} \subset O$ be a compact set. A hybrid controller, denoted by \mathcal{H}_c , that renders the set \mathcal{A} asymptotically stable for (6.3) is designed. This hybrid controller confers to the closed-loop system a margin of robustness to noise in the measurements of the state x . The proposed controller prevents the closed-loop system from being vulnerable to measurement noise in scenarios like the ones discussed in the previous sections.

Hybrid controller

The hybrid controller \mathcal{H}_c measures the output $y := x + e$ of (6.3), has logic (or discrete) state q that takes value in the finite set $Q := \{1, 2, \dots, m\}$, $m \in \mathbb{N}$, has continuous dynamics

$$\dot{q} = 0 \quad (y, q) \in C_c ,$$

discrete dynamics

$$q^+ \in Q_c(y, q) \quad (y, q) \in D_c ,$$

and output

$$u = \kappa(y, q) ,$$

where C_c, D_c are subsets of $O \times Q$, $Q_c : O \times Q \rightrightarrows Q$ is a set-valued map that defines the update law for the discrete state q , and κ is a function that defines the control law applied to (6.3).

Assume there exists a family of open sets $O_q \subset \mathbb{R}^n$ such that $O := \cup_{q \in Q} O_q$ and $\mathcal{A} \subset O$. Suppose that there exist functions $V_q : O \rightarrow [0, \infty]$ that are C^1 on O_q , for every $z \in O \setminus O_q$ are such that $V_q(z) = \infty$, and as $|x| \rightarrow \infty$ or $x \rightarrow \partial O_q$ are such that $V_q(x) \rightarrow \infty$; a family of C^0 functions $\kappa_q : O_q \rightarrow \mathbb{R}^m$; functions $\alpha_1, \alpha_2 \in \mathcal{K}_\infty$; a continuous, positive-definite function $\rho : \mathbb{R}_{\geq 0} \rightarrow \mathbb{R}_{\geq 0}$; and a proper indicator³ ω of \mathcal{A} on O such that

$$\alpha_1(\omega(x)) \leq \min_{p \in Q} V_p(x) \leq \alpha_2(\omega(x)) \quad \forall x \in O , \quad (6.4)$$

and, for each $q \in Q$,

$$\langle \nabla V_q(x), f_p(x, \kappa_q(x)) \rangle \leq -\rho(V_q(x)) \quad \forall x \in O_q . \quad (6.5)$$

In some control problems, like in the regulation to a disconnected set of points (see Section 6.1.1), for each $q \in Q$, there exist a proper indicator ω_q of \mathcal{A} on O_q and functions $\alpha_1^q, \alpha_2^q \in \mathcal{K}_\infty$ satisfying

$$\alpha_1^q(\omega_q(x)) \leq V_q(x) \leq \alpha_2^q(\omega_q(x)) \quad \forall x \in O_q . \quad (6.6)$$

The function $\omega : O \rightarrow \mathbb{R}_{\geq 0}$ constructed as $\omega(x) := \min_{q \in Q} \omega_q(x)$ for each $x \in O$ is a proper indicator of \mathcal{A} on O and the functions $\alpha_1, \alpha_2 \in \mathcal{K}_\infty$ given by $\alpha_1(s) := \min_{p \in Q} \alpha_1^p(s)$, $\alpha_2(s) := \max_{p \in Q} \alpha_2^p(s)$ for each $s \in \mathbb{R}_{\geq 0}$ satisfy (6.4).

³A function $\omega : U \rightarrow \mathbb{R}_{\geq 0}$ is a proper indicator of a compact set $\mathcal{A} \subset U$ with respect to an open set U if it is continuous, positive definite with respect to \mathcal{A} , and such that $\omega(x) \rightarrow \infty$ as $x \rightarrow \partial U$ (boundary of U) or $|x| \rightarrow \infty$.

Assumption 6.9 (V_q condition on $\mathcal{A} \times Q$) *There exists $\gamma > 0$ such that $(x, q) \in \mathcal{A} \times Q$ and $V_q(x) > 0$ imply $V_q(x) > \gamma$.*

Assumption 6.9 is automatically satisfied when, for each $q \in Q$, V_q is positive definite with respect to \mathcal{A} since, in this case, it is impossible to have $(x, q) \in \mathcal{A} \times Q$ and $V_q(x) > 0$. In scenarios where V_q is non-zero on a subset of \mathcal{A} , for example when \mathcal{A} is a disconnected set like in Section 6.1.1, then the constant γ consists of a uniform lower bound on $V_q(x)$ on that subset.

Define constants $\mu > 1$ and $\lambda \in (0, \mu - 1)$. Let $\gamma > 0$ be given by Assumption 6.9. The hybrid controller \mathcal{H}_c defines the feedback law

$$u = \kappa(y, q) := \kappa_q(y)$$

when $(y, q) \in C_c := C_c^a \cup C_c^b$, where

$$C_c^a := \left\{ (x', q') \in O \times Q \mid V_{q'}(x') \leq \mu \min_{p \in Q} V_p(x') \right\} \quad (6.7)$$

$$C_c^b := \{(x', q') \in O \times Q \mid V_{q'}(x') \leq \gamma\}, \quad (6.8)$$

and has discrete dynamics given by

$$q^+ \in Q_c(y, q) := \{q' \in Q \mid V_q(y) \geq (\mu - \lambda)V_{q'}(y)\}$$

when $(y, q) \in D_c$, where D_c is given by

$$\left\{ (x', q') \in O \times Q \mid V_{q'}(x') \geq (\mu - \lambda) \min_{p \in Q} V_p(x') \right\}. \quad (6.9)$$

The design parameters of the controller are μ and λ .

The basic idea in this construction is as follows. The discrete mode q selects the control law that is to be applied to system (6.3). A change in the mode occurs only if the Lyapunov function for the current mode, V_q , gets larger or equal than the Lyapunov function for some other mode, say $V_{q'}$, multiplied by $\mu - \lambda > 1$. Points $(x, q) \in O \times Q$ with this property define the set D_c . Then, jumps are only allowed to modes that, at the current state, have a Lyapunov function $\frac{1}{(\mu - \lambda)} < 1$ times smaller than the Lyapunov function at the current mode. Flows are allowed when the Lyapunov function for the current mode is smaller or equal than μ times the minimum of the Lyapunov functions for the other modes. Then, with (6.5), the Lyapunov function for the current mode is decreasing along solutions. Global asymptotic stability of the compact set \mathcal{A} is achieved in this way. This stability property and its robustness to external state perturbations is addressed in the next section.

Closed-loop system properties

From the construction of \mathcal{H}_c , the nominal closed-loop hybrid system, denoted \mathcal{H}_{cl} , can be written as

$$\left. \begin{aligned} \dot{x} &= f_p(x, \kappa(x, q)) \\ \dot{q} &= 0 \end{aligned} \right\} (x, q) \in C_c \quad (6.10)$$

$$\left. \begin{aligned} x^+ &= x \\ q^+ &\in Q_c(x, q) \end{aligned} \right\} (x, q) \in D_c. \quad (6.11)$$

With the regularity properties of f_p , V_q , and κ_q on O_q for each $q \in Q$ and the construction of the flow and jump sets in (6.7)-(6.8) and (6.9), respectively, the resulting data (\bar{O}, F, C, G, D) of the hybrid system \mathcal{H}_{cl} with

state $\xi := [x^T \ q^T]$ given by

$$\tilde{O} := O \times \mathbb{R}, \quad F(\xi) := \begin{bmatrix} f_p(x, \kappa(x, q)) \\ 0 \end{bmatrix}, \quad G(\xi) := \begin{bmatrix} x \\ Q_c(x, q) \end{bmatrix}, \quad C := C_c, \quad D := D_c$$

satisfies the hybrid basic conditions. Recall that these conditions guarantee, among other things, that hybrid systems have several structural properties, including the property that the limit of a sequence of solutions to hybrid systems is itself a solution.

Lemma 6.10 (hybrid basic conditions) *Under Assumption 6.8 and 6.8, for every $\gamma > 0$ the closed-loop system \mathcal{H}_{cl} satisfies the hybrid basic conditions. Moreover, $C_c \subset \cup_{q \in Q} O_q \times \{q\}$ and $C_c \cup D_c = O \times Q$.*

Proof. By definition, $C_c \subset O \times Q \subset \tilde{O}$. By continuity of V_q for each $q \in Q$, $C = \overline{C}$. Then

$$\overline{C} \cap \tilde{O} = C \cap (O \times \mathbb{R}) = C.$$

Then, C is relatively closed in \tilde{O} . Proceeding similarly, $D_c \subset O \times Q$ and it can be shown that D is relatively closed in \tilde{O} .

By definition of C_c , if $(x, q) \in C_c$ then $V_q(x) < \infty$, and since by Assumption 6.8 this holds only if $(x, q) \in O_q \times \{q\}$, then $C_c \subset \cup_{q \in Q} (O_q \times \{q\})$. Every point in $(\cup_{q \in Q} (O_q \times \{q\})) \setminus C_c^a$ satisfies, in particular, $V_q(x) > \mu \min_{p \in Q} V_p(x)$. By definition of D_c , every such point is in D_c . Moreover, every point $(x, q) \in (O \times Q) \setminus (\cup_{q \in Q} (O_q \times \{q\}))$ is such that $V_q(x) = \infty$. By definition of O , for each such point there exists $q' \in Q$ such that $V_{q'}(x) < \infty$. Then, every such point is in D_c . This establishes that $C_c \cup D_c = O \times Q$.

Since for each $q \in Q$, $\kappa(x, q) = \kappa_q(x)$ for each $x \in O_q$ and κ_q, f_p are continuous, F is continuous on its domain of definition and nonempty for each point in $\cup_{q \in Q} (O_q \times \{q\})$, in particular, for each point in C_c .

By construction of D_c and Q_c , $Q_c(x, q) \neq \emptyset$ and $Q_c(x, q) \subset C_c$ for every $(x, q) \in D_c$. For every $(x, q) \in D_c$ and every sequence x_i, q_i such that $(x_i, q_i) \in D_c$ and $x_i \rightarrow x, q_i \rightarrow q$ it holds that

$$V_{q_i}(x_i) \geq (\mu - \lambda)V_{p_i}(x_i) \tag{6.12}$$

where $p_i \in Q_c(x_i, q_i)$. For q_i and p_i to converge, $p_i = p$ and $q_i = q$ for large enough i , for some $p, q \in Q$. Taking limit at each side of (6.12) and using the continuity properties of V_q for each $q \in Q$ yields

$$V_q(x) \geq (\mu - \lambda)V_p(x). \tag{6.13}$$

Then, $p \in Q_c(x, q)$ and Q_c is outer semicontinuous in its domain of definition. \square

As discussed in the previous section, the construction of the hybrid controller is such that the logic mode q is updated so that the Lyapunov function for the closed-loop hybrid system \mathcal{H}_{cl} given by $W(x, q) := V_q(x)$ decreases along solutions. This leads to the following ‘‘global’’ asymptotic stability result of the compact set $\mathcal{A} \times Q$.

Theorem 6.11 (nominal asymptotic stability of \mathcal{A}) *Under Assumptions 6.8 and 6.9, the compact set $\mathcal{A} \times Q$ is asymptotically stable with basin of attraction $\mathcal{B}_{\mathcal{A}} = O \times Q$ for the hybrid system \mathcal{H}_{cl} .*

In the case that noise e corrupts the measurement of the state x , that is, the controller measures the output $y = x + e$, statements about robustness of the above asymptotic stability property can be made by perturbation analysis. Roughly speaking, the main idea is to model the measurement noise as a state perturbation of size $\delta^* > 0$ and replace the instances in (6.10) and (6.11) where the controller measures the state by the state

perturbation $x + \delta^* \overline{\mathbb{B}}$ (these places are the first argument of κ , C_c , Q_c , and D_c). Then, the resulting perturbed hybrid system will have the original data (\tilde{O}, F, C, G, D) perturbed and, by construction, satisfying certain conditions that guarantee that the stability property is semiglobally and practically preserved. The following result uses this technique to show that $\mathcal{A} \times Q$ is semiglobally practically asymptotically stable under small enough measurement noise.

Theorem 6.12 (robustness of \mathcal{H}_{cl} to measurement noise) *For given parameters $\mu > 1$ and $\lambda \in (0, \mu - 1)$ of the controller \mathcal{H}_c , there exists $\beta \in \mathcal{KLL}$ and for each $\varepsilon > 0$ and each compact set $K \subset O$ there exists $\delta^* > 0$, such that for each admissible measurement noise $e : \text{dom } e \rightarrow \delta \overline{\mathbb{B}}$ with $\delta \in [0, \delta^*]$, solutions (x, q) to \mathcal{H}_{cl} exist, are complete, and for initial conditions $(x^0, q^0) \in K \times Q$ satisfy*

$$\omega(x(t, j)) \leq \beta(\omega(x^0), t, j) + \varepsilon \quad \forall (t, j) \in \text{dom}(x, q) .$$

Theorem 6.12 guarantees that for each compact set of initial conditions, the closed-loop system \mathcal{H}_{cl} tolerates a nonzero level $\delta^* > 0$ of measurement noise. This corresponds to the margin of robustness that the hybrid control strategy confers to the closed-loop system. This margin of robustness to measurement noise overcomes the issues described in the control problems in Section 6.1.1.

An estimate of this margin of robustness can be computed from the sets C_c and D_c . Figure 6.4 shows these sets, along with level sets of the Lyapunov functions, for the problem of globally stabilizing a disconnected set of points in Section 6.1.1. Given points $\mathcal{A}_1, \mathcal{A}_2$ with associated Lyapunov functions V_1, V_2 and control laws κ_1, κ_2 satisfying the conditions in Section 6.1.3, respectively, and parameters $\mu > 1$, $\lambda \in (0, \mu - 1)$, the set C_c and D_c can be written as

$$C_c := (C_{c1} \times \{1\}) \cup (C_{c2} \times \{2\}), \quad D_c := (D_{c1} \times \{1\}) \cup (D_{c2} \times \{2\}) \quad (6.14)$$

where $C_{c1}, C_{c2}, D_{c1}, D_{c2} \subset O$. Figure 6.4 depicts these sets and a solution to \mathcal{H}_{cl} . The solution, which starts from a point in the flow set with $q = 1$, experiences a jump when in the jump set that maps q to 2. From there, the solution flows with $q = 2$ until, once in the jump set again, a jump maps q to 1. From there on, the solution stays in the flow set with mode $q = 1$ and approaches \mathcal{A}_1 . From this discussion, it follows that under the presence of measurement noise, for the closed-loop system to experience the nonrobust behavior discussed in Section 6.1.1, the size of the measurement noise needs to be so that fast switching between the modes occurs. This is only possible from certain points of the state space if the measurement noise is larger than the minimum distance between the sets D_{c1} and D_{c2} . Then, this analysis suggests that the maximum measurement noise for which solutions approach the target set without experiencing the phenomenon described in Theorem 6.5 and Corollary 6.7 is given by

$$\delta_1 := \min_{z_1 \in D_{c1}, z_2 \in D_{c2}} |z_1 - z_2| . \quad (6.15)$$

This level depends proportionally on μ , and therefore, can be tuned by varying this control parameter. For the setting in Figure 6.4, as μ increases, the set D_{c1} (D_{c2}) becomes smaller and centered around the set \mathcal{A}_2 (\mathcal{A}_1). Clearly, the maximum margin of robustness to measurement noise that can be obtained with this control strategy is upper bounded by the distance between \mathcal{A}_1 and \mathcal{A}_2 .

As discussed in Section 3.3, measurement noise in hybrid systems can lead to nonexistence of solutions, even when the measurement noise is arbitrarily small. The overlap between the set C_c and D_c obtained from using μ in the definition of C_c and $\mu - \lambda$ in the definition of D_c guarantees such existence for measurement noise smaller than the minimum overlap given by

$$\begin{aligned} \delta_2 &:= \min\{\delta_{21}, \delta_{22}\}, \quad \delta_{21} := \min_{z_1 \in O \setminus D_{c1}, z_2 \in O \setminus C_{c1}} |z_1 - z_2|, \\ \delta_{22} &:= \min_{z_1 \in O \setminus D_{c2}, z_2 \in O \setminus C_{c2}} |z_1 - z_2| , \end{aligned}$$

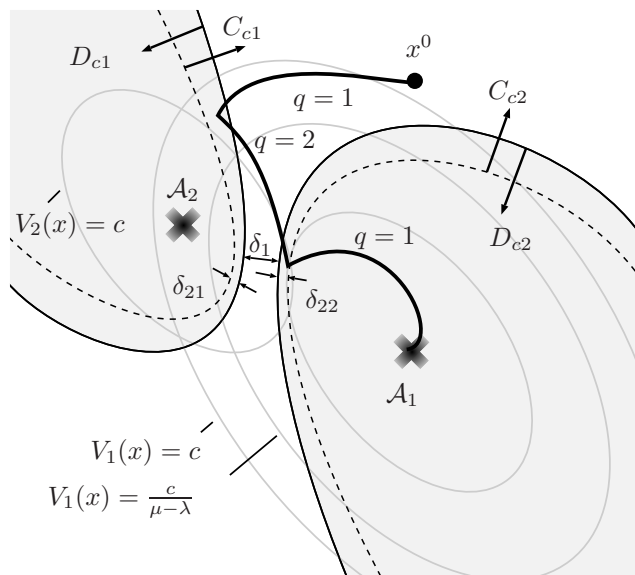


Figure 6.4. Flow set C_c and jump set D_c for the regulation to disconnected set of points problem. A solution converges to \mathcal{A}_1 after switching mode two times. The minimum distances δ_1, δ_{21} and δ_{22} between sets are used to compute an estimate of the margin of robustness to measurement noise.

which depends proportionally on the parameter $\lambda > 0$. The overlap between the sets C_{c1} and D_{c1} , and between the sets C_{c2} and D_{c2} . in Figure 6.4 correspond to the overlap between the sets C_c and D_c .

From the discussion above, an estimate of the margin of robustness to measurement noise is given by $\min\{\delta_1, \delta_2\}$. The examples in the next section illustrate this as well as the construction of the control law designed in the previous sections.

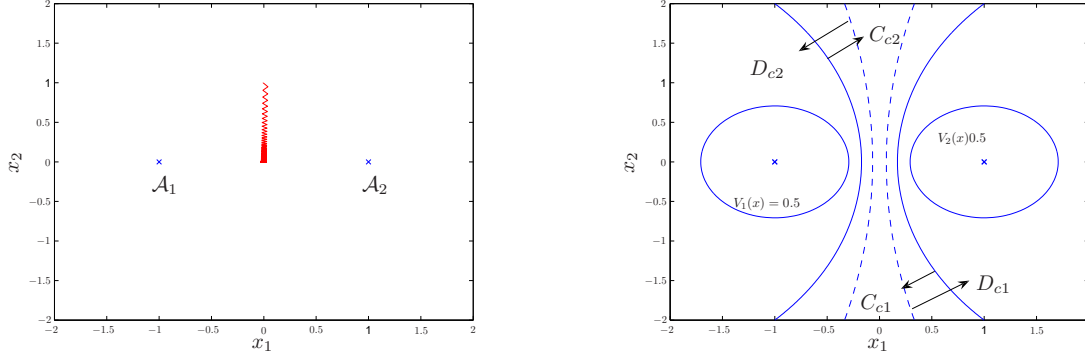
6.1.4 Two numerical examples

Robotic task

Consider the problem of transporting objects from a source to two isolated destinations with a controlled robotic arm. Suppose that there exist control algorithms that can transport the objects from the source to each destination but the switching rule between the algorithms is to be designed. Suppose also that full measurement of the state of the robotic arm is available but it is corrupted with noise. The goal is to design a switching control strategy between the control algorithms that is robust to measurement noise. As the focus will be on the problem of switching between the control algorithms, simple dynamics for the robotic arm are assumed. Consequently, consider a planar model for the robotic arm given by $\dot{x} = u$, $x = [x_1, x_2]^T$, $u = [u_1, u_2]^T$. Let \mathcal{A}_1 and \mathcal{A}_2 define sets in \mathbb{R}^2 that correspond to the location of each destination, which are assumed to be given by $\mathcal{A}_1 = \{(-1, 0)\}$ and $\mathcal{A}_2 = \{(1, 0)\}$, and let the source be located on the x_2 axis (and be represented by a small neighborhood around it). With this formulation, the task is to design a switching rule between two control algorithms that robustly steers the trajectories of the robotic arm system to the compact set $\mathcal{A} := \mathcal{A}_1 \cup \mathcal{A}_2$ (c.f. first example in Section 6.1.1). The state space O is given by \mathbb{R}^2 .

Consider quadratic Lyapunov functions V_1, V_2 that are zero at $\mathcal{A}_1, \mathcal{A}_2$, respectively, and steepest descent control laws $\kappa_i(x) = -\nabla V_i(x)$, $i = 1, 2$. A simple switching rule is the following: if $x \in \mathcal{M}_1 := \{x \in \mathbb{R}^2 \mid x_1 < 0\}$

then $u = \kappa_1(x)$, while if $x \in \mathcal{M}_2 := \{x \in \mathbb{R}^2 \mid x_1 \geq 0\}$ then $u = \kappa_2(x)$. This switching strategy globally asymptotically stabilizes the system to \mathcal{A} . However, for initial conditions arbitrarily close to the set $\mathcal{M} = \{x \in \mathbb{R}^2 \mid x_1 = 0\}$, there exists arbitrarily small measurement noise that causes the trajectories to stay in a neighborhood of that set as stated in Corollary 6.7. Figure 6.5(a) depicts a possible trajectory with measurement noise that is such that it stays far away from the target set \mathcal{A} .



(a) A possible trajectory with a simple switching logic with $x(0) = (-0.005, 1)$. The trajectory (with binary noise of amplitude 0.08 and period 0.1s) “chatters” around $x_1 = 0$ and does not reach the set \mathcal{A} .

(b) Sets C_c and D_c (see (6.14)) for the hybrid controller \mathcal{H}_c . Noise levels with magnitude larger than the systems’ robustness level (determined by the separation between the lines) would prevent the trajectories from approaching \mathcal{A} .

Figure 6.5. Global stabilization of a robotic arm to two isolated destinations.

The hybrid controller introduced in Section 6.1 solves this problem. Let $Q = \{1, 2\}$, $\mu = 2$, $\lambda = 0.7$, and $\gamma = 0.5$. Figure 6.5(b) depicts the resulting sets C_c and D_c obtained from (6.7)-(6.8) and (6.9), respectively, as well as γ -level sets of the Lyapunov functions and a sample trajectory. The set C_c defines flow set and D_c defines jump set.

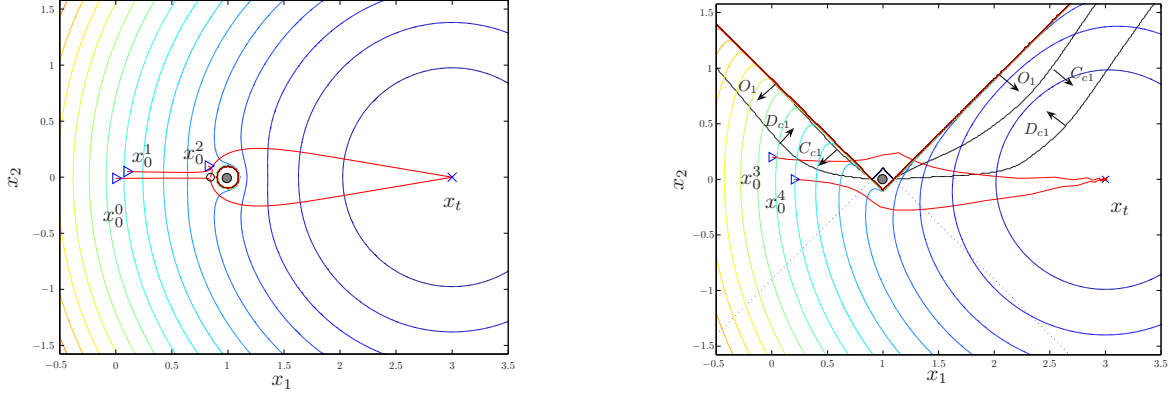
A trajectory starting in the set $C_{c1} \times \{1\} \subset C_c$ can flow as long as its x component is in C_{c1} , and can jump when its x component reaches D_{c1} . Jumps from this set map the logic state q to 2. Similarly for solutions starting in the set C_{c2} . Solutions starting in the set D_c with x component in $D_{c1} \setminus C_{c1}$ initially jumps, the logic state q is mapped to 2, and then flows with x in C_{c2} . Similarly for solutions starting in D_c with x component not in $D_{c2} \setminus C_{c2}$. By construction, solutions starting in $C_c \cup D_c$ approach either the set \mathcal{A}_1 or \mathcal{A}_2 (depending on the initial condition). Note that asymptotic stability of \mathcal{A} is guaranteed by Theorem 6.11.

As discussed above, the largest noise that the system tolerates is determined by the minimum separation between the boundaries of D_{c1} and D_{c2} , between the boundary of C_{c1} and D_{c1} , and of C_{c2} and D_{c2} . This corresponds to an estimate of the robustness margin for asymptotic stability of the set \mathcal{A} and is ≈ 0.1 .

Target acquisition and obstacle avoidance

Suppose that it is desired to steer a vehicle from its initial location to a target while avoiding an obstacle as depicted in Figure 6.2(a). As in Section 6.1.4, simple dynamics for the vehicle given by $\dot{x} = u$ will be assumed, where $x, u \in \mathbb{R}^2$. The obstacle \mathcal{N} is modeled as a ball on the plane of radius $\delta > 0$ at $x_o := (x_{o1}, x_{o2})$, while the target is located at $x_t := (x_{t1}, x_{t2})$. The state space O is given by $\mathbb{R}^2 \setminus (x_o + \delta\mathbb{B})$.

The control strategy described in Section 6.1.1 solves the control task nominally; however, under the presence of measurement noise, the same pathology around the line \mathcal{M} arises. Another potential solution to solve this



(a) The vehicle is denoted by \triangleright and its position relative to the coordinate system is given by (x_1, x_2) , the target is denoted by x with coordinates $x_t = (3, 0)$, and the obstacle (static) by the circular gray area with coordinates $x_o = (1, 0)$ and radius $\delta = 1/(20\sqrt{2})$. Trajectories (without noise) starting at x_0^0 and x_0^1 converge to the target while the trajectory starting at x_0^2 (with noise) approaches the saddle node point denoted by \circ .

(b) Hybrid controller sets and trajectories. The region O_1 is defined by all points below the two lines from where the arrows labeled as so originate; similarly for the other region O_2 for points above the dotted lines. The level sets of V_1 are plotted as well. Also for $q = 1$, the figure depicts the sets C_{c1} and D_{c1} , respectively, for $\mu = 1.1$ and $\lambda = 0.09$. The trajectory that starts at $x_0^3 = (0, 0.2)$, $q_0^3 = 1$, is pushed into D_{c1} by binary noise of magnitude 0.08, but the controller's mode jumps to $q = 2$ and steers it to the target. The trajectory starting from $x_0^4 = (0.2, 0)$, $q_0^4 = 1$, converges to the target from below the obstacle without jumping.

Figure 6.6. Global stabilization with obstacle avoidance.

task is to define a Lyapunov function that is positive definite with respect to the target, and then steer the vehicle to the target with a steepest descent controller. To this end, consider the Lyapunov function defined by

$$V(x) := \frac{1}{2}(x - x_t)^2 + B(d(x)) \quad (6.16)$$

where $B : \mathbb{R}_{\geq 0} \rightarrow \mathbb{R}$ is a continuously differentiable barrier function defined as $B(z) := \max\{0, (z - 1)^2 \ln \frac{1}{z}\}$, and $d : \mathbb{R}^2 \rightarrow \mathbb{R}_{\geq 0}$ is a continuously differentiable function that measures the distance from any point in O to the obstacle \mathcal{N} . The control law is given by the steepest descent control $u = -\nabla V(x)$. Figure 6.6(a) shows simulation results of the closed-loop system. Without noise, the trajectories starting at $x_0^0 = (0, -0.01)$ and $x_0^1 = (0.1, 0.05)$ avoid the obstacle and arrive at the target. Figure 6.6(a) denotes by \circ the saddle point present in the function V . Trajectories starting from that point stay at that point. The presence of measurement noise can cause that trajectories starting nearby the saddle point eventually reach it. The trajectory starting at $x_0^2 = (0.824, 0.1)$ is such that reaches the saddle point (such measurement noise was generated with a controller that locally stabilizes the vehicle's trajectories to the saddle point) and stays there for ever. Therefore, there exists a trajectory that does not reach the target.

To solve this problem robustly with the hybrid control strategy in Section 6.1, define a box $\tilde{\mathcal{N}}$ around the obstacle and two sets $O_1, O_2 \subset \mathbb{R}^2$ as depicted in Figure 6.6(b). Let $O = \mathbb{R}^2 \setminus \tilde{\mathcal{N}}$ and let $V_q : O \rightarrow \mathbb{R}_{\geq 0}$, $q \in Q := \{1, 2\}$, given by (6.16) with d replaced by d_q which is a continuously differentiable function that measures the distance from any point to the set $\mathbb{R}^2 \setminus O_q$. The control law is given by $u = \kappa(x, q) := -\nabla V_q(x)$.

Figure 6.6(b) depicts the flow and jump sets C_c and D_c as in (6.14), respectively, of the hybrid controller and two trajectories, one starting from x_0^3 and another from x_0^4 . (The set construction is given in (6.7)-(6.8) and (6.9), respectively.) Note that in this case, by construction, there is no saddle point. For the particular selection of the parameters, $\mu = 1.1$ and $\lambda = 0.09$, solutions reach the target by avoiding the box containing the

obstacle.

For every point away from the obstacle, the margin of robustness with respect to measurement noise is nonzero and gets larger as the vehicle is farther away from the obstacle (recall that the largest noise that the system tolerates is determined by the separation between the boundaries the jump sets, the boundary of C_{c1} and D_{c1} , and the boundary C_{c2} and D_{c2}).

6.2 Throw-and-catch control

6.2.1 An intuitive control strategy

Given the nonlinear control system

$$\dot{x} = f_p(x, u) \tag{6.17}$$

with output given by $y = x + e$ where e is a bounded measurement error signal, suppose that the goal is to design a controller that measures the output y , acts on the input u , and that steers the trajectories of the nonlinear system (6.17) to a neighborhood of a compact set \mathcal{A} , a subset of the state space. The idea is to accomplish this robust stability task with a hybrid controller that combines several control laws. More precisely, suppose that for the nonlinear system (6.17), it is known how to steer the trajectories from a neighborhood S_1 of some compact set \mathcal{A}_1 to a neighborhood E_1 of the compact set \mathcal{A} , perhaps just in an open-loop manner by a function of time α . Moreover, suppose that local state feedback controllers for (6.17) can be designed, given by $\kappa(\cdot)$ and $\kappa_1(\cdot)$, to locally asymptotically stabilize the compact sets \mathcal{A} and \mathcal{A}_1 , respectively. With this information, an intuitive control strategy is as follows:

- 1) If the state x is near \mathcal{A}_1 , then apply $\kappa_1(x)$;
- 2) When the state x reaches the set S_1 , apply $\alpha(t)$.
- 3) When the state x approaches the set E_1 , apply $\kappa(x)$.

This control strategy consists basically of two modes of operation. In 2), the trajectories of the nonlinear system (6.17) are transferred from nearby points of \mathcal{A}_1 to nearby points of \mathcal{A} . This task can be interpreted as “throwing” the state from an initial location to another location. This stage is called *throw mode*. In 3), the trajectories are steered to \mathcal{A} by the local stabilizer κ when they approach the set E_1 and are nearby \mathcal{A} . This logic can be seen as “catching” the trajectories, and consequently, it is referred to as the *catch mode*.

Figure 6.7 depicts a sample trajectory resulting from the nominal closed-loop system with this control strategy. When noise is added to the measurements of x , the robustness properties conferred by our control strategy rely on the construction of the sets that define the jumps of the resulting hybrid closed-loop system. Additionally, since during the “throw” mode the controller does not use any information about the state of the system, if due to external perturbations the control law α fails to steer the trajectory to a neighborhood of E_1 then the controller should be able to steer back the trajectory to a “safe” controller. This capability is added to the system as an additional mode: *“recovery” mode*.

This control technique can be used in several engineering applications to confer robust stability properties to the closed-loop system. For instance, in the problem of swinging up a multi-link pendulum, it is usually the case that local stabilization around the resting and upright equilibrium point of the system is possible. Moreover, open-loop control laws that are capable to drive the trajectories of the system from any point to nearby points of resting equilibrium, and from there to nearby points of the upright equilibrium can be computed. This can be done by solving a two-point boundary value problem, or in a simpler manner, by trial and error. Figure 6.8 depicts this scenario for the case of a three-link pendulum.

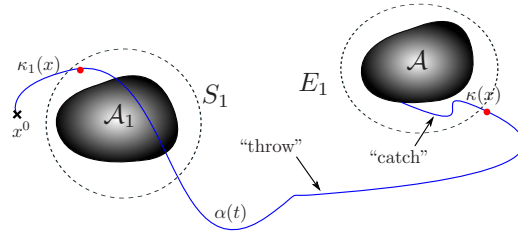


Figure 6.7. A trajectory starting at $x(0) = x^0$ for the nonlinear system with the local state feedback law κ_1 reaches the set S_1 from where the controller switches to the control law $\alpha(t)$ in order to steer the trajectory to points nearby E_1 . When the trajectory reaches a small enough neighborhood of \mathcal{A} , the controller switches to the local state feedback law κ to drive the trajectory to \mathcal{A} . The dots along the trajectory denote the locations where the control strategy decide the controller to be used.

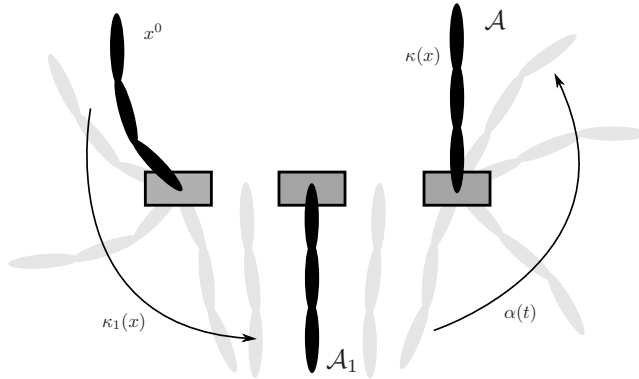


Figure 6.8. Swing up of a multi-link pendulum on a cart. The set \mathcal{A}_1 corresponds to the state at the stable resting equilibrium while the set \mathcal{A} corresponds to the upright position. Control law κ_1 (almost globally) stabilizes the resting equilibrium and control law κ locally stabilizes the upright position. The open-loop control law α steers the trajectory from nearby points of \mathcal{A}_1 to nearby points of \mathcal{A} .

The problem of steering autonomous vehicles with limited information is another example where the throw-and-catch strategy can be applied. In such a scenario, vehicle sensors usually have a limited area of coverage. Consequently, relative measurements to a target destination are only available in a neighborhood of that destination. Then, position feedback control is not a global solution. In this situation, open-loop control laws that steer the vehicle from nearby points of one location to nearby points of another location, where position measurements are available, can be combined with feedback laws. Figure 6.9 depicts this idea for a single autonomous vehicle.

6.2.2 Control design and analysis

In this section, nonlinear control systems of the following form are considered:

$$\dot{x} = f_p(x, u) \quad (6.18)$$

where $f : \mathbb{R}^n \times \mathbb{R}^m \rightarrow \mathbb{R}^n$, $x \in \mathbb{R}^n$ is the state, and $u \in \mathbb{R}^m$ is the control input. Let $\mathcal{A} \subset \mathbb{R}^n$ be compact; $P := \{1, 2, \dots, p_{\max}\} \subset \mathbb{N}$, $p_{\max} \geq 1$; for each $j \in P$, $Q_j := \{1, 2, \dots, q_{\max}^j\} \subset \mathbb{N}$, $q_{\max}^j \geq 2$; and $R :=$

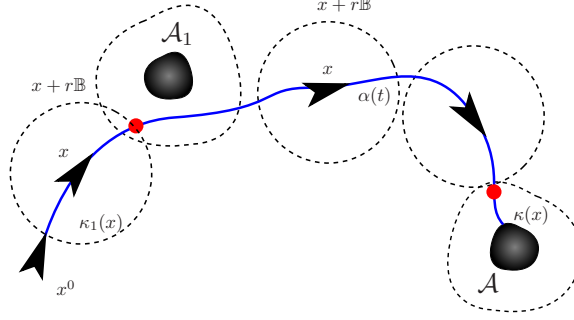


Figure 6.9. Control of autonomous vehicles with limited position measurements. The autonomous vehicle is only capable of measuring its position relative to $\mathcal{A}, \mathcal{A}_1$ with the radius of coverage given by r . With the knowledge of an open-loop control law that is able to steer (“throw”) the vehicle from nearby points of \mathcal{A}_1 to nearby points of \mathcal{A} , once the vehicle is able to obtain (relative) position measurements of the destination, the local controllers can “catch” the vehicle and take it to the desired destination.

$\cup_{k \in P} (Q_k \times \{k\})$. The following assumption guarantees that the control laws needed for the throw-and-catch strategy outlined in the previous section exist.

Assumption 6.13 (conditions for throw-and-catch control) *The function $f_p : \mathbb{R}^n \times \mathbb{R}^m \rightarrow \mathbb{R}^n$ is continuous. For each $(i, j) \in R$, there exist:*

1. *Disjoint compact sets $\mathcal{A}_{i,j} \subset \mathbb{R}^n$ satisfying $\mathcal{A}_{i,j} = \mathcal{A}$ for each $i = q_{\max}^j, j \in P$.*
2. *When $i > 1$, continuous state-feedback laws $\kappa_{i,j} : \mathbb{R}^n \rightarrow \mathbb{R}^m$ such that the compact set $\mathcal{A}_{i,j}$ is asymptotically stable with basin of attraction $\mathcal{B}_{\mathcal{A}_{i,j}} \subset \mathbb{R}^n$ for $\dot{x} = f_p(x, \kappa_{i,j}(x))$.*
3. *When $i < q_{\max}^j$, piecewise-continuous functions $\alpha_{(i,j) \rightarrow (i+1,j)} : \mathbb{R}_{\geq 0} \rightarrow \mathbb{R}^m$ that are capable of steering trajectories of (6.18) from a set $S_{i,j}$ to an open set $E_{i,j}$ in finite time with maximum time $\tau_{i,j}^* \geq 0$, where $S_{i,j} \subset \mathbb{R}^n$ contains an open neighborhood of $\mathcal{A}_{i,j}$, $E_{i,j}$ contains an open neighborhood of $\mathcal{A}_{i+1,j}$ and is such that an open $\delta_{i,j}^c$ -neighborhood of itself, $\delta_{i,j}^c > 0$, is contained in $\mathcal{B}_{\mathcal{A}_{i+1,j}}$.*

Moreover, there exists:

4. *Continuous state-feedback law $\kappa_0 : \mathbb{R}^n \rightarrow \mathbb{R}^m$, such that, for each solution x to $\dot{x} = f_p(x, \kappa_0(x))$ there exists finite $T > 0$ such that $x(T)$ is in the union of each of the sets $E_{i,j} + \frac{\delta_{i,j}^c}{2}\mathbb{B}$ and $S_{i,j}$ above (this corresponds to a “bootstrap” feedback controller).*

In most applications, the compact sets $\mathcal{A}_{i,j}, (i, j) \in R$, are given by single points, in particular equilibrium points, for which local regulation of the trajectories of (6.18) is known with the state-feedback laws $\kappa_{i,j}$. The functions $\alpha_{(i,j) \rightarrow (i+1,j)}$ are functions of time that can be recorded in the memory of the digital controller.

Note that the compact sets $\mathcal{A}_{i,j}, (i, j) \in R$, define a *directed tree* in the sense that for every compact set $\mathcal{A}_{i,j}$ with $i < q_{\max}^j, j \in P$, there exists an open-loop control law that transfers the state from nearby points of $\mathcal{A}_{i,j}$ to nearby points of $\mathcal{A}_{i+1,j}$. Every path has the last node in common and first independent nodes defining a path, which eventually, merges with another paths. This connectivity between nodes is denoted in Figure 6.10 by a directed arc joining the node $\mathcal{A}_{i,j}$ with the node $\mathcal{A}_{i+1,j}$. Note that Assumption 6.13.4 guarantees the existence of a state-feedback law κ_0 such that, when the trajectories are away from the basin of attraction of the local stabilizers or at points where the open-loop control laws are not able to transfer the state to the next node, the trajectories are steered back to the tree.

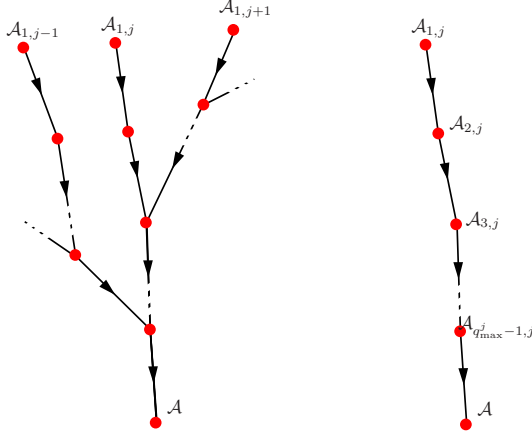


Figure 6.10. General case of directed tree (left) and j -th path (right).

Control Design

Now, the state-feedback hybrid controller, denoted by \mathcal{H}_c , that performs the switching between the feedback control laws κ_0 , $\kappa_{i,j}$, and $\alpha_{(i,j) \rightarrow (i+1,j)}$ in Assumption 6.13 is designed. The controller state is given by $[q \ p \ \tau]^T$ with logic states q taking value in $Q \cup \{0\} \subset \mathbb{N}$ and p taking value in $P \cup \{0\} \subset \mathbb{N}$, and timer state τ taking value in \mathbb{R} . The set Q is given by

$$Q := \bigcup_{k \in P} (Q_k^c \cup Q_k^t), \quad Q_k^c := (-Q_k) \setminus \{-1\}, \quad Q_k^t := Q_k \setminus \{q_{\max}^k\}. \quad (6.19)$$

They logic states store the running mode of the system:

- “Catch mode” at the $|q|$ -th node of the p -th path when $q \in Q_p^c$, $p \in P$.
- “Throw mode” at the q -th node of the p -th path when $q \in Q_p^t$, $p \in P$.
- “Recovery mode” when $q = p = 0$.

Basically, the sets Q_j^c , $j \in P$, contain the values of the logic variable q for “catch mode”, while the sets Q_j^t , $j \in P$, contain the values of the logic variable q for “throw mode”.

With the definitions above, the logic states as a pair (q, p) take value in

$$L := \bigcup_{k \in P} ((Q_k^c \cup Q_k^t) \times \{k\}) \cup (0, 0). \quad (6.20)$$

For convenience in what follows, the sets Q_k^t are combined with the corresponding path index k in the set

$$L^t := \bigcup_{k \in P} (Q_k^t \times \{k\}). \quad (6.21)$$

The output of the hybrid controller is given by

$$\kappa_c(x, q, p, \tau) := \begin{cases} \kappa_{|q|,p}(x) & \text{if } q \in Q_p^c \\ \alpha_{(q,p) \rightarrow (q+1,p)}(\tau) & \text{if } q \in Q_p^t \\ \kappa_0(x) & \text{if } q = 0. \end{cases} \quad (6.22)$$

The following sets are part of the control logic.

I) Sets for “Catch mode” update logic

For each $(i, j) \in L^t$, let $E_{i,j}$ and $\delta_{i,j}^c$ be given as in Assumption 6.13.3, and define

$$D_{i,j}^c = E_{i,j} + \delta_{i,j}^c \overline{\mathbb{B}}, \quad C_{i,j}^c = \overline{\mathbb{R}^n \setminus D_{i,j}^c} + \frac{\delta_{i,j}^c}{2} \overline{\mathbb{B}}.$$

II) Sets for “Throw mode” update logic

For each $(i, j) \in L^t$, let $S_{i,j}$ be given as in Assumption 6.13.3, and define $D_{i,j}^t$ to be a closed set such that for some $\delta_{i,j}^t > 0$ satisfies

$$\mathcal{A}_{i,j} + \delta_{i,j}^t \mathbb{B} \subset D_{i,j}^t, \quad D_{i,j}^t + \frac{\delta_{i,j}^t}{2} \mathbb{B} \subset S_{i,j}.$$

Then, for each $(i, j) \in L^t$, let $C_{i,j}^t$ be given by

$$C_{i,j}^t := \overline{\mathbb{R}^n \setminus D_{i,j}^t} + \frac{\delta_{i,j}^t}{2} \overline{\mathbb{B}}.$$

III) Sets for “Recovering mode” update logic

For each $(i, j) \in \cup_{k \in P} (Q_k^c \times \{k\})$, for some $\delta_{i,j}^r > 0$, define

$$C_{i,j}^r := \text{reach}_{i,j}(D_{|i|-1,j}^c) + \delta_{i,j}^r \overline{\mathbb{B}} \tag{6.23}$$

where $\text{reach}_{i,j}(D_{|i|-1,j}^c)$ is the reachable set of $\dot{x} = f_p(x, \kappa_{|i|,j}(x))$ from $D_{|i|-1,j}^c$. Also, define $D_{i,j}^r$ as

$$D_{i,j}^r := \overline{\mathbb{R}^n \setminus C_{i,j}^r} + \frac{\delta_{i,j}^r}{2} \overline{\mathbb{B}}. \tag{6.24}$$

Define $C_{0,0}^r$ and $D_{0,0}^r$ as follows. For each $(i, j) \in \cup_{k \in P} (Q_k \times \{k\})$ define an auxiliary set $\tilde{D}_{i,j}^r$ to be a closed set such that for some $\delta_{i,j}^r > 0$ satisfies

$$\mathcal{A}_{i,j} + \delta_{i,j}^r \mathbb{B} \subset \tilde{D}_{i,j}^r, \quad \tilde{D}_{i,j}^r + \frac{\delta_{i,j}^r}{2} \mathbb{B} \subset D_{i-1,j}^c \cup D_{i,j}^t,$$

where $D_{0,j}^c = D_{q_{\max},j}^t = \emptyset$ for all $j \in P$. Then, $C_{0,0}^r$ and $D_{0,0}^r$ are given by

$$D_{0,0}^r := \bigcup_{(i,j) \in \cup_{k \in P} (Q_k \times \{k\})} \tilde{D}_{i,j}^r, \quad C_{0,0}^r := \overline{\mathbb{R}^n \setminus D_{0,0}^r} + \frac{\delta_{0,0}^r}{2} \overline{\mathbb{B}}$$

where $\delta_{0,0}^r$ is the minimum $\delta_{i,j}^r$ over $\cup_{k \in P} (Q_k \times \{k\})$.

With these definitions, the update laws are designed as follows. If in *throw mode* and the state x is such that a “catch” is possible, i.e.

$$(q, p) \in Q_p^t \times \{p\}, \quad x \in D_{q,p}^c, \tag{6.25}$$

then jumps to catch mode are enabled with update law $q^+ = -(|q| + 1)$. If in *catch mode* and the state x is such that a “throw” is possible, i.e.

$$(q, p) \in (Q_p^c \setminus \{-q_{\max}^p\}) \times \{p\}, \quad x \in D_{|q|,p}^t, \tag{6.26}$$

then jumps to throw mode are enabled with update law $q^+ = |q|$.

If in *throw mode* and the timer state τ is larger than $\tau_{q,p}^*$ or if in *catch mode* and the state x is such that $x \in D_{q,p}^r$ then jumps to *recovery mode* are enabled with update law $q^+ = 0, p^+ = 0$. While in this mode, the controller enables updates of (q, p) to a pair in $\cup_{k \in P} ((Q_k^c \cup Q_k^t) \times \{k\})$ when $x \in D_{0,0}^r$.

The construction of the sets in I)-III) define the flow and jump sets of the hybrid controller (while in mode $q \in Q$ and in path $p \in P$, the sets $C_{|q|,p}^c$ and $D_{|q|,p}^c$; $C_{|q|,p}^t$ and $D_{|q|,p}^t$; and $C_{-|q|,p}^r$, $D_{-|q|,p}^r$ and $D_{0,0}^r$ define the flow and jump sets for jumps to *catch*, *throw*, and *recovery mode*, respectively). Figure 6.11 illustrates the sets used in the update law and a sample trajectory for the i -th compact set in the j -th path, $(i, j) \in L$, $i \in \{2, 3, \dots, q_{\max}^j - 1\}$.

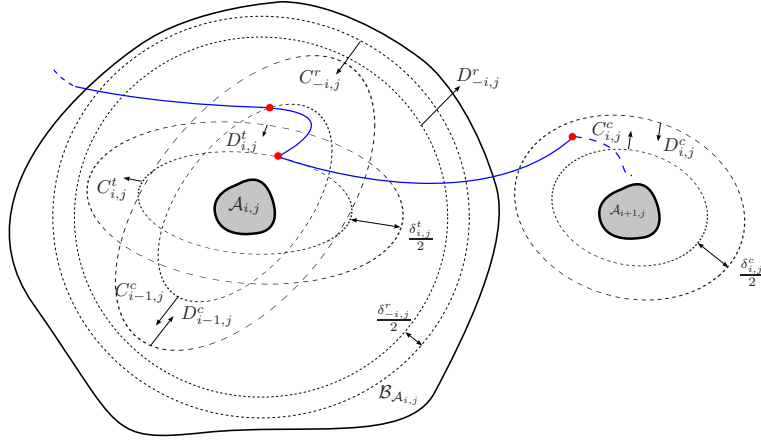


Figure 6.11. The compact set $\mathcal{A}_{i,j}$, $(i, j) \in L$, $i \in \{2, 3, \dots, q_{\max}^j - 1\}$; the associated flow sets $C_{i,j}^c, C_{i,j}^t, C_{-i,j}^r$; and the jump sets $D_{i,j}^c, D_{i,j}^t, D_{-i,j}^r$ are depicted. The sets $C_{-i-1,j}^c$ and $D_{-i-1,j}^c$ associated with the compact set $\mathcal{A}_{i-1,j}$ are also shown for the computation of $C_{-i,j}^r$ and $D_{-i,j}^r$. Vaguely, the control strategy is such that with $q = i - 1$ and $p = j$, a jump can occur as soon as the trajectory enters the set $D_{-i-1,j}^c$, from where the local state feedback law $\kappa_{i,j}$ is applied. A jump that activates the control law $\alpha_{(i,j) \rightarrow (i+1,j)}$ can be triggered as soon as the trajectory hits the set $D_{i,j}^t$. The local stabilizer for $\mathcal{A}_{i+1,j}$ is enabled when the trajectory enters the set $D_{i+1,j}^c$. The sequence is repeated until the compact set $\mathcal{A}_{i^*,j}$, $i^* = q_{\max}^j$, is reached.

Hybrid controller

Let $O_c := \mathbb{R}^n \times L \times \mathbb{R}$, $\bar{\tau} = \max \tau_{i,j}^*$ for all $(i, j) \in L^t$ where $\tau_{i,j}^*$ is given by Assumption 6.13.3, and $\xi := [x^T \ q \ p \ \tau]^T$. The hybrid controller, denoted by \mathcal{H}_c , is

$$\mathcal{H}_c \begin{cases} (\dot{q}, \dot{p}) = (0, 0), \quad \dot{\tau} = 1, & \xi \in C_c \\ (q, p)^+ \in g_c(\xi), \quad \tau^+ = 0, & \xi \in D_c \end{cases}$$

where the sets C_c and D_c are given by

$$C_c := C_{c1} \cup C_{c2} \cup C_{c3}$$

where

$$\begin{aligned}
C_{c1} &:= \left\{ \xi \in O_c \mid q \in Q_p^c \setminus \{-q_{\max}^p\}, x \in C_{|q|,p}^t \cap C_{q,p}^r \right\} \cup \left\{ \xi \in O_c \mid q = -q_{\max}^p, x \in C_{q,p}^r \right\} \\
C_{c2} &:= \left\{ \xi \in O_c \mid q \in Q_p^t, x \in C_{q,p}^c, \tau \leq \tau_{q,p}^* \right\}, \\
C_{c3} &:= \left\{ \xi \in O_c \mid q = p = 0, x \in C_{0,0}^r \right\},
\end{aligned}$$

and

$$D_c := D_{c1} \cup D_{c2} \cup D_{c3},$$

where

$$\begin{aligned}
D_{c1} &:= \left\{ \xi \in O_c \mid q \in Q_p^t, x \in D_{q,p}^c, \tau \leq \tau_{q,p}^* \right\} \cup \left\{ \xi \in O_c \mid (q,p) = (0,0), (q',p') \in L^t, x \in D_{q',p'}^c \cap D_{0,0}^r \right\}, \\
D_{c2} &:= \left\{ \xi \in O_c \mid q \in Q_p^c \setminus \{-q_{\max}^p\}, x \in D_{|q|,p}^t \right\} \cup \left\{ \xi \in O_c \mid (q,p) = (0,0), (q',p') \in L^t, x \in D_{q',p'}^t \cap D_{0,0}^r \right\}, \\
D_{c3} &:= \left\{ \xi \in O_c \mid q \in Q_p^t, \tau \geq \tau_{q,p}^* \right\} \cup \left\{ \xi \in O_c \mid q \in Q_p^c, x \in D_{|q|,p}^r \right\},
\end{aligned}$$

and the jump map g_c is given by

$$g_c(\xi) := \begin{cases} g_{c1}(\xi) & \xi \in D_{c1} \\ g_{c2}(\xi) & \xi \in D_{c2} \\ (0,0) & \xi \in D_{c3} \end{cases}$$

$$g_{c1}(\xi) := \begin{cases} (-|q| - 1, p) & \text{if } (q,p) \in L^t, \\ \{(-|q'| - 1, p') \mid (q',p') \in L^t, x \in D_{q',p'}^c\} & \text{if } (q,p) = (0,0) \end{cases}$$

$$g_{c2}(\xi) := \begin{cases} (|q|, p) & \text{if } q \in Q_p^c \setminus \{-q_{\max}^p\}, \\ \{(q',p') \mid (q',p') \in L^t, x \in D_{q',p'}^t\} & \text{if } (q,p) = (0,0) \end{cases}$$

and output κ_c given in (6.22).

The jump map g_{c1} and jump set D_{c1} implement the logic for *catch mode*, while g_{c2} and D_{c2} implement the logic *throw mode*. The first pieces of these sets correspond to the conditions in (6.25) and (6.26), while the second pieces allow jumps from *recovering to catch* or *throw mode*. Moreover, the definitions of D_{c1} and D_{c2} differ from the corresponding ones in (6.25)-(6.26) as they implement jumps that update the path state p to a correct one. Similarly for g_{c1} and g_{c2} . (This mechanism is needed when the initialization of the logic states is not correct.) The jump set D_{c3} states the conditions for jumps to *recovery mode*. The flow set C_c includes all points at which jumps are not allowed, and to guarantee robust existence of solutions, it overlaps with the jump set D_c .

Note that this construction is such that the resulting hybrid closed-loop system given in the next section satisfies the hybrid basic conditions.

Stability and robustness to measurement noise

The closed-loop system resulting from controlling the nonlinear system (6.18) with the controller \mathcal{H}_c is given by

$$\left. \begin{aligned} \dot{x} &= f_p(x, \kappa_c(\xi)) \\ (\dot{q}, \dot{p}) &= (0, 0) \\ \dot{\tau} &= 1 \end{aligned} \right\} \xi \in C_c$$

$$\left. \begin{array}{l} x^+ = x \\ (q, p)^+ \in g_c(\xi) \\ \tau^+ = 0 \end{array} \right\} \xi \in D_c .$$

This hybrid system is denoted by \mathcal{H}_{cl} . The hybrid controller \mathcal{H}_c confers the following stability property.

Theorem 6.14 (nominal asymptotic stability) *Let Assumption 6.13 hold. For the hybrid system \mathcal{H}_{cl} , the compact set $\mathcal{A} \times (\cup_{j \in P} (\{-q_{\max}^j\} \times \{j\})) \times [0, \bar{\tau}]$ is asymptotically stable with basin of attraction $\mathcal{B}_{\mathcal{A}} := C_c \cup D_c$.*

This result states that every solution to \mathcal{H}_{cl} is such that the x component converges to \mathcal{A} and that every solution with initial x close to \mathcal{A} stays close for all time. This corresponds to global asymptotic stability of \mathcal{A} for the the nonlinear system (6.18) controlled by \mathcal{H}_c . The proof of this result follows from the control logic implemented in \mathcal{H}_c . The open-loop schedules are used to steer trajectories from a neighborhood of one node to a neighborhood of the following node, and the state-feedback control laws steer the trajectories toward the nodes of the tree. The control logic in \mathcal{H}_c is such that for every point in the state space, by measuring the state, a sequence of switches between the control laws takes the state of the system to \mathcal{A} .

The hybrid controller \mathcal{H}_c confers a margin of robustness to measurement noise e on the state x . This is stated in the following result. Below, $|x|_{\mathcal{A}} = \inf_{y \in \mathcal{A}} |x - y|$. Also, recall that $\text{dom}(x, q, p, \tau)$ denotes the domain of the solution (x, q, p, τ) to \mathcal{H}_{cl} .

Theorem 6.15 (robustness to measurement noise) *Let Assumption 6.13 hold. Then, there exists $\beta \in \mathcal{KL}$, for each $\varepsilon > 0$ and each compact set $K \subset \mathcal{B}_{\mathcal{A}}$ there exists $\delta^* > 0$, such that for each measurement noise $e : \mathbb{R}_{\geq 0} \rightarrow \delta^* \mathbb{B}$, solutions (x, q, p, τ) to \mathcal{H}_{cl} exist, are complete, and for initial conditions $(x^0, q^0, p^0, \tau^0) \in K$ the x component of the solutions satisfies*

$$|x(t, j)|_{\mathcal{A}} \leq \beta(|x^0|_{\mathcal{A}}, t + j) + \varepsilon \quad \forall (t, j) \in \text{dom}(x, q, p, \tau).$$

In addition to the property in Theorem 6.15, the hybrid controller \mathcal{H}_c confers an additional robustness property to the closed-loop system when the open-loop schedules are in the loop. When a disturbance or failure prevents a “throw” from being successful, the recovery logic implemented in the hybrid controller steers the state of the system back to the tree and retries the “throw-catch” sequence.

6.2.3 Application: robust global pendubot swing-up control

Consider the dynamical system given in Figure 6.12 consisting of a pendulum with two links, the *pendubot*. For

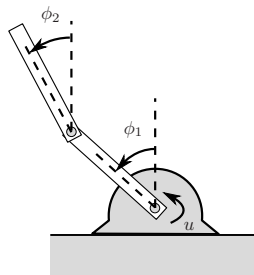


Figure 6.12. The pendubot system: a two-link pendulum with torque actuation u in the first link.

the problem of robustly globally stabilizing both links of the pendubot to the upright position using only torque actuation in the first link, the hybrid controller proposed in the previous section is designed.

Let ϕ_1 and ϕ_2 denote the angles relative to the upright position, ω_1 and ω_2 the angular velocities, and $u \in \mathbb{R}$ the control input. The dynamical model of this system can be obtained with the Lagrange method. The resulting equations are of the form

$$\begin{aligned}\dot{\phi}_1 &= \omega_1, & \dot{\omega}_1 &= f_1(x, u) \\ \dot{\phi}_2 &= \omega_2, & \dot{\omega}_2 &= f_2(x, u),\end{aligned}\tag{6.27}$$

where $x := [\phi_1 \ \omega_1 \ \phi_2 \ \omega_2]^T \in \mathbb{R}^4$ and $f_1, f_2 : \mathbb{R}^4 \times \mathbb{R} \rightarrow \mathbb{R}$ are nonlinear, locally Lipschitz functions that define the dynamics of the pendulum. Let $f(x, u) := [\omega_1 \ f_1(x, u) \ \omega_2 \ f_2(x, u)]^T$. It is considered that ϕ_1 and ϕ_2 are given by the angle of a vector in the unit circle $Z := \{z \in \mathbb{R}^2 \mid \|z\|_2 = 1\}$. More precisely, for each $i = 1, 2$, ϕ_i is given by the angle of the vector $z_i \in Z$. Note that, with this embedding technique, the problem of globally stabilizing the pendubot to the upright position is equivalent to globally stabilizing the system to the compact set defined by $z_1 = z_2 = [1 \ 0]^T$, $\omega_1 = \omega_2 = 0$.

The pendubot system has four equilibrium points:

- Resting (\mathcal{A}_r): $\phi_1 = -\pi$, $\omega_1 = 0$, $\phi_2 = -\pi$, $\omega_2 = 0$;
- Upright (\mathcal{A}_u): $\phi_1 = \omega_1 = \phi_2 = \omega_2 = 0$;
- Upright/Resting (\mathcal{A}_{ur}): $\phi_1 = \omega_1 = 0$, $\phi_2 = -\pi$, $\omega_2 = 0$;
- Resting/Upright (\mathcal{A}_{ru}): $\phi_1 = -\pi$, $\omega_1 = \phi_2 = \omega_2 = 0$.

These equilibrium points are depicted in Figure 6.13.

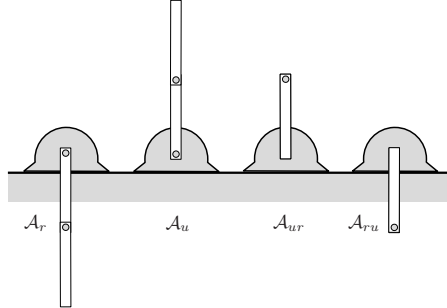


Figure 6.13. Equilibrium configurations of the pendubot.

The control laws needed in the throw-and-catch strategy are designed below.

Local state-feedback stabilizers κ_u and κ_r

The construction of local state-feedback stabilizers κ_u for the upright equilibrium \mathcal{A}_u and κ_r for the resting equilibrium \mathcal{A}_r are designed to steer points nearby \mathcal{A}_u and \mathcal{A}_r to the equilibrium point itself, respectively. Such controllers can be designed by linearization and pole placement. For example, for κ_u , let $A := \partial f(x, u) / \partial x|_{x=\mathcal{A}_u, u=0}$ and $B := \partial f(x, u) / \partial u|_{x=\mathcal{A}_u, u=0}$, choose $K \in \mathbb{R}^4$ and $P \in \mathbb{R}^{4 \times 4}$, $P = P^T > 0$, such that

$$(A - BK^T)^T P + P(A - BK^T) < 0, \tag{6.28}$$

and let $\kappa_u(x) := K^T x$. (Such K and P exist as (A, B) is controllable.) The basin of attraction of this controller can be estimated with a sublevel set $L_{V_u}(r_u)$ of the Lyapunov function $V_u(x) := x^T P x$.

Open-loop control laws for steering from/to neighborhoods of points to $\mathcal{A}_r, \mathcal{A}_u, \mathcal{A}_{ur}$, and \mathcal{A}_{ru}

Construct open-loop controllers $\alpha_{r \rightarrow u}$, $\alpha_{ur \rightarrow r}$, and $\alpha_{ru \rightarrow r}$ such that

- a) $\alpha_{r \rightarrow u}(t)$ steers the trajectories of (6.27) from points nearby the *resting* equilibrium \mathcal{A}_r to points nearby the *upright* equilibrium \mathcal{A}_u ;
- b) $\alpha_{ur \rightarrow r}(t)$ steers the trajectories of (6.27) from points nearby the *upright/resting* equilibrium \mathcal{A}_{ur} to points nearby the *resting* equilibrium \mathcal{A}_r ;
- c) $\alpha_{ru \rightarrow r}(t)$ steers the trajectories of (6.27) from points nearby the *resting/upright* equilibrium \mathcal{A}_{ru} to points nearby the *resting* equilibrium \mathcal{A}_r .

For example, for item a), it is possible to construct a piecewise-continuous function of time $\alpha_{r \rightarrow u} : \mathbb{R}_{\geq 0} \rightarrow \mathbb{R}$ such that for the initial condition $x^0 = \mathcal{A}_r, t^0 = 0$, the solution to $\dot{x} = f(x, \alpha_{r \rightarrow u}(t))$ is in a small neighborhood of \mathcal{A}_u . Then, by continuity with respect to initial conditions to (6.27), there exist a neighborhood S of \mathcal{A}_r and a neighborhood E of \mathcal{A}_u such that solutions to $\dot{x} = f(x, \alpha_{r \rightarrow u}(t))$ starting from S reach E in finite time $\tau_{r \rightarrow u}^* > 0$. Controls $\alpha_{ur \rightarrow r}$ and $\alpha_{ru \rightarrow r}$ are designed similarly. One technique that can be used to design these open-loop controllers is to define a parameterized basis function for the control law and then determine its parameters by trial and error. A different approach is to solve a two-point boundary value problem (or some other constrained optimal control problem) with boundary constraints corresponding to neighborhoods of $\mathcal{A}_r, \mathcal{A}_u, \mathcal{A}_{ur}$, and \mathcal{A}_{ru} .

Bootstrap stabilizer κ_0

The main task of this controller is to steer trajectories starting from every point not in $\mathcal{A}_r \cup \mathcal{A}_u \cup \mathcal{A}_{ur} \cup \mathcal{A}_{ru}$ to a small enough neighborhood of $\mathcal{A}_r \cup \mathcal{A}_u \cup \mathcal{A}_{ur} \cup \mathcal{A}_{ru}$. One such controller is $\kappa_0 \equiv 0$ as the natural damping present in the system steer the trajectories to $\mathcal{A}_r \cup \mathcal{A}_u \cup \mathcal{A}_{ur} \cup \mathcal{A}_{ru}$ with zero control input. In the next section, to obtain better performance, a more sophisticated control law which removes energy from the system much faster is used.

With the control ingredients designed in 1), 2), and 3), the basic tasks that our control strategy performs are:

- For points nearby \mathcal{A}_r , apply the state-feedback law κ_r to steer the state to the set S corresponding to $\alpha_{r \rightarrow u}$ and then apply $\alpha_{r \rightarrow u}$ to steer the trajectories to a neighborhood of \mathcal{A}_u ;
- For points nearby \mathcal{A}_u , apply the state feedback law κ_u to stabilize the trajectories to \mathcal{A}_u ;
- For points nearby \mathcal{A}_{ur} and \mathcal{A}_{ru} , apply the open-loop control laws $\alpha_{ur \rightarrow r}$ and $\alpha_{ru \rightarrow r}$, respectively, to steer the trajectories to a neighborhood of \mathcal{A}_r ;
- For any other point in \mathbb{R}^4 , apply the law κ_0 to steer the trajectories to a neighborhood of $\mathcal{A}_r \cup \mathcal{A}_u \cup \mathcal{A}_{ur} \cup \mathcal{A}_{ru}$.

Figure 6.14 shows the combination of these tasks to accomplish global stabilization to the point \mathcal{A}_u of the pendubot.

The control strategy, interpreted as a *directed tree or graph* with nodes given by the equilibrium points, has two paths given by $\mathcal{A}_{ur} \rightarrow \mathcal{A}_r \rightarrow \mathcal{A}_u$ and $\mathcal{A}_{ru} \rightarrow \mathcal{A}_r \rightarrow \mathcal{A}_u$.

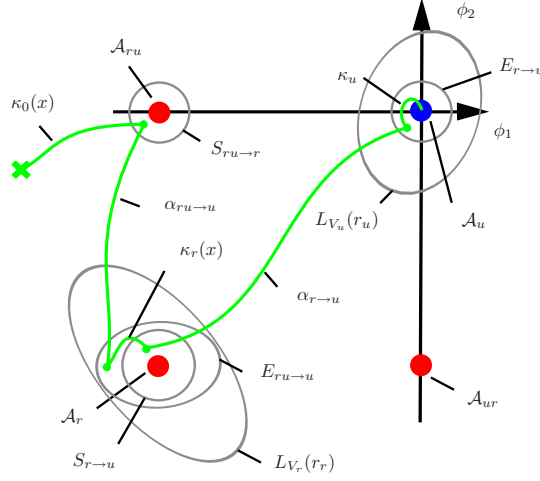


Figure 6.14. Control strategy for robust global stabilization of the pendubot to the point \mathcal{A}_u . A sample trajectory in the ϕ_1, ϕ_2 plane resulting from our control strategy is depicted. From the initial point \times , the trajectory is steered to the neighborhood $S_{r_u \rightarrow r}$ of \mathcal{A}_{r_u} with $\kappa_0(x)$, from which it is “thrown” to the neighborhood $E_{r_u \rightarrow r}$ of \mathcal{A}_r with the control law $\alpha_{r_u \rightarrow r}$. The local stabilizer κ_r “catches” the state to a point in $S_{r \rightarrow u}$ from where the open-loop law $\alpha_{r \rightarrow u}$ is applied. Finally, after the “throw”, the state reaches a point in $E_{r \rightarrow u}$ and the last “catch” by the local stabilizer κ_u steers the trajectory to \mathcal{A}_u .

The nodes in each of the paths are numbered, starting from \mathcal{A}_{ur} and \mathcal{A}_{ru} and finishing at \mathcal{A}_u , by the pairs $(i, j) \in \{1, 2, 3\} \times \{1, 2\}$ where i indicates the node number and j the path number. Then, the two paths are

Path 1: $(1, 1) \rightarrow (2, 1) \rightarrow (3, 1)$ (i.e. $\mathcal{A}_{ur} \rightarrow \mathcal{A}_r \rightarrow \mathcal{A}_u$).

Path 2: $(1, 2) \rightarrow (2, 2) \rightarrow (3, 2)$ (i.e. $\mathcal{A}_{ru} \rightarrow \mathcal{A}_r \rightarrow \mathcal{A}_u$).

Then controller logic states, q and p , are such that $(q, p) \in \{-3, -2, 0, 1, 2\} \times \{1, 2\}$. The timer state is $\tau \in \mathbb{R}$. Recall that the state q indicates the mode of the controller, p indicates the current path of the trajectories, and τ keeps track of the time that the system has been in open loop. Let $\tau_{1,1}^* = \tau_{ur \rightarrow r}^*$, $\tau_{1,2}^* = \tau_{ru \rightarrow r}^*$, and $\tau_{2,1}^* = \tau_{2,2}^* = \tau_{r \rightarrow u}^*$. The control logic is summarized as follows:

- *Catch mode* when $q < 0$. This mode indicates that the state x is steered to the $(|q|, p)$ -th node of the current path p . If $q = -2$ then the control law applied is κ_r , while if $q = -3$ then the control law applied is κ_u .
- *Throw mode* when $q > 0$. This mode indicates that the trajectories are being steered from a neighborhood of the (q, p) -th node to a neighborhood of the $(q + 1, p)$ -th node of the current path p . If $q = 1, p = 1$, then the control law applied is $\alpha_{ur \rightarrow r}$; if $q = 1, p = 2$, then $\alpha_{ru \rightarrow r}$ is applied; and if $q = 2$ then $\alpha_{r \rightarrow u}$ is applied.
- *Recovery mode* when $q = p = 0$. This mode indicates that the trajectories are being steered to the tree with the control law κ_0 .

The hybrid controller updates its state under the following events:

- (C) **“Throw-to-catch” transitions:** when the state x is in some neighborhood E of an open-loop control law and in *throw mode* ($q > 0$), the controller jumps to *catch mode* (q updated to $-(|q| + 1)$). The timer state τ is reset to zero.

- (T) **“Catch-to-throw” transitions:** when the state x is in some neighborhood S of an open-loop control law and in *catch mode* ($q < 0$), the controller jumps to *throw mode* (q updated to $|q|$). The timer state τ is reset to zero.
- (R) **“Throw- or catch- to-recovery” transitions:** when the trajectories
- while in *throw mode*, do not reach a neighborhood of the associated set E in the expected amount of time (that is, $q > 0$ and $\tau \geq \tau_{q,p}^*$); or
 - while in *catch mode*, leave the basin of attraction of the current local stabilizer;
- then the controller jumps to *recovery mode* (q, p updated to $q = p = 0$).

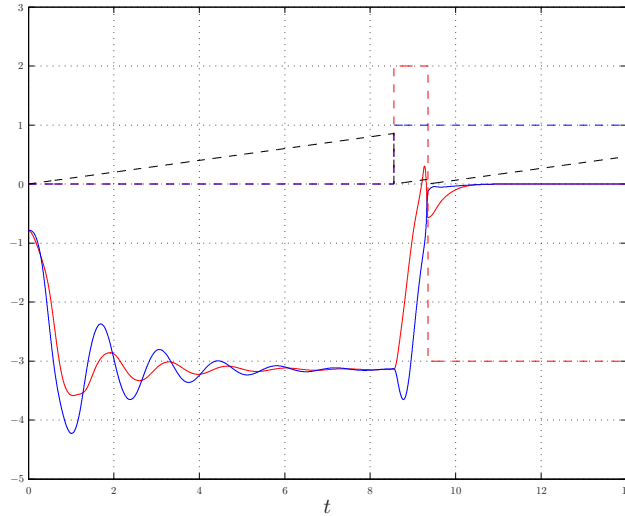


Figure 6.15. Simulation of the pendubot system with our hybrid control strategy. Initial conditions: $x^0 = [-\pi/4, 0, -\pi/4, 0]^T$, $q^0 = p^0 = 1$, $\tau^0 = 0$. The figure depicts: pendubot angles ϕ_1 (trajectory with larger overshoot) and ϕ_2 , logic state q (dashed, transitions: $0 \rightarrow 2 \rightarrow -3$), logic state p (dashed, transitions: $0 \rightarrow 1$), and timer state τ (dashed, seesaw trajectory). After an initial switch to recovery mode, when x reaches a neighborhood of $[-\pi, 0, -\pi, 0]^T$, a “throw” is performed (at around 8.5sec.) from the resting configuration (node (2, 1), \mathcal{A}_r) to a neighborhood of the upright configuration (node (3, 1), \mathcal{A}_u). Finally, a switch to the local stabilizer κ_r ($q = -3$) (at around 9.5sec.) steers x to the origin.

Figure 6.15 shows a simulation of the closed-loop system resulting from controlling the pendubot with our hybrid controller. The initial state of the pendubot is such that it is far away from the regions where the open-loop laws and the local stabilizer κ_u are applicable. Therefore, the hybrid controller initially switches to *recovery mode* ($q = p = 0$) and applies κ_0 . (In this case, the controller κ_0 was designed to be given by $-L_g V := -\langle \nabla V(x), g(x) \rangle$ where V is the kinetic plus potential energy of the pendubot and g is such that $f(x, u) = \tilde{f}(x) + g(x)u$. This controller removes energy faster than $\kappa_0 \equiv 0$.) With this controller, the angles of the pendulums reach a neighborhood of $-\pi$ and the angular velocities a neighborhood of 0. Then, the hybrid controller switches to *throw mode* in the first path and from node (2, 1) to node (3, 1) ($q = 2, p = 1$). The open-loop control law applied is $\alpha_{r \rightarrow u}$ which steers the state x to a neighborhood of the origin. In that event, a switch to the local stabilizer κ_u follows, and the state x converges to the origin asymptotically.

6.3 Trajectory tracking control for a class of juggling systems

6.3.1 Introduction

Mechanical systems with impacts are nonsmooth dynamical systems with trajectories that have intervals of continuity (*flow*) and points of discontinuity (*jumps*). Among a number of important stabilization tasks for these systems, the problem of stabilization to rhythmic patterns has received great attention from the engineering and neuroscience community because of its relevance in robotics and nature. A widely used benchmark system for this type of task is the simple, but rich in dynamics, model of a mechanical system with impacts consisting of a ball vertically bouncing on an actuated robot. This particular class of systems is referred to as *juggling systems*. Studies on juggling systems include feedback control strategies in for phase-lock stabilization to rhythmic patterns generated by a reference clock of one and two-dimensional juggling systems with only measurement of the ball state at impacts, and also open-loop strategies for the same stabilization task.

In this chapter, the juggling problem is viewed as a trajectory tracking problem for hybrid systems. Juggling systems are modeled as hybrid dynamical systems and a (feedback) hybrid controller is designed to accomplish the trajectory tracking tasks. The main goal of this chapter is to provide a general control design framework for general juggling systems with multiple impacting objects and reference trajectories. For the particular system for which the main ideas and concepts are introduced, the one degree-of-freedom juggler, the tracking problem translates into the problem of stabilizing *multiple balls* to *multiple periodic patterns* with a single actuated device. Figure 6.16 depicts the one degree-of-freedom juggler which consists of a point-mass ball, the plant, that impacts with a point-mass platform, the juggler.

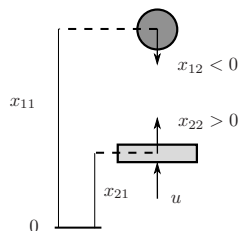


Figure 6.16. Juggling system of interest: one ball (plant) and an actuated robot. Their positions are denoted by x_{11}, x_{21} and their velocities by x_{12}, x_{22} , respectively.

The main challenge of this trajectory tracking problem for juggling systems is that the controller has to stabilize the trajectories of the balls to a reference signal with specific impact times by only taking measurements of the balls at impacts.

Our hybrid control algorithm accomplishes this task by, at impacts, planning the future impacts and, in between them, steering the actuated robot to satisfy the results from the planning stage. At every impact, the controller measures the ball state and its reference, and computes: 1) the time for the next impact, and 2) the position and velocity of the actuated robot at the next impact time. Then, the controller generates an input for the actuated robot to satisfy these constraints. An appropriately designed logic in the controller supervises the tracking of each of the balls to each reference trajectory. The proposed hybrid control strategy accomplishes finite-time practical tracking of the reference trajectories. It is demonstrated by simulations that it takes only three bounces for each ball to approach the reference trajectories.

6.3.2 Trajectory tracking approach to juggling control

The juggling problem outlined in Section 6.3.1 consists of designing a controller for system \mathcal{H} so that, with only information of the state of the ball at impacts, the ball state x_1 *tracks* a given reference trajectory r (on an appropriate hybrid time domain). Since both x_1 and r are given on hybrid time domains, and those are not necessarily the same, *tracking* between x_1 and r means that their graphs are close after a finite amount of time. More precisely, given $\varepsilon > 0$, $x_1 : \text{dom } x_1 \rightarrow \mathbb{R}^2$, and $r : \text{dom } r \rightarrow \mathbb{R}^2$, x_1 and r are ε -close after $T \geq 0$ if

- (a) for all $(t, j) \in \text{dom } x_1$ with $(t, j) \succeq (T, J)$ for some $J, (T, J) \in \text{dom } x_1$, there exists $(t', j') \in \text{dom } r$, $|t - t'| < \varepsilon$, and

$$|x_1(t, j) - r(t', j')| < \varepsilon, \quad (6.29)$$

- (b) for all $(t, j) \in \text{dom } r$ with $(t, j) \succeq (T, J)$ for some $J, (T, J) \in \text{dom } r$, there exists $(t', j') \in \text{dom } x_1$, $|t - t'| < \varepsilon$, and

$$|r(t, j) - x_1(t', j')| < \varepsilon. \quad (6.30)$$

When this property holds for x_1 and a given reference trajectory r , it is called *finite-time ε -tracking*, and it will be said that “ x_1 finite-time ε -tracks r ” (cf. Definition 3.8).

Figure 6.17 shows the ball position component of the solution shown in Figure 6.19 and the reference trajectory shown in Figure 6.18. Note that the hybrid time domains of these trajectories do not coincide. These trajectories are such that the state x_{11} and the reference r are ε -close after t_3 . Figure 6.17 shows the way properties (a) and (b) verify at points with time t in a neighborhood of t_3 . Notice that the closeness property

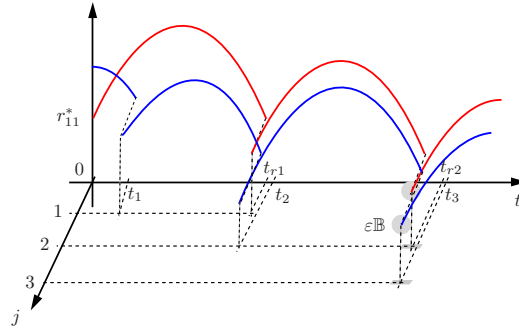


Figure 6.17. A ball position trajectory (trajectory jumping first at t_1) and a reference trajectory (trajectory jumping first at t_{r1}) with different hybrid time domains. The trajectories are ε -close for points with t such that $|t - t_3| < \varepsilon$ since each trajectory has points in a ε -neighborhood (denoted by $\varepsilon\mathbb{B}$) of the other trajectory.

above does not insist on the trajectories to satisfy (6.29) and (6.30) for the same index j , but rather for different indexes for which the trajectories are close at nearby times.⁴

As mentioned above, reference trajectories are given on hybrid time domains. Periodic reference trajectories are generated by the hybrid system \mathcal{H}_r :

$$\begin{aligned} \dot{r}_{11} &= r_{12}, \quad \dot{r}_{12} = -\gamma & r_{11} - r_{11}^* \geq 0, \\ r_{11}^+ &= r_{11}, \quad r_{12}^+ = -r_{12} & r_{11} - r_{11}^* \leq 0 \text{ and } r_{12} \leq 0, \end{aligned}$$

⁴This is the main difference between this notion of closeness and (τ, ε) -closeness in Definition 3.8.

where r_{11}^* is the reference height and r_{12}^* is the reference velocity after the impact. Let $r := [r_{11} \ r_{12}]^T$. Given an initial condition r^0 , the solution r to \mathcal{H}_r defines a reference trajectory on a hybrid time domain $\text{dom } r$. Figure 6.18 shows a sample reference trajectory which describes a periodic pattern.

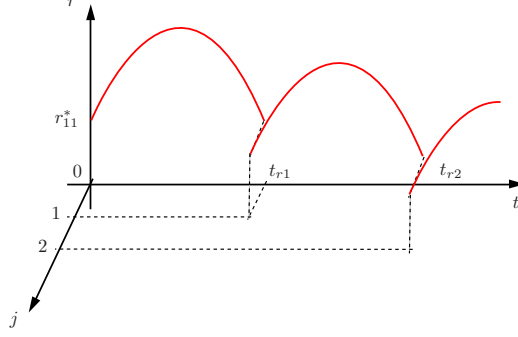


Figure 6.18. Reference trajectory describing a periodic pattern generated by \mathcal{H}_r for a given initial condition r^0 . The constant r_{11}^* is the desired height for the pattern.

The hybrid system \mathcal{H}_r is considered to be an external signal generator to the juggling system and hybrid controller.

6.3.3 Single-ball juggling

A model for a hybrid system given by a ball and a juggler in Section 6.3.1 is derived first. The dynamics of the ball are given by Newton laws

$$\dot{x}_1 = \begin{bmatrix} x_{12} \\ -\gamma \end{bmatrix} =: f_1(x_1) \quad (6.31)$$

where $x_1 := [x_{11} \ x_{12}]^T \in \mathbb{R}^2$ with x_{11} being the height and x_{12} the velocity of the ball, and γ is the gravity constant. The mass of the plant is denoted by m_1 . The actuated robot is assumed to have double integrator dynamics given by

$$\dot{x}_2 = \begin{bmatrix} x_{22} \\ u \end{bmatrix} =: f_2(x_2, u) \quad (6.32)$$

where $x_2 := [x_{21} \ x_{22}]^T \in \mathbb{R}^2$ with x_{21} being the height and x_{22} the velocity of the actuated robot, and $u \in \mathbb{R}$ the control input. The mass of the actuated robot is denoted by m_2 .

The impacts between the ball and the actuated robot are given by the following impact rule with conservation of momentum

$$\begin{aligned} x_{12}^+ - x_{22}^+ &= -e(x_{12} - x_{22}), \\ m_1 x_{12}^+ + m_2 x_{22}^+ &= m_1 x_{12} + m_2 x_{22} \end{aligned}$$

where $e \in (0, 1)$ is the restitution coefficient. Let $\lambda = \frac{m_1}{m_1 + m_2}$. The resulting update law at impacts for x_{12} and x_{22} is given by

$$\begin{bmatrix} x_{12}^+ \\ x_{22}^+ \end{bmatrix} = \begin{bmatrix} \lambda - (1 - \lambda)e & (1 - \lambda)(1 + e) \\ \lambda(1 + e) & 1 - \lambda - \lambda e \end{bmatrix} \begin{bmatrix} x_{12} \\ x_{22} \end{bmatrix} =: \Gamma(\lambda, e) \begin{bmatrix} x_{12} \\ x_{22} \end{bmatrix},$$

while the update law for x_{11} and x_{21} are given by

$$\begin{bmatrix} x_{11}^+ \\ x_{21}^+ \end{bmatrix} = \begin{bmatrix} x_{11} \\ x_{21} \end{bmatrix}.$$

The impacts between the ball and the actuated robot occur when $x_{11} \leq x_{21}$ and $x_{12} \leq x_{22}$.

Then, the one degree-of-freedom juggler system in Figure 6.16 is given by the hybrid system \mathcal{H} with flows

$$\left. \begin{array}{l} \dot{x}_{11} = x_{12}, \quad \dot{x}_{12} = -\gamma \\ \dot{x}_{21} = x_{22}, \quad \dot{x}_{22} = u \end{array} \right\} x_{11} - x_{21} \geq 0,$$

and jumps

$$\left. \begin{array}{l} x_{11}^+ = x_{11} \\ x_{12}^+ = [1 \quad 0] \Gamma(\lambda, e) \begin{bmatrix} x_{12} \\ x_{22} \end{bmatrix} \\ x_{21}^+ = x_{21} \\ x_{22}^+ = [0 \quad 1] \Gamma(\lambda, e) \begin{bmatrix} x_{12} \\ x_{22} \end{bmatrix} \end{array} \right\} x_{11} - x_{21} \leq 0 \text{ and } x_{12} - x_{22} \leq 0.$$

Figure 6.19 depicts the x_{11} and x_{21} components of a solution to \mathcal{H} for a particular choice of control input u . At hybrid times $(t_1, 0)$, $(t_2, 1)$, $(t_3, 2)$ the ball and the actuated robot impact and the jump map g computes the new value of the state at $(t_1, 1)$, $(t_2, 2)$, $(t_3, 3)$, respectively. The continuous evolution of the solution is governed by the differential equations (6.31) and (6.32).

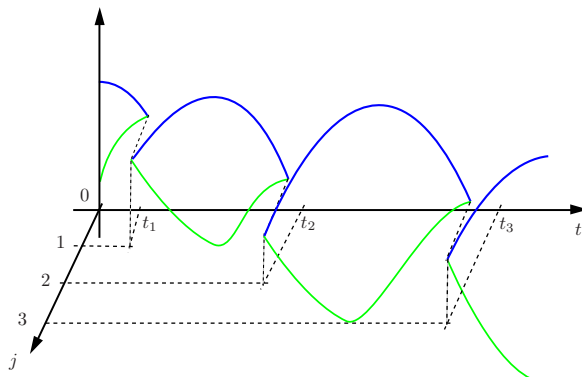


Figure 6.19. Position components of a solution to \mathcal{H} on hybrid time domains: ball height (top, dark) and actuator robot height (bottom, gray).

The main control task to accomplish in this section is

(\star) For every feasible initial condition, level of tracking accuracy $\varepsilon > 0$, and a reference trajectory r , the ball state component x_1 of the solutions to the closed-loop system finite-time ε -tracks the reference trajectory r .

To solve this problem, the state of the balls can only be measured and controlled at the impact times. A *feasible initial condition* is any initial condition of the closed-loop system for which an impact between the plant and the actuated robot occurs in finite time.

Control strategy

The main control idea to accomplish the tracking problem in (\star) is summarized in the following algorithm:

Algorithm for Single-ball Juggling

At every impact between the ball and the actuated robot (say it occurs at hybrid time $(t_0, 0)$) compute:

- Step 1)** the apex time of the ball position trajectory x_{11} resulting from the impact (denote this time by t_a);
- Step 2)** the time of the next two consecutive impacts to t_a in the reference r (denote these impact times by t_1 and t_2 , respectively);
- Step 3)** the ball trajectory x_1 at $(t_1, 0)$;
- Step 4)** the value of the state x_2 at $(t_1, 0)$, denoted by x'_2 , required for the impact at $(t_2, 1)$ to occur with x_1 equal to the reference trajectory r ;
- Step 5)** a *virtual reference trajectory* z that at time $(t_1, 0)$ is equal to the value of x_2 , given by x'_2 , computed in step 4).

Finally, the control law applied to the actuated robot is designed so that x_2 tracks the virtual reference trajectory computed in Step 5).

Note that the steps above can be computed by solving for the dynamics of the ball in (6.31). The virtual reference trajectory z needed in Step 5) is basically a trajectory initialized at the impact time such that, when tracked, the next impact between the ball and the actuated robot occurs at the appropriate time with value equal to x'_2 .

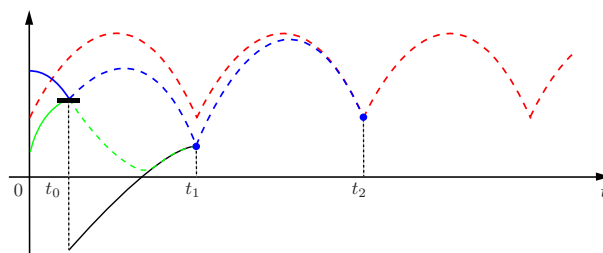


Figure 6.20. Main control idea to track a reference trajectory r (r_{11} component, dashed, jumping first at t_1). At the impact at $t = t_0$, the controller computes the resulting ball position trajectory x_{11} (dashed, jumping first at t_0) at time t_1 and the required value of the state x_2 at t_1 such that the next desired impact time t_2 of the reference, x_{11} equals r_1 . The virtual reference trajectory z (solid) resulting from this computation is tracked by the actuated robot (dashed, gray).

Figure 6.20 depicts the computations in Steps 1)-5) that the control algorithm performs at the impact at $(t_0, 0)$. For simplicity, the trajectories are plotted projected to the ordinary time axis t . Figure 6.21 illustrates the sequence of events of the juggling system executing the control algorithm.

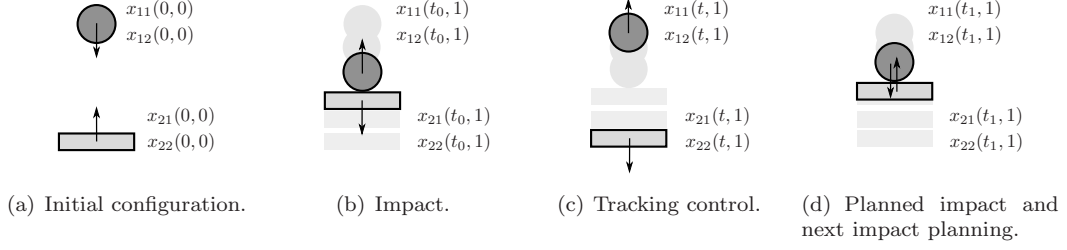


Figure 6.21. Sequence of events during ball-robot impact. From the initial configuration at $(0,0)$ (see (a)), at the impact at hybrid time $(t_0,0)$ (see (b)), the controller executes Steps 1)-5) of the control algorithm. After the impacts, the actuated robot tracks the virtual reference (see (c)). The next impact occurs at the desired hybrid time $(t_1,1)$ with desired actuated robot state (see (d)) given by x'_2 . The next impact is then planned.

Hybrid Controller

The control algorithm above is implemented in a hybrid controller which is denoted by \mathcal{H}_c . The state of the controller is given by the virtual reference state $z = [z_{11} \ z_{12}]^T \in \mathbb{R}^2$. The controller performs three main tasks:

- At every impact, perform the computations in Step 1)-4).
- At every impact, reset z to a value such that the continuous dynamics of z generate a virtual reference trajectory that matches the impact constraint in Step 4).
- In between impacts, control the actuated robot to track the virtual reference trajectory.

The continuous dynamics of the state z are defined by a copy of the dynamics of the actuated robot. Then, the flows of \mathcal{H}_c are given by

$$\dot{z}_{11} = z_{12}, \quad \dot{z}_{12} = \alpha \quad (6.33)$$

where $\alpha < 0$. This constant is chosen so that the z_{11} components of the solution to (6.33) are described by concave parabolas (see [80] for more details). The jump map for \mathcal{H}_c is given by

$$\begin{bmatrix} z_{11} \\ z_{12} \end{bmatrix}^+ \in \kappa_c(x_1, z, r) \quad (6.34)$$

where $\kappa_c : \mathbb{R}^2 \times \mathbb{R}^2 \times \mathbb{R}^2 \rightrightarrows \mathbb{R}^2$ is a set-valued mapping that updates the state z for the generation of the virtual trajectory. The output of the controller is given by

$$u = \kappa(x_2, z) .$$

This corresponds to the control input for the actuated robot. Note that the hybrid controller \mathcal{H}_c only uses state and reference information at impacts for the update of z . The only measurements that are needed permanently are the state of the actuated robot and z .

The closed-loop system \mathcal{H}_{cl} resulting from controlling the juggling system \mathcal{H} with the hybrid controller \mathcal{H}_c can be written as the following hybrid system:

$$\left. \begin{aligned} \dot{x}_{11} &= x_{12}, & \dot{x}_{12} &= -\gamma \\ \dot{x}_{21} &= x_{22} \\ \dot{x}_{22} &= \kappa(x_2, z) \\ \dot{z}_{11} &= z_{12}, & \dot{z}_{12} &= \alpha \end{aligned} \right\} x_{11} - x_{21} \geq 0 ,$$

$$\left. \begin{aligned} x_{11}^+ &= x_{11} \\ x_{12}^+ &= [1 \ 0] \Gamma(\lambda, e) \begin{bmatrix} x_{12} \\ x_{22} \end{bmatrix} \\ x_{21}^+ &= x_{21} \\ x_{22}^+ &= [0 \ 1] \Gamma(\lambda, e) \begin{bmatrix} x_{12} \\ x_{22} \end{bmatrix} \\ \begin{bmatrix} z_{11} \\ z_{12} \end{bmatrix}^+ &\in \kappa_c(x_1, z, r) \end{aligned} \right\} x_{11} - x_{21} \leq 0 \text{ and } x_{12} - x_{22} \leq 0 .$$

This construction is such that \mathcal{H}_{cl} satisfies the hybrid basic conditions.

Control Design

To design the update law κ_c of the hybrid controller \mathcal{H}_c , the dynamics of the actuated robot in \mathcal{H} are initially replaced by the dynamics of the state z in \mathcal{H}_c , i.e.,

$$\left. \begin{aligned} \dot{x}_{11} &= x_{12}, & \dot{x}_{12} &= -\gamma \\ \dot{z}_{11} &= z_{12}, & \dot{z}_{12} &= \alpha \end{aligned} \right\} x_{11} - z_{11} \geq 0 ,$$

$$\left. \begin{aligned} x_{11}^+ &= x_{11} \\ x_{12}^+ &= [1 \ 0] \Gamma(\lambda, e) \begin{bmatrix} x_{12} \\ z_{12} \end{bmatrix} \\ \begin{bmatrix} z_{11} \\ z_{12} \end{bmatrix}^+ &\in \kappa_c(x_1, z, r) \end{aligned} \right\} x_{11} - z_{11} \leq 0 \text{ and } x_{12} - z_{12} \leq 0 .$$

This system is denoted by \mathcal{H}_v , meaning *virtual juggling system*. The main idea for control design is to define the set-valued map κ_c such that the control task (\star) is accomplished for \mathcal{H}_v and then design a control law κ that acts on the actuated robot and accomplishes (standard) tracking between x_2 and r . To that end, a result for the solutions to \mathcal{H}_v is first stated.

Lemma 6.16 (property of solutions to \mathcal{H}_v) *For every feasible initial condition*

$$[x_{11}(0,0) \ x_{12}(0,0) \ z_{11}(0,0) \ z_{12}(0,0)]^T$$

for \mathcal{H}_v , the next impact occurs at time $(t_1, 0)$ provided that

$$z_{11}(0,0) = -\frac{\gamma + \alpha}{2} t_1^2 + (x_{12}(0,0) - z_{12}(0,0)) t_1 + x_{11}(0,0) . \quad (6.35)$$

Moreover, the position and velocity of the ball after the impact at $(t_1, 0)$, denoted by $x_{11}(t_1, 1)$ and $x_{12}(t_1, 1)$, respectively, are given by

$$x_{11}(t_1, 1) = -\frac{\gamma}{2} t_1^2 + x_{12}(0,0) t_1 + x_{11}(0,0), \quad (6.36)$$

$$x_{12}(t_1, 1) = [1 \ 0] \Gamma(\lambda, e) \begin{bmatrix} x_{12}(0,0) - \gamma t_1 \\ \alpha t_1 + z_{12}(0,0) \end{bmatrix}. \quad (6.37)$$

Proof. Given a feasible initial condition $[x_{11}(0,0) \ x_{12}(0,0) \ z_{11}(0,0) \ z_{12}(0,0)]^T$, that is, an initial condition for which there exists $t_1 > 0$ such that an impact between the ball and the virtual reference occurs at $(t_1, 0)$, then, up to $(t_1, 0)$, the ball trajectory is given by

$$x_{11}(t, 0) = -\frac{\gamma}{2} t^2 + x_{12}(0,0) t + x_{11}(0,0) \quad (6.38)$$

$$x_{12}(t, 0) = -\gamma t + x_{12}(0,0) \quad (6.39)$$

and for the virtual reference

$$z_{11}(t, 0) = \frac{\alpha}{2}t^2 + z_{12}(0, 0)t + z_{11} \quad (6.40)$$

$$z_{12}(t, 0) = \alpha t + z_{12}(0, 0) . \quad (6.41)$$

For the impact to occur at $(t_1, 0)$, $x_{11}(t_1, 0) = z_{11}(t_1, 0)$ and $x_{12}(t_1, 0) \leq z_{12}(t_1, 0)$. The first condition implies (6.35). The second condition is satisfied by the initial condition being feasible.

Finally, (6.36) and (6.37) are given by applying the jump map of \mathcal{H}_v to x and z at $(t_1, 0)$. \square

Lemma 6.16 can be shown by solving the continuous dynamics of the ball and state z . In fact, equation (6.35) follows from solving the system backward in time from the jump condition of \mathcal{H}_v , equation (6.36) follows from the fact that the x_{11} component of the solution is mapped to itself at jumps, and equation (6.37) is derived from the impact rule used for the impacts of \mathcal{H}_v .

Let $J : \mathbb{R}^2 \times \mathbb{R}^2 \times \mathbb{R}^2 \rightrightarrows \mathbb{R}^2$ be the set-valued mapping

$$J(x_1, z, r) = \begin{cases} \frac{r_{12} + r_{12}^*}{\gamma} & \text{if } \frac{ax_{12} + bz_{12}}{\gamma} < \frac{r_{12} + r_{12}^*}{\gamma} \\ \left\{ \frac{r_{12} + r_{12}^*}{\gamma}, \frac{r_{12} + r_{12}^*}{\gamma} + T_r \right\} & \text{if } \frac{ax_{12} + bz_{12}}{\gamma} = \frac{r_{12} + r_{12}^*}{\gamma} \\ \frac{r_{12} + r_{12}^*}{\gamma} + T_r & \text{if } \frac{ax_{12} + bz_{12}}{\gamma} > \frac{r_{12} + r_{12}^*}{\gamma} \end{cases} \quad (6.42)$$

where $T_r = 2r_{12}^*/\gamma$ and

$$a = [1 \quad 0] \Gamma(\lambda, e) \begin{bmatrix} 1 \\ 0 \end{bmatrix}, \quad b = [1 \quad 0] \Gamma(\lambda, e) \begin{bmatrix} 0 \\ 1 \end{bmatrix} .$$

The proposed control algorithm first computes the time for the next impact t_1 in Step 1) and then computes Step 2)-5) to generate a virtual trajectory. Regarding Step 1), the set-valued mapping J contains the time(s) to the next impact t_1 from the current state. The value of t_1 is chosen so that if the apex time of the trajectory x_{11} is smaller than the time for the next impact of the reference, then t_1 is given by the next impact time of the reference. If it is larger, then the impact is postponed for one period T_r . When t_1 is equal to the apex time both times are possible, and therefore, J is set-valued. Regarding Step 2)-5), for each $t_1 \in J(x_1, z, r)$, the reset value z^* for z is computed by two applications of Lemma 6.16. This is done by setting $x_{11}(t_1 + T_r, 3) = r_{11}^*$ and $x_{12}(t_1 + T_r, 3) = r_{12}^*$ (see Figure 6.20). Then, the set-valued mapping $\kappa_c(x_1, z, r)$ is given by all points $z^* = [z_{11}^* \quad z_{12}^*]^T$ such that

$$z_{11}^* = -\frac{\gamma + \alpha}{2}t_1^2 + (ax_{12} + bz_{12} - z_{12}^*)t_1 + x_{11} \quad (6.43)$$

$$z_{12}^* = \frac{r_{11}^* + \frac{\gamma}{2}T_r^2 + \frac{\gamma}{2}t_1^2 - (ax_{12} + bz_{12})t_1 - x_{11}}{bT_r} + \frac{(a\gamma - b\alpha)t_1 - a(ax_{12} + bz_{12})}{b} . \quad (6.44)$$

The control law κ is designed so that the trajectories of the platform system track the trajectories of the virtual platform system. Let $e_1 := x_{21} - z_{11}$, $e_2 := x_{22} - z_{12}$. Then, the error system is

$$\dot{e}_1 = e_2, \quad \dot{e}_2 = u - \alpha .$$

Given $k_1, k_2 > 0$, a particular choice of the control law κ to accomplish the tracking between x_2 and r is given by

$$\kappa(x_2, z) = \alpha - k_1(x_{21} - z_{11}) - k_2(x_{22} - z_{12}) .$$

Tracking properties

In a perfect tracking scenario, when the error between the actuated robot state and the virtual trajectory is zero, the control algorithm achieves *finite-time 0-tracking*. That is, given $x_1 : \text{dom } x_1 \rightarrow \mathbb{R}^2$, and $r : \text{dom } r \rightarrow \mathbb{R}^2$, x_1 finite-time 0-tracks r after $T \geq 0$ if

- (a) for all $(t, j) \in \text{dom } x_1$ with $(t, j) \succeq (T, J)$ for some J , $(T, J) \in \text{dom } x_1$, there exists $(t, j') \in \text{dom } r$ and

$$|x_1(t, j) - r(t, j')| = 0, \quad (6.45)$$

- (b) for all $(t, j) \in \text{dom } r$ with $(t, j) \succeq (T, J)$ for some J , $(T, J) \in \text{dom } r$, there exists $(t', j) \in \text{dom } x_1$ and

$$|r(t, j) - x_1(t', j)| = 0. \quad (6.46)$$

This is the case for the virtual juggling system \mathcal{H}_v as shown next.

Theorem 6.17 (finite-time 0-tracking) *For each reference trajectory r generated from \mathcal{H}_r and each feasible initial condition, each solution to \mathcal{H}_v is bounded and the x_1 component finite-time 0-tracks the reference trajectory r . Moreover, the trajectories coincide after three impacts.*

Proof. The result follows by the construction of the update law κ_c . Suppose that an impact, the first impact, occurs at $(T_0, 0)$. Let $T_1, T_2 > 0$ be such that subsequent impact, the second impact, and the following impact, the third impact, occur at $(T_1, 1)$, $(T_2, 2)$, respectively. The impact times T_1 and T_2 are planned as follows.

- To accomplish finite-time 0-tracking, assume $x_{11}(T_2, 3) = r_{11}^*$, $x_{12}(T_2, 3) = r_{12}^*$, and $x_{11}(T_1, 2) = -\frac{\gamma}{2}(T_1 - T_0)^2 + x_{12}(T_0, 1)(T_1 - T_0) + x_{11}(T_0, 1)$. Then, using (6.37) and (6.35), solving for $x_{12}(T_1, 2)$ yields

$$x_{12}(T_1, 2) = \frac{r_{11}^* + \frac{\gamma}{2}(T_2 - T_1)^2 - x_{11}(T_1, 2)}{T_2 - T_1} \quad (6.47)$$

- Given $x_{11}(T_1, 2)$ and $x_{12}(T_1, 2)$ as above, solve for z_1^* and z_2^* using (6.37) and (6.35). This results in

$$z_2^* = \frac{x_{12}(T_1, 2) + [1 \ 0] \Gamma(\lambda, e) \left(\begin{bmatrix} 1 \\ 0 \end{bmatrix} (\gamma T' - x_{12}(T_0, 1)) - [0 \ 1] \alpha T' \right)}{[1 \ 0] \Gamma(\lambda, e) \begin{bmatrix} 0 \\ 1 \end{bmatrix}} \quad (6.48)$$

$$z_1^* = -\frac{\gamma + \alpha}{2} T'^2 + (x_{12}(T_0, 1) - v_4) T' + x_{11}(T_0, 1). \quad (6.49)$$

The time $T' = T_1 - T_0$, the time to the next impact, is computed measuring the velocity of the reference ball, given by r_{12} and using the fact that in between jumps, r_{12} decreases linearly with rate γ from r_{12}^* . Then, the time to the next impact in the reference signal is given by $\frac{r_{12} + \gamma T_{12}}{\gamma}$. Assuming that the velocity of the platform at impacts is positive, the impact times should only occur when the velocity of the ball is negative. In this way, the impacts are programmed to occur no sooner than the apex time for the trajectory, which when an impact occurs with velocity of the ball x_{12} and velocity of the virtual reference state z_{12} is given by $\frac{ax_{12} + bz_{12}}{\gamma}$. The set-valued mapping J in (6.42) performs this computation. Note that this choice of T_1 is so that if the apex time is smaller than the time for the next impact of the reference, then the time for the next impact is given by the next impact time of the reference. Otherwise, the impact is postponed for one period T_r .

Then, combining (6.47), (6.48), (6.49), and (6.42) at each impact time, the control inputs to the virtual reference are given by (6.43) and (6.44). By construction, the ball's trajectory coincides with the reference trajectory from the third onwards. \square

The proof of Theorem 6.17 follows from the construction of the update law κ_c in Section 6.3.3 which is designed so that the ball component of solutions to \mathcal{H}_v converge to the reference trajectory in finite time.

The fact that it is possible to select the parameters k_1, k_2 of the tracking law κ so that the actuated robot tracks the the virtual state z fast enough, suggests that the following conjecture is true:

For each $\varepsilon > 0$, each reference trajectory r generated from \mathcal{H}_r , and each feasible initial condition, each solution to \mathcal{H}_{cl} is bounded and the x_1 component finite-time ε -tracks the reference trajectory r . Moreover, only three impacts are required for x_1 and r to be ε -close.

The numerical simulations in the following section are indicators of truthfulness of this conjecture.

Numerical simulations

The closed-loop system \mathcal{H}_{cl} with a reference trajectory generated by \mathcal{H}_r with $r_{11}^* = 0, r_{12}^* = 10, r^0 = [0 \ 10]^T$ is simulated in Simulink.

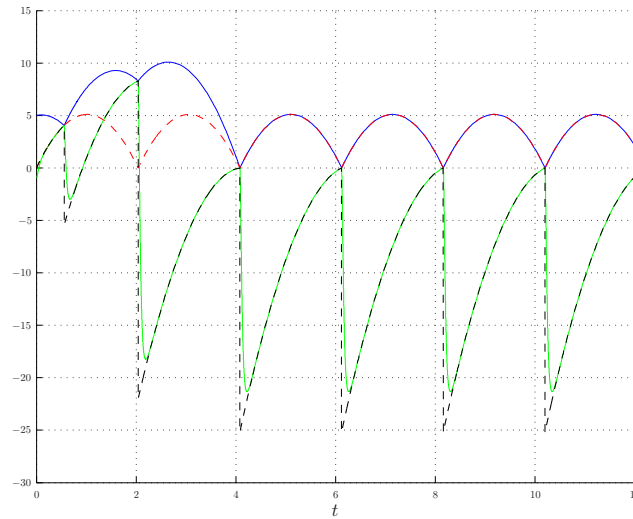


Figure 6.22. Simulation of closed-loop system \mathcal{H}_{cl} . System parameters: $m_1 = 1, m_2 = 9, e = 0.8, \gamma = 9.8$. Controller parameters: $\alpha = -9.8, k_1 = 2000, k_2 = 100$. Initial condition: $x_{11}(0, 0) = 5, x_{12}(0, 0) = 1, x_{21}(0, 0) = -1, x_{22}(0, 0) = 0$. The trajectory of the ball (top) impacts with the actuated robot (gray). Finite-time ε -tracking is achieved at the third bounce when the ball trajectory approaches the reference trajectory (dashed, periodic pattern). The virtual reference z is depicted with a black, dashed line (bottom).

Figure 6.22 shows a simulation of the closed-loop system. For simplicity in plotting the results, trajectories are projected to the ordinary time t axis. The ball trajectory approaches the reference trajectory in the neighborhood of the time corresponding to the third bounce. Note that the parameters of the control law κ

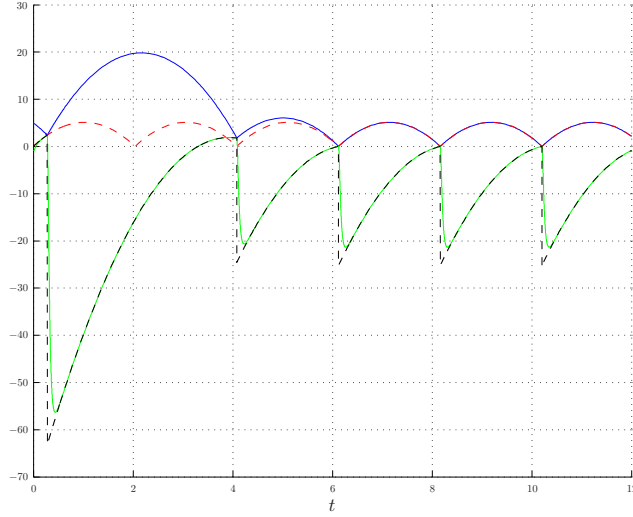


Figure 6.23. Simulation of closed-loop system \mathcal{H}_{cl} . System parameters: $m_1 = 1, m_2 = 9, e = 0.8, \gamma = 9.8$. Controller parameters: $\alpha = -9.8, k_1 = 2000, k_2 = 100$. Initial condition: $x_{11}(0, 0) = 5, x_{12}(0, 0) = 1, x_{21}(0, 0) = -1, x_{22}(0, 0) = 0$. The trajectory of the ball (top) impacts with the actuated robot (gray). Finite-time ε -tracking is achieved at the third bounce when the ball trajectory approaches the reference trajectory (dashed, periodic pattern). The virtual reference z is depicted with a black, dashed line (bottom).

steer the actuated robot to a very small neighborhood of the virtual reference as the figure indicates. This can be adjusted appropriately with the parameters k_1 and k_2 .

The simulation in Figure 6.23 is for the same reference trajectory but for different initial conditions of the ball. It illustrates the decision that the controller makes when the apex time of the trajectory after the first bounce is larger than the next impact of the reference trajectory. As a difference to the simulation in Figure 6.22, the second impact is planned for $t_1 = 4r_{12}^*/\gamma$ rather than for $t_1 = 2r_{12}^*/\gamma$. Recall that the control algorithm is so that, if the apex time coincides with the impact time of the reference trajectory, both choices are possible.

6.3.4 Multiple-balls juggling control

In this section, the multiple balls juggling problem is considered. Suppose that n reference trajectories, n balls, and one actuated robot are given as in Figure 6.24. The goal is the following:

($\star\star$) For every feasible initial condition and n reference trajectories with distinct impact times, the i -th ball state component x_1^i of the solutions to the closed-loop system finite-time ε -tracks the i -th reference trajectory r^i .

Recall that the state of the balls can only be measured and controlled at the impact times.

A *feasible initial condition* in this multiple trajectory tracking problem means any initial condition for which each ball impacts with the actuated robot in finite time and in an ordered manner: every n impacts, each ball has impacted only once, and the order is preserved for all time.

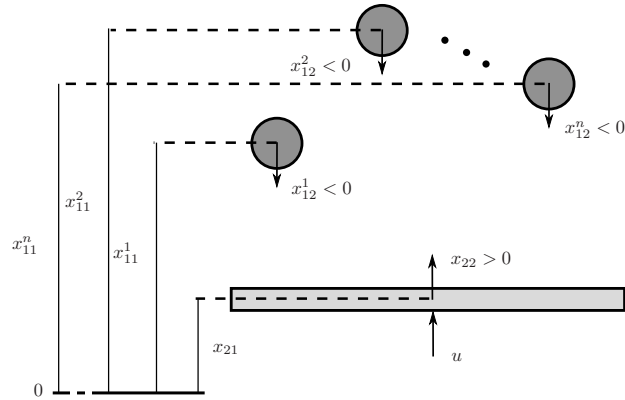


Figure 6.24. Juggling system of interest: n balls (plant) and one actuated robot. The ball positions and velocities are denoted by x_{11}^i, x_{12}^i , respectively, and the actuated robot position and velocity by x_{12}, x_{22} , respectively.

Control Strategy and Hybrid Controller

The control strategy proposed here combines the control algorithm introduced in Section 6.3.3 to plan the impacts for each ball individually and uses additional logic to select the ball to control. Let $Q := \{1, 2, \dots, n\}$ and q be a logic state, $q \in Q$. Let $z^q \in \mathbb{R}^2$ be the virtual reference state of the q -th ball. The reference trajectory for q -th ball is generated by the hybrid system \mathcal{H}_r^q . It is assumed that for each q , \mathcal{H}_r^q is defined as \mathcal{H}_r . Moreover, it is assumed that the reference trajectories are such that the impact times do not occur at the same time and that they have the above ordering property: every n impacts, each reference trajectory has only one impact, and the order is preserved for all time.

The control logic for multi-ball juggling is as follows.

Algorithm for Multiple-balls Juggling

At an impact between the q -th ball and the actuated robot:

- Step 1)** With reference trajectory r^q , compute Step 1)-5) of the *Algorithm for Single-ball Juggling* to obtain z^{q*} . Update the state z^q with this value.
- Step 2)** Update the logic state q by $q^+ = \text{mod}(q, n) + 1$.
- Step 3)** Apply to the actuated robot a control law that tracks the virtual reference z^q .

This logic is implemented in a hybrid controller resulting in the closed-loop system \mathcal{H}_{cl}^M given by

$$\left. \begin{array}{l} \dot{x}_{11}^1 = x_{12}^1, \quad \dot{x}_{12}^1 = -\gamma \\ \dot{x}_{11}^2 = x_{12}^2, \quad \dot{x}_{12}^2 = -\gamma \\ \vdots \\ \dot{x}_{11}^n = x_{12}^n, \quad \dot{x}_{12}^n = -\gamma \\ \dot{x}_{21} = x_{22} \\ \dot{x}_{22} = \kappa(x_2, z^q) \\ \dot{z}_{11}^1 = z_{12}^1, \quad \dot{z}_{12}^1 = \alpha \\ \dot{z}_{11}^2 = z_{12}^2, \quad \dot{z}_{12}^2 = \alpha \\ \vdots \\ \dot{z}_{11}^n = z_{12}^n, \quad \dot{z}_{12}^n = \alpha \\ \dot{q} = 0 \end{array} \right\} x_{11}^q - x_{21} \geq 0 ,$$

$$\left. \begin{array}{l} \left[\begin{array}{l} x_{12}^q \\ x_{21} \end{array} \right]^+ = \Gamma(\lambda, e) \left[\begin{array}{l} x_{12}^q \\ x_{21} \end{array} \right] \\ \left[\begin{array}{l} z_{11}^q \\ z_{12}^q \end{array} \right]^+ \in \kappa_c(x_1^q, z^q, r^q) \\ q^+ = \text{mod}(q, 2) + 1 \end{array} \right\} x_{11}^q - x_{21} \leq 0 \text{ and } x_{12}^q - x_{22} \leq 0 ,$$

where in the jump map and jump set, the components of the state that remain constant at jumps were omitted. Note that this construction is such that \mathcal{H}_{cl}^M satisfies the hybrid basic conditions.

Tracking properties

By construction, the closed-loop system \mathcal{H}_{cl}^M inherits the same properties than the ones of \mathcal{H}_{cl} . The main difference in the multiple trajectory tracking problem is that feasible initial conditions need to satisfy more restrictive ordering constraints. This leads to a smaller set of initial conditions from where finite-time ε -tracking is achieved. The following conjecture is expected to be true:

For each $\varepsilon > 0$, q reference trajectories r^q generated from \mathcal{H}_r^q , $q \in Q$, and each feasible initial condition, each solution to \mathcal{H}_{cl}^M is bounded and the x_1^q component finite-time ε -tracks the reference trajectory r^q , $q \in Q$. Moreover, for each $q \in Q$, only three impacts are required for x_1^q and r^q to be ε -close.

Numerical simulations

The case of juggling two balls is considered first. References r^1 and r^2 are such that r^1 is generated by \mathcal{H}_r^1 with $r_{11}^{1*} = 0, r_{12}^{1*} = 10, r^{10} = [0 \ 10]^T$ and r^2 by \mathcal{H}_r^2 with $r_{11}^{2*} = 0, r_{12}^{2*} = 10, r^{20} = [0 \ 10]^T$. (Reference r^1 and r^2 have a 180deg phase difference as show in Figure 6.25.) The closed-loop trajectories in Figure 6.25 show that at the third impact with each ball, each reference trajectory is ε -tracked for all future time. Figure 6.26 shows the switches of the logic state q that select the appropriate state z^q for tracking and update at impacts.

Finally, Figure 6.27 shows a simulation result for the case of juggling three balls. Notice that tracking is also accomplished at the third bounce of each one of the balls.

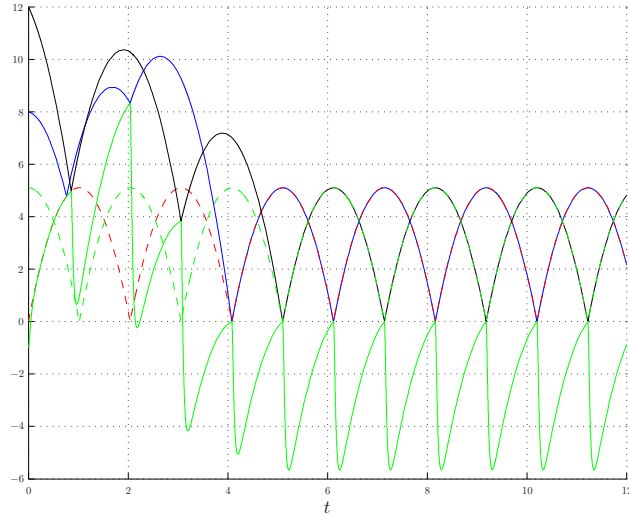


Figure 6.25. Simulation of the closed-loop system \mathcal{H}_r^M for two balls. System parameters: $m_1^1 = m_1^2 = 1, m_2 = 9, e = 0.8, \gamma = 9.8$. Controller parameters: $\alpha = -9.8, k_1 = 2000, k_2 = 100$. Initial condition: $x_{11}^1(0,0) = 8, x_{12}^1(0,0) = -0.5, x_{11}^2(0,0) = 12, x_{22}^2(0,0) = -4, x_{21}(0,0) = -1, x_{22}(0,0) = 0$. The trajectory of the first ball (top, the one jumping first, $q = 1$) and the trajectory of the second ball (black, $q = 2$) bounce on the actuated robot (top, the one jumping second) and approach the respective reference trajectories r^q (dashed, periodic patterns) at the third bounce.

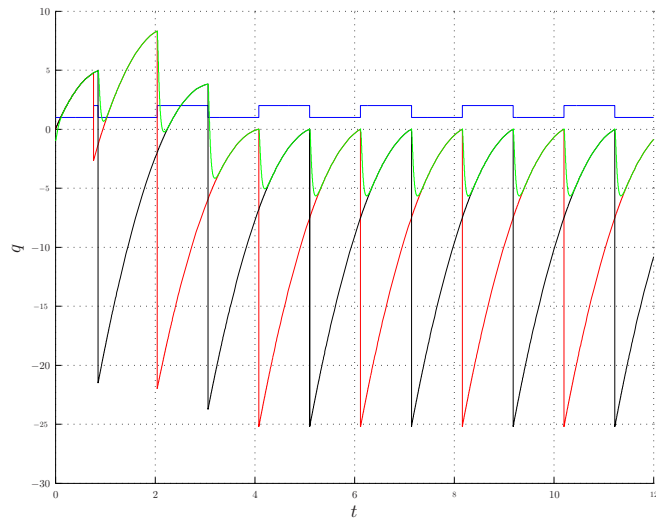


Figure 6.26. Simulation of the closed-loop system \mathcal{H}_r^M for two balls. The states z_{11}^q are plotted (bottom, second one with a large negative peak, $q = 1$; bottom, first one with a large negative peak, $q = 2$) along with the logic state $q \in \{1,2\}$. The tracking law switches reference after each bounce.

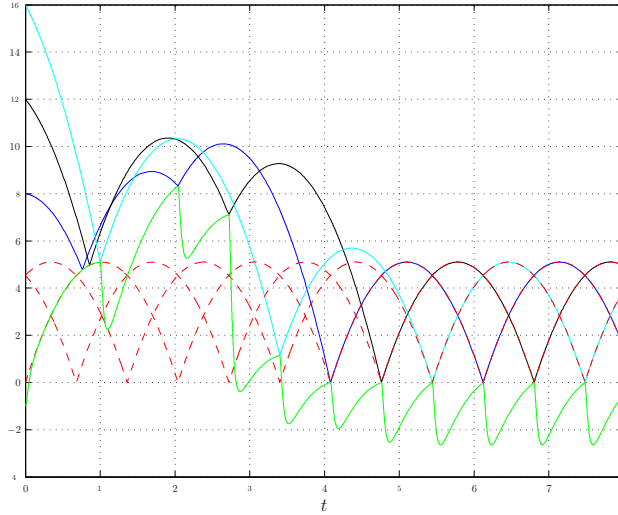


Figure 6.27. Simulation of the closed-loop system \mathcal{H}_r^M for three balls. System parameters: $m_1^1 = m_1^2 = m_1^3 = 1, m_2 = 9, e = 0.8, \gamma = 9.8$. Controller parameters: $\alpha = -9.8, k_1 = 2000, k_2 = 100$. For the given initial conditions, the trajectories approach their respective reference trajectories (in red, dashed) at their third bounce.

6.4 Summary

Hybrid control strategies for nonlinear and hybrid systems have been introduced. These accomplish particular tasks, treated as stabilization problems, globally (for the control strategies in Section 6.1 and 6.2) and robustly. Examples including numerical simulations illustrated the strategies.

6.5 Notes and references

For techniques to design the feedback laws in the obstacle avoidance problem in Section 6.1.1 using MPC see [57, 58, 101].

In the context of control, Carathéodory solutions for systems with discontinuous right-hand side have been considered in, for example, [3] and [8]. Control-related conditions on the right-hand side f that guarantee existence of Carathéodory solutions to (6.1) can be found in [3].

Control strategies for local and nominal stabilization of the pendubot appeared in the literature; these include energy pumping [35], trajectory tracking [51], and jerk control [1].

Other frameworks for modeling mechanical systems with impacts, in particular, juggling systems, different from the hybrid systems framework proposed in Section 6.3 include Poincaré map modeling [19, 104, 107, 94], dynamical systems with unilateral constraints [16, 107, 17], measure differential inclusions [72, 71], among others. Studies on juggling systems include the feedback control strategies in [107, 94, 80] for phase-lock stabilization to rhythmic patterns generated by a reference clock of one and two-dimensional juggling systems with only measurement of the ball state at impacts, and the open-loop strategies for the same stabilization task in [93, 78].

The model for juggling systems used in Section 6.3 for the one-degree of freedom juggler is applicable to the following more general juggling systems. Consider juggling systems with *plant* (for the one-degree of freedom juggler with one ball, the ball plays the role of the plant) given by

$$\dot{x}_1 = f_1(x_1) \tag{6.50}$$

where $x_1 = [x_{11} \ x_{12}]^T \in \mathbb{R}^{n_1}$ is the state, and *actuated robot* given by

$$\dot{x}_2 = f_2(x_2, u) \tag{6.51}$$

where $x_2 = [x_{21} \ x_{22}]^T \in \mathbb{R}^{n_2}$ is the state and $u \in \mathbb{R}^m$ is the input. The first components x_{11} and x_{21} of the states x_1 and x_2 correspond to the position state, and the second components x_{12} and x_{22} correspond to the velocity state of the plant and actuated robot, respectively. Define $x := [x_1 \ x_2]^T$ and $f(x, u) := [f_1(x_1) \ f_2(x_2, u)]^T$. The restitution law at impacts is modeled by the difference equations

$$x_1^+ = g_1(x), \quad x_2^+ = g_2(x). \tag{6.52}$$

Let $g(x) := [g_1(x) \ g_2(x)]^T$. The impacts between the plant and the actuated robot are assumed to occur when for a continuously differentiable function h , the state x and input u satisfy

$$h(x) = 0 \text{ and } \langle \nabla h(x), f(x, u) \rangle \leq 0. \tag{6.53}$$

Then, these juggling systems are given by the hybrid system

$$\left. \begin{aligned} \dot{x}_1 &= f_1(x_1) \\ \dot{x}_2 &= f_2(x_2, u) \end{aligned} \right\} h(x) \geq 0, \tag{6.54}$$

$$\left. \begin{aligned} x_1^+ &= g_1(x) \\ x_2^+ &= g_2(x) \end{aligned} \right\} \begin{aligned} &h(x) \leq 0 \text{ and} \\ &\langle \nabla h(x), f(x, u) \rangle \leq 0, \end{aligned} \tag{6.55}$$

where the right-hand side of the differential equations (the function f) and the state constraint in (6.54) define the *flow map* and *flow set*, respectively, and the right-hand sides of the difference equations (the function g) and the state constraints in (6.55) define the *jump map* and *jump set*, respectively. Extensions of the control strategy for the one-degree of freedom juggler to these systems is work under progress.

The remainder proofs of the results in this chapter can be found in Section B.4.

Chapter 7

Simulation Theory

7.1 Introduction

The theory of numerical simulation for differential equations is well-developed and several textbooks in the subject are available. The properties of integration schemes for differential equations are generally studied as dynamical systems. The analysis of stability and convergence of one-step integration schemes (like Euler and Runge-Kutta), multi-step algorithms (like Adams method and backward differentiation), and their variable step versions establishes conditions on the step size for integration and on the discrete map used to approximate the solutions of the system so that the simulations are close to the actual solutions. The ultimate goal in these numerical integration schemes is to reproduce with arbitrary precision the trajectories to the mathematical model under simulation. In other words, it is desired that the simulated solutions are close to the solutions to the actual model, and that this level of closeness can be adjusted with the integration step size of the numerical solver. Moreover, it is also desired that when the dynamical system to be simulated has an asymptotically stable set, the simulated model preserves that asymptotic stability in a practical sense. Results of this type, though currently not available for hybrid systems, can be found for differential equations and inclusions in the numerical analysis literature.

In this chapter, a *hybrid simulator model* for hybrid systems \mathcal{H} is proposed. Conditions on the data of the hybrid simulator are established to show the following sequence of results:

- 1) On compact hybrid time domains, every simulation to a hybrid system is arbitrarily close to a solution of the hybrid system;
- 2) Asymptotically stable compact sets for a hybrid system are semiglobally practically asymptotically stable compact sets for the hybrid simulator;
- 3) Asymptotically stable compact sets for the hybrid simulator are continuous in the step size s .

These conditions basically consist of a closeness property for the integration scheme that is used to simulate the flows of the hybrid system, plus additional conditions on inflations of the jump mapping and the jump and flow sets. To generate these results, jumps are not assumed to be “forced” when the trajectories hit the boundary of the jump set, sometimes considered as *forcing* or *triggering semantics*. Alternatively, trajectories are allowed to “enter” the jump set, sometimes referred to as *enabling semantics*.

7.2 Simulation model

Given a hybrid system $\mathcal{H} = (O, F, C, G, D)$, a *hybrid simulator for \mathcal{H}* will be given by the family of systems $\mathcal{H}_s = (O, F_s, C_s, G_s, D_s)$ parameterized by the step size $s > 0$, where

- $F_s : O \rightrightarrows \mathbb{R}^n$ is the integration scheme for the flows of \mathcal{H} ;
- $G_s : O \rightrightarrows \mathbb{R}^n$ is the jump mapping;
- C_s is a subset of the state space O where the integration scheme F_s is allowed;
- D_s is a subset of the state space O where the mapping G_s is allowed.

Following (2.1), the hybrid simulator \mathcal{H}_s can be written as

$$\mathcal{H}_s : \quad x \in O \quad \begin{cases} x^+ \in F_s(x) & x \in C_s \\ x^+ \in G_s(x) & x \in D_s . \end{cases} \quad (7.1)$$

Comparing (2.1) with (7.1), the dynamics for the continuous flows of the hybrid system \mathcal{H} have been replaced by the integration scheme $x^+ \in F_s(x)$, where F_s is constructed from F by a particular integration scheme (e.g. forward Euler, Runge-Kutta, etc.). The discrete dynamics of \mathcal{H} have been replaced by the discrete mapping G_s , and the flow and jump sets C and D by the sets C_s and D_s , respectively.

Note that the dynamics of the hybrid simulator \mathcal{H}_s are purely discrete. For that reason, the solutions to \mathcal{H}_s will be given on discrete versions of hybrid time domains.

Definition 7.1 (discrete time domain) *A subset $E \subset \mathbb{N} \times \mathbb{N}$ is a compact discrete time domain if*

$$E = \bigcup_{j=0}^{J-1} \bigcup_{k=K_j}^{K_{j+1}} (k, j)$$

for some finite sequence $0 = K_0 \leq K_1 \leq K_2 \dots \leq K_J$, $K_j \in \mathbb{N}$ for every $j \leq J$, $j \in \mathbb{N}$. It is a discrete time domain if for all $(K, J) \in E$, $E \cap (\{0, 1, \dots, K\} \times \{0, 1, \dots, J\})$ is a compact discrete time domain.

Solutions to \mathcal{H}_s are parameterized by the discrete variables j and k where k keeps track of the step of the integration scheme for flows and j counts the steps of the simulation.

Definition 7.2 (discrete arc) *A function $x_s : E \rightarrow \mathbb{R}^n$ is a discrete arc if E is a discrete time domain.*

Simulations to \mathcal{H} are defined as solutions to the hybrid simulator \mathcal{H}_s .

Definition 7.3 (simulation to \mathcal{H}) *A discrete arc $x_s : \text{dom } x_s \mapsto O$ is a simulation to the hybrid system \mathcal{H} with a hybrid simulator \mathcal{H}_s for a given $s > 0$ if $x_s(0, 0) \in C_s \cup D_s$, $x_s(k, j) \in O$ for all $(k, j) \in \text{dom } x_s$, and*

(S1') for all $k, j \in \mathbb{N}$ such that $(k, j), (k+1, j) \in \text{dom } x_s$,

$$x_s(k, j) \in C_s, \quad x_s(k+1, j) \in F_s(x_s(k, j)); \quad (7.2)$$

(S2') for all $k, j \in \mathbb{N}$ such that $(k, j), (k, j+1) \in \text{dom } x_s$,

$$x_s(k, j) \in D_s, \quad x_s(k, j+1) \in G_s(x_s(k, j)) . \quad (7.3)$$

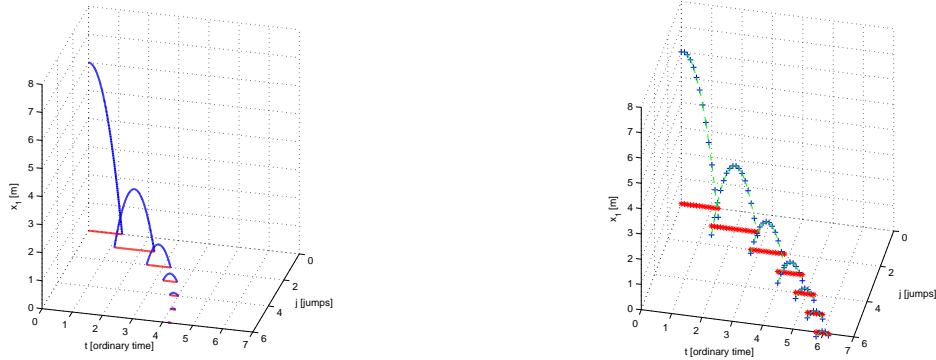


Figure 7.1. Solution and simulation to the bouncing ball model: (a) Solution for initial conditions $x_1(0,0) = 6\text{m}$, $x_2(0,0) = 0.1\text{m/s}$, constants $g = 9.8\text{m/s}^2$, $\gamma = 0.6$; position x_1 and hybrid time domain are plotted; (b) Simulation to the bouncing ball model with step size $s = 0.1\text{sec}$, initial conditions $x_1(0,0) = 6\text{m}$, $x_2(0,0) = 0.1\text{m/s}$, and constants $g = 9.8\text{m/s}^2$, $\gamma = 0.6$; discrete arc x_s denoted with +, hybrid arc ξ_s denoted with --, and discrete domain denoted with *.

One way to translate a simulation x_s on the discrete time domain $\text{dom } x_s$ to a hybrid arc ξ_s on a hybrid time domain $\text{dom } \xi_s$ is by piecewise linear interpolation of the flows:

- for every (t, j) such that $(k, j), (k+1, j) \in \text{dom } x_s$, $ks \leq t \leq (k+1)s$,

$$\begin{aligned} \xi_s(t, j) &= x_s(k, j) + \frac{1}{s}(t - ks)(x_s(k+1, j) - x_s(k, j)), \\ t_j &= ks, \quad t_{j+1} = (k+1)s; \end{aligned} \quad (7.4)$$

- for every (t, j) such that $(k, j), (k, j+1) \in \text{dom } x_s$, $t = ks$,

$$\xi_s(t, j) = x_s(k, j), \quad t_j = t_{j+1} = ks; \quad (7.5)$$

- $J = \sup_{(k,j) \in \text{dom } x_s} j$ and the hybrid time domain $\text{dom } \xi_s$ is the union of a finite or infinite sequence of intervals $[t_j, t_{j+1}] \times \{j\}$, $j \in \{0, 1, \dots, J\}$ with the “last” interval possibly of the form $[t_j, +\infty) \times \{j\}$.

To illustrate the transformation of a simulation x_s into a hybrid arc ξ_s , consider the model for a bouncing ball. A solution x starting at $x_1(0,0), x_2(0,0) > 0$ on a hybrid time domain is depicted in Figure 7.1(a). Taking $s = 0.2\text{sec}$ and using the forward Euler scheme for the flows, a simulation x_s to the bouncing ball with $x_s(0,0) = x(0,0)$ and its discrete domain are shown in Figure 7.1(b) along with its respective hybrid arc ξ_s .

7.3 From hybrid to discrete

The hybrid simulator model proposed above suggests a discretization of the data of \mathcal{H} . Such operation has to be done so that the solutions of the simulator \mathcal{H}_s and of the hybrid system \mathcal{H} are “close” on compact hybrid time domains defined by the simulation horizon. The following assumption establishes conditions on (O, F_s, C_s, G_s, D_s) in terms of (O, F, C, G, D) for that purpose.

Below, given a sequence of sets $\{S_i\}_{i=1}^\infty$, each S_i subset of \mathbb{R}^n , its *outer limit*, denoted by $\limsup_{i \rightarrow \infty} S_i$, is the set of all points $x \in \mathbb{R}^n$ for which there exists a subsequence $\{S_{i_k}\}_{k=1}^\infty$ and points $x_{i_k} \in S_{i_k}$, $k = 1, 2, \dots$ such that $x_{i_k} \rightarrow x$.

Assumption 7.4 (hybrid simulator data) *The data of the hybrid simulator $\mathcal{H}_s = (O, F_s, C_s, G_s, D_s)$ for the hybrid system $\mathcal{H} = (O, F, C, G, D)$ satisfies*

(R1) F_s implements a specific integration algorithm and is such that, for each compact set $\mathcal{K} \subset O$, there exists $\rho \in \mathcal{K}_\infty$ such that for each $x \in C_s \cap \mathcal{K}$ and each $s > 0$

$$F_s(x) \subset x + s\rho(s)\mathbb{B} + s\overline{\text{co}}F(x + \rho(s)\mathbb{B});$$

(R2) G_s is such that $G_0(x) \subset G(x)$ where G_0 is the outer graphical limit of G_{s_i} , for any $s_i \searrow 0$;

(R3) C_s and D_s are such that for any sequence $s_i \searrow 0$,

$$\left(\limsup_{i \rightarrow \infty} C_{s_i} \right) \cap O \subset C, \quad \left(\limsup_{i \rightarrow \infty} D_{s_i} \right) \cap O \subset D$$

where $\limsup_{i \rightarrow \infty} C_{s_i}$ and $\limsup_{i \rightarrow \infty} D_{s_i}$ are the outer limits of the sequence of sets C_{s_i} and D_{s_i} , respectively.

Assumption (R1) is a condition on the integrator scheme for flows. It implies that, given a compact set $\mathcal{K} \subset \mathbb{R}^n$, at every point in $C_s \cap \mathcal{K}$ where the integration scheme is active, the new value is close to a perturbed solution to $\dot{x} \in F(x)$. When simulating a hybrid system, the projection function is required since there is no guarantee that the integration step s keeps the simulations in $C_s \cup D_s$, even if it keeps them in O . For Assumption (R2) recall that G_0 is the outer graphical limit of G_{s_i} when $\text{gph } G_0 = \limsup_{i \rightarrow \infty} \text{gph } G_{s_i}$ and G_{s_i} is locally eventually bounded with respect to O (for a definition of locally eventually bounded, see Section 3.4). Assumption (R3) is a condition on the inflation by s of the flow and jump sets. Both conditions (R2) and (R3) are satisfied when G_s, C_s , and D_s are outer perturbations of G, C , and D , respectively. More precisely, given a continuous function $\alpha : O \rightarrow \mathbb{R}_{\geq 0}$ such that, for all $x \in O$, $x + \alpha(x)\mathbb{B} \subset O$, the outer perturbation of G, C , and D for $\delta \in (0, 1)$ is given by the set-valued mapping G_δ and sets C_δ, D_δ defined by

$$\begin{aligned} G_\delta &:= \{y \mid y \in \eta + \delta\alpha(\eta)\mathbb{B}, \eta \in G(x + \delta\alpha(x)\mathbb{B})\} \\ C_\delta &:= \{x \in O \mid (x + \delta\alpha(x)\mathbb{B}) \cap C \neq \emptyset\} \\ D_\delta &:= \{x \in O \mid (x + \delta\alpha(x)\mathbb{B}) \cap D \neq \emptyset\} \end{aligned}$$

which satisfy (R2)-(R3). However, very often, when simulating hybrid systems the jump mapping G and the sets C and D are such that it is sufficient to choose $G_s \equiv G$, $C_s = C$, and $D_s = D$ (this is a reasonable situation when G, C , and D are known precisely).

Example 7.5 (forward Euler method) The simplest numerical method to approximate solutions to differential equations/inclusions is the forward Euler rule. This method is based on the first-order Taylor's expansion of the continuous right-hand side around $x \in \mathbb{R}^n$ and is given by

$$F_s^E(x) = x + sF(x) .$$

Condition (R1) is automatically satisfied. □

Example 7.6 (p -stage Runge-Kutta consistent methods) For differential inclusions (or equations) $\dot{x} \in F(x)$ with locally bounded $F : \mathbb{R}^n \rightrightarrows \mathbb{R}^n$, the update law for p -stage Runge-Kutta integration schemes, $p \geq 1$, is given by

$$F_s^{RK}(x) = x + s \sum_{i=1}^p b_i \xi_i \quad (7.6)$$

where $b_i \in \mathbb{R}$ and $\xi_i \in F(Y_i)$, $i \in I := \{1, 2, \dots, p\}$. The variables Y_i are called *stage variables* and are given by

$$Y_i = x + s \sum_{j=1}^p a_{ij} \xi_j, \quad \xi_j \in F(Y_j) \quad (7.7)$$

where $a_{ij} \in \mathbb{R}$, $(i, j) \in I \times I$. (When $a_{ij} = 0$ for all $j \geq i$, the method is called *explicit* since the stage variables can be solved without recursion.)

Provided that the equations (7.7) are solvable, either in a explicit or implicit manner, for every compact set $\mathcal{K} \subset \mathbb{R}^n$ there exists $\rho \in \mathcal{K}_\infty$ such that the stage variables satisfy

$$Y_i \in x + s\rho(s) \quad \forall i \in I .$$

Moreover, when the Runge-Kutta method is consistent, the coefficients b_i satisfy

$$\sum_{i=1}^p b_i = 1 . \quad (7.8)$$

Then, the sum in (7.6) corresponds to a convex hull condition and Assumption (R1) is satisfied since

$$F_s^{RK}(x) \subset x + s \operatorname{co}_{i \in I} F(Y_i) \subset x + s \operatorname{co} F(x + \rho(s)) .$$

□

7.4 Closeness and continuity properties

The hybrid simulator $\mathcal{H}_s = (O, F_s, C_s, G_s, D_s)$ is considered as a perturbation of the hybrid system $\mathcal{H} = (O, F, C, G, D)$. The following result exploits this idea to show that for a given simulation horizon (T, J) , by a proper choice of the step size, every simulation to the hybrid system is close in the graphical sense to some solution of the hybrid system with a desired level of closeness.

Theorem 7.7 (closeness on compact domains) *Assume that \mathcal{H} satisfies the hybrid basic conditions and that, for some compact set $K \subset O$, it is forward complete at every $x^0 \in K$. Assume that the family of hybrid systems \mathcal{H}_s satisfies Assumption 7.4. Then, for any $\varepsilon > 0$ and any simulation horizon $(T, J) \in \mathbb{R}_{\geq 0} \times \mathbb{N}$ there exists $s^* > 0$ with the following property: for any $s \in (0, s^*]$ and any simulation x_s to \mathcal{H}_s with $x_s(0, 0) = x_s^0 \in (K + \varepsilon \mathbb{B}) \cap O$ there exists a solution x to \mathcal{H} with $x(0, 0) \in K$ such that for all $(k, j) \in \operatorname{dom} x_s$ with $ks \leq T$, $j \leq J$, there exists m such that $(m, j) \in \operatorname{dom} x$, $|ks - m| \leq \varepsilon$, and*

$$|x_s(k, j) - x(m, j)| \leq \varepsilon . \quad (7.9)$$

Proof. Let $\varepsilon > 0$ and a simulation horizon $(T, J) \in \mathbb{R}_{\geq 0} \times \mathbb{N}$ be given. Let $\operatorname{reach}_{(T, J)}^{\mathcal{H}_s}(\mathcal{K})$ be the finite-time (up to (T, J)) reachable set of \mathcal{H}_s from the compact set \mathcal{K} , i.e.,

$$\operatorname{reach}_{(T, J)}^{\mathcal{H}_s}(\mathcal{K}) := \{x_s(k, j) | x_s \text{ is a simulation to } \mathcal{H}_s, x_s(0, 0) \in \mathcal{K}, (k, j) \in \operatorname{dom} x_s, ks \leq T, j \leq J\} .$$

By Definition 7.3, any simulation $x_s : \text{dom } x_s \rightarrow O$ to \mathcal{H} , $\text{dom } x_s \subset [0, T] \times \{0, \dots, J\}$, satisfies (S1_s) and (S2_s), and can be extended to a hybrid arc $\xi_s : \text{dom } \xi_s \rightarrow O$ on a hybrid time domain $\text{dom } \xi_s$ constructed as in (7.4)-(7.5). Note that for each $(t, j) \in \text{dom } \xi_s$ such that $(k, j), (k+1, j) \in \text{dom } \xi_s$, $ks \leq t \leq (k+1)s$, by (R1) in Assumption 7.4 we have that

$$|\xi_s(ks, j) - \xi_s(t, j)| \leq |x_s(k, j) - x_s(k+1, j)| \leq s\delta'(s) \quad (7.10)$$

where

$$\delta'(s) := \max_{\eta \in \text{reach}_{(T, J)}^{\mathcal{K}}(\mathcal{K}) \cap C_s} \text{co } F((\eta + \rho(s)\mathbb{B}) \cap O) + \rho(s)\mathbb{B}.$$

Then, using (R1) in Assumption 7.4 and (7.10), for every $(t, j) \in \text{dom } \xi_s$ so that $(k, j), (k+1, j) \in \text{dom } x_s$, $ks \leq t \leq (k+1)s$, ξ_s satisfies

$$\begin{aligned} \dot{\xi}_s(t, j) &= \frac{x_s(k+1, j) - x_s(k, j)}{s} \in \text{co } F((\xi_s(ks, j) + \rho(s)\mathbb{B}) \cap O) + \rho(s)\mathbb{B} \\ \Rightarrow \quad \dot{\xi}_s(t, j) &\in \overline{\text{co}}F((\xi_s(t, j) + (s\delta'(s) + \rho(s))\mathbb{B}) \cap O) + (s\delta'(s) + \rho(s))\mathbb{B} \end{aligned}$$

and

$$\xi_s(t, j) \in \{x \in O \mid (x + s\delta'(s)\mathbb{B}) \cap C_s \neq \emptyset\}.$$

By construction of ξ_s , for every (t, j) so that $(k, j), (k, j+1) \in \text{dom } x_s$, $t = ks$,

$$\xi_s(t, j) \in D_s, \quad \xi_s(t, j+1) \in G_s(\xi_s(t, j)).$$

Given $\delta > 0$ pick $s > 0$ such that $s\delta'(s) + \rho(s) \leq \delta$. Define

$$\begin{aligned} F_\delta(x) &:= \overline{\text{co}}F((x + \delta\mathbb{B}) \cap O) + \delta\mathbb{B}, & G_\delta(x) &:= G_{s(\delta)}(x), \\ C_\delta &:= \{x \in O \mid (x + \delta\mathbb{B}) \cap C_{s(\delta)} \neq \emptyset\}, & D_\delta &:= D_{s(\delta)} \end{aligned}$$

where the dependence of s on δ is explicitly indicated. In fact, s approaches zero as $\delta \rightarrow 0$.

From the properties of ξ_s above, hybrid arcs ξ_s obtained from simulations x_s to \mathcal{H} are solutions to the perturbed hybrid system $\mathcal{H}_\delta := (O, F_\delta, C_\delta, G_\delta, D_\delta)$. For any arbitrary sequence $\{\delta_i\}_{i=1}^\infty$ with $1 > \delta_1 > \delta_2 > \dots > 0$ converging to zero, sequences $C_i = C_{\delta_i}$, $D_i = D_{\delta_i}$, $F_i = F_{\delta_i}$, $G_i = G_{\delta_i}$ satisfy assumptions (C1), (C2), (C3), and (C4) in [39, Section 5]. Assumption 7.4 automatically implies that C_i, D_i , and G_i satisfy (C1), (C2), (C3), and (C4). The proof that F_i satisfies (C2) and (C3) can be found in Lemma 5.4 in [39] which follows by the fact that F_i is an outer perturbation of F .

It follows that using the techniques in [22], a version of Corollary 5.5 in [39] without completeness assumptions holds. Then, given $\varepsilon > 0$ there exists $\delta^* > 0$ such that for each $\delta \in (0, \delta^*]$, each $s > 0$ such that $s\delta'(s) + \rho(s) \leq \delta$, and each solution to \mathcal{H}_δ starting from $\mathcal{K} + \delta\mathbb{B}$, in particular, every hybrid arc ξ_s obtained from a simulation x_s , $\text{dom } x_s \subset [0, T] \times \{0, \dots, J\}$, there exists a solution x to \mathcal{H} with $x(0, 0) \in \mathcal{K}$ such that for every $(k, j) \in \text{dom } x_s$ with $ks \leq T$, $j \leq J$, there exists m such that $(m, j) \in \text{dom } x$, $|ks - m| \leq \varepsilon$, $|x_s(k, j) - x(m, j)| \leq \varepsilon$. To finish the proof, let $s^* > 0$ be the maximum s satisfying $s\delta'(s) + \rho(s) \leq \delta^*$. \square

When a hybrid system \mathcal{H} has an asymptotically stable compact set \mathcal{A} , the hybrid simulator \mathcal{H}_s has the same set semiglobally practically asymptotically stable.

Theorem 7.8 (practical semiglobal stability of simulations) *Suppose that $\mathcal{H} = (O, F, C, G, D)$ satisfies the hybrid basic conditions and that \mathcal{A} is an asymptotically stable compact set with basin of attraction $\mathcal{B}_\mathcal{A}$ open*

relative to $C \cup D$. Let $U \subset O$ be any open set such that $\mathcal{B}_A = (C \cup D) \cap U$. Assume that the family of hybrid systems $\mathcal{H}_s = (O, F_s, C_s, G_s, D_s)$ satisfies Assumption 7.4. Then, the set \mathcal{A} is semiglobally practically asymptotically stable for \mathcal{H}_s , i.e., for each proper indicator $\omega : U \rightarrow \mathbb{R}_{\geq 0}$ of \mathcal{A} with respect to U , each compact set $K \subset \mathcal{B}_A$, and each $\varepsilon > 0$ there exists $\beta \in \mathcal{KLL}$ and $s^* > 0$ such that for each $s \in (0, s^*]$ every simulation x_s to \mathcal{H} starting from K satisfies, for each $(k, j) \in \text{dom } x_s$,

$$\omega(x_s(k, j)) \leq \beta(\omega(x_s(0, 0)), ks, j) + \varepsilon. \quad (7.11)$$

Proof. It follows that using the techniques in [22], a version of Theorem B.14 without completeness assumptions holds. Then, for each proper indicator $\omega : U \rightarrow \mathbb{R}_{\geq 0}$ of \mathcal{A} with respect to U there exists $\beta \in \mathcal{KLL}$ such that for each solution x to \mathcal{H} with $x(0, 0) \in \mathcal{B}_A$, for all $(t, j) \in \text{dom } x$,

$$\omega(x(t, j)) \leq \beta(\omega(x(0, 0)), t, j).$$

By Assumption 7.4, we proceed as in Theorem 7.7 to construct a perturbed hybrid system \mathcal{H}_δ such that every hybrid arc ξ_s obtained from a simulation x_s to \mathcal{H} is a solution to it. By construction, \mathcal{H}_δ satisfies (C1), (C2), (C3), and (C4) in [39, Section 5]. Then, by Theorem B.15, for each compact set $\mathcal{K} \subset \mathcal{B}_A$ and each $\varepsilon > 0$ there exists $\delta^* > 0$ such that for each $\delta \in (0, \delta^*]$, $s > 0$ such that $s\delta'(s) + \rho(s) \leq \delta$, every hybrid arc ξ_s obtained from a simulation x_s starting from \mathcal{K} satisfies, for all $(t, j) \in \text{dom } \xi_s$,

$$\omega(\xi_s(t, j)) \leq \beta(\omega(\xi_s(0, 0)), t, j) + \varepsilon.$$

Let $s^* > 0$ be the largest s that satisfies $s\delta'(s) + \rho(s) \leq \delta$. Hence, by the construction of ξ_s from x_s , (7.11) holds. \square

Theorem 7.8 implies that simulations starting from K with unbounded discrete time domain approach the compact set $\mathcal{A}_\varepsilon := \{x \in O \mid \omega(x) \leq \varepsilon\}$. This property holds for small enough step size s . Clearly, as the desired level of closeness to \mathcal{A} which is given by ε decreases, the required step size s decreases as well.

In order to guarantee that simulations exist for arbitrarily large simulation horizon as required in the definition of asymptotic stability in Definition 4.1, we strengthen assumptions (R1) and (R2) in Assumption 7.4 as follows.

Assumption 7.9 (conditions on \mathcal{H}_s for completeness)

The data of the hybrid simulator $\mathcal{H}_s = (O, F_s, C_s, G_s, D_s)$ for the hybrid system $\mathcal{H} = (O, F, C, G, D)$ satisfies the following conditions: for each compact set $K \subset O$ there exists $s^* > 0$ such that for all $s \in (0, s^*]$

(R1_c) $F_s(C_s \cap K) \subset C_s \cup D_s$ and for each $x \in C_s \cap K$, $F_s(x) \neq \emptyset$;

(R2_c) $G_s(D_s \cap K) \subset C_s \cup D_s$ and for each $x \in D_s \cap K$, $G_s(x) \neq \emptyset$.

Theorem 7.10 (continuity of asymptotically stable sets) *Let Assumption 7.4 and 7.9 hold. Suppose that the hybrid system $\mathcal{H} = (O, F, C, G, D)$ satisfies the hybrid basic conditions and that \mathcal{A} is an asymptotically stable compact set with basin of attraction \mathcal{B}_A which is open relative to $C \cup D$. Then, there exists s^* such that for all $s \in (0, s^*]$, the hybrid simulator \mathcal{H}_s has an asymptotically stable set \mathcal{A}_s which satisfies*

$$d_H(\mathcal{A}_s, \mathcal{A}) \rightarrow 0 \quad \text{as } s \searrow 0. \quad (7.12)$$

Proof. Let \mathcal{K} be any compact set such that for some $\varepsilon^* > 0$, $\mathcal{A} + \varepsilon^* \mathbb{B} \subset \mathcal{K} \subset O$. Let $\beta \in \mathcal{KLL}$ and $s^* > 0$ come from Theorem 7.8 with \mathcal{K} , $\varepsilon \in (0, \varepsilon^*]$, and $\omega(\cdot) = |\cdot|_{\mathcal{A}}$. Using Assumption 7.9, redefine s^* above so that (R1_c)

and (R2_c) hold. Then, every simulation to \mathcal{H} starting from \mathcal{K} exists for arbitrarily large simulation horizon (T, J) .

By Assumption 7.4, we proceed as in Theorem 7.7 to construct a perturbed hybrid system \mathcal{H}_δ such that every hybrid arc ξ_s obtained from a simulation x_s to \mathcal{H} is a solution to it. By construction, \mathcal{H}_δ satisfies (C1), (C2), (C3), and (C4) in [39, Section 5]. Let

$$B_\varepsilon := \overline{\text{reach}^{\mathcal{H}_\delta}(\mathcal{A} + 2\varepsilon\mathbb{B})}$$

where $\text{reach}^{\mathcal{H}_\delta}(\mathcal{A} + 2\varepsilon\mathbb{B})$ is the reachable set of \mathcal{H}_δ from $\mathcal{A} + 2\varepsilon\mathbb{B}$, i.e.,

$$\text{reach}^{\mathcal{H}_\delta}(\mathcal{A} + 2\varepsilon\mathbb{B}) := \{\xi(t, j) \mid \xi \text{ is a solution to } \in \mathcal{H}_\delta, \xi_s(0, 0) \in (\mathcal{A} + 2\varepsilon\mathbb{B})\} .$$

By Theorem 7.8, B_ε is bounded. Since B_ε is closed by definition, it follows that it is compact. We now show that it is forward invariant. Let $\tilde{\xi}^0 \in B_\varepsilon$ and let $\tilde{\xi}$ be a solution to \mathcal{H}_δ from $\tilde{\xi}^0$. Suppose that there exists $(t', j') \in \text{dom}\tilde{\xi}$ for which $\tilde{\xi}(t', j') \notin B_\varepsilon$. By definition of B_ε , since $\tilde{\xi}^0 \in B_\varepsilon$, the solution $\tilde{\xi}$ belongs to B_ε for all $(t, j) \in \text{dom}\tilde{\xi}$. This is a contradiction. Then, B_ε is forward invariant. To show that solutions to \mathcal{H}_δ starting from \mathcal{K} converge to B_ε uniformly, note that, Theorem 7.8 implies that there exists $N > 0$ such that for every solution ξ to \mathcal{H}_δ with $\xi(0, 0) \in \mathcal{K}$, we have

$$|\xi(t, j)|_{\mathcal{A}} \leq \beta(|\xi(0, 0)|_{\mathcal{A}}, t, j) + \varepsilon \leq 2\varepsilon \quad (7.13)$$

for all $(t, j) \in \text{dom}\xi$, $t + j \geq N$, for large enough simulation horizon. Then, since B_ε is compact, forward invariant, and uniformly attractive from \mathcal{K} , by Proposition 6.2 in [39], B_ε is an asymptotically stable set for \mathcal{H}_δ . Hence, it is an asymptotically stable set for \mathcal{H}_s .

Finally, note that $B_0 = \overline{\text{reach}^{\mathcal{H}_\delta}(\mathcal{A})} = \mathcal{A}$ and that as $\varepsilon \searrow 0$, $d_H(B_\varepsilon, B_0) \rightarrow 0$. Then, since ε and s are related through Theorem 7.8 and are such that $s \searrow 0$ as $\varepsilon \searrow 0$, with some abuse of notation, the claim holds with $\mathcal{A}_s = B_\varepsilon$. \square

7.4.1 Numerical example

Consider the bouncing ball example in Section 2.2.1 with regular data which, for convenience, is rewritten below:

$$O := \mathbb{R}^2, f(x) := \begin{bmatrix} x_2 \\ -g \end{bmatrix}, C := \{x \in \mathbb{R}^2 \mid x_1 \geq 0\} \quad (7.14)$$

$$g(x) := \begin{bmatrix} x_1 \\ -\lambda x_2 \end{bmatrix}, D := \{x \in \mathbb{R}^2 \mid x_1 = 0, x_2 \leq 0\} \quad (7.15)$$

where $g > 0$ is the gravity constant and $\lambda \in [0, 1)$ is the restitution coefficient. Denote this system by \mathcal{H}^{BB} .

A hybrid simulator for the bouncing ball system is given by

$$\begin{aligned} f_s(x) &= x + sf(x), & C_s &= C, \\ g_s(x) &= g(x), & D_s &= \{x \in O \mid -\alpha(s)|x_2| \leq x_1 \leq 0, x_2 \leq 0\}, \end{aligned}$$

where $s > 0$ is the integration step for the integration scheme for flows and $\alpha : \mathbb{R}_{\geq 0} \rightarrow \mathbb{R}_{\geq 0}$ is a continuous function satisfying $\alpha(s) > s$ for all $s > 0$, $\alpha(0) = 0$. Note that $\mathcal{H}_s = (O, f_s, C_s, g_s, D_s)$ satisfies Assumption 7.4. Note that one of the perturbations included is due to the integration scheme for the flows which is implemented as a forward Euler rule. Moreover, the jump set D is perturbed in order to satisfy Assumption 7.9 and consequently, guarantee that simulations to the bouncing ball starting in $C \cup D$ exist for all simulation horizon.

The bouncing ball example is appropriate to illustrate that simulations to \mathcal{H}^{BB} are close to some solution to \mathcal{H}^{BB} (Theorem 7.7) since its solutions can be analytically computed. Given a finite simulation horizon (T, J) , a level of closeness ε , and a compact set $K \subset \mathbb{R}^2$ of initial conditions, there exists s^* so that for each $0 < s \leq s^*$ the simulations x_s to \mathcal{H}^{BB} are ε -close to solution to \mathcal{H}^{BB} . The solution to which each simulation is close to is uniquely defined since \mathcal{H}^{BB} has unique solutions. In Figure 7.2, the first component of a solution x and the first component of a simulation x_s to \mathcal{H}^{BB} are plotted in a compact domain and for a particular step size s . It is clear to see that the level of closeness can only be satisfied on compact time domains. In Figure 7.3 a zoomed in version of the trajectories is shown to indicate that at points $(k, j) \in \text{dom } x_s$ (denoted by \circ) for which $x_s(k, j)$ enters the set D_s closeness between x and x_s is not possible for the same hybrid time (k, j) . The desired level of closeness is obtained by considering the distance between graphs of x and x_s .

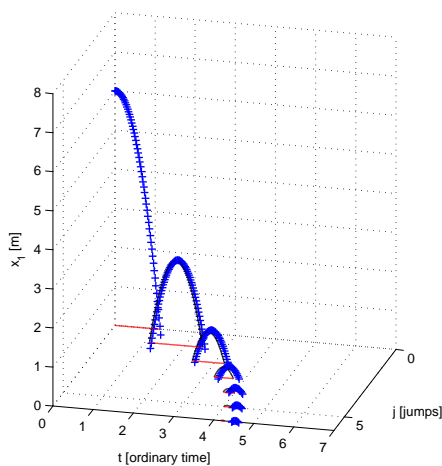


Figure 7.2. Closeness of simulations to solutions. Step size $s = 0.02\text{sec}$, $\alpha(s) = 2s$, initial conditions $x_1(0, 0) = 6\text{m}$, $x_2(0, 0) = 0.1\text{m/s}$, constants $g = 9.8\text{m/s}^2$, $\lambda = 0.6$. Discrete arc x_s denoted with $+$, exact hybrid arc solution x denoted with solid line and exact hybrid time domain with solid line (floor). The graphs of the simulation and of the solution are close until some finite hybrid time (T', J') . The closeness property can be tuned with the step size s .

It can be shown with invariance principles for hybrid systems, like the ones in [87], that the compact set $\mathcal{A} = (0, 0)$ is a globally asymptotically stable set for \mathcal{H}^{BB} . By Theorem 7.8, the set \mathcal{A} is semiglobally practically asymptotically stable for \mathcal{H}_s^{BB} . Provided a desired neighborhood of \mathcal{A} for the convergence of the simulations, it is possible to obtain an upper bound on the sampling time s so that simulations to \mathcal{H}^{BB} approach $\mathcal{A} + \varepsilon\mathbb{B}$ for large enough simulation horizon.

The bouncing ball example illustrates the closeness between the graph of the simulation and the graph of the exact solution to the bouncing ball. As stated in the results above, this closeness property is on compact hybrid/discrete time domains. As a matter of fact, the hybrid simulator is able to approximate the Zeno trajectories to the bouncing ball with arbitrary precision for any finite simulation horizon (finite flow time and number of jumps) by choosing sufficiently small step size. In general, simulations obtained on finite simulation horizons have the closeness property to some exact solution by virtue of a proper choice of the step size. Note that the hybrid simulator model does not require event/zero-cross detection algorithms to trigger the jumps. The jumps are detected by only checking whether the simulation has reached the jump set D_s or not. The step

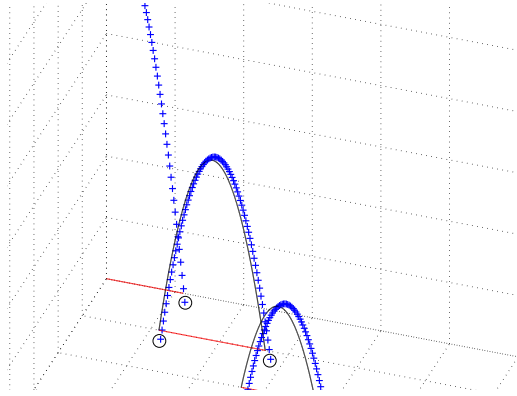


Figure 7.3. Detail on closeness of solutions. The circled points of simulation x_s are not close in the “standard” sense to the exact solution x . The closeness property is between the graphs of x_s and x .

size required to detect jumps is expected to be small when the jump set D , and consequently its approximation D_s , are very thin. Indeed, in the limiting case when those sets have measure zero, no matter how small the step size is chosen, the hybrid simulator may not detect the jump. However, in this case, there will exist a solution to the hybrid system (solutions will be non unique) that does not jump when the jump set is reached (cf. Example 3.3). This is the solution that is close to the simulation that did not jump when the jump was not detected. Note that the usage of some type of detection algorithm for the jumps would prevent this from happening, but at the same time, alters the hybrid system \mathcal{H} under simulation.

7.5 Summary

A general model for simulations of hybrid systems \mathcal{H} , referred to as a *hybrid simulator for \mathcal{H}* and denoted by \mathcal{H}_s , was proposed. Solutions to \mathcal{H}_s are simulations to \mathcal{H} and are given by discrete arcs on discrete time domains satisfying certain conditions given by the data (O, F_s, C_s, G_s, D_s) and the step size s of the hybrid simulator. Closeness and stability properties of the hybrid simulator \mathcal{H}_s related to the hybrid system \mathcal{H} are shown and illustrated in a numerical example.

7.6 Notes and references

For more details about integration rules see [5, Chapter 3], [33, Chapter 2]. Consistency of these methods is defined in [96, Definition 3.4.2]. Condition (7.8) is usually required for stability of the Runge-Kutta integration method, see [50] and [41].)

The forward Euler integration scheme used in the example in Section 7.4.1 has been used to simulate the continuous dynamics of hybrid systems in the literature before, see e.g. [64, 73].

The simulations of the bouncing ball in Section 7.4.1 were coded in Matlab/Simulink. The simulation algorithm executes the discrete events of the hybrid simulator model \mathcal{H}_s^{BB} . Since the integration rule employed was the forward Euler, it was not necessary to use any of the integration schemes available in the software. However, the simulations of the hybrid systems in previous chapters were implemented in Matlab/Simulink with a technique that is described in Appendix A.

Chapter 8

Conclusion

In this thesis, a dynamical systems approach to modeling, analysis, and design of hybrid systems was pursued from a robust stability point of view. A summary of the contents of this document and several future research thrusts emerging from this thesis are the focus of this chapter.

8.1 Summary

A general modeling framework for hybrid control systems was introduced in Chapter 2. Hybrid systems were modeled by *hybrid equations* with a state space, a flow map (given by a single-valued function or a set-valued mapping), a flow set, a jump map (given by a single-valued function or a set-valued mapping), and a jump set. Solutions were defined as hybrid arcs and parametrized both by flow time t and jump time j on hybrid time domains, which are subsets of $\mathbb{R}_{\geq 0} \times \mathbb{N}$. Several examples were presented to illustrate the modeling framework.

In Chapter 3, it was shown that the robustness properties of hybrid systems are very sensitive to the properties of the data defining the hybrid equations. Several examples illustrated the effect of this perturbation in the system behavior. Mild conditions on these objects, the hybrid basic conditions, were motivated and shown to capture the effect of arbitrarily small state perturbations in the nominal set of solutions of what we called a regularized hybrid system. The regularization procedure and the solutions to the resulting regularized system followed the regularization and solution notion introduced by Krasovskii in [55].

Structural properties of solutions guaranteed by the hybrid basic conditions allowed the development of the stability and invariance results in Chapter 4. Stability and convergence tools for hybrid systems \mathcal{H} presented include hybrid versions of the classical Lyapunov stability theorem and of LaSalle's invariance principle. Special cases of these results, and more general invariance principles and their connections to detectability were also derived. The application of these tools were illustrated in several examples.

In Chapter 5, robustness of asymptotic stability for classes of closed-loop systems resulting from hybrid control was established. Results for perturbations arising from the presence of measurement noise, unmodeled sensor and actuator dynamics, control smoothing, and sample-and-hold devices were derived. These results guarantee that, for small enough perturbations, nominally asymptotically stable compact sets (or points) are semiglobally practically asymptotically stable. The problem of globally stabilizing the one-link pendulum on a cart to the upright condition was used as benchmark to test the robustness properties of the hybrid control strategies proposed.

Several engineering control applications were studied in Chapter 6. The problem of robustness in stabiliza-

tion of nonlinear systems with certain topological structure was investigated. A general nonrobustness result for such problems and a hybrid controller featuring hysteresis were given. The hybrid control guarantees robust, global asymptotic stability. These results were illustrated in autonomous vehicle control problems like that of steering a vehicle to a disconnected set of points and to a target with obstacle avoidance. In a subsequent section, a novel hybrid control strategy combining local state-feedback and open-loop laws for robust, global stabilization of nonlinear systems was introduced. A decision-making algorithm was implemented in a hybrid controller by combining logic variables and timers. The problem of stabilizing the trajectories to the pendubot system to the upright configuration was used to illustrate the design procedure and functionality. Finally, a tracking control strategy for a class of juggling systems was presented and developed for the problem of juggling multiple balls with a single actuator. The proposed control algorithm provides finite-time practical tracking of reference trajectories.

A general model for simulation of hybrid systems was introduced in Chapter 7. Solutions to the hybrid simulator were given by discrete arcs on discrete time domains satisfying certain conditions given by the data and the step size of the hybrid simulator. The main properties of the hybrid simulator consist of a closeness property between solutions and simulations on compact time domains, and practical semiglobal asymptotic stability and upper semicontinuity of compact sets that are asymptotically stable for the original hybrid system. A numerical example about the simulation of a bouncing ball system was given.

These results are currently being compiled into a textbook on hybrid dynamical systems. Other results that were not included in this thesis are the hybrid control strategy for a class of nonlinear systems that renders the closed-loop system uniformly input-to-state stable with respect to measurement noise in [92], the hybrid control algorithm with hysteresis for robust contact detection and force regulation of robotic manipulators in [24], and the hybrid control methodology for the problem of commanding autonomous vehicles to locate a radiation source using only measurements of the radiation strength in [68].

8.2 Future directions

The following research directions arise from the results in this thesis.

- **Control of hybrid system with inputs:** The stability results and invariance principles for “closed” systems (that is, systems without inputs) in Chapter 4 can be used to develop tools for analysis and design of “open” hybrid systems (that is, hybrid systems with inputs). The concept of “control-Lyapunov function” and related control design methods for classical nonlinear systems can be generalized to the hybrid setting. This will lead to new tools for systematic design of hybrid and non-hybrid control algorithms for hybrid systems with inputs. The coupling between the control inputs and the flow/jump sets, which is present in the general input case, is one of the challenges in Lyapunov design of control laws for hybrid systems with inputs.
- **Singular perturbation analysis:** The results in Chapter 5 on robustness to a particular class of singularly perturbed hybrid systems can be taken as the first step on the development of a general theory on this topic, one that parallels the perturbation theory of classical nonlinear systems. This theory would enable the application of standard nonlinear control design techniques to hybrid systems with inputs.
- **Advanced hybrid control methods for robotics and aerospace systems:** The hybrid control strategies in Chapter 6 are applicable to other relevant problems in robotics and aerospace systems. For instance, the throw-and-catch strategy in Section 6.2 can be used to develop control algorithms with decision-making capabilities and robustness for multiple autonomous vehicles. Robust algorithms for such purposes seem to be missing from the literature. The hybrid tracking control strategy in Section 6.3 for juggling systems is applicable to more general mechanical systems with impacts, including walking and jumping robots.

- **Embedded systems:** The analysis of the effect of sample-and-hold devices on the robust stability properties of closed-loop systems resulting from interconnecting a nonlinear system with a hybrid controller in Section 5.3 of Chapter 5 can be specialized to different classes of embedded systems to derive minimum rates for sample-and-hold devices and software computation. These results would serve as guidelines for embedded system design. Moreover, the hybrid system framework introduced in this thesis is also useful to capture the dynamics of models of computation used in embedded computing, thus enabling the application of the new systematic tools to that area as well.
- **Simulation:** The initial efforts in Chapter 7 are an indicator that classical results in the simulation theory of continuous-time systems can also be extended to the hybrid setting. A simulation theory for hybrid systems seems to be missing from the literature. The simulation framework introduced in Chapter 7 is suitable for its future development.

Other areas of science and engineering that would benefit from the theoretical and practical results in this thesis include several problems in biology, especially those dealing with biological networks and mutual synchronization. We believe this thesis contributes both to the theory and applications of hybrid control systems by introducing new modeling, analysis, and design tools that are useful for the control community and other related fields.

Appendix A

Simulating Hybrid Systems in Matlab/Simulink

A.1 Simulink Model

Hybrid systems $\mathcal{H} = (O, f, C, g, D)$ can be simulated in Matlab/Simulink. Figure A.1 shows a Simulink implementation used in this thesis.

Five basic blocks are used to define the dynamics of the hybrid system:

- The flow map is implemented in a *Matlab function block* executing the function `f.m`. Its input is the state of the system x , its output is the value of the flow map f which is connected to the integrator's input.
- The flow set is implemented in a *Matlab function block* executing the function `C.m`. Its input is the state of the *Integrator* system x' , its output is equal to 1 if the state belongs to the set C and is 0 otherwise.
- The jump map is implemented in a *Matlab function block* executing the function `g.m`. Its input is the state of the *Integrator* system x' , its output is the value of the jump map g .
- The jump set is implemented in a *Matlab function block* executing the function `D.m`. Its input is the state of the *Integrator* system x' , its output is equal to 1 if the state belongs to D and equal to 0 otherwise.
- The state space is implemented in a *Matlab function block* executing the function `O.m`. Its input is the state of the *Integrator* system x' , its output is equal to 1 if the state belongs to O and equal to 0 otherwise.

The flows and jumps of the hybrid system are computed by the *Integrator* system. This is depicted in Figure A.2.

The main component of the *Integrator* system is the integrator block. Its state is $[t \ j \ x^T]^T$ where t and j parametrize the result of the simulation of the hybrid system \mathcal{H} which is stored in the state component x . That is, the integrator generates both the time variables and the state trajectory.

The integrator is configured with the following special settings:

- External reset: “level hold”¹.

¹This corresponds to the setting for Simulink/Matlab R2007a. For previous versions, as older as R14 SP3, this reset setting corresponds to *level*.

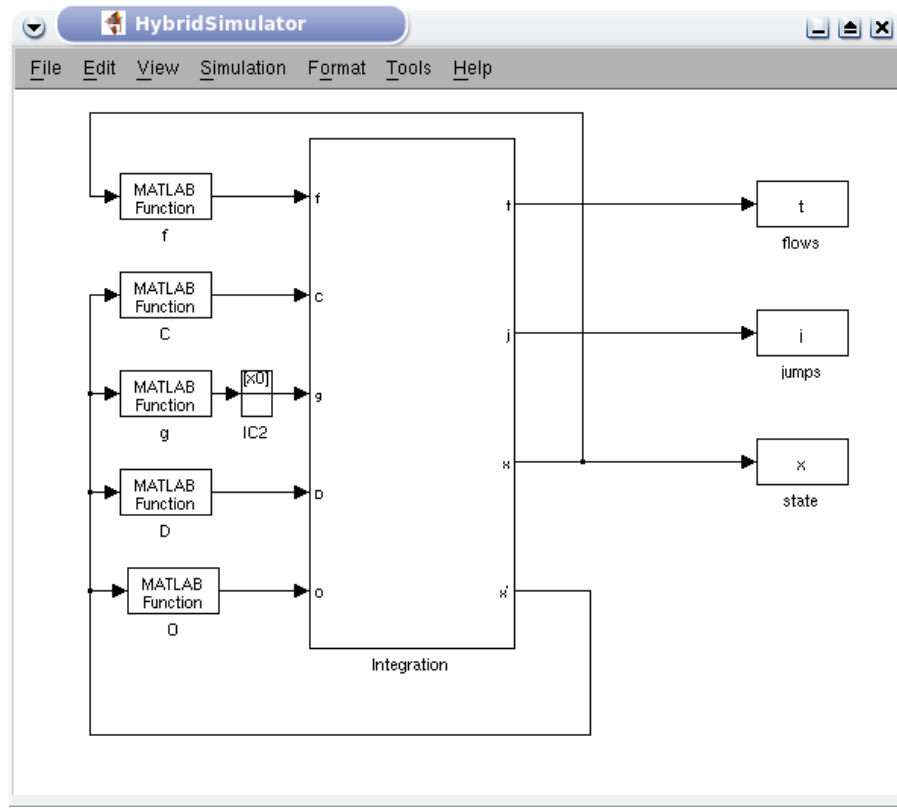


Figure A.1. Matlab/Simulink implementation of a hybrid system $\mathcal{H} = (O, f, C, g, D)$.

- Initial condition source: “external”.
- Show state port: checked.

Zero cross detection is globally disabled. The ODE solver is set to be the variable-step algorithm ode23 (Bogacki-Shampine) with default options.

The subsystems of the *Integrator* system perform the following main tasks:

1. Continuous dynamics: compute continuous dynamics of the hybrid system.
2. Jump logic: trigger jumps.
3. Update logic: update the state of the system and the simulation time (t, j) at jumps.
4. Stop logic: stop simulation.

The following parameters have to be defined for this implementation to work:

- x_0 : the initial condition for the state x .
- T and J : simulation horizon for the flows and for the jumps, respectively.

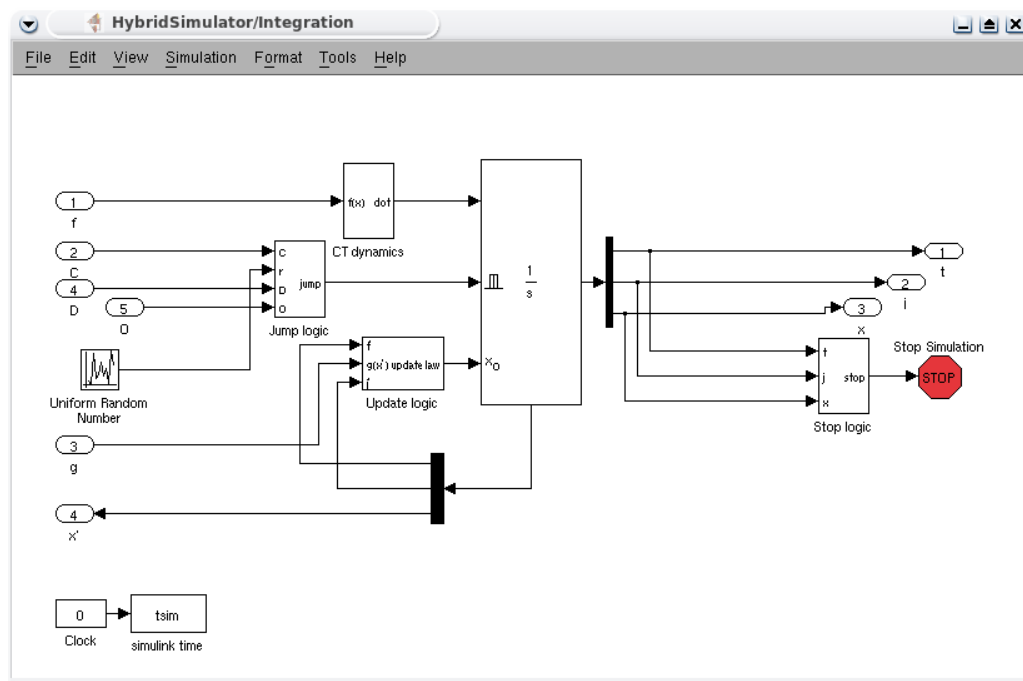


Figure A.2. Integrator.

- *rule*: rule for priority of flows/jumps to use. $rule = 1$ indicates that jumps have the highest priority (forced jumps), $rule = 2$ indicates that flows have the highest priority (forced flows), $rule = 3$ indicates that at points where both flows and jumps are possible, the selection is done randomly.

The following sections describe each of these subsystems in detail.

A.2 Continuous dynamics

This block defines the continuous dynamics of the state $[t \ j \ x^T]^T$. These are given by

$$\dot{t} = 1, \quad \dot{j} = 0, \quad \dot{x} = f(x) .$$

Figure A.3 depicts this implementation. Note that input port 1 takes the value of $f(x)$ through the output of the *Matlab function block f* in Figure A.1.

A.3 Jump Logic

The inputs to the jump logic block are the output of the blocks C, D , and O indicating whether the state is in those sets or not, and a random signal with uniform distribution in $[0, 1]$. Figure A.4 shows that these signals are the input a Matlab function block called *jump priority*. (The initial condition blocks set the initial value of the signals. These depend on the initial condition x_0 .) The *jump priority* block runs the following function (jumpPriority.m):

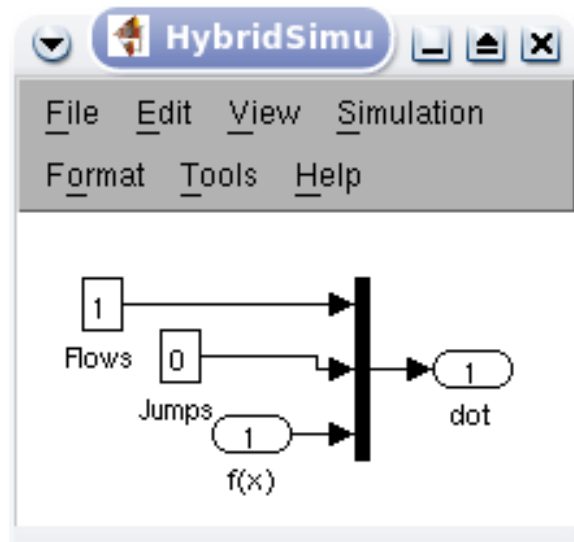


Figure A.3. Continuous dynamics.

```
function out = jumpPriority(u,rule)

% state
flowFlag = u(1);
jumpFlag = u(2);
stateFlag = u(3);
randomInput = u(4);

% rule = 1 -> priority for jumps
% rule = 2 -> priority for flows
% rule = 3 -> no priority, random selection
%           when simultaneous conditions

if (rule == 1) & (jumpFlag == 1)
    out = 1;
elseif (rule == 1) & (jumpFlag == 0)
    out = 0;
elseif (rule == 2) & (flowFlag == 1)
    out = 0;
elseif (rule == 2) & (flowFlag == 0) & (jumpFlag == 0)
    out = 0;
elseif (rule == 2) & (flowFlag == 0) & (jumpFlag == 1)
    out = 1;
elseif (rule == 3)
    if (flowFlag == 1) & (jumpFlag == 0)
        out = 0;
    elseif (flowFlag == 0) & (jumpFlag == 1)
        out = 1;
    elseif (flowFlag == 1) & (jumpFlag == 1)

```

```

    if (randomInput >= 0.5)
        out = 1;
    else
        out = 0;
    end
else
    out = 0;
end
end
end

```

The output of this function is equal to one only when the output of the D block is equal to one and $rule = 1$, or when the output of the D block is equal to one, $rule = 3$, and the random signal r is larger or equal than 0.5. Under either event, the output of this block, which is connected to the integrator external reset input, triggers a reset of the integrator, that is, a jump of \mathcal{H} . The reset or jump is activated since the configuration of the reset input is set to “level hold”, which executes resets when this external input is equal to one (if this input remains set to one, multiple resets would be triggered).

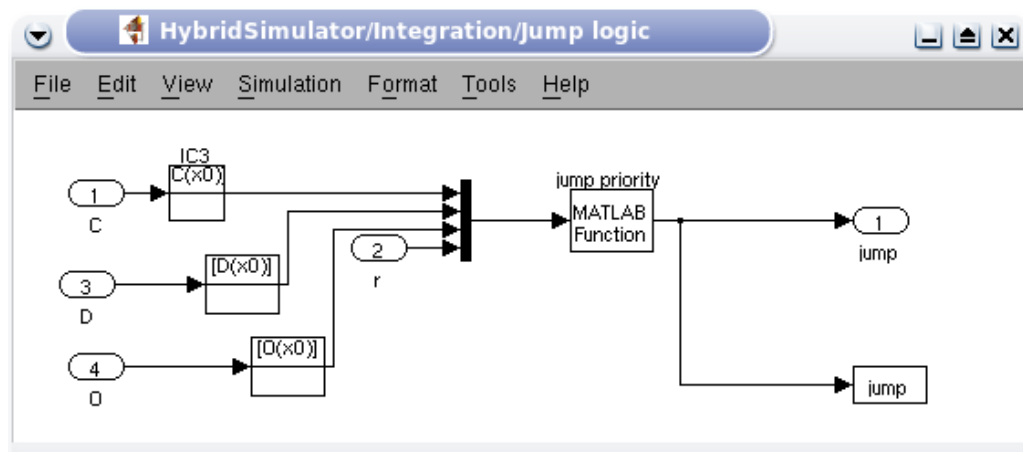


Figure A.4. Jump Logic.

A.4 Update Logic

The update logic uses the *state port* information of the integrator. This port reports the value of the state of the integrator, $[t \ j \ x^T]^T$, at the exact instant that the reset condition becomes true. Notice that x' differs from x since at a jump, x' indicates the value of the state that triggers the jump, that is, $x \in D$, while x at that same time is equal to the value assigned at the jump by the update logic. This value is given by $g(x')$ as Figure A.5 illustrates. It also shows that the flow time t is kept constant at jumps and that j is incremented by one by the Matlab function block $j + 1$. More precisely

$$t^+ = t', \quad j^+ = j', \quad x^+ = g(x')$$

where $[t' \ j' \ x'^T]^T$ is the state that triggers the jump.

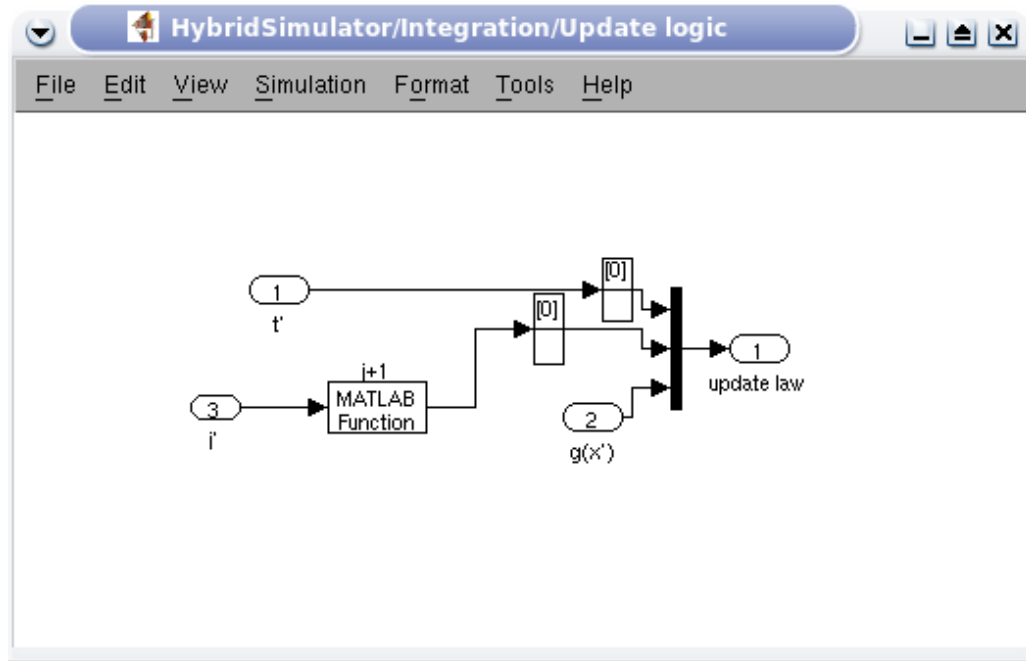


Figure A.5. Update Logic.

A.5 Stop Logic

This block stops the simulation under any of the following events:

- The flow time is larger or equal than the maximum flow time specified by T .
- The jump time is larger or equal than the maximum number of jumps specified by J .
- The state of the hybrid system x is neither in C nor in D , or it is not in O .

Under any of these events, the output of the logic operator connected to the *Stop block* becomes one, stopping the simulation. Note that the blocks computing whether the state is in C , D , and O use the current value of the state x .

A.6 Examples

The examples below illustrate the use of the implementation above. The following functions are used to generate the plots:

- `plotflows(t,j,x)`: plots (in blue) the projection of the trajectory x onto the flow time axis t . The value of the trajectory for intervals $[t_j, t_{j+1}]$ with empty interior is marked with * (in blue). Dashed lines (in red) connect the value of the trajectory before and after the jump.

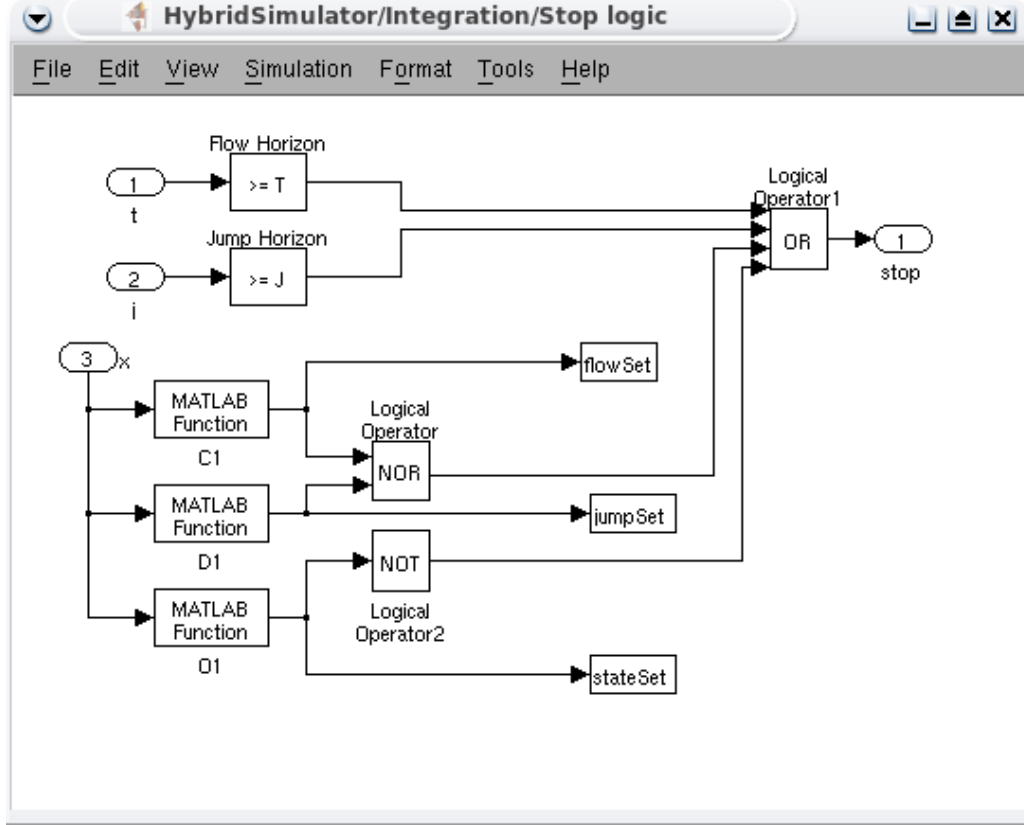


Figure A.6. Stop Logic.

- `plotjumps(t,j,x)`: plots (in red) the projection of the trajectory x onto the jump time j . The initial and final value of the trajectory on each interval $[t_j, t_{j+1}]$ is denoted by $*$ (in red) and the continuous evolution of the trajectory on each interval is depicted with a dashed line (in blue).
- `plotHybridArc(t,j,x)`: plots (in blue) the trajectory x on hybrid time domains. The intervals $[t_j, t_{j+1}]$ indexed by the corresponding j are depicted in the $t - j$ plane (in red).

Example A.1 (bouncing ball) For the simulation of the bouncing ball system in Section 2.2.1 with regular data given by

$$O := \mathbb{R}^2, f(x) := \begin{bmatrix} x_2 \\ -\gamma \end{bmatrix}, C := \{x \in \mathbb{R}^2 \mid x_1 \geq 0\} \quad (\text{A.1})$$

$$g(x) := \begin{bmatrix} 0 \\ -\lambda x_2 \end{bmatrix}, D := \{x \in \mathbb{R}^2 \mid x_1 \leq 0, x_2 \leq 0\} \quad (\text{A.2})$$

where $\gamma > 0$ is the gravity constant and $\lambda \in [0, 1)$ is the restitution coefficient. The Matlab scripts in each of the function blocks of the implementation above are given as follows. The constants for the bouncing ball system are $g = 9.8$ and $\lambda = 0.8$.

```
function out = f(u)
```

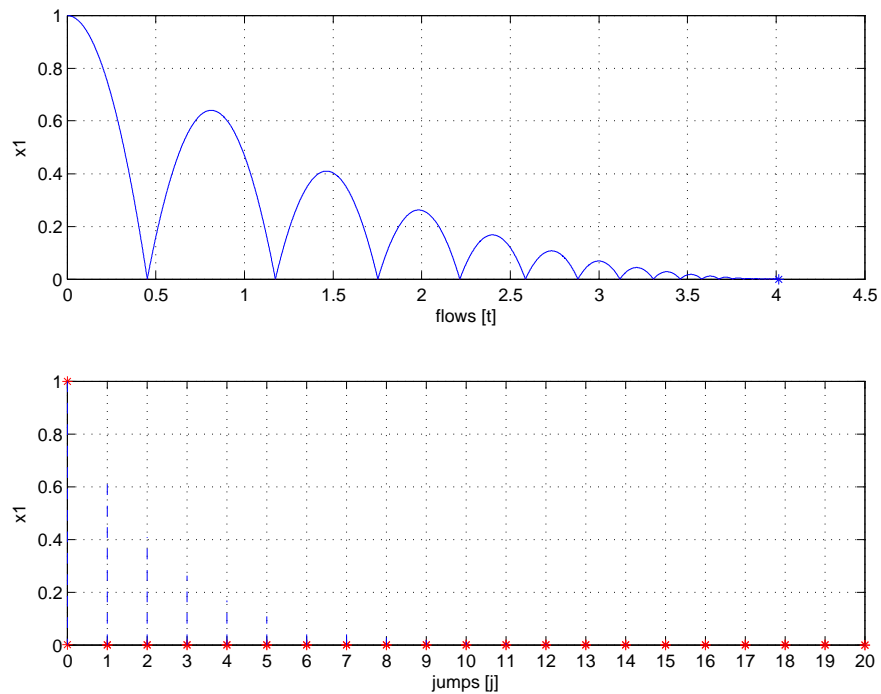


Figure A.7. Solution to the bouncing ball example: height.

```

% state
x1 = u(1);
x2 = u(2);
% flow map
x1dot = x2;
x2dot = -9.8;
out = [x1dot; x2dot];

function [v] = C(u)
% state
x1 = u(1);
x2 = u(2);
if (x1 >= 0) % flow condition
    v = 1; % report flow
else
    v = 0; % do not report flow
end

function out = g(u)
% state
x1 = u(1);

```

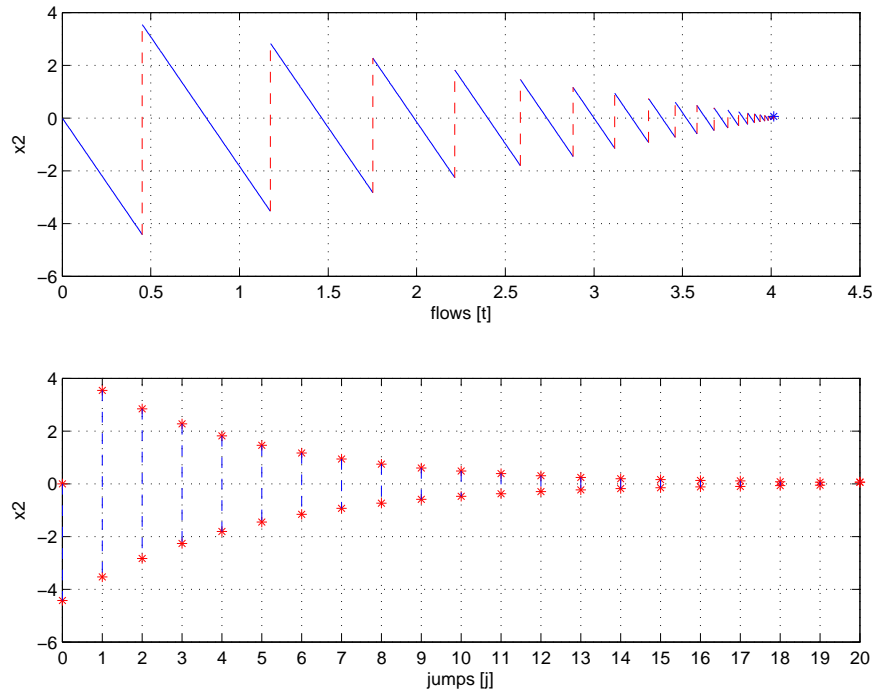


Figure A.8. Solution to the bouncing ball example: velocity.

```

x2 = u(2);
% jump map
x1plus = 0;
x2plus = -0.8*x2;
out = [x1plus; x2plus];

function [v] = D(u)
% state
x1 = u(1);
x2 = u(2);
if (x1 <= 0 && x2 <= 0) % jump condition
    v = 1; % report jump
else
    v = 0; % do not report jump
end

function [v] = O(u)
v = 1; % in the state space

```

A solution to the bouncing ball system from $[1, 0]$ and with $T = 10, J = 20, rule = 1$, is depicted in Figure A.7 (height) and Figure A.8 (velocity). Both the projection onto t and j are shown. Figure A.9 depicts the corresponding hybrid arc.

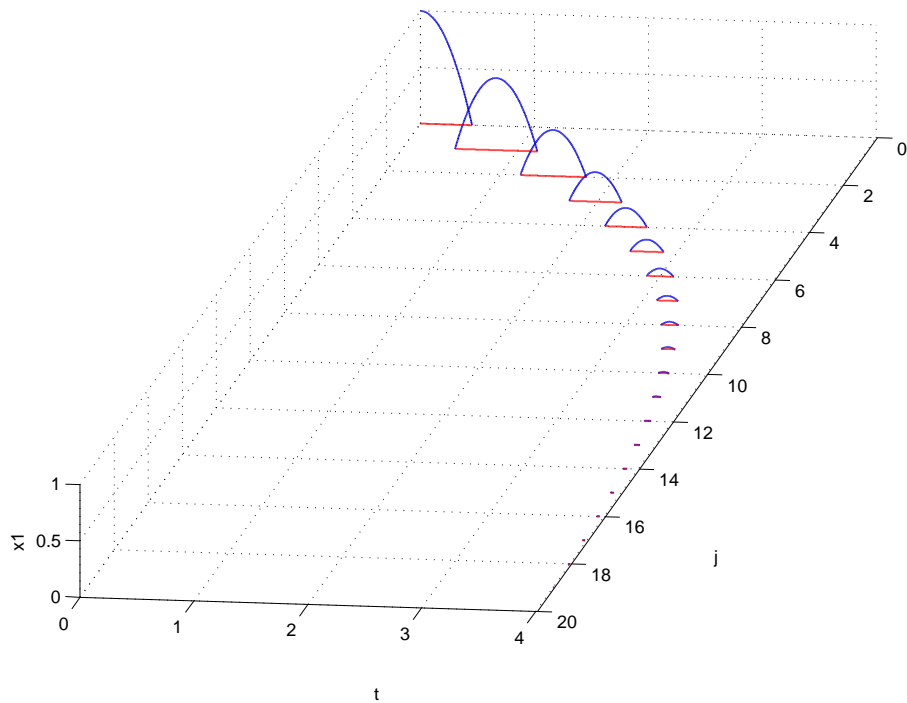


Figure A.9. Hybrid arc corresponding to a solution to the bouncing ball example: height.

These simulations reflect the expected behavior of the bouncing ball model. However, if instead

$$\{x \in \mathbb{R}^2 \mid x_1 = 0, x_2 \leq 0\}$$

is used as D , the effect of the discretization of the flows would prevent the *Jump Logic block* from detecting the jumps since it is very unlikely that the computed solution would hit $x_1 = 0$ exactly. The enlarged jump set prevents this from happening. Another way to prevent such behavior is by adding special Simulink blocks with zero-cross detection.

Also note that using $[x_1, -\gamma x_2]^T$ as the jump map would cause the simulation to stop after the first jump. In fact, at the jump, due to the discretization effect of the flows mentioned above, $x_1, x_2 < 0$. With this new jump map, $x_1^+ < 0, x_2^+ > 0$ and this state is neither in C nor in D . Hence, the simulation is stopped after the first jump.

□

Example A.2 (a simple example)

Consider the hybrid system with data

$$O := \mathbb{R}, f(x) := -x, C := [0, 1], g(x) := 1 + \text{mod}(x, 2), D := \{1\} \cup \{2\}.$$

Note that solutions from $\xi = 1$ and $\xi = 2$ are nonunique. The following simulations show the use of the *variable rule* in the *Jump Logic block*.

Jumps enforced:

A solution from $x_0 = 1$ with $T = 10, J = 20, rule = 1$ is depicted in Figure A.10. The solution jumps from 1 to 2, and from 2 to 1 repetitively.

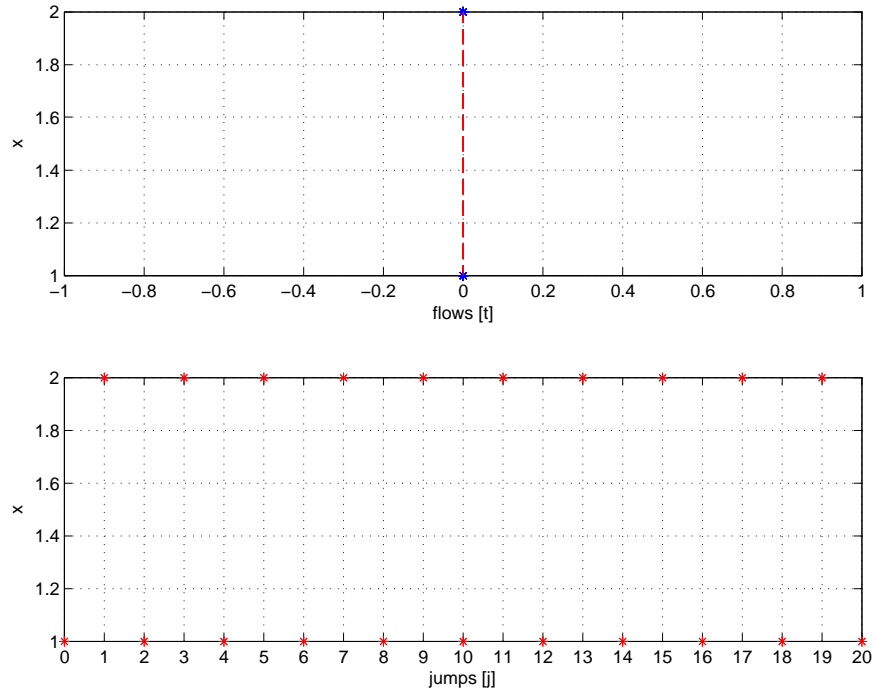


Figure A.10. Solution to Example A.2 with forced jumps logic.

Flows enforced:

A solution from $x_0 = 1$ with $T = 10, J = 20, rule = 2$ is depicted in Figure A.11. The solution flows for all time and converges exponentially to zero.

Random rule:

A solution from $x_0 = 1$ with $T = 10, J = 20, rule = 3$ is depicted in Figure A.12. The solution jumps to 2, then jumps to 1 and flows for the rest of the time converging to zero exponentially.

Enlarging D to

$$D := [1/50, 1] \cup \{2\}$$

causes the overlap between C and D to be “thicker”. The simulation result is depicted in Figure A.13 with the same parameters used in the simulation in Figure A.12. The plot suggests that the solution jumps several times

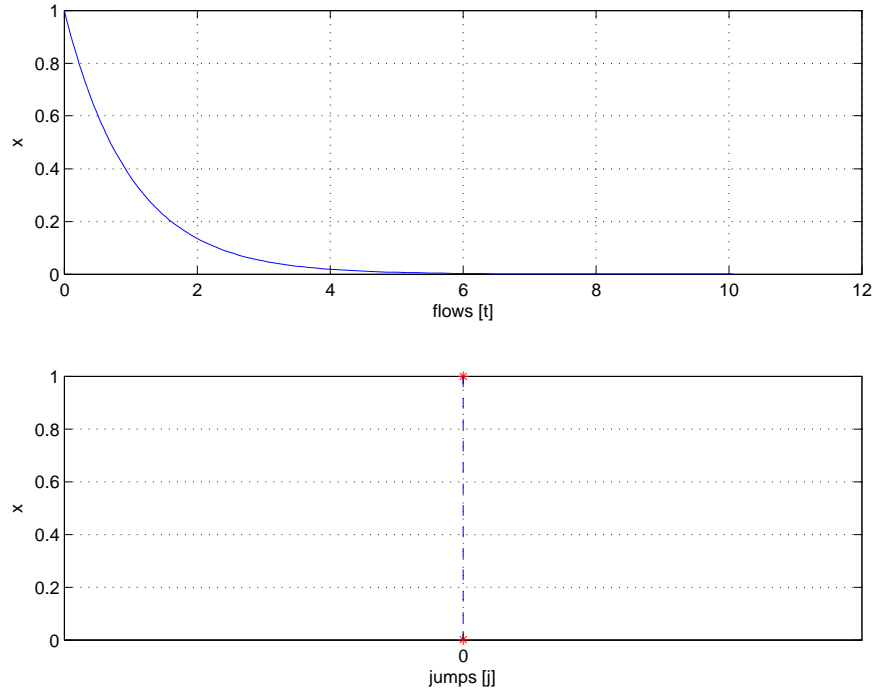


Figure A.11. Solution to Example A.2 with forced flows logic.

until $x < 1/50$ from where it flows to zero. However, Figure A.14, a zoomed version of Figure A.13, shows that initially the solution flows and that at $(t, j) = (0.2e - 3, 0)$ it jumps. After the jump, it continues flowing, then it jumps a few times, then it flows, etc. The combination of flowing and jumping occurs while the solution is in the intersection of C and D , where the selection of whether flowing or jumping is done randomly due to using $rule = 3$.

This simulation also reveals that this implementation does not precisely generate hybrid arcs. The maximum step size was set to $0.1e - 3$. The solution flows during the first two steps of the integration of the flows with maximum step size. The value at $t = 0.1e - 3$ is very close to 1. At $t = 0.2e - 3$, instead of assuming a value given by the flow map, the value of the solution is about 0.5, which is the result of the jump occurring at $(0.2e - 3, 0)$. This is the value stored in x at such time by the integrator. Note that the value of x' at $(0.2e - 3, 0)$ is the one given by the flow map that triggers the jump, and if available for recording, it should be stored in $(0.2e - 3, 0)$. This is a limitation of the current implementation.

□

The following simulations show the *Stop Logic block* stopping the simulation at different events.

Solution outside O :

Replacing O by $(-1, 2)$, a solution starting from $x_0 = 1$ with $T = 10, J = 20, rule = 1$ fails to exist after the first jump. This is depicted in Figure A.15 (cf. Figure A.10)

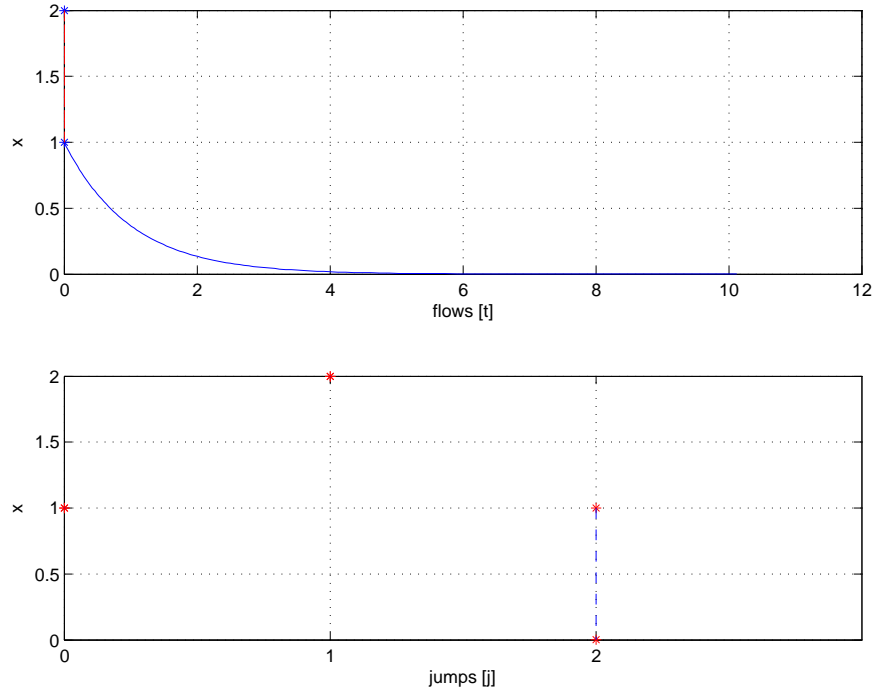


Figure A.12. Solution to Example A.2 with random logic for flowing/jumping.

Solution outside $C \cup D$:

The same behavior as the one just outlined arises with $O = \mathbb{R}$ but with $D = \{1\}$. The simulation stops since the solution leaves $C \cup D$. (See also `Overlap3.zip`).

Solution reaches the boundary of C from where jumps are not possible:

Finally, taking $O = \mathbb{R}$ and replacing the flow set by $[1/2, 1]$ a solution starting from $x_0 = 1$ with $T = 10$, $J = 20$ and $rule = 2$ flows for all time until it reaches the boundary of C where jumps are not possible. Figure A.16 shows this.

Note that in this implementation, the Stop Logic is such that when the state of the hybrid system is not in $(C \cup D) \cap O$, then the simulation is stopped. In particular, if this condition becomes true while flowing, then the last value of the computed solution will not belong to either C or O , or both, depending on the situation. It could be desired to be able to recompute the solution so that its last point belongs to the corresponding set. From that point, it should be the case that solutions cannot be continued.

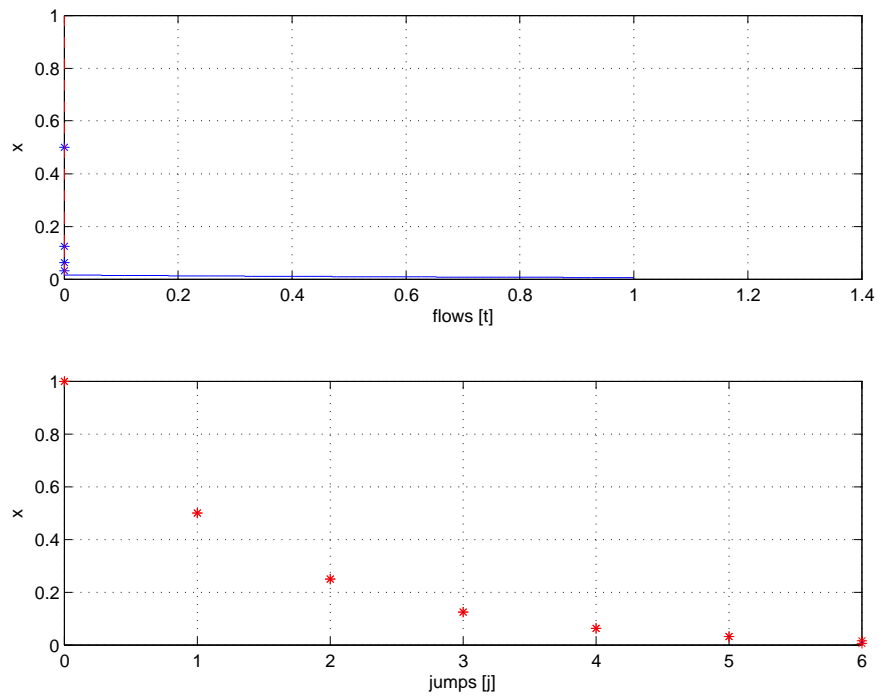


Figure A.13. Solution to Example A.2 with random logic for flowing/jumping.

A.7 Notes

Matlab/Simulink files corresponding to the simulation technique described in this appendix can be found at the authors' website, currently at

<http://www.ccdc.ece.ucsb.edu/~rsanfelice/>.

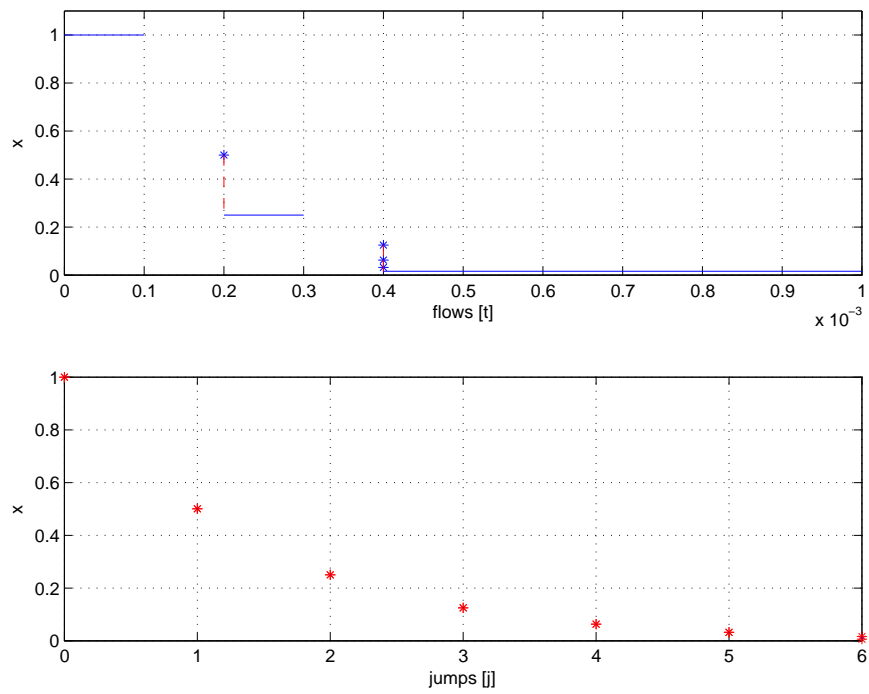


Figure A.14. Solution to Example A.2 with random logic for flowing/jumping. Zoomed version.

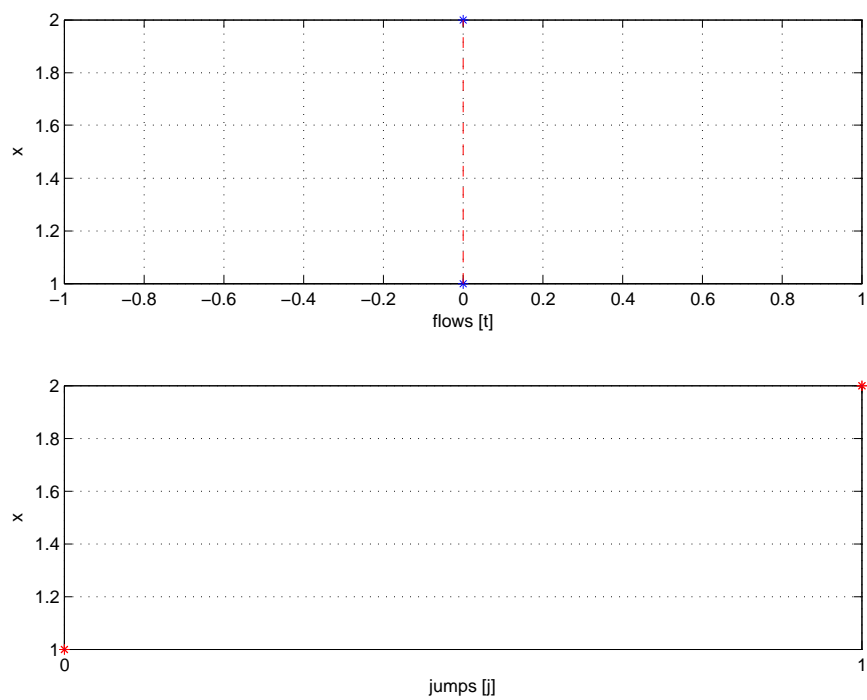


Figure A.15. Solution to Example A.2 with forced jump logic and different O .

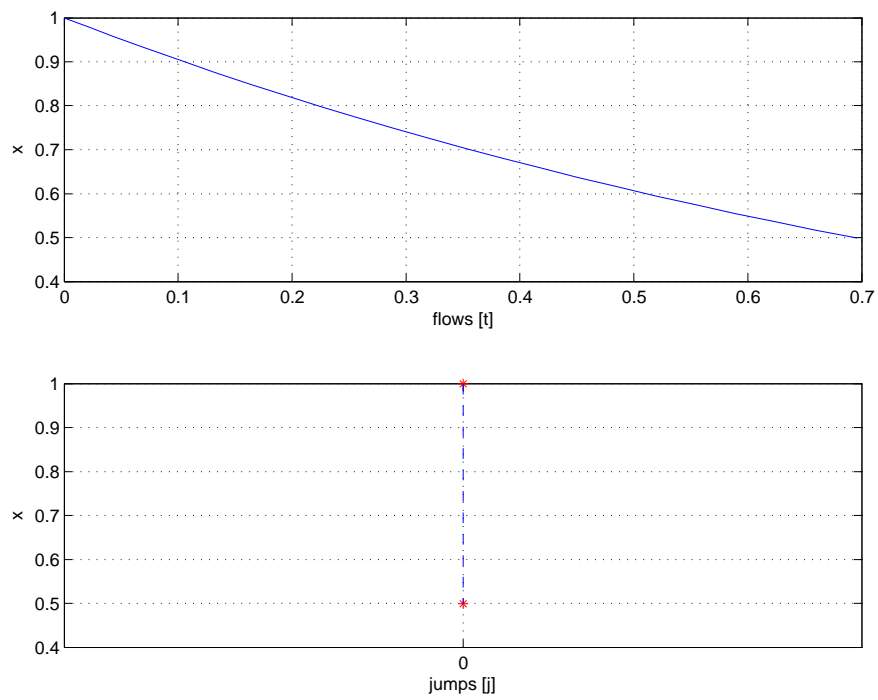


Figure A.16. Solution to Example A.2 with forced flow logic.

Appendix B

Proofs

This appendix contains proofs that, for clarity of the exposition, were omitted throughout the thesis.

B.1 Proofs of results in Chapter 3

B.1.1 Proof of Theorem 3.11 and Corollary 3.15

The proof of these results is divided in two parts. In the next two sections, it is shown that Krasovskii solutions are (control) Hermes solutions, and in the last section, it is shown that (control) Hermes solutions are Krasovskii solutions.

Krasovskii solutions are Hermes

Theorem B.3 below is an extension of Theorem 5.5 in [42] to differential equations with a constraint $x(t) \in C$. Our proof is also different (and shorter) than that given in [42]. We will need the corollary of [42, Lemma 3.3] below.

Assumption B.1 (*f* and *g* assumptions) *The set $O \subset \mathbb{R}^n$ is open. The sets C and D are subsets of O . The function $f : C \rightarrow \mathbb{R}^n$ is locally bounded on O . The set-valued mapping $G : D \rightrightarrows \mathbb{R}^n$ is locally bounded with respect to O on O .*

Lemma B.2 (auxiliary lemma) *Let f satisfy Assumption B.1 and let $\psi : [0, T] \rightarrow O$ be an absolutely continuous function that satisfies, for almost all $t \in [0, T]$, $\dot{\psi}(t) \in \bar{f}(\psi(t))$. Then, for every $\varepsilon > 0$, there is a closed null-set Z and a Lipschitz function $z : [0, T] \rightarrow O$ such that $|\psi(t) - z(t)| \leq \varepsilon$ for all $t \in [0, T]$ and which is piecewise linear in the sense that $\dot{z}(t) = \dot{\psi}(\alpha)$ for all t in any component (α, β) of $[0, T] \setminus Z$, and for any such component, $\dot{\psi}(\alpha) \in \bar{f}(\psi(\alpha))$.*

Above, by a component of (the open set) $[0, T] \setminus Z$ we understand any of the (at most countably many) mutually disjoint intervals (α, β) covering $[0, T] \setminus Z$. In what follows, we will refer to the family of all such intervals as \mathcal{I} . Below, we will also use the term “piecewise constant” to mean that a function is constant on each $(\alpha, \beta) \in \mathcal{I}$. Finally, we note that directly from the proof of the result above one can deduce that the size of the intervals (α, β) in \mathcal{I} can be made arbitrarily small.

Theorem B.3 (continuous-time Krasovskii is Hermes) *Let f satisfy Assumption B.1 and let $\psi : [0, T] \rightarrow O$ be an absolutely continuous function that satisfies, for almost all $t \in [0, T]$, $\psi(t) \in \overline{C}$, $\dot{\psi}(t) \in \overline{f}(\psi(t))$. Then, for any $\varepsilon > 0$ such that $\text{rge } \psi + \varepsilon \mathbb{B} \subset O$ and any $\varphi_0 \in C$ such that $|\varphi_0 - \psi(0)| < \varepsilon$, there exists a Lipschitz and piecewise linear $\varphi : [0, T] \rightarrow O$ with $\varphi(0) = \varphi_0$ and a measurable $e : [0, T] \rightarrow \mathbb{R}^n$ such that $\sup_{t \in [0, T]} |e(t)| \leq \varepsilon$, $\varphi + e$ is piecewise constant on $[0, T]$,*

$$\varphi(t) + e(t) \in C \quad \text{for all } t \in [0, T], \quad \dot{\varphi}(t) = f(\varphi(t) + e(t)) \quad \text{for almost all } t \in [0, T],$$

and $|\psi(t) - \varphi(t)| \leq \varepsilon$ for all $t \in [0, T]$.

Proof. Fix $\varepsilon > 0$ so that $\text{rge } \psi + \varepsilon \mathbb{B} \subset O$, pick $\varphi_0 \in C$ so that $|\varphi_0 - \psi(0)| < \varepsilon$, and pick any $\varepsilon' \in (0, \varepsilon - |\varphi_0 - \psi(0)|)$. Let $L > 0$ be a bound on f on $\text{rge } \psi + \varepsilon' \mathbb{B}$ (so in particular, L is a Lipschitz constant for ψ). Use Lemma B.2 to obtain $z : [0, T] \rightarrow O$ with $|\psi(t) - z(t)| \leq \varepsilon'/8$ in a way that $\beta - \alpha \leq \frac{\varepsilon'}{8(1+L)}$ for each component (α, β) of $[0, T] \setminus Z$. Then, in particular, $|\psi(t) - \psi(\alpha)| \leq \varepsilon'/8$ for all $t \in (\alpha, \beta)$ and all intervals (α, β) in \mathcal{I} . For each segment $(\alpha, \beta) \in \mathcal{I}$, by the definition of \overline{f} and since $\dot{\psi}(\alpha) \in \overline{f}(\psi(\alpha))$, there exist points $\psi_j^\alpha \in C$, $j = 1, 2, \dots, n+1$, so that $|\psi_j^\alpha - \psi(\alpha)| \leq \varepsilon'/8$ and constants $\lambda_j^\alpha \geq 0$, $j = 1, 2, \dots, n+1$, so that $\sum_{j=1}^{n+1} \lambda_j^\alpha = 1$ and

$$\left| \left(\sum_{j=1}^{n+1} \lambda_j^\alpha f(\psi_j^\alpha) \right) - \dot{\psi}(\alpha) \right| \leq \frac{\varepsilon'}{8(1+T)}.$$

Divide (α, β) into $n+1$ subintervals $(\gamma_{j-1}^\alpha, \gamma_j^\alpha)$ with $\gamma_0^\alpha = \alpha$, $\gamma_{n+1}^\alpha = \beta$ of lengths $\lambda_j^\alpha(\beta - \alpha)$. Now define a piecewise linear function $v : [0, T] \rightarrow \mathbb{R}^n$ almost everywhere by $v(t) = f(\psi_j^\alpha)$ on $(\gamma_{j-1}^\alpha, \gamma_j^\alpha)$. Note that $v \in L_1[0, T]$, and consequently, the function $\varphi : [0, T] \rightarrow \mathbb{R}^n$ defined by

$$\varphi(t) = \varphi_0 + \int_0^t v(\tau) d\tau$$

is absolutely continuous. Furthermore, $\dot{\varphi}(t) = v(t)$ for almost all $t \in [0, T]$ (in fact, whenever $t \in (\gamma_{j-1}^\alpha, \gamma_j^\alpha)$, $j = 1, 2, \dots, n+1$). Also, define $e : [0, T] \rightarrow \mathbb{R}^n$ as follows: set

$$e(t) = \psi_j^\alpha - \varphi(t) \quad \text{if } t \in (\gamma_{j-1}^\alpha, \gamma_j^\alpha)$$

and note that this defines e for almost all $t \in [0, T]$, and that for those t 's, we have $\dot{\varphi}(t) = f(\varphi(t) + e(t))$ as well as $\varphi(t) + e(t) \in C$. For each t at which $e(t)$ has not been defined yet, one can find $c_t \in C$ such that $|c_t - \psi(t)| < \varepsilon'/4$ and then set $e(t) = c_t - \varphi(t)$. Then $\varphi(t) + e(t) \in C$ for all $t \in [0, T]$. Also, $\varphi(t) + e(t)$ is constant on each $(\gamma_{j-1}^\alpha, \gamma_j^\alpha)$, as so $\varphi + e$ is piecewise constant on $[0, T]$. We claim that φ and e have the other desired properties.

For each initial point $\bar{\alpha}$ of some interval $(\alpha, \beta) \in \mathcal{I}$

$$\begin{aligned} |\varphi(\bar{\alpha}) - z(\bar{\alpha})| &\leq |\varphi(0) - z(0)| + \left| \int_0^{\bar{\alpha}} (\dot{\varphi}(t) - \dot{z}(t)) dt \right| \\ &\leq |\varphi_0 - z(0)| + \sum_{(\alpha, \beta) \in \mathcal{I}, \beta \leq \bar{\alpha}} \left| \int_\alpha^\beta \dot{\varphi}(t) dt - \dot{\psi}(\alpha)(\beta - \alpha) \right| \\ &\leq |\varphi_0 - \psi(0)| + |\psi(0) - z(0)| + \sum_{(\alpha, \beta) \in \mathcal{I}, \beta \leq \bar{\alpha}} \frac{\varepsilon'(\beta - \alpha)}{8(1+T)} \\ &\leq |\varphi_0 - \psi(0)| + \varepsilon'/8 + \frac{\varepsilon'}{8(1+T)} \sum_{(\alpha, \beta) \in \mathcal{I}, \beta \leq \bar{\alpha}} (\beta - \alpha) \\ &= |\varphi_0 - \psi(0)| + \varepsilon'/8 + \frac{\varepsilon'}{8(1+T)} \bar{\alpha} \end{aligned}$$

$$\leq |\varphi_0 - \psi(0)| + \varepsilon'/4$$

where the sum above is over all intervals $(\alpha, \beta) \in \mathcal{I}$ with $\beta \leq \bar{\alpha}$ (so that in particular, $\sum(\beta - \alpha) = \bar{\alpha}$) and the last inequality above relies on $\bar{\alpha} < T$.¹ Furthermore, for each interval (α, β) and any $\tau \in (\alpha, \beta)$,

$$\left| \int_{\alpha}^{\tau} \dot{\varphi}(t) dt - \dot{\psi}(\alpha)(\tau - \alpha) \right| \leq 2L(\tau - \alpha) \leq 2L(\beta - \alpha) \leq \varepsilon'/4$$

since both $\dot{\varphi}$ and $\dot{\psi}$ are bounded by L . Consequently,

$$|\varphi(t) - z(t)| \leq |\varphi_0 - \psi(0)| + \varepsilon'/2$$

for all $t \in [0, T]$, and hence

$$|\varphi(t) - \psi(t)| \leq |\varphi_0 - \psi(0)| + 5\varepsilon'/8 < \varepsilon$$

for all $t \in [0, T]$.

For the error bound, one obtains, for t in one of the intervals $(\gamma_{j-1}^{\alpha}, \gamma_j^{\alpha})$,

$$\begin{aligned} |e(t)| &\leq |\psi_j^{\alpha} - \psi(\alpha)| + |\psi(\alpha) - \psi(t)| + |\psi(t) - \varphi(t)| \\ &\leq \varepsilon'/8 + \varepsilon'/8 + |\varphi_0 - \psi(0)| + 5\varepsilon'/8 \\ &= |\varphi_0 - \psi(0)| + 7\varepsilon'/8 < \varepsilon. \end{aligned}$$

For the remaining t 's,

$$|e(t)| \leq |c_t - \psi(t)| + |\psi(t) - \varphi(t)| \leq \varepsilon'/4 + |\varphi_0 - \psi(0)| + 5\varepsilon'/8 < \varepsilon$$

by the choice of c_t and the previously established bound on $|\psi(t) - \varphi(t)|$. Thus $|e(t)| \leq \varepsilon$ for all $t \in [0, T]$. \square

Theorem B.4 (Krasovskii solution is close to a Hermes solution) *Let Assumption B.1 hold and let $\psi : \text{dom } \psi \rightarrow O$ be a Krasovskii solution to the hybrid system $\mathcal{H} = (O, f, C, g, D)$. Pick any $\varepsilon > 0$ and any $(T, J) \in \text{dom } \psi$. Let $E = \text{dom } \psi \cap ([0, T] \times \{0, 1, \dots, J\})$ and express E as $\bigcup_{j=0}^J ([t_j, t_{j+1}] \times \{j\})$. Then, there exist a measurable function $e : \text{dom } e \rightarrow \mathbb{R}^n$, $\text{dom } e = E$ and a hybrid arc $\varphi : \text{dom } \varphi \rightarrow O$, $\varphi(0, 0) = \psi(0, 0)$, $\text{dom } \varphi = E$ such that $\sup_{(t,j) \in \text{dom } e} |e(t, j)| \leq \varepsilon$ and*

(V1) for all $j = 0, 1, \dots, J$,

$$\varphi(t, j) + e(t, j) \in C \text{ for all } t \in [t_j, t_{j+1}), \quad \dot{\varphi}(t, j) = f(\varphi(t, j) + e(t, j))$$

for almost all $t \in [t_j, t_{j+1}]$;

(V2) for all $j = 0, 1, \dots, J - 1$,

$$\varphi(t_{j+1}, j) + e(t_{j+1}, j) \in D, \quad \varphi(t_{j+1}, j + 1) \in g(\varphi(t_{j+1}, j) + e(t, j));$$

¹We used the fact that by the construction of v , for any (α, β) in \mathcal{I} ,

$$\int_{\alpha}^{\beta} \dot{\varphi}(t) dt = \sum_{j=1}^{n+1} \int_{\gamma_{j-1}^{\alpha}}^{\gamma_j^{\alpha}} v(t) dt = \sum_{j=1}^{n+1} \lambda_j^{\alpha} (\beta - \alpha) f(\psi_j^{\alpha}) = (\beta - \alpha) \sum_{j=1}^{n+1} \lambda_j^{\alpha} f(\psi_j^{\alpha})$$

and thus

$$\left| \int_{\alpha}^{\beta} \dot{\varphi}(t) dt - \dot{\psi}(\alpha)(\beta - \alpha) \right| \leq (\beta - \alpha) \left| \sum_{j=1}^{n+1} \lambda_j^{\alpha} f(\psi_j^{\alpha}) - \dot{\psi}(\alpha) \right| \leq \frac{\varepsilon'(\beta - \alpha)}{8(1 + T)}.$$

and $|\varphi(t, j) - \psi(t, j)| \leq \varepsilon$ for every $(t, j) \in \text{dom } \varphi$.

Proof. Fix $\varepsilon > 0$ small enough so that $\psi(t, j) + \varepsilon\mathbb{B} \subset O$ for all $(t, j) \in E$. Note that for each $j = 0, 1, \dots, J-1$ there exists $z_j \in D$ and $w_{j+1} \in g(z_j)$ such that $|z_j - \psi(t_{j+1}, j)| \leq \frac{\varepsilon}{8}$ and $|w_{j+1} - \psi(t_{j+1}, j+1)| \leq \frac{\varepsilon}{8}$. Indeed, for any $x \in \overline{D}$ and $\varepsilon > 0$, we have:

$$\overline{g(x)} \subset \overline{g((x + \varepsilon\mathbb{B}) \cap D)} \cap O \subset (g((x + \varepsilon\mathbb{B}) \cap D) + \varepsilon\mathbb{B}) \cap O,$$

where the first inclusion above comes from the definition of $\overline{g(x)}$, and the second one from the definition of the closure of a set. Consequently, for each $y \in \overline{g(x)}$, there exists $z \in (x + \varepsilon\mathbb{B}) \cap D$ and $w \in g(z)$ such that $y \in g(y) + \varepsilon\mathbb{B}$.

On each segment $[t_j, t_{j+1}] \times \{j\}$ that is *nontrivial*, i.e., with $t_{j+1} > t_j$, by Theorem B.3, there exists an absolutely continuous function $\varphi_j : [t_j, t_{j+1}] \rightarrow O$ starting at $\varphi_j^0 \in \psi(t_j, j) + \frac{\varepsilon}{8}\mathbb{B}$, where $\varphi_j^0 = w_j$ if $j > 0$, $\varphi_j^0 = \psi(0, 0)$ if $j = 0$, and a measurable function $e_j : [t_j, t_{j+1}] \rightarrow \mathbb{R}^n$ with $\sup_{t \in [t_j, t_{j+1}]} |e_j(t)| \leq \frac{\varepsilon}{4}$ satisfying

$$\varphi_j(t) + e_j(t) \in C \quad \text{for all } t \in [t_j, t_{j+1}], \quad \dot{\varphi}_j(t) = f(\varphi_j(t) + e_j(t))$$

for almost all $t \in [t_j, t_{j+1}]$, and such that

$$|\varphi_j(t) - \psi(t, j)| \leq \frac{\varepsilon}{4} \quad \text{for all } t \in [t_j, t_{j+1}].$$

We now construct the measurement noise e . On each segment $[t_j, t_{j+1}] \times \{j\} \subset E$ that is *trivial*, i.e segments with $t_{j+1} = t_j$, let $e'_j = z_j - w_j$ if $J > j > 0$, $e'_j = z_0 - \psi(0, 0)$ if $j = 0$, and $e'_j = 0$ if $j = J$. On each nontrivial segment $[t_j, t_{j+1}] \times \{j\}$, let $e'_j(t) = e_j(t)$ for all $(t, j) \in [t_j, t_{j+1}] \times \{j\}$, $e'_j(t_{j+1}) = z_j - \varphi_j(t_{j+1})$ if $j < J$, $e'_j(t_{j+1}) = 0$ if $j = J$.

Then, φ and e are given by

$$\begin{aligned} \varphi(t, j) &:= \begin{cases} \varphi_j(t) & \text{if } (t, j) \in [t_j, t_{j+1}] \times \{j\} \text{ nontrivial} \\ w_j & \text{if } (t, j) = [t_j, t_{j+1}] \times \{j\} \text{ trivial} \end{cases} \\ e(t, j) &:= \begin{cases} e'_j(t) & \text{if } (t, j) \in [t_j, t_{j+1}] \times \{j\} \text{ nontrivial} \\ e'_j & \text{if } (t, j) = [t_j, t_{j+1}] \times \{j\} \text{ trivial} . \end{cases} \end{aligned}$$

By construction, φ and e satisfy (V1) and (V2). It follows that $|\varphi(t, j) - \psi(t, j)| \leq \varepsilon$ for all $(t, j) \in \text{dom } \varphi$ since on every trivial segment

$$|\varphi(t, j) - \psi(t, j)| = |w_j - \psi(t, j)| \leq \frac{\varepsilon}{8}$$

and on every nontrivial segment $[t_j, t_{j+1}] \times \{j\}$

$$|\varphi(t, j) - \psi(t, j)| = |\varphi_j(t) - \psi(t, j)| \leq \frac{\varepsilon}{4} \quad \forall t \in [t_j, t_{j+1}].$$

Moreover, $\sup_{(t, j) \in \text{dom } e} |e(t, j)| \leq \varepsilon$ since on every trivial interval

$$\begin{aligned} |e(t, j)| &= |z_j - w_j| \leq |z_j - \psi(t, j)| + |\psi(t, j) - w_j| \leq \frac{\varepsilon}{4} & \text{if } J > j > 0 \\ |e(t, j)| &= |z_0 - \psi^0| \leq \frac{\varepsilon}{8} & \text{if } j = 0 \\ |e(t, j)| &= 0 & \text{if } j = J, \end{aligned}$$

and on every nontrivial segment $[t_j, t_{j+1}] \times \{j\}$

$$\begin{aligned} |e(t, j)| &= |e'_j(t)| = |e_j(t)| \leq \frac{\varepsilon}{4} & \forall t \in [t_j, t_{j+1}] \\ |e(t, j)| &= |z_j - \varphi_j(t)| \leq |z_j - \psi(t, j)| + |\psi(t, j) - \varphi_j(t)| \leq \frac{\varepsilon}{2} \end{aligned}$$

for all $(t, j) = (t_{j+1}, j)$ if $j < J$, and $|e(t, j)| = 0$ if $j = J$. □

Corollary B.5 (Krasovskii solutions are Hermes solutions) *Under Assumption B.1, if a hybrid arc is a hybrid Krasovskii solution to \mathcal{H} then it is also a Hermes solution to \mathcal{H} .*

Proof. Let $\psi : \text{dom } \psi \rightarrow O$ be a Krasovskii solution to \mathcal{H} . Pick $(T, J) \in \text{dom } \psi$ (when $\text{dom } \psi$ is compact, it is enough to consider $(T, J) = \sup \text{dom } \psi$). Let ψ' be the truncation of ψ to $\text{dom } \psi' = \text{dom } \psi \cap ([0, T] \times \{0, 1, \dots, J\})$. By Theorem B.4, there exist $e_i : \text{dom } \psi' \rightarrow \mathbb{R}^n$ and $\varphi_i : \text{dom } \psi' \rightarrow O$ such that $\sup_{(t,j) \in \text{dom } e_i} |e_i(t, j)| \leq \frac{1}{i}$ and which satisfy conditions (V1) and (V2) of Theorem B.4 (with e replaced by e_i and φ replaced by φ_i) and also $|\psi(t, j) - \varphi_i(t, j)| \leq 1/i$ for every $(t, j) \in \text{dom } \varphi_i$. The last bound implies that φ_i converge graphically to ψ' . Since $\sup_{(t,j) \in \text{dom } e_i} |e_i(t, j)| \leq \frac{1}{i}$, ψ is a Hermes solution to \mathcal{H} . \square

Krasovskii solutions are control Hermes solutions

Below, we consider f and g given as in Corollary 3.11 with the assumption therein which, for convenience, we rewrite below. The result to follow is a corollary of Theorem B.3.

Assumption B.6 (f and g assumptions (control)) *The set $O \subset \mathbb{R}^n$ is open. The sets C and D are subsets of O . The function $f' : O \times \mathbb{R}^{m_c} \rightarrow \mathbb{R}^n$ is locally Lipschitz continuous in the first argument, locally uniformly in the second argument. The function $g' : O \times \mathbb{R}^{m_d} \rightarrow O$ is continuous in the first argument, locally uniformly in the second argument. The functions $\kappa_c : C \rightarrow \mathbb{R}^{m_c}$, $\kappa_d : D \rightarrow \mathbb{R}^{m_d}$ are locally bounded on O .*

Corollary B.7 (continuous-time Krasovskii is control Hermes) *Let f satisfy Assumption B.6, and let $\psi : [0, T] \rightarrow \mathbb{R}^n$ be an absolutely continuous function that satisfies, for almost all $t \in [0, T]$, $\psi(t) \in \overline{C}$, $\dot{\psi}(t) \in \overline{f}(\psi(t))$. Let $\varepsilon > 0$ be small enough so that $\text{rge } \psi + 2\varepsilon\mathbb{B} \subset O$ and let L be a Lipschitz constant for $f(\cdot, u)$ on $\text{rge } \psi + 2\varepsilon\mathbb{B} \subset O$ for any $u \in \kappa_c(\text{rge } \psi + 2\varepsilon\mathbb{B})$. Then, for every φ_0 such that $|\varphi_0 - \psi(0)| < \varepsilon e^{-LT}$, there exists a measurable function $e : [0, T] \rightarrow \mathbb{R}^n$ and an absolutely continuous function $\varphi : [0, T] \rightarrow O$, $\varphi(0) = \varphi_0$, such that $\sup_{t \in [0, T]} |e(t)| \leq \varepsilon$,*

$$\varphi(t) + e(t) \in C, \quad \text{for all } t \in [0, T],$$

$$\dot{\varphi}(t) = f'(\varphi(t), \kappa_c(\varphi(t) + e(t))) \quad \text{for almost all } t \in [0, T],$$

and $|\varphi(t) - \psi(t)| \leq \varepsilon$ for all $t \in [0, T]$.

Proof. Let $\varepsilon > 0$ be as assumed, and let $\varepsilon' = \varepsilon e^{-LT} < \varepsilon$. By Theorem B.3, there exists an absolutely continuous function $z : [0, T] \rightarrow O$ with $z(0) = \varphi_0$ and a measurable function $e' : [0, T] \rightarrow \mathbb{R}^n$ such that

$$\dot{z}(t) = f'(z(t) + e'(t), \kappa_c(z(t) + e'(t))) \quad \text{for almost all } t \in [0, T],$$

and $|z(t) - \psi(t)| \leq \varepsilon'$, $|e'(t)| \leq \varepsilon'$, and $z(t) + e'(t) \in C$ for all $t \in [0, T]$. Note that $|(z(t) + e'(t)) - \psi(t)| \leq 2\varepsilon'$. Furthermore, $z + e'$ is piecewise constant on $[0, T]$, so $\kappa_c(z(t) + e'(t))$ is measurable, and so the mapping $(x, t) \mapsto f'(x, \kappa_c(z(t) + e'(t)))$ is a Carathéodory mapping: continuous in x for a fixed t and measurable in t for a fixed x . Consequently, there exists a solution $\varphi : [0, T] \rightarrow O$ to

$$\dot{\varphi}(t) = f'(\varphi(t), \kappa_c(z(t) + e'(t))) \quad \text{a.e. and } \varphi(0) = \varphi_0$$

for which $\varphi(0) = z(0)$,

$$|\dot{\varphi}(t) - \dot{z}(t)| \leq L|\varphi(t) - z(t) - e'(t)| \leq L|\varphi(t) - z(t)| + L\varepsilon'$$

and thus $|\varphi(t) - z(t)| \leq \varepsilon'(e^{LT} - 1)$ for all $t \in [0, T]$. Consequently, for all $t \in [0, T]$,

$$|\varphi(t) - \psi(t)| \leq |\varphi(t) - z(t)| + |z(t) - \psi(t)| \leq \varepsilon' e^{LT} = \varepsilon.$$

Let $e(t) := z(t) + e'(t) - \varphi(t)$, so that $z(t) + e'(t) = \varphi(t) + e(t)$. Then, since $z(t) + e'(t) \in C$, we have $\varphi(t) + e(t) \in C$ for all $t \in [0, T]$. Furthermore, $\dot{\varphi}(t) = f(\varphi(t), \kappa_c(\varphi(t) + e(t)))$. Finally,

$$|e(t)| \leq |\varphi(t) - z(t)| + |e'(t)| \leq \varepsilon'(e^{LT} - 1) + \varepsilon' = \varepsilon' e^{LT} = \varepsilon.$$

□

The next result combines Corollary B.7 above, and the ideas of Theorem B.4.

Corollary B.8 (Krasovskii solution is close to a control Hermes solution) *Let Assumption B.6 hold, and let $\psi : \text{dom } \psi \rightarrow O$ be a Krasovskii solution to $\mathcal{H} = (O, f, C, g, D)$ with f and g as given in Corollary 3.15. Pick any $\varepsilon > 0$ and any $(T, J) \in \text{dom } \psi$. Let $E = \text{dom } \psi \cap ([0, T] \times \{0, 1, \dots, J\})$ and express E as $\bigcup_{j=0}^J ([t_j, t_{j+1}] \times \{j\})$. Then, there exist a measurable function $e : \text{dom } e \rightarrow \mathbb{R}^n$, $\text{dom } e = E$ and a hybrid arc $\varphi : \text{dom } \varphi \rightarrow O$, $\varphi(0, 0) = \psi(0, 0)$, $\text{dom } \varphi = E$ such that $\sup_{(t,j) \in \text{dom } e} |e(t, j)| \leq \varepsilon$ and*

(V1') for all $j = 0, 1, \dots, J$,

$$\varphi(t, j) + e(t, j) \in C \text{ for all } t \in [t_j, t_{j+1}), \quad \dot{\varphi}(t, j) = f'(\varphi(t, j), \kappa_c(\varphi(t, j) + e(t, j)))$$

for almost all $t \in [t_j, t_{j+1}]$;

(V2') for all $j = 0, 1, \dots, J - 1$,

$$\varphi(t_{j+1}, j) + e(t_{j+1}, j) \in D, \quad \varphi(t_{j+1}, j + 1) = g'(\varphi(t_{j+1}, j), \kappa_d(\varphi(t, j) + e(t, j)));$$

and $|\varphi(t, j) - \psi(t, j)| \leq \varepsilon$ for every $(t, j) \in \text{dom } \varphi$.

Proof. Let $S := \text{dom } \psi \cap ([0, T] \times \{0, 1, \dots, J\})$, fix $\varepsilon > 0$ so that $\psi(t, j) + 2\varepsilon\mathbb{B} \subset O$ for all $(t, j) \in S$, and let L be a Lipschitz constant for $f(\cdot, u)$ on $\{\psi(t, j) + 2\varepsilon\mathbb{B} \mid (t, j) \in S\}$. Note that for any $\delta > 0$, at each jump of ψ on S , i.e. at each point $(t, j) \in S$ such that there exists $(t, j + 1) \in S$, we can find $z_j \in D$ arbitrarily close to $\psi(t, j)$ that satisfies $|g(z_j, \kappa_d(z_j)) - \psi(t, j + 1)| \leq \delta/2$. This was already justified in the proof of Theorem B.4. Since g is continuous in the first variable, locally uniformly in the second variable varying over compact sets, we can pick z_j so that $|g(\psi(t, j), \kappa_d(z_j)) - \psi(t, j + 1)| \leq \delta$. Thus, by using $\delta = \min\{\frac{\varepsilon}{8}, \frac{\varepsilon}{4}e^{-LT}\}$, for every jump of ψ we obtain points $z_j \in D$ such that $|z_j - \psi(t, j)| \leq \frac{\varepsilon}{8}$ and $|g(\psi(t, j), \kappa_d(z_j)) - \psi(t, j + 1)| \leq \min\{\frac{\varepsilon}{8}, \frac{\varepsilon}{4}e^{-LT}\}$.

On each segment $[t_j, t_{j+1}] \times \{j\} := S \cap (\mathbb{R}_{\geq 0} \times \{j\}) \subset S$ that is *nontrivial*, i.e segments with $t_{j+1} > t_j$, by Corollary B.7, there exists an absolutely continuous function $\varphi_j : [t_j, t_{j+1}] \rightarrow O$ starting at $\varphi_j^0 \in \psi(t_j, j) + \min\{\frac{\varepsilon}{8}, \frac{\varepsilon}{4}e^{-LT}\}\mathbb{B}$, where $\varphi_j^0 = g(\psi(t_j, j), \kappa_d(z_{j-1}))$ if $j > 0$, $\varphi_j^0 = \psi^0$ if $j = 0$, and a measurable function $e_j : [t_j, t_{j+1}] \rightarrow \mathbb{R}^n$ with $\sup_{t \in [t_j, t_{j+1}]} |e_j(t)| \leq \frac{\varepsilon}{4}$ satisfying for almost all $t \in [t_j, t_{j+1}]$

$$\varphi_j(t) + e_j(t) \in C, \quad \dot{\varphi}_j(t) = f'(\varphi_j(t) + e_j(t), \kappa_c(\varphi(t) + e(t)))$$

and for all $t \in [t_j, t_{j+1}]$

$$|\varphi_j(t) - \psi(t, j)| \leq \frac{\varepsilon}{4}. \tag{B.1}$$

The rest of the proof is analogous to that of Theorem B.4. □

With Corollary B.8 at hand, the result below can be shown exactly in the same fashion as Corollary B.5.

Corollary B.9 (Krasovskii solutions are control Hermes solutions) *Under Assumption B.6, if a hybrid arc is a hybrid Krasovskii solution to \mathcal{H} then it is also a control Hermes solution to \mathcal{H} .*

Hermes and control Hermes solutions are Krasovskii solutions

Let $\rho : O \rightarrow (0, \infty)$ be an admissible radius of perturbation, that is, a continuous function such that for all $x \in O$, $x + \rho(x)\mathbb{B} \subset O$. For each $\delta \in (0, 1)$, let $\widehat{\mathcal{H}}^\delta$ denote the hybrid system defined by sets

$$\overline{C}^\delta := \{x \in O \mid x + \delta\rho(x)\mathbb{B} \cap \overline{C} \neq \emptyset\}, \quad \overline{D}^\delta := \{x \in O \mid x + \delta\rho(x)\mathbb{B} \cap \overline{D} \neq \emptyset\}$$

and mappings

$$\begin{aligned} \overline{f}^\delta(x) &:= \text{co} \overline{f}((x + \delta\rho(x)\mathbb{B}) \cap C) + \delta\rho(x)\mathbb{B}, \\ \overline{g}^\delta(x) &:= \{\xi + \delta\rho(\xi)\mathbb{B} \mid \xi \in \overline{g}((x + \delta\rho(x)\mathbb{B}) \cap D)\}. \end{aligned}$$

Such ‘‘inﬂations’’ of the hybrid system $\widehat{\mathcal{H}}$ were discussed in detail in [39]. A key property of such perturbations of $\widehat{\mathcal{H}}$ is that, thanks to properties of $\widehat{\mathcal{H}}$ given by the hybrid basic conditions and subject to minor local boundedness conditions, a sequence of solutions to $\widehat{\mathcal{H}}^\delta$ with decreasing δ is a solution to $\widehat{\mathcal{H}}$. We will use this below.

Proposition B.10 (control Hermes solution is close to a Krasovskii solution) *Under Assumption B.6, if a hybrid arc is a control Hermes solution to \mathcal{H} , then it is also a Krasovskii solution to \mathcal{H} .*

Proof. Let $\varphi : \text{dom } \varphi \rightarrow O$ be a control Hermes solution to $\mathcal{H} = (O, f, C, g, D)$. Pick $(T, J) \in \text{dom } \varphi$ and let φ' be the truncation of φ to $\text{dom } \varphi'$ given by $\text{dom } \varphi \cap ([0, T] \times \{0, 1, \dots, J\})$. Let the sequences of φ_i 's, e_i 's, and ε_i 's correspond to φ' . In particular, for all i and all $(t, j) \in \text{dom } e_i$, $|e_i(t, j)| \leq \varepsilon_i$ and $\lim_{i \rightarrow \infty} \varepsilon_i = 0$.

For each $j \in \{0, 1, \dots, J\}$, $\varphi_i(\cdot, j)$ converge graphically to $\varphi'(\cdot, j)$; this comes directly from the definition of graphical convergence. Since, for each j , the graphs of $\varphi_i(\cdot, j)$ are connected and the graph of $\varphi'(\cdot, j)$ is compact (in fact a compact subset of $\mathbb{R}_{\geq 0} \times \mathbb{N} \times O$), for each j the graphs of $\varphi_i(\cdot, j)$ are eventually bounded with respect to O . This can be shown in the same fashion as [79, Corollary 4.12]. Consequently, there exists a compact set $K \subset O$ and an index i^0 such that $\varphi_i(t, j) \in K$ for all $i > i^0$, all $(t, j) \in \text{dom } \varphi_i$, $j \leq J$.

Let ρ be any admissible perturbation radius. Then let $i_k > i^0$ be such that $|\varepsilon_{i_k}| \leq k^{-1} \min\{\rho(x) \mid x \in K\}$, and let ψ_k be the truncation of φ_{i_k} to $\text{dom } \psi_k := \{(t, j) \in \text{dom } \varphi_{i_k} \mid j \leq J\}$. Fix k . For all k and almost all t such that $(t, j) \in \text{dom } \psi_k$ we have $\psi_k(t, j) + e_{i_k}(t, j) \in C \subset \overline{C}$ and since $|e_{i_k}(t, j)| \leq k^{-1}\rho(\psi_k(t, j))$, we have

$$(\psi_k(t, j) + k^{-1}\rho(\psi_k(t, j))) \cap \overline{C} \neq \emptyset$$

and consequently $\psi_k(t, j) \in \overline{C}^{1/k}$. Furthermore, since for any $\delta \in (0, 1)$ and any x ,

$$f'(x, \kappa_c((x + \delta\rho(x)\mathbb{B}) \cap C)) \subset f((x + \delta\rho(x)\mathbb{B}) \cap C) \subset \overline{f}((x + \delta\rho(x)\mathbb{B}) \cap C) \subset \overline{f}^\delta(x),$$

we have, for all k and almost all t such that $(t, j) \in \text{dom } \psi_k$, $\psi_k(t, j) \in \overline{f}^{1/k}(\psi_k(t, j))$. Similar arguments show that for all $(t, j) \in \text{dom } \psi_k$ such that $(t, j+1) \in \text{dom } \psi_k$ we have $\psi_k(t, j) \in \overline{D}^{1/k}$ and $\psi_k(t, j+1) \in \overline{g}^{1/k}(\psi_k(t, j))$. Consequently, ψ_k is a solution to $\widehat{\mathcal{H}}^{1/k}$, for $k = 1, 2, \dots$. Since the sequence of φ_i 's converges graphically to φ' , by the very definition of graphical convergence, so does the sequence of ψ_k 's. Now, since $\{\psi_k\}_{k=1}^\infty$ is eventually bounded, its graphical limit, that is φ' , is a solution to \mathcal{H} ; see [39, Theorem 5.1 and Theorem 5.4]. Thus, φ' is a Krasovskii solution to \mathcal{H} . Since (T, J) was an arbitrary point in $\text{dom } \varphi$, this is sufficient to guarantee that φ is a Krasovskii solution to \mathcal{H} . \square

In the proof above, the local boundedness and continuity properties from Assumption B.6 are only needed to guarantee that f and g meet Assumption B.1, so that [39, Theorem 5.1 and Theorem 5.4] can be invoked. Furthermore, the proof can be repeated with little change for the case of a set valued g , as considered for Hermes solutions. The results of [39] still apply, and thus we obtain:

Corollary B.11 (Hermes solutions are Krasovskii solutions) *Under Assumption B.1, if a hybrid arc is a Hermes solution to \mathcal{H} , then it is also a Krasovskii solution to \mathcal{H} .*

Proof. Let $\psi : \text{dom } \psi \rightarrow O$ be a Krasovskii solution to \mathcal{H} . Pick $(T, J) \in \text{dom } \psi$ (when $\text{dom } \psi$ is compact, it is enough to consider $(T, J) = \sup \text{dom } \psi$). Let ψ' be the truncation of ψ to $\text{dom } \psi' = \text{dom } \psi \cap ([0, T] \times \{0, 1, \dots, J\})$. By Theorem B.4, there exist $e_i : \text{dom } \psi' \rightarrow \mathbb{R}^n$ and $\varphi_i : \text{dom } \psi' \rightarrow O$ such that $\sup_{(t,j) \in \text{dom } e_i} |e_i(t, j)| \leq \frac{1}{i}$ and which satisfy conditions (V1) and (V2) of Theorem B.4 (with e replaced by e_i and φ replaced by φ_i) and also $|\psi(t, j) - \varphi_i(t, j)| \leq 1/i$ for every $(t, j) \in \text{dom } \varphi_i$. The last bound implies that φ_i converge graphically to ψ' . Since $\sup_{(t,j) \in \text{dom } e_i} |e_i(t, j)| \leq \frac{1}{i}$, ψ is a Hermes solution to \mathcal{H} . \square

B.2 Proofs of results in Chapter 4

B.2.1 Proof of Theorem 4.3

Stability of \mathcal{A} is guaranteed by Theorem 4.16. To show attractivity, pick $\delta > 0$ as in the last paragraph of the proof of Theorem 4.16. Pick any $z \in \mathcal{A} + \delta\mathbb{B}$ and any $x \in \mathcal{S}_{\mathcal{H}}(z)$. Then $\Omega_{\mathcal{H}}(x) \subset N$, where N is given by (B.3), and in particular, $\Omega(x) \subset \mathcal{U}$. Given any $z' \in \Omega(x)$, let $\xi \in \mathcal{S}_{\mathcal{H}}(z')$ be any solution to \mathcal{H} verifying the forward invariance of $\Omega(x)$, i.e. $\text{rge } \xi \subset \Omega(x)$. By Lemma B.12, V is constant along ξ . Suppose that $V(\xi(t, j)) = d > 0$ for all $(t, j) \in \text{dom } \xi$, so in particular $\Omega(x) \cap \mathcal{A} = \emptyset$. If assumptions (a) and (b) hold, then by (a) and Lemma B.12, ξ is instantaneously Zeno since $\Omega(x) \subset N$. Hence, by (b), it converges to \mathcal{A} . But this contradicts V being constant along ξ . If assumptions (a') and (b') hold, then by (a') and Lemma B.12, ξ has no jumps, i.e. it is a complete continuous solution. Hence, by (b'), it converges to \mathcal{A} . This again contradicts V being constant along ξ . Thus, $V(\xi(t, j)) = 0$ for all $(t, j) \in \text{dom } \xi$ and consequently, $\Omega(x) \subset \mathcal{A}$. This implies that x converges to \mathcal{A} .

B.2.2 Proof of Theorem 4.14

The bound (4.4) holds with u_c, u_d replaced by u_C, u_D , for any trajectory x with $\text{rge } x \subset \mathcal{U}$. Consequently, by Theorem 4.17, any precompact trajectory x with $\overline{\text{rge } x} \subset \mathcal{U}$ approaches the largest weakly invariant set in (4.10) for some $r \in V(\mathcal{U})$ (with $G = g$), and here, the reachable set $G(u_D^{-1}(0))$ is just $G(u_D^{-1}(0))$. Since u_C is upper semicontinuous and nonpositive on \mathcal{U} , the set $u_C^{-1}(0)$ is closed, and the closure can be omitted. The same reasoning applies when assumptions involve v_C or w_C , however since these functions need not be upper semicontinuous, the closures are necessary.

B.2.3 Proof of Corollary 4.15

If x is Zeno, then the weak invariance of $\Omega(x)$ can be verified by instantaneous Zeno trajectories. More specifically, given $z \in \Omega(x)$ with $x(t_i, j_i) \rightarrow z$ for some increasing and unbounded sequence of (t_i, j_i) 's, the sequence of trajectories $x_i(t, j) := x(t + t(j_i), j + j_i - 1)$ has a graphically convergent subsequence, the limit ξ of which has the domain equal to $\{0\} \times \mathbb{N}$ (see also the proof of Lemma 4.13) and is such that $\xi(0, 1) = z$. Using this limit in the proof of Lemma B.13 shows that $z \in u_d^{-1}(0) \cap G(u_d^{-1}(0))$.

Regarding (b), note that we can truncate x (and we won't relabel it) so that, for some $\gamma > 0$, $t_{j+1} - t_j \geq \gamma$ for all $j \geq 0$ such that $(t_j, j), (t_{j+1}, j) \in \text{dom } x$. Pick $\bar{z} \in \Omega(x)$ and an increasing and unbounded sequence (t_i, j_i) with the property that $x(t_i, j_i) \rightarrow \bar{z}$. Suppose that the sequence given by $x_i(t, j) := x(t + t_i, j + j_i)$ graphically converges, say to a trajectory $\bar{x} \in \mathcal{S}_{\mathcal{H}}$, and $\bar{x}(0, 0) = \bar{z}$ (consult the proof of Lemma 4.13). If $[0, \gamma/3] \times \{0\} \subset \text{dom } \bar{x}$, then using \bar{x} in the proof of Lemma B.13 shows that $\bar{z} \in u_c^{-1}(0)$. In the opposite case, a graphically convergent subsequence can be extracted from the sequence given by $x'_i(t, j) := x(t + t_i - \gamma/3, j + j_i)$

so that its limit \bar{x}' is such that $[0, \gamma/3] \times \{0\} \subset \text{dom } \bar{x}'$. Furthermore $\bar{x}'(\gamma/3, 0) = \bar{z}$ and $\text{rge } \bar{x}' \subset \Omega(x)$ (so \bar{x}' verifies the weak backward invariance of $\Omega(x)$ at \bar{z}), and using \bar{x}' in the proof of Lemma B.13 shows that $\bar{z} \in \overline{u_c^{-1}(0)}$.

B.2.4 Proof of Theorem 4.16

Assume (\star) and let $\epsilon > 0$ be small enough so that $\mathcal{A} + 2\epsilon\mathbb{B} \subset \mathcal{U}$. We claim that there exists c_ϵ such that

$$\begin{aligned} V(z) \leq c_\epsilon, z \in (\mathcal{A} + 2\epsilon\mathbb{B}) \cap (C \cup D) \\ \Rightarrow z \in (\mathcal{A} + \epsilon\mathbb{B}) \cap (C \cup D), G(z) \subset (\mathcal{A} + \epsilon\mathbb{B}) \cap (C \cup D). \end{aligned} \quad (\text{B.2})$$

Certainly, as V is positive definite on $C \cup D$ with respect to \mathcal{A} , there exists $r'_\epsilon > 0$ so that for $z \in (\mathcal{A} + 2\epsilon\mathbb{B}) \cap (C \cup D)$, $V(z) \leq r'_\epsilon$ implies $z \in (\mathcal{A} + \epsilon\mathbb{B}) \cap (C \cup D)$. Now note that as $u_D(z) \leq 0$ for all $z \in \mathcal{A}$ and V is positive definite on $C \cup D$ with respect to \mathcal{A} , $G(\mathcal{A} \cap (C \cup D)) \subset \mathcal{A} \cap (C \cup D)$. By outer semicontinuity and local boundedness, the mapping G is ‘‘upper semicontinuous’’, in particular there exists $\gamma > 0$ so that $G(\mathcal{A} + \gamma\mathbb{B}) \subset \mathcal{A} + \epsilon\mathbb{B}$. Using positive definiteness of V again, one can find $r''_\epsilon > 0$ so that $z \in (\mathcal{A} + 2\epsilon\mathbb{B}) \cap (C \cup D)$ and $V(z) \leq r''_\epsilon$ imply $z \in (\mathcal{A} + \gamma\mathbb{B}) \cap (C \cup D)$. To make the implication (B.2) true, one now takes $r_\epsilon = \min\{r'_\epsilon, r''_\epsilon\}$.

Based on (B.2), we claim that the set

$$N = \{z \in (\mathcal{A} + \epsilon\mathbb{B}) \cap (C \cup D) \mid V(z) \leq r_\epsilon\} \quad (\text{B.3})$$

is (strongly) forward invariant for \mathcal{H} , that is for any $x \in \mathcal{S}_{\mathcal{H}}(z)$ with $z \in N$, $\text{rge } x \subset N$. Indeed, pick any $z \in N$ and let $x \in \mathcal{S}_{\mathcal{H}}(z)$. If $(0, 1) \in \text{dom } x$, then $x(0, 1) \in G(z) \subset (\mathcal{A} + \epsilon\mathbb{B}) \cap (C \cup D)$. If $[0, T] \times \{0\} \subset \text{dom } x$ and for some $t' \in (0, T]$, $x(t', 0) \notin N$, then by continuity of $t \mapsto x(t, 0)$, for some $t'' \in (0, t']$, $x(t'', 0) \notin N$ but $x(t'', 0) \in (\mathcal{A} + \epsilon\mathbb{B}) \cap (C \cup D)$ and $V(x(t'', 0)) \leq r_\epsilon$ (the latter is true as V is nonincreasing along x). By equation (B.2), $x(t'', 0) \in N$. This is a contradiction. Thus $x([0, T], 0) \subset N$. The facts just shown are enough to conclude that N is forward invariant.

Finally, by continuity of V , given any small enough $\epsilon > 0$ and $r_\epsilon > 0$ so that (B.2) holds, we can find $\delta \in (0, \epsilon)$ so that $z \in (\mathcal{A} + \delta\mathbb{B}) \cap (C \cup D)$ implies $V(z) \leq r_\epsilon$. Relying on forward invariance of N , each maximal $x \in \mathcal{S}_{\mathcal{H}}(z)$ with $z \in \mathcal{A} + \delta\mathbb{B}$ is so that $\text{rge } x \subset \mathcal{A} + \epsilon\mathbb{B}$. Thus, \mathcal{A} is stable.

Now assume (\star) and $(\star\star)$. To show attractivity, note that given $\epsilon > 0$ with $\mathcal{A} + 2\epsilon\mathbb{B} \subset \mathcal{U}$, we can find $r_\epsilon \in (0, r)$, r as in condition $(\star\star)$ so that N in (B.3) is forward invariant (i.e. one can pick r_ϵ in the proof of stability of \mathcal{A} arbitrarily small). In particular, if δ is associated with ϵ as in the paragraph above, any $x \in \mathcal{S}_{\mathcal{H}}(z)$ with $z \in \mathcal{A} + \delta\mathbb{B}$ is precompact. As such, by Theorem 4.14, it converges to the largest weakly invariant subset of the set given by (4.6). It must be the case that $r' \leq r_\epsilon$ as V is nonincreasing along x , and then $r' < r^*$. As $\Omega(x)$ is nonempty, x converges to the largest weakly invariant subset of (4.6) with $r = 0$ which, by positive definiteness of V , is a subset of \mathcal{A} . Hence, \mathcal{A} is attractive.

B.2.5 Proof of Theorem 4.17

The next two lemmas allow us to establish the V invariance principle for hybrid trajectories.

Lemma B.12 (V constant on $\Omega(x)$) *Suppose a function $V : O \rightarrow \mathbb{R}$ is nonincreasing along a hybrid trajectory x . If V is lower semicontinuous, then for some $r \in \mathbb{R}$, $V(\Omega(x)) \subset (-\infty, r]$. If V is continuous, then for some $r \in \mathbb{R}$, $V(\Omega(x)) = r$.*

Proof. If $\Omega(x) = \emptyset$, there is nothing to prove. Otherwise, pick any $\bar{z} \in \Omega(x)$. By the definition of $\Omega(x)$, there exists $\{(t_i, j_i)\}_{i=1}^\infty$, an increasing and unbounded sequence in $\text{dom } x$, satisfying $x(t_i, j_i) \rightarrow \bar{z}$. Let $\bar{r} =$

$\liminf_{i \rightarrow \infty} V(x(t_i, j_i))$. Pick any $z \in \Omega(x)$, and an increasing and unbounded sequence $\{(t_k, j_k)\}_{k=1}^\infty$ in $\text{dom } x$ with $x(t_k, j_k) \rightarrow z$. There exists a subsequence $\{(t_{k_i}, j_{k_i})\}_{i=1}^\infty$ of $\{(t_k, j_k)\}_{k=1}^\infty$ such that for $i = 1, 2, \dots$, $(t_i, j_i) \preceq (t_{k_i}, j_{k_i})$, and as V is nonincreasing along x , $V(x(t_i, j_i)) \geq V(x(t_{k_i}, j_{k_i}))$. If V is lower semicontinuous, taking limits as $i \rightarrow \infty$ yields $\bar{r} \geq \liminf_{i \rightarrow \infty} V(x(t_{k_i}, j_{k_i})) \geq V(z)$. If V is continuous, then let $\bar{r} = \lim V(x(t_i, j_i)) = V(\bar{z})$, and considering a subsequence $\{(t_{i_k}, j_{i_k})\}_{k=1}^\infty$ of $\{(t_i, j_i)\}_{i=1}^\infty$ so that $(t_k, j_k) \preceq (t_{i_k}, j_{i_k})$ and $V(x(t_k, j_k)) \geq V(x(t_{i_k}, j_{i_k}))$ yields, in the limit, that $V(z) \geq \bar{r}$. Thus, if V is continuous, $V(z) = \bar{r}$. \square

Lemma B.13 (invariant sets with constant V) *Let $V : O \rightarrow \mathbb{R}$, $u_c, u_d : O \rightarrow [-\infty, +\infty]$ be any functions, the set $\mathcal{U} \subset O$ be such that $u_c(z) \leq 0$, $u_d(z) \leq 0$ for all $z \in \mathcal{U}$ and such that for any trajectory $\xi \in \mathcal{S}_{\mathcal{H}}$ with $\text{rge } \xi \subset \mathcal{U}$, (4.4) holds for any $(t, j), (t', j') \in \text{dom } \xi$ such that $(t, j) \preceq (t', j')$. Let $\mathcal{M} \subset \mathcal{U}$ be a set such that $V(\mathcal{M}) = r$ for some $r \in \mathbb{R}$. If \mathcal{M} is weakly forward invariant, then $\mathcal{M} \subset \overline{u_c^{-1}(0)} \cup u_d^{-1}(0)$. If \mathcal{M} is weakly backward invariant, then $\mathcal{M} \subset \overline{u_c^{-1}(0)} \cup G(u_d^{-1}(0))$. If \mathcal{M} is weakly invariant, then*

$$\mathcal{M} \subset \overline{u_c^{-1}(0)} \cup (u_d^{-1}(0) \cap G(u_d^{-1}(0))).$$

Proof. For any trajectory $x \in \mathcal{S}_{\mathcal{H}}$ such that $x(t, j) \in \mathcal{M}$ for $(t, j) \in \text{dom } x$ with $(\underline{t}, \underline{j}) \preceq (t, j) \preceq (\bar{t}, \bar{j})$ for some $(\underline{t}, \underline{j})$ and (\bar{t}, \bar{j}) in $\text{dom } x$, the fact that V is constant along trajectories in \mathcal{M} gives

$$\int_{\underline{t}}^{\bar{t}} u_c(x(s, j(s))) ds + \sum_{i=\underline{j}+1}^{\bar{j}} u_d(x(t(i), i-1)) = 0.$$

Pick any $z \in \mathcal{M}$. If \mathcal{M} is weakly forward invariant, then there exists a nontrivial $x \in \mathcal{S}_{\mathcal{H}}(z)$ with $\text{rge } x \subset \mathcal{M}$. If $(0, 1) \in \text{dom } x$, applying the above equation to $(\underline{t}, \underline{j}) = (0, 0)$, $(\bar{t}, \bar{j}) = (0, 1)$ yields $u_d(x(0, 0)) = 0$, which shows that $z \in \overline{u_d^{-1}(0)}$. If $(T, 0) \in \text{dom } x$ for some $T > 0$, then applying the equation to $(0, 0)$, $(T, 0)$ yields $\int_0^T u_c(x(s, 0)) ds = 0$. As u_c is nonpositive, it must be the case that $u_c(x(s, 0)) = 0$ for almost all $s \in [0, T]$. Hence, $z \in \overline{u_c^{-1}(0)}$. If \mathcal{M} is weakly backward invariant, then there exists $x \in \mathcal{S}_{\mathcal{H}}(z^*)$, $z^* \in \mathcal{M}$, such that $x(t^*, j^*) = z$, $t^* + j^* > 1$, and $x(t, j) \in \mathcal{M}$ for all $(t, j) \preceq (t^*, j^*)$. If $(t^*, j^* - 1) \in \text{dom } x$, then the inequality above with $(\underline{t}, \underline{j}) = (t^*, j^* - 1)$, $(\bar{t}, \bar{j}) = (t^*, j^*)$ shows that $u_d(x(t^*, j^* - 1)) = 0$ and so $z = x(t^*, j^*) \in G(u_d^{-1}(0))$. If $(t^* - T, j^*) \in \text{dom } x$ for some $T > 0$, then an argument similar to the one for forward invariance can be given. \square

For any precompact trajectory x , from Lemma 4.13 we know that x approaches its ω -limit, which is weakly invariant. This ω -limit is the same as the ω -limit of the truncation of x to (t, j) 's with $(T, J) \preceq (t, j) \in \text{dom } x$. By (4.4), the function V is nonincreasing along the truncation. Thus V is constant on $\Omega(x)$ by Lemma B.12. Now note that $\Omega(x)$ is a subset of \mathcal{U} intersected with $\{\text{rge } \xi \mid \xi \in \mathcal{S}_{\mathcal{H}}, \text{rge } \xi \subset \mathcal{U}\}$. In turn, this intersection meets the conditions placed on the set \mathcal{U} in Lemma B.13. Thus, invoking Lemma B.13, with \mathcal{M} also replaced by $\Omega(x)$, finishes the proof.

B.2.6 Proof of Theorem 4.31

(1 \Rightarrow 2) Let \mathcal{M} be the largest weakly invariant set in K . Suppose that there exists $z \in \mathcal{M} \setminus \mathcal{A}$. Let $\epsilon = |z|_{\mathcal{A}}$. By stability of \mathcal{A} relative to K , there exists $\delta > 0$ such that every hybrid trajectory $\xi \in \mathcal{S}_{\mathcal{H}}$ with $\text{rge } \xi \subset K$ and $\xi(0, 0) \in \mathcal{A} + \delta\mathbb{B}$ satisfies $\text{rge } \xi \subset \mathcal{A} + \frac{\epsilon}{2}\mathbb{B}$. By weak backward invariance of \mathcal{M} , there exists a trajectory $x_1 \in \mathcal{S}_{\mathcal{H}}$ such that for some $(t_1, j_1) \in \text{dom } x_1$, $t_1 + j_1 \geq 1$, $x_1(t_1, j_1) = z$ and $x_1(t, j) \in \mathcal{M}$ for all $(t, j) \preceq (t_1, j_1)$, $(t, j) \in \text{dom } x_1$ (in particular $x_1(0, 0) \in \mathcal{M}$). Note that by stability, since $x_1(t_1, j_1) \notin \mathcal{A} + \frac{\epsilon}{2}\mathbb{B}$, we have $x_1(t, j) \in \mathcal{M} \setminus (\mathcal{A} + \delta\mathbb{B})$ for all $(t, j) \in \text{dom } x_1$, $(t, j) \preceq (t_1, j_1)$. In this way, we can construct a sequence $x_i \in \mathcal{S}_{\mathcal{H}}$

such that for every $i > 0$, there exists $(t_i, j_i) \in \text{dom } x_i$, $t_i + j_i \geq i$ with $x_i(t_i, j_i) = z$ and $x_i(t, j) \in \mathcal{M} \setminus (\mathcal{A} + \delta\mathbb{B})$ for all $(t, j) \preceq (t_i, j_i)$, $(t, j) \in \text{dom } x_i$. As K is compact, the sequence $\{x_i\}_{i=1}^\infty$ is locally eventually bounded. By the hybrid basic conditions, it has a subsequence (that we won't relabel) converging to some $x \in \mathcal{S}_{\mathcal{H}}$, with $x_i(0, 0) \rightarrow x(0, 0) \in \mathcal{M}$. Since $\text{dom } x_i$ are ‘‘increasing’’, x is complete; see [39, Lemma 3.5]. Finally, $\text{rge } x \subset \mathcal{M} \setminus (\mathcal{A} + \delta\mathbb{B})$, and also $\text{rge } x \subset K$. The second inclusion, by detectability of \mathcal{A} relative to K , relative stability of \mathcal{A} , and Lemma 4.29, implies that x converges to \mathcal{A} . This is a contradiction with the first inclusion.

(2 \Rightarrow 1) Any trajectory $x \in \mathcal{S}_{\mathcal{H}}$ with $\text{rge } x \subset K$ is precompact, by compactness of K , and as such, it converges to its ω -limit. Since the ω -limit is invariant and a subset of K , it must be a subset of \mathcal{A} . Hence, x converges to \mathcal{A} .

B.3 Proofs of results in Chapter 5

Some of the following results use theorems from [39], which for completeness are reproduced below.

Theorem B.14 (*KLL-bound* [39, Theorem 6.5]) *Suppose that the basin of attraction $\mathcal{B}_{\mathcal{A}}$ of a compact set $\mathcal{A} \subset O$ is open relative to $C \cup D$. Let $U \subset O$ be any open set such that $\mathcal{B}_{\mathcal{A}} = (C \cup D) \cap U$. For each proper indicator $\omega : U \rightarrow \mathbb{R}_{\geq 0}$ of \mathcal{A} with respect to U there exists $\beta \in \text{KLL}$ such that, for all solutions x starting in $\mathcal{B}_{\mathcal{A}}$,*

$$\omega(x(t, j)) \leq \beta(\omega(x(0, 0)), t, j) \quad \forall (t, j) \in \text{dom } x. \quad (\text{B.4})$$

Theorem B.15 (*KLL-bound under perturbations* [39, Theorem 6.6]) *Suppose that the basin of attraction $\mathcal{B}_{\mathcal{A}}$ of a compact set $\mathcal{A} \subset O$ is open relative to $C \cup D$, $U \subset O$ is any open set such that $\mathcal{B}_{\mathcal{A}} = (C \cup D) \cap U$, and $\omega : U \rightarrow \mathbb{R}_{\geq 0}$ is a proper indicator of \mathcal{A} with respect to U , and $\beta \in \text{KLL}$ is such that, for all solutions starting in $\mathcal{B}_{\mathcal{A}}$, (B.4) holds. Assume that the family of perturbed hybrid systems \mathcal{H}_δ , $\delta \in (0, 1)$, has the convergence property (CP) in [39, Section V]. Then, for each compact set $K \subset \mathcal{B}_{\mathcal{A}}$ and each $\varepsilon > 0$ there exists $\delta^* > 0$ such that for each $\delta \in (0, \delta^*]$, the solutions x_δ of \mathcal{H}_δ from K satisfy, for all $(t, j) \in \text{dom } x_\delta$,*

$$\omega(x_\delta(t, j)) \leq \beta(\omega(x_\delta(0, 0)), t, j) + \varepsilon \quad \forall (t, j) \in \text{dom } x.$$

B.3.1 Proof of Theorem 5.12

To show Theorem 5.12, we first exploit the asymptotic stability of \mathcal{A} with respect to \mathcal{H}_{cl} . Using the properties of the data defining the closed-loop system \mathcal{H}_{cl} to invoke the converse Lyapunov theorems for hybrid systems in [23], there exists a smooth function $V : \mathbb{R}^{n_p} \times \mathbb{R}^{n_c} \rightarrow \mathbb{R}_{\geq 0}$ and class- \mathcal{K}_∞ functions α_1, α_2 satisfying

$$\text{i) } \forall (x, x_c) \in \mathbb{R}^{n_p} \times \mathbb{R}^{n_c} : \alpha_1(|(x, x_c)|_{\mathcal{A}}) \leq V(x, x_c) \leq \alpha_2(|(x, x_c)|_{\mathcal{A}}), \quad (\text{B.5})$$

$$\text{ii) } \forall (x, x_c) \in C_c : \langle \nabla V(x, x_c), [f_p(x, \kappa(x, x_c))^T, f_c(x, x_c)^T]^T \rangle \leq -V(x, x_c), \quad (\text{B.6})$$

$$\text{iii) } \forall (x, x_c) \in D_c : \max_{\xi \in G_c(x, x_c)} V(x, \xi) \leq e^{-1} V(x, x_c), \quad (\text{B.7})$$

where we have used the properties of the data of \mathcal{H}_{cl} .

By using continuity of V and (B.6), for each $0 < \delta_s \leq \Delta_s < \infty$ there exists $\bar{\delta} > 0$ and $\gamma_0 \in (0, 1)$ such that for all $(x, x_c) \in (C_c + \bar{\delta}\mathbb{B}) \cap \Omega_{\mathcal{A}}(\delta_s, \Delta_s)$

$$\langle \nabla V(x, x_c), [f(x, \kappa_c(x, x_c))^T, f_c(x, x_c)^T]^T \rangle \leq -\gamma_0 V(x, x_c).$$

By local boundedness of $(x, x_c) \mapsto f_p(x, \kappa_c(x, x_c))$ and f_c , there exists $M > 0$ such that for all $(x, x_c) \in (C_c + \bar{\delta}\mathbb{B}) \cap \Omega_{\mathcal{A}}(0, \Delta_s)$

$$|[f_p(x, \kappa_c(x, x_c))^T, f_c(x, x_c)^T]^T| \leq M .$$

Let $0 < \delta < \bar{\delta}$ and pick T_s and T_c so that $\max\{T_s, T_c\} < \delta/M$. Note that with this construction, when flows are enabled, points in C_c are not reachable from $\mathbb{R}^n \times \mathbb{R}^{n_c} \setminus (C_c + \delta\mathbb{B})$ and points in $\mathbb{R}^n \times \mathbb{R}^{n_c} \setminus (C_c + \delta\mathbb{B})$ are not reachable from C_c .

We extend the hybrid system $\mathcal{H}_{cl}^{S/H}$ with two auxiliary states: a continuous state denoted by \tilde{z}_h and a discrete state denoted by q . The continuous state \tilde{z}_h is so that its update law is equal to the one for z_c , while its continuous dynamics are so that the flows of \tilde{z}_h are governed by f_c , i.e.

$$\dot{\tilde{z}}_h = f_c(x, \tilde{z}_h) \tag{B.8}$$

when $\tau_s \in [0, T_s]$ and $\tau_c \in [0, T_c]$.

The discrete state q assumes values in the set $\{0, 1\}$. We design the update law for q so that it is equal to 1 when the new values of (z_m, z_h) are in the proximity of the flow set C_c , and zero when they are away from the flow set C_c . During flows, q remains constant. We denote the extended hybrid system by \mathcal{H}_{cl}^{S/H_e} .

Let $\lambda_1, \lambda_2, \lambda_3 \in \mathbb{R}$ be constants satisfying $\lambda_1, \lambda_2 > 0$, $\lambda_3 < 0$, and let $W(x, \tilde{z}_h, \tau_s, \tau_c, q)$ be given by

$$W(x, \tilde{z}_h, \tau_s, \tau_c, q) := \exp(\lambda_1 \tau_s) \exp(\lambda_2 q \tau_c) \exp(\lambda_3 (1 - q) \tau_c) V(x, \tilde{z}_h) . \tag{B.9}$$

The function W is constructed by combining the Lyapunov function V for the nominal closed-loop system \mathcal{H}_{cl} and exponential terms that depend on the timers τ_s, τ_c and the logic state q . The purpose of the exponential terms in W is to balance the increase of

$$\langle \nabla V(x, \tilde{z}_h), [f(x, \kappa_c(z_s, z_c))^T, f_c(x, \tilde{z}_h)^T]^T \rangle$$

along flows and of $V(x, \tilde{z}_h^+) - V(x, \tilde{z}_h)$ at jumps. Clearly, during flows, the terms $\exp(\lambda_1 \tau_s)$ and $\exp(\lambda_2 q \tau_c)$ for $q = 1$ decrease. However, at jumps, the terms $\exp(\lambda_2 q \tau_c)$ and $\exp(\lambda_3 (1 - q) \tau_c)$ may increase or decrease depending on the value of q^+ . Therefore, the constants λ_1, λ_2 , and λ_3 have to be designed carefully to obtain decrease both at flows . Let

$$e_1 := \tilde{z}_h - g_f(z_m, z_c), \quad e_2 := z_m - x, \quad e_3 := z_c - \tilde{z}_h, \quad e_4 := z_s - x .$$

The partial closed-loop system state $[x, \tilde{z}_h, \tau_s, \tau_c, q]^T$ has continuous dynamics given by

$$\tilde{f}(x, \tilde{z}_h, \tau_s, \tau_c, q) := [f(x, \kappa_c(z_s, z_c))^T, f_c(x, \tilde{z}_h)^T, 1, 1, 0]^T .$$

The following lemma states a decrease property of W along flows for a proper choice of its constants.

Lemma B.16 (decrease along flows) *Let Assumptions 5.1, 5.2, and 5.3 hold. Then, for each positive number δ_s and Δ_s satisfying $0 < \delta_s \leq \Delta_s < \infty$ there exist $\varepsilon > 0$ and constants $\lambda_1 > 0$, $\lambda_2 > 0$, and $\lambda_3 < 0$ of W such that*

$$\langle \nabla W(x, \tilde{z}_h, \tau_s, \tau_c, q), \tilde{f}(x, \tilde{z}_h, \tau_s, \tau_c, q) \rangle \leq -\varepsilon W(x, \tilde{z}_h, \tau_s, \tau_c, q)$$

for points

$$(F1) \quad (x, \tilde{z}_h, \tau_s, \tau_c, q, |[e_3^T, e_4^T]^T|) \in ((C_c + \delta\mathbb{B}) \cap \Omega_{\mathcal{A}}(\delta_s, \Delta_s)) \times [0, T_s] \times [0, T_c] \times \{1\} \times \delta_{34}\mathbb{B};$$

$$(F2) \quad (x, \tilde{z}_h, \tau_s, \tau_c, q, |[e_3^T, e_4^T]^T|) \in \Omega_{\mathcal{A}}(\delta_s, \Delta_s) \times [0, T_s] \times [0, T_c] \times \{0\} \times \delta_{34}\mathbb{B};$$

for some $\delta_{34} > 0$.

Proof. When $\tau_s \leq T_s$ and $\tau_c \leq T_c$, with the closed-loop dynamics we obtain

$$\langle \nabla W(x, \tilde{z}_h, \tau_s, \tau_c, q), \tilde{f}(x, \tilde{z}_h, \tau_s, \tau_c, q) \rangle \leq (\lambda_1 + \lambda_2 q + \lambda_3(1 - q)) \exp(\lambda_1 \tau_s) \exp(\lambda_2 q \tau_c) \exp(\lambda_3(1 - q) \tau_c) V(x, \tilde{z}_h) + \exp(\lambda_1 \tau_s) \exp(\lambda_2 q \tau_c) \exp(\lambda_3(1 - q) \tau_c) \langle \nabla V(x, \tilde{z}_h), [f(x, \kappa_c(z_s, z_c))^T, f_c(x, \tilde{z}_h)^T]^T \rangle.$$

By operating with the last term, we can rewrite the inequality as follows:

$$\langle \nabla W(x, \tilde{z}_h, \tau_s, \tau_c, q), \tilde{f}(x, \tilde{z}_h, \tau_s, \tau_c, q) \rangle \leq (\lambda_1 + \lambda_2 q + \lambda_3(1 - q)) \exp(\lambda_1 \tau_s) \exp(\lambda_2 q \tau_c) \exp(\lambda_3(1 - q) \tau_c) V(x, \tilde{z}_h) + \exp(\lambda_1 \tau_s) \exp(\lambda_2 q \tau_c) \exp(\lambda_3(1 - q) \tau_c) \langle \nabla V(x, \tilde{z}_h), [f(x, \kappa_c(x, \tilde{z}_h))^T, f_c(x, \tilde{z}_h)^T]^T \rangle \exp(\lambda_1 \tau_s) \exp(\lambda_2 q \tau_c) \exp(\lambda_3(1 - q) \tau_c) \tilde{\rho}(x, \tilde{z}_h, \tau_s, \tau_c, q, e_3, e_4)$$

where

$$\tilde{\rho}(x, \tilde{z}_h, \tau_s, \tau_c, q, e_3, e_4) := |\nabla V(x, \tilde{z}_h)| |f(x, \kappa_c(x + e_4, \tilde{z}_h + e_3)) - f(x, \kappa_c(x, \tilde{z}_h))|.$$

The function $\tilde{\rho}$ is continuous and for every $(x, \tilde{z}_h, \tau_s, \tau_c, q) \in \mathbb{R}^n \times \mathbb{R}^m \times \mathbb{R}_{\geq 0}^2 \times \{0, 1\}$ then we have

$$\tilde{\rho}(x, \tilde{z}_h, \tau_s, \tau_c, q, 0, 0) = 0.$$

For all $(x, \tilde{z}_h) \in (C_c + \delta\mathbb{B}) \cap \Omega_{\mathcal{A}}(\delta_s, \Delta_s)$ and $q = 1$, with the property of V in (B.8) there exists $\lambda_1 > 0$, $\lambda_2 > 0$, and $\varepsilon > 0$ satisfying $-\gamma_0 + \lambda_1 + \lambda_2 < -2\varepsilon$ that yields

$$\langle \nabla W(x, \tilde{z}_h, \tau_s, \tau_c, q), \tilde{f}(x, \tilde{z}_h, \tau_s, \tau_c, q) \rangle \leq \exp(\lambda_1 \tau_s) \exp(\lambda_2 \tau_c) (-2\varepsilon V(x, \tilde{z}_h) + \tilde{\rho}(x, \tilde{z}_h, \tau_s, \tau_c, q, e_3, e_4)).$$

Since $\tilde{\rho}$ is continuous and vanishes with (e_3, e_4) , there exists small enough $\delta_{34} > 0$ so that $(x, \tilde{z}_h, \tau_s, \tau_c, |[e_3^T, e_4^T]^T|)$ in

$$\Omega_{\mathcal{A}}(\delta_s, \Delta_s) \times [0, T_s] \times [0, T_c] \times \delta_{34}\mathbb{B}$$

implies

$$\tilde{\rho}(x, \tilde{z}_h, \tau_s, \tau_c, q, e_3, e_4) < \varepsilon V(x, \tilde{z}_h).$$

Then

$$\langle \nabla W(x, \tilde{z}_h, \tau_s, \tau_c, q), \tilde{f}(x, \tilde{z}_h, \tau_s, \tau_c, q) \rangle \leq -\varepsilon W(x, \tilde{z}_h, \tau_s, \tau_c, q)$$

for all $(x, \tilde{z}_h, \tau_s, \tau_c, q, |[e_3^T, e_4^T]^T|) \in ((C_c + \delta\mathbb{B}) \cap \Omega_{\mathcal{A}}(\delta_s, \Delta_s)) \times [0, T_s] \times [0, T_c] \times \{1\} \times \delta_{34}\mathbb{B}$.

When $q = 0$ we have that

$$\langle \nabla W(x, \tilde{z}_h, \tau_s, \tau_c, q), \tilde{f}(x, \tilde{z}_h, \tau_s, \tau_c, q) \rangle \leq (\lambda_1 + \lambda_3) \exp(\lambda_1 \tau_s) \exp(\lambda_3 \tau_c) V(x, \tilde{z}_h) + \exp(\lambda_1 \tau_s) \exp(\lambda_3 \tau_c) \langle \nabla V(x, \tilde{z}_h), [f(x, \kappa_c(x, \tilde{z}_h))^T, f_c(x, \tilde{z}_h)^T]^T \rangle + \exp(\lambda_1 \tau_s) \exp(\lambda_3 \tau_c) \tilde{\rho}(x, \tilde{z}_h, \tau_s, \tau_c, q, e_3, e_4).$$

Let M_V be such that

$$\max_{(x, \tilde{z}_h) \in \Omega_{\mathcal{A}}(\delta_s, \Delta_s)} \{|\nabla V(x, \tilde{z}_h)| |[f(x, \kappa_c(x, \tilde{z}_h))^T, f_c(x, \tilde{z}_h)^T]^T|\} < M_V.$$

Let $\mu \geq \frac{M_V}{\alpha_1(\delta_s)}$. It follows by (B.5) that

$$|\langle \nabla V(x, \tilde{z}_h), [f(x, \kappa_c(x, \tilde{z}_h))^T, f_c(x, \tilde{z}_h)^T]^T \rangle| \leq \mu V(x, \tilde{z}_h)$$

for all $(x, \tilde{z}_h) \in \Omega_{\mathcal{A}}(\delta_s, \Delta_s)$. Then choose $\lambda_3 < 0$ so that $\lambda_1 + \lambda_3 + \mu < -\frac{3}{2}\varepsilon$. Proceeding as for $q = 1$, we obtain

$$\langle \nabla W(x, \tilde{z}_h, \tau_s, \tau_c, q), \tilde{f}(x, \tilde{z}_h, \tau_s, \tau_c, q) \rangle \leq -\varepsilon W(x, \tilde{z}_h, \tau_s, \tau_c, q)$$

for all $(x, \tilde{z}_h, \tau_s, \tau_c, q, |[e_3^T, e_4^T]^T|) \in \Omega_{\mathcal{A}}(\delta_s, \Delta_s) \times [0, T_s] \times [0, T_c] \times \{0\} \times \delta_{34}\mathbb{B}$. \square

Lemma B.17 (decrease along jumps) *Let Assumptions 5.1, 5.2, and 5.3 hold. Then for each positive number δ_s and Δ_s satisfying $0 < \delta_s \leq \Delta_s < \infty$ and each constants $\lambda_1 > 0$, $\lambda_2 > 0$, and $\lambda_3 < 0$ of W and $T_c, T_s > 0$ satisfying $T_c \lambda_3 \in (-1, 0)$ there exists $\rho \in (0, 1)$ such that*

$$W(x^+, \tilde{z}_h^+, \tau_s^+, \tau_c^+, q^+) \leq \rho W(x, \tilde{z}_h, \tau_s, \tau_c, q)$$

for points

$$(J1) \quad (x, \tilde{z}_h, \tau_s, \tau_c, q) \in \Omega_{\mathcal{A}}(\delta_s, \Delta_s) \times [T_s, +\infty) \times [0, T_c] \times \{0, 1\};$$

$$(J2) \quad (z_m, z_c) \in C_c, (x, \tilde{z}_h, \tau_s, \tau_c, q, |e_1|) \in \Omega_{\mathcal{A}}(\delta_s, \Delta_s) \times [0, T_s] \times [T_c, +\infty) \times \{1\} \times \delta_1\mathbb{B};$$

$$(J3) \quad (z_m, z_c) \in D_c, (x, \tilde{z}_h, \tau_s, \tau_c, q, |[e_2^T, e_3^T]^T|) \in \Omega_{\mathcal{A}}(\delta_s, \Delta_s) \times [0, T_s] \times [T_c, +\infty) \times \{0, 1\} \times \delta_{23}\mathbb{B};$$

for some $\delta_1, \delta_{23} > 0$.

Proof. When $\tau_s \geq T_s$, for every $\lambda_1 > 0$, $T_s > 0$ there exists $\rho_1 \in (0, 1)$ that satisfies $\rho_1 > \exp(-\lambda_1 T_s)$ and yields

$$W(x^+, \tilde{z}_h^+, \tau_s^+, \tau_c^+, q^+) = \exp(\lambda_2 q \tau_c) \exp(\lambda_3 (1 - q) \tau_c) V(x, \tilde{z}_h) \leq \rho_1 W(x, \tilde{z}_h, \tau_s, \tau_c, q)$$

for all $(x, \tilde{z}_h, \tau_s, \tau_c, q) \in \Omega_{\mathcal{A}}(\delta_s, \Delta_s) \times [T_s, +\infty) \times [0, T_c] \times \{0, 1\}$ since $\lambda_2 > 0$.

When $\tau_c \geq T_c$, $(z_m, z_c) \in C_c \setminus D_c$, and $q = 1$, the update law yields

$$W(x^+, \tilde{z}_h^+, \tau_s^+, \tau_c^+, q^+) = \exp(\lambda_1 \tau_s) V(x, g_{f_c}(z_m, z_c)). \quad (\text{B.10})$$

Since V is smooth on \mathbb{R}^n , for every $\delta' > 0$ there exists $L > 0$ such that $|\eta_1 - \eta_2| \leq \delta'$, $\eta_1, \eta_2 \in \Omega_{\mathcal{A}}(0, \Delta_s) \cap \mathbb{R}^n$ implies

$$|V(\eta_1) - V(\eta_2)| \leq L \delta'. \quad (\text{B.11})$$

Let $\delta_1 > 0$ to be fixed later. Using (B.11) with $\delta' = \delta_1$ in (B.10), for every $(x, \tilde{z}_h, \tau_s, \tau_c, q, |e_1|) \in \Omega_{\mathcal{A}}(\delta_s, \Delta_s) \times [0, T_s] \times [T_c, +\infty) \times \{1\} \times \delta_1\mathbb{B}$ we obtain

$$W(x^+, \tilde{z}_h^+, \tau_s^+, \tau_c^+, q^+) \leq \exp(\lambda_1 \tau_s) (V(x, \tilde{z}_h) + L \delta_1).$$

Since $V(x, \tilde{z}_h) \geq \alpha_1(\delta_s)$ for every $(x, \tilde{z}_h) \in \Omega_{\mathcal{A}}(\delta_s, \Delta_s)$, for every $\lambda_2 > 0$, $T_c > 0$ there exists $\rho_2 \in (0, 1)$ satisfying $\rho_2 > \exp(-\lambda_2 T_c)$ and by fixing δ_1 to satisfy $\delta_1 < \frac{1}{L} \alpha_1(\delta_s) (\rho_2 \exp(\lambda_2 T_c) - 1)$ we obtain

$$W(x^+, \tilde{z}_h^+, \tau_s^+, \tau_c^+, q^+) \leq \rho_2 W(x, \tilde{z}_h, \tau_s, \tau_c, q) \quad (\text{B.12})$$

for all $(z_m, z_c) \in C_c \setminus D_c$, $(x, \tilde{z}_h, \tau_s, \tau_c, q, |e_1|) \in \Omega_{\mathcal{A}}(\delta_s, \Delta_s) \times [0, T_s] \times [T_c, +\infty) \times \{1\} \times \delta_1\mathbb{B}$.

When $\tau_c \geq T_c$ and $(z_m, z_c) \in D_c \setminus D_c$, the update law yields

$$W(x^+, \tilde{z}_h^+, \tau_s^+, \tau_c^+, q^+) = \exp(\lambda_1 \tau_s) V(x, g_c(z_m, z_c)) \quad (\text{B.13})$$

Let $\delta_{23} > 0$ to be fixed later. Using $\delta' = \delta_{23}$ in (B.11) and the property of V at jumps in (B.7), for every $(x, \tilde{z}_h, \tau_s, \tau_c, q, |e_2|) \in \Omega_{\mathcal{A}}(\delta_s, \Delta_s) \times [0, T_s] \times [T_c, +\infty) \times \{1\} \times \delta_{23}\mathbb{B}$ we obtain

$$W(x^+, \tilde{z}_h^+, \tau_s^+, \tau_c^+, q^+) \leq \exp(\lambda_1 \tau_s)(e^{-1}V(z_m, z_c) + L\delta_{23})$$

Using the smoothness of V again, for every

$$(x, \tilde{z}_h, \tau_s, \tau_c, q, |[e_2^T, e_3^T]^T|) \in \Omega_{\mathcal{A}}(\delta_s, \Delta_s) \times [0, T_s] \times [T_c, +\infty) \times \{1\} \times \delta_{23}\mathbb{B}$$

it follows that

$$W(x^+, \tilde{z}_h^+, \tau_s^+, \tau_c^+, q^+) \leq \exp(\lambda_1 \tau_s)(e^{-1}V(x, \tilde{z}_h) + L\delta_{23}(1 + e^{-1})).$$

Since $V(x, \tilde{z}_h) \geq \alpha_1(\delta_s)$ for every $(x, \tilde{z}_h) \in \Omega_{\mathcal{A}}(\delta_s, \Delta_s)$, for every $T_c \lambda_3 \in (-1, 0)$ there exists $\rho_3 \in (0, 1)$ satisfying $\rho_3 > \exp(-\lambda_3 T_c - 1)$ and by fixing δ_{23} to satisfy $\delta_{23} < \frac{1}{L(1+e)}\alpha_1(\delta_s)(\rho_3 \exp(\lambda_3 T_c + 1) - 1)$ we obtain

$$W(x^+, \tilde{z}_h^+, \tau_s^+, \tau_c^+, q^+) \leq \rho_3 W(x, \tilde{z}_h, \tau_s, \tau_c, q). \quad (\text{B.14})$$

for all $(z_m, z_c) \in D_c \setminus C_c$, $(x, \tilde{z}_h, \tau_s, \tau_c, q, |[e_2^T, e_3^T]^T|) \in \Omega_{\mathcal{A}}(\delta_s, \Delta_s) \times [0, T_s] \times [T_c, +\infty) \times \{0, 1\} \times \delta_{23}\mathbb{B}$. Following the last two cases of the proof it is easy to show a similar result for points $(z_m, z_c) \in D_c \cap C_c$. \square

In order to keep overall boundedness, the timer constants $T_s, T_c > 0$ need to be designed so that during flows and jumps the error states e_i , $i = 1, 2, 3, 4$, remain bounded. We establish this as follows.

Lemma B.18 (errors boundedness) *Let Assumptions 5.1, 5.2, and 5.3 hold. For each positive numbers δ_s and Δ_s satisfying $0 \leq \delta_s \leq \Delta_s < \infty$, given $\delta' > 0$ there exists $T_c, T_s > 0$ so that for every solution ξ_e to \mathcal{H}_{cl}^{S/H_e} with $(x^0, \tilde{z}_h^0) \in \Omega_{\mathcal{A}}(\delta_s, \Delta_s)$ there exists $(T^*, J^*) \in \text{dom } \xi_e$ so that*

$$|e_2(t, j)| \leq \delta', \quad |e_3(t, j)| \leq \delta', \quad |e_4(t, j)| \leq \delta', \quad (\text{B.15})$$

for every $(t, j) \succeq (T^*, J^*)$, $(t, j) \in \text{dom } \xi_e$.

Proof. Recall that the dynamics of \mathcal{H}_{cl}^{S/H_e} are such that during flows

$$\dot{e}_2 = -f(x, \kappa_c(z_s, z_c)), \quad \dot{e}_3 = -f_c(x, \tilde{z}_h), \quad \dot{e}_4 = -f(x, \kappa_c(z_s, z_c)); \quad (\text{B.16})$$

at jumps due to $\tau_s \geq T_s$

$$e_2^+ = e_2, \quad e_3^+ = e_3, \quad e_4^+ = 0; \quad (\text{B.17})$$

and at jumps due to $\tau_c \geq T_c$

$$e_2^+ = e_4, \quad e_3^+ = 0, \quad e_4^+ = e_4. \quad (\text{B.18})$$

Let $M_0 = |[e_2(0)^T, e_3(0)^T, e_4(0)^T]^T| + \delta' + 1$. Let M_1 and M_2 be two positive numbers satisfying

$$\max_{(x, \tilde{z}_h) \in \Omega_{\mathcal{A}}(\delta_s, \Delta_s)} |f_c(x, \tilde{z}_h)| \leq M_1, \quad (\text{B.19})$$

$$\max_{(x, \tilde{z}_h) \in \Omega_{\mathcal{A}}(\delta_s, \Delta_s)} |f(x, \kappa_c(x + M_0\mathbb{B}, \tilde{z}_h + M_0\mathbb{B}))| \leq M_2 \quad (\text{B.20})$$

Since the jumps of \mathcal{H}_{cl}^{S/H_e} are triggered by the timers τ_s and τ_c , for every solution ξ_e there exists $(T^*, J^*) \in \text{dom } \xi_e$ such that the jump mappings (B.17) and (B.18) have already been executed at least once, independently of the

point with $(x^0, \tilde{z}_h^0) \in \Omega_{\mathcal{A}}(\delta_s, \Delta_s)$ from where ξ_e started from. Then, for all $(t, j) \succeq (T^*, J^*)$, $(t, j) \in \text{dom } \xi_e$, using (B.19)-(B.16), $|e_3|$ cannot grow more than $M_1 T_c$, $M_1 T_c < 1$, and $|e_4|$ cannot grow more than $M_2 T_s$, $M_2 T_s < 1$, during flows. From (B.17) and (B.18), $|e_3|$ and $|e_4|$ do not increase during jumps. Then choose T_c so that $M_1 T_c \leq \min\{1, \frac{\delta'}{2}\}$ and T_s so that $M_2 T_s \leq \min\{1, \frac{\delta'}{2}\}$ to show

$$|e_3(t, j)| \leq \frac{\delta'}{2}, \quad |e_4(t, j)| \leq \frac{\delta'}{2}, \quad (\text{B.21})$$

for every $(t, j) \succeq (T^*, J^*)$, $(t, j) \in \text{dom } \xi_e$. Since e_2 is reset to e_4 at jumps triggered by $\tau_c \geq T_c$, using (B.21) the error $|e_2|$ cannot increase more than $\delta' + M_2 T_c$, $M_2 T_c < 1$. Then choose T_c so that $M_2 T_c < \min\{1, \frac{\delta'}{2}\}$ to show

$$|e_4(t, j)| \leq \delta' \quad (\text{B.22})$$

for every $(t, j) \succeq (T^*, J^*)$, $(t, j) \in \text{dom } \xi_e$. \square

We are now ready to show Theorem 5.12. The state of \mathcal{H}_{cl}^{S/H_e} is given by

$$[x^T, z_c^T, z_s^T, \tau_s, \tau_c, z_m^T, \tilde{z}_h^T, q]^T$$

but for this analysis we consider the state vector with the error signals given by $[x^T, \tilde{z}_h^T, \tau_s, \tau_c, q, e^T]^T$ (all the signals can be recovered from the errors as well), where $e := [e_1^T, e_2^T, e_3^T, e_4^T]^T$. First note the following observation based on the design of δ :

- (\diamond) Solutions to \mathcal{H}_{cl}^{S/H_e} cannot flow for more than $\max\{T_c, T_s\}$ units of time. By design, $\max\{T_c, T_s\} < \delta/M$ which implies that solutions that flow with components (x, \tilde{z}_h) in $C_c \cap \Omega_{\mathcal{A}}(\delta_s, \Delta_s)$ cannot reach the set $\mathbb{R}^n \setminus (C_c + \delta\mathbb{B})$ before experiencing a jump, and that solutions flowing in $(\mathbb{R}^n \setminus (C_c + \delta\mathbb{B})) \cap \Omega_{\mathcal{A}}(\delta_s, \Delta_s)$ cannot continue flowing and reach the set C_c without jumping.

This observation has the following implication: solutions with components (x, \tilde{z}_h, q) starting in the set (or eventually entering the set)

$$\mathcal{R}_0 := (C_c \cap \Omega_{\mathcal{A}}(\delta_s, \Delta_s)) \times \{q = 0\} \quad (\text{B.23})$$

leave it in finite time and never return to it. To show this, consider first that there is an instantaneous jump due to the timer τ_c . Since $(z_m, z_c) \in C_c$, the jump mapping g_{logic} will update q to one and consequently, the component of the solution (x, \tilde{z}_h, q) will leave the set \mathcal{R}_0 . If we assume instead that there is an instantaneous jump due to τ_s , z_m and z_c will be remapped to their initial values before the jump, event that will be repeated until a jump due to τ_c occurs. Instead, if the solution flows, by (\diamond), it will stay in $C_c + \delta\mathbb{B}$. From there, a future jump due to $\tau_c \geq T_c$ would map it outside \mathcal{R}_0 since the mapping used would be $g_{fc}(z_s, z_c)$. This shows that solutions with components starting in \mathcal{R}_0 leave it in finite time. As the solution leaves this set, q is necessarily mapped to one. For q to be mapped back to zero and (z_m, z_c) to C_c , a jump due to $\tau_c > T_c$ should occur with $(z_s, g_{\mathcal{H}_c}(z_m, z_c)) \in (C_c + \delta\mathbb{B})$ and $q^+ = 0$. This is impossible by the definition of g_{logic} . It follows that, after leaving the set \mathcal{R}_0 , q indicates if $(z_s, z_c) \in (C_c + \delta\mathbb{B})$ with $q = 1$ or if it is in $(z_s, z_c) \in \mathbb{R}^n \setminus (C_c + \delta\mathbb{B})$ with $q = 0$. Based on this discussion, we will not consider solutions with components in C_c and with $q = 0$ since such a condition is not reachable after finite time.

Let ξ_e be any solution to \mathcal{H}_{cl}^{S/H_e} with $x(0) = x^0$, $\tilde{z}_h(0) = z_c^0$, $(x^0, \tilde{z}_h^0) \in \Omega_{\mathcal{A}}(\delta_s, \Delta_s)$

Obtain δ_{34} from Lemma B.16, and δ_1 and δ_{23} from Lemma B.17.

Then from Lemma B.18 with $\delta' = \min\{\delta_{23}, \delta_{34}\}$, there exists $T_c^{*1} > 0$, $T_s^{*1} > 0$, and $(T^*, J^*) \in \text{dom } \xi_e$ such that for all $(t, j) \succeq (T^*, J^*)$, $(t, j) \in \text{dom } \xi_e$, $|e_i(t, j)| \leq \delta'$, for each $i = 2, 3, 4$. With some abuse of notation, we redefine the solution ξ_e (but we don't relabel it) so that for each $i = 2, 3, 4$; $|e_i(t, j)| \leq \delta'$ for all $(t, j) \in \text{dom } \xi_e$.

Let $\tilde{\delta}_3 = \tilde{\delta}_4 = \delta'$. Since $||[e_3^T, e_4^T]^T|| \leq \delta'$, it follows from Lemma B.16 that for every $(t, j) \in \text{dom } \xi_e$ for which ξ_e flows and its components satisfy the condition (F1)

$$(x, \tilde{z}_h) \in (C_c + \delta\mathbb{B}) \cap \Omega_{\mathcal{A}}(\delta_s, \Delta_s) \text{ and } (\tau_s, \tau_c, q) \in [0, T_s] \times [0, T_c] \times \{1\}$$

or the condition (F2)

$$(x, \tilde{z}_h, \tau_s, \tau_c, q) \in \Omega_{\mathcal{A}}(\delta_s, \Delta_s) \times [0, T_s] \times [0, T_c] \times \{0\},$$

we have

$$\dot{W}(x(t, j), \tilde{z}_h(t, j), \tau_s(t, j), \tau_c(t, j), q(t, j)) \leq -\varepsilon W(x(t, j), \tilde{z}_h(t, j), \tau_s(t, j), \tau_c(t, j), q(t, j))$$

for every $\varepsilon \in (0, \varepsilon^*]$, where ε^* is imposed by Lemma B.16.

Since g_{f_c} is consistent with f_c , there exists $\rho \in \mathcal{K}_\infty$ and $T_c^{*2} > 0$ such that for all $T_c \in (0, T_c^{*2})$, at every jump point $(t, j) \in \text{dom } \xi_e$ due to $\tau_c \geq T_c$

$$|g_{f_c}(z_m(t, j), z_c(t, j)) - \tilde{z}_h(t, j)| \leq T_c \rho(T_c) \leq \delta_1.$$

Let $\tilde{\delta}_1 = \delta_1$. Then, when $\tau_c(t, j) \geq T_c$ and $q(t, j) = 1$ we have $|e_1(t, j)| \leq \delta_1$. Let $\tilde{\delta}_2 = \delta_{23}$. Then, for every jump point (t, j) of ξ_e due to $\tau_s \geq T_s$ with components of ξ_e satisfying condition (J1)

$$(x, \tilde{z}_h, \tau_s, \tau_c, q) \in \Omega_{\mathcal{A}}(\delta_s, \Delta_s) \times [T_s, +\infty) \times [0, T_c] \times \{0, 1\}$$

or for every jump point (t, j) of ξ_e due to $\tau_c \geq T_c$ with components of ξ_e satisfying condition (J2) $(z_m, z_c) \in C_c$ and

$$(x, \tilde{z}_h, \tau_s, \tau_c, q) \in \Omega_{\mathcal{A}}(\delta_s, \Delta_s) \times [0, T_s] \times [T_c, +\infty) \times \{1\},$$

or condition (J3) $(z_m, z_c) \in D_c$ and

$$(x, \tilde{z}_h, \tau_s, \tau_c, q) \in \Omega_{\mathcal{A}}(\delta_s, \Delta_s) \times [0, T_s] \times [T_c, +\infty) \times \{0, 1\}$$

we have

$$W(x(t, j+1), \tilde{z}_h(t, j+1), \tau_s(t, j+1), \tau_c(t, j+1), q(t, j+1)) \leq \rho W(x(t, j), \tilde{z}_h(t, j), \tau_s(t, j), \tau_c(t, j), q(t, j)).$$

This implies that provided we choose $T_c \leq \min\{T_c^{*0}, T_c^{*1}, T_c^{*2}\}$ and $T_s \leq \min\{T_s^{*0}, T_s^{*1}\}$, trajectories with components $(x, \tilde{z}_h) \in \Omega_{\mathcal{A}}(\delta_s, \Delta_s)$ satisfy during flows

$$\dot{W}(x(t, j), \tilde{z}_h(t, j), \tau_s(t, j), \tau_c(t, j), q(t, j)) \leq -\varepsilon W(x(t, j), \tilde{z}_h(t, j), \tau_s(t, j), \tau_c(t, j), q(t, j)), \quad (\text{B.24})$$

and during jumps

$$W(x(t, j+1), \tilde{z}_h(t, j+1), \tau_s(t, j+1), \tau_c(t, j+1), q(t, j+1)) \leq \rho W(x(t, j), \tilde{z}_h(t, j), \tau_s(t, j), \tau_c(t, j), q(t, j)) \quad (\text{B.25})$$

with $|e_i(t, j)| \leq \tilde{\delta}_i$, $i = 1, 2, 3, 4$ for all $(t, j) \in \text{dom } \xi_e$.

Then, for every solution ξ_e to $\mathcal{H}_{cl}^{S/He}$ starting at

$$(x^0, \tilde{z}_h^0, \tau_s^0, \tau_c^0, q^0, e^0) \in \Omega_{\mathcal{A}}(\delta_s, \Delta_s) \times \mathbb{R}_{\geq 0}^2 \times \{0, 1\} \times \tilde{\delta}\mathbb{B},$$

$e = [e_1^T, e_2^T, e_3^T, e_4^T]^T$ and $\tilde{\delta} = \min_{i \in \{1, 2, 3, 4\}} \tilde{\delta}_i$,

- during flows ξ_e satisfies (B.24) and therefore, for each $t \in [t_j, t_{j+1}]$, $t_{j+1} > t_j$, $(t, j) \in \text{dom } \xi_e$,

$$W(\zeta(t, j)) \leq \exp(-\varepsilon(t - t_j))W(\zeta(t_j, j)), \quad (\text{B.26})$$

where for clarity in the exposition, we define

$$\zeta(t, j) =: (x(t, j), \tilde{z}_h(t, j), \tau_s(t, j), \tau_c(t, j), q(t, j)), \zeta^0 = \zeta(0, 0).$$

- during jumps ξ_e satisfies (B.25) and therefore, for each $(t, j) \in \text{dom } \xi_e$ so that $(t, j + 1) \in \text{dom } \xi_e$,

$$W(\zeta(t, j + 1)) \leq \rho W(\zeta(t, j)) . \quad (\text{B.27})$$

Combining (B.26) and (B.27) we obtain a bound on $|(x, \tilde{z}_h)|_{\mathcal{A}}$ on compact hybrid time domains. Let $T = \min\{T_s, T_c\}$. Then for every $(T^*, J^*) \in \text{dom } \zeta$ and defining $n = \lfloor \frac{T^*}{T} \rfloor$

$$W(\zeta(T^*, J^*)) \leq \rho^{J^*} \exp(-\varepsilon T n) \exp(-\varepsilon(T^* - nT))W(\zeta^0)$$

which combined with (B.5) gives

$$|(x, \tilde{z}_h)|_{\mathcal{A}} \leq \alpha_1^{-1} \left(\frac{1}{a_1} \rho^{J^*} \exp(-\varepsilon T n) \exp(-\varepsilon(T^* - nT))W(\zeta^0) \right).$$

Solving this equation when $|(x, \tilde{z}_h)|_{\mathcal{A}} = \delta_s$ gives an explicit value of (T^*, J^*) such that $(x(T^*, J^*), \tilde{z}_h(T^*, J^*)) \in \Omega_{\mathcal{A}}(0, \delta_s)$.

We now fix δ_s and Δ_s to satisfy the given set of initial conditions K and the level of closeness ε to the set \mathcal{A} .

From the definition of W in (B.9) and the bounds for V in (B.5) we obtain

$$a_1 \alpha_1 (|(x, x_c)|_{\mathcal{A}}) \leq a_1 V(x, x_c) \leq W(x, \tilde{z}_h, \tau_s, \tau_c, q) \leq a_2 V(x, x_c) \leq a_2 \alpha_2 (|(x, x_c)|_{\mathcal{A}}) \quad (\text{B.28})$$

where $a_1 = \exp(\lambda_3 T_c)$ and $a_2 = \exp(\lambda_1 T_s + \lambda_2 T_c)$ and we used the fact that the timer τ_s and τ_c do not grow more than T_s and T_c , respectively.

Let $\Delta'_s > 0$ be such that $K \subset \Omega_{\mathcal{A}}(0, \Delta'_s)$ and let $\Delta_s = \alpha_1^{-1} \left(\frac{a_2}{a_1} \alpha_2(\Delta'_s) \right)$.

For initial conditions

$$(x^0, \tilde{z}_h^0, \tau_s^0, \tau_c^0, q^0, e^0) \in \Omega_{\mathcal{A}}(0, \Delta'_s) \times \mathbb{R}_{\geq 0}^2 \times \{0, 1\} \times \tilde{\delta}\mathbb{B}, \quad (\text{B.29})$$

where the solution ζ to \mathcal{H}_{cl}^{S/H_e} starts, using (B.28), we have

$$W(\zeta(0, 0)) \leq a_2 \alpha_2(\Delta'_s) .$$

Suppose that there exists a first hybrid instant $(t', j') \in \text{dom } \zeta$ at which

$$(x(t', j'), \tilde{z}_h(t', j')) \notin \Omega_{\mathcal{A}}(0, \Delta_s) .$$

Then, for all $(t, j) \prec (t', j')$, $(t, j) \in \text{dom } \zeta$, W decreases along the solution and with (B.28) gives

$$a_1 \alpha_1 (|(x(t, j), \tilde{z}_h(t, j))|_{\mathcal{A}}) \leq W(\zeta(t, j)) < W(\zeta^0) \leq a_2 \alpha_2(\Delta'_s)$$

which implies

$$|(x(t, j), \tilde{z}_h(t, j))|_{\mathcal{A}} \leq \alpha_1^{-1} \left(\frac{a_2}{a_1} \alpha_2(\Delta'_s) \right) = \Delta_s .$$

Then, the solution ζ (and every solution with initial points satisfying the condition in (B.29)) never leaves the set $\Omega_{\mathcal{A}}(0, \Delta_s)$.

The jumps from the set $\Omega_{\mathcal{A}}(0, \delta_s)$ may land outside of that set since W is no longer decreasing for $(x, \tilde{z}_h) \in \Omega_{\mathcal{A}}(0, \delta_s)$. Let $\delta'_s > 0$ be such that after the jump from $\Omega_{\mathcal{A}}(0, \delta_s)$, $\delta_s \leq |(x^+, \tilde{z}_h^+)|_{\mathcal{A}} \leq \delta'_s$. This can be established by choosing δ_s small enough and using continuity of W . Let $\delta'_s = \alpha_1^{-1} \left(\frac{a_2}{a_1} \alpha_2(\delta''_s) \right)$. Then by the same argument used above, the solution after the jump cannot leave the set $\Omega_{\mathcal{A}}(0, \delta'_s)$. More precisely, say that the jump from $\Omega_{\mathcal{A}}(0, \delta_s)$ occurred at $(t^*, j^*) \in \text{dom } \zeta$. Then for all $(t, j) \succ (t^*, j^*)$, $(t, j) \in \text{dom } \zeta$ until (x, \tilde{z}_h) enters $\Omega_{\mathcal{A}}(0, \delta_s)$ again

$$a_1 \alpha_1(|(x(t, j), \tilde{z}_h(t, j))|_{\mathcal{A}}) \leq W(\zeta(t, j)) < W(\zeta^0) \leq a_2 \alpha_2(\delta''_s)$$

which implies

$$|(x(t, j), \tilde{z}_h(t, j))|_{\mathcal{A}} \leq \alpha_1^{-1} \left(\frac{a_2}{a_1} \alpha_2(\delta''_s) \right) = \delta'_s$$

Let $\delta'_s < \varepsilon$ and use $\delta''_s = \alpha_2^{-1} \left(\frac{a_1}{a_2} \alpha_1(\delta'_s) \right)$ in the continuity argument above to obtain δ_s .

Finally, the bounds on x and \tilde{z}_h can be extended to z_c and combined into a \mathcal{KLL} function satisfying along solutions the properties in the claim.

B.4 Proofs of results in Chapter 6

B.4.1 Proof of Theorem 6.5

The following auxiliary lemma will be needed.

Lemma B.19 (middle point lemma) *Let $\mathcal{B} \subset O$. If $z_i \in \mathcal{M}_i$ and $z_j \in \mathcal{M}_j$ with $i \neq j$ and the line segment connecting z_i and z_j is contained in \mathcal{B} then there exists a point on the line segment connecting z_i and z_j that belongs to \mathcal{M} .*

Proof. Since the line segment is contained in the open set \mathcal{B} there exists a neighborhood \mathcal{N}' of the line segment contained in \mathcal{B} . We cover the line segment with an increasing number of open balls with decreasing radius, each centered at points on the line segment and such that each ball is contained in \mathcal{N}' . The radius is taken to be $\frac{1}{k}$ with k a sufficiently large integer. Since the endpoints belong to different index sets, at least one ball intersects more than one index set. We use y_k to denote the center of the ball of radius $\frac{1}{k}$ intersecting more than one index set. The sequence y_i has a subsequence converging to a point y on the line segment. We claim that $y \in \mathcal{M}$. Suppose not. Then there exists $\rho > 0$ and i such that $\xi \in \mathcal{M}_i$ for all $\xi \in \{y\} + \rho\mathbb{B}$. But since $\{y_k\} + \frac{1}{k}\mathbb{B} \subset \{y\} + \rho\mathbb{B}$ for k sufficiently large, this provides a contradiction. \square

By Assumption 6.2, $m < +\infty$. Then, given $\rho', \rho'' > 0$, every solution x to $\dot{x} = f(x)$ from x^0 is such that if there exists T_1 such that $x(T_1) \notin x^0 + \rho'\mathbb{B}$, then the minimum such time T_1 satisfies

$$T_1 \geq \frac{\rho'}{m}, \quad (\text{B.30})$$

while if there exists T_2 such that $x(T_2) \notin \mathcal{B}$, then the minimum such time T_2 satisfies

$$T_2 \geq \frac{\rho''}{m}, \quad (\text{B.31})$$

Then, $T^* := \min\{T_1, T_2\} \geq \frac{\min\{\rho', \rho''\}}{m}$.

Let $x_0^0 = x^0$ and i be such that $x_0^0 \in \mathcal{M}_i$. Since $x_0^0 \in \mathcal{M} + \varepsilon\mathbb{B}$, there exists $z \in \mathcal{M}$ such that $|x_0^0 - z| < \varepsilon$. Pick $j \neq i$ and using Assumption 6.4, let z_j be such that $|z_j - z| < \min\{\frac{\varepsilon}{2}, \varepsilon - |x_0^0 - z|\}$ and $x_j(t) \in \mathcal{M}_j \setminus \mathcal{M} \subset \mathcal{B}$ for all $t \in [0, T]$ where $x_j : [0, T] \rightarrow O$ is a Carathéodory solution to $\dot{x} = f(x)$, $x_j(0) = z_j$. Note that such z_j exists by choosing small enough $\rho > 0$. Also note that

$$|x_0^0 - z_j| < |x_0^0 - z| + |z - z_j| < \varepsilon. \quad (\text{B.32})$$

Let $x : [0, T] \rightarrow \mathbb{R}^n$ satisfy $\dot{x} = f(x_j(t))$ with $x(0) = x_0^0$, that is, it satisfies

$$x(t) = x_0^0 + \int_0^t f(x_j(\tau))d\tau \quad (\text{B.33})$$

for all $t \in [0, T]$. Let $e(t) := x_j(t) - x(t)$ for all $t \in [0, T]$. It follows that x is also a Carathéodory solution to the initial value problem $\dot{x} = f(x + e)$, $x(0) = x_0^0$, since

$$x(t) = x_0^0 + \int_0^t f(x(\tau) + e(\tau))d\tau = x_0^0 + \int_0^t f(x_j(\tau))d\tau \quad (\text{B.34})$$

for all $t \in [0, T]$. Note that since x_j is a Carathéodory solution to the initial value problem $\dot{x} = f(x)$, $x_j(0) = z_j$, it satisfies

$$x_j(t) = z_j + \int_0^t f(x_j(\tau))d\tau \quad (\text{B.35})$$

for all $t \in [0, T]$. Combining (B.35) with (B.34), $e(t) = z_j - x_0^0$. From (B.32), $|e(t)| < \varepsilon$ for all $t \in [0, T]$. Note that by construction, for $x(t)$ to leave $\mathcal{M} + \varepsilon\mathbb{B}$ it is required that $|x_j(t) - z_j| > \frac{\varepsilon}{2}$, and that the minimum time for that to happen is $\frac{\varepsilon}{2m}$.

Let $t_1 \in [0, \min\{T, T^*, \frac{\varepsilon}{2m}\}]$ be such that, for all $t \in [0, t_1]$, $\left| \int_0^t f(x(\tau) + e(\tau))d\tau \right| < \varepsilon$. It follows that $x(t) \in (x_0^0 + \varepsilon\mathbb{B}) \cap \mathcal{B} \cap (x_0^0 + \rho'\mathbb{B})$ for all $t \in [0, t_1]$. Let $t'_1 \in (0, t_1]$ and suppose that $x(t'_1) \in \mathcal{M}_k$ for some $k \neq i$. Since $x(t) \in \mathcal{B}$ for all $t \in [0, t_1]$, by Lemma B.19, there exists a line connecting x^0 and $x(t'_1)$ that has a point that is in \mathcal{M} . Denote this point by z' . Then

$$|x(t'_1) - z'| < |x(t'_1) - x_0^0| = \left| \int_0^{t'_1} f(x(\tau) + e(\tau))d\tau \right| < \varepsilon. \quad (\text{B.36})$$

Instead, if $x(t'_1) \in \mathcal{M}_i$, using again Lemma B.19, the line connecting $x(t'_1)$ and $x(t'_1) + e(t'_1)$ contains a point that is in \mathcal{M} since $x(t) + e(t) = x_j(t) \in \mathcal{M}_j$, $j \neq i$, for all $t \in [0, T]$. Denote this point by z' . It follows that

$$|x(t'_1) - z'| \leq |x(t'_1) - x(t'_1) - e(t'_1)| = |e(t'_1)| < \varepsilon.$$

Continuing in this way, provided that $x(t_i) \in (x^0 + \rho'\mathbb{B}) \cap \mathcal{B}$, $i = 1, 2, \dots$, this argument can be repeated with constants $\varepsilon_i = \varepsilon$ and $\rho'_i = \rho'$, picking ρ'_i so that $x(t_i) + \rho'_i\mathbb{B} \subset \mathcal{B}$, and with $x_0^0 = x(t_i)$ to obtain a sequence of times $t_{i+1} > 0$, $i = 1, 2, \dots$, defining a Carathéodory solution x to $\dot{x} = f(x)$, $x(0) = x^0$, with measurement noise e and with the property that, for all $t \in [0, T'] \subset \text{dom } x$, $T' := \sum_{i=1}^{\infty} t_i$ (possibly unbounded, in which case x is complete), $x(t) \in (\mathcal{M} + \varepsilon\mathbb{B}) \cap \mathcal{B} \cap (x^0 + \rho'\mathbb{B})$ and $|e(t)| \leq \varepsilon$. Note that by construction, $T' \geq T^*$. If T' is finite, then $\lim_{t \rightarrow T'} x(t) \notin \mathcal{B} \cup (x^0 + \rho'\mathbb{B})$. If $\lim_{t \rightarrow T'} x(t) \notin O$, then x is maximal; otherwise x (and the measurement noise e) can be further extended to obtain a maximal solution.

B.4.2 Proof of Corollary 6.7

Following the definition in [55] (see also [42]), a function $x : \text{dom } x \rightarrow \mathbb{R}^n$ is a *Krasovskii solution* to $\dot{x} = f(x)$, $f : O \rightarrow \mathbb{R}^n$, if

$$\dot{x}(t) \in F(x(t)) \quad \text{for almost all } t \in \text{dom } x,$$

where, for each $\xi \in O$,

$$F(\xi) = \bigcap_{\delta > 0} \overline{\text{co}}f(\xi + \delta\mathbb{B}).$$

Corollary B.20 (Krasovskii solution on \mathcal{M}) *For every $x^0 \in \mathcal{M} \cap \mathcal{B}$ there exists a maximal Krasovskii solution x to $\dot{x} = f(x)$ with $x(0) = x^0$ such that $x(t) \in \mathcal{M} \cap \mathcal{B}$ for all $t \in \text{dom } x$. Moreover, this solution either leaves \mathcal{B} or is complete.*

Proof. Pick any $\rho' > 0$ and any $\rho'' > 0$ such that $x^0 + \rho'\mathbb{B} \subset O$ and $x^0 + \rho''\mathbb{B} \subset \mathcal{B}$. For each $i \in \mathbb{N}$, let $\rho'_i, \rho''_i > 0$, $\varepsilon_i = \frac{1}{i}$, and x_i^0 be such that $\rho'_i \rightarrow \rho'$, $\rho''_i \rightarrow \rho''$, and $x_i^0 \rightarrow x^0$ as $i \rightarrow \infty$. Using Theorem 6.5 with the constants just defined, obtain, for each $i \in \mathbb{N}$, $x_i : \text{dom } x_i \rightarrow O$ and $e_i : \text{dom } e_i \rightarrow \frac{1}{i}\mathbb{B}$, $\text{dom } x_i = \text{dom } e_i$, such that

$$x_i(t) \in \left(\mathcal{M} + \frac{1}{i}\mathbb{B} \right) \cap \mathcal{B} \cap (x_i^0 + \rho'_i\mathbb{B}) \quad \forall t \in [0, T'_i) \subset \text{dom } x_i, \quad (\text{B.37})$$

where $T'_i \geq T_i^* := \frac{\min\{\rho'_i, \rho''_i\}}{m_i}$, $m_i := \sup \{1 + |f(\eta)| \mid \eta \in x_i^0 + \rho'_i\mathbb{B}\}$. In the limit, the truncation of $\{x_i\}_{i=1}^\infty$ to $[0, T'_i)$ uniformly converge to $x : [0, T^*] \rightarrow O$, $x(0) = x^0$, and the truncation of $\{e_i\}_{i=1}^\infty$ to $[0, T'_i)$ uniformly converge to the zero function on (in \mathbb{R}^n) on $[0, T^*]$, where $T^* = \frac{\min\{\rho', \rho''\}}{m}$, $m := \sup \{1 + |f(\eta)| \mid \eta \in x^0 + \rho'\mathbb{B}\}$. Then, x satisfies $x(t) \in \mathcal{M}$ for all $t \in [0, T^*]$. It follows by Theorem 4.3 in [42] that x is a Krasovskii solution to $\dot{x} = f(x)$. Now we show that if $x(T^*) \in \mathcal{B}$ then x can be extended further while in $\mathcal{M} \cap \mathcal{B}$. By contradiction, suppose it is maximal. Pick a sequence \tilde{x}_i^0 such that $\lim_{i \rightarrow \infty} \tilde{x}_i^0 = x(T^*)$. Using Theorem 6.5 again with the the constants above, obtain $\{\tilde{x}_i\}_{i=1}^\infty$ and $\{\tilde{e}_i\}_{i=1}^\infty$ such that they satisfy (B.37) (replacing x_i^0 by \tilde{x}_i^0 in T_i^* and m_i). Then, \tilde{x}_i converge uniformly to $\tilde{x} : [0, \tilde{T}'] \rightarrow \mathbb{R}^n$ where $\tilde{T}' > T^*$. This is a contradiction since \tilde{x} is an extension of x and the concatenation of x and \tilde{x} is a Krasovskii solution to $\dot{x} = f(x)$. \square

With Corollary B.20, the proof of Corollary 6.7 follows from Corollary 4.5 in [90]. In fact, by Corollary B.20 with $x^0 = z$, there exists a maximal Krasovskii solution \tilde{x} to $\dot{x} = \tilde{f}(x, \kappa_c(x))$ with $\tilde{x}(0) = z$ and $\tilde{x}(t) \in \mathcal{M} \cap \mathcal{B}$ for all $t \in \text{dom } \tilde{x}$. Let $\tilde{T} > 0$ be the largest time such that $[0, \tilde{T}) \subset \text{dom } \tilde{x}$. Let $T' \in (0, \tilde{T})$. Then, by Corollary 4.5 in [90] with $C = O$, for every $x^0 \in O$ such that $|x^0 - \tilde{x}(0)| < \varepsilon' e^{-LT'}$ where $\varepsilon' > 0$ is small enough so that $\text{rge } \tilde{x} + 2\varepsilon'\mathbb{B} \subset O$ and $\varepsilon' < \varepsilon$, and L is a Lipschitz constant for $\tilde{f}(\cdot, u)$ on $\text{rge } \tilde{x} + 2\varepsilon'\mathbb{B}$ for any $u \in \kappa_c(\text{rge } \tilde{x} + 2\varepsilon'\mathbb{B})$, there exists a measurable function $e : [0, T'] \rightarrow \mathbb{R}^n$ and an absolutely continuous function $x : [0, T'] \rightarrow O$, $x(0) = x^0$, such that $\sup_{t \in [0, T']} |e(t)| \leq \varepsilon'$,

$$\dot{x}(t) = \tilde{f}(x(t), \kappa_c(x(t) + e(t))) \quad \text{for almost all } t \in [0, T'] , \quad (\text{B.38})$$

and $|x(t) - \tilde{x}(t)| \leq \varepsilon'$ for all $t \in [0, T']$, that is, $x(t) \in (\mathcal{M} + \varepsilon\mathbb{B}) \cap \mathcal{B}$. The horizon T' can be chosen arbitrarily close to \tilde{T} by picking sufficiently small ε' . The remainder of the proof follows the proof of Theorem 6.5.

B.4.3 Proof of Theorem 6.11

By Lemma 6.10, the closed-loop system \mathcal{H}_{cl} satisfies the hybrid basic conditions. Then, for each $(x, q) \in C_c \cup D_c$, if $(x, q) \in D_c$ then $Q_c(x, q) \neq \emptyset$; otherwise (VC) in Proposition 2.4 in [39] holds by construction of C_c

and the continuity properties of V_q on O_q for each $q \in Q$. Then, using Proposition 2.4 in [39], there exists a nontrivial solution from each $\xi \in C_c \cup D_c$, and since

$$G(\xi) := \begin{bmatrix} x \\ Q_c(x, q) \end{bmatrix}$$

is such that $G(D_c) \subset C_c \cup D_c$, each solution is either complete or has a bounded hybrid time domain. Suppose that a solution $(x(t, j), q(t, j))$ has a bounded hybrid time domain with T and J being the supremum of $\text{dom}(x, q)$ in the t and j direction, respectively. Since $G(D_c) \subset C_c \cup D_c$, if $(x(T, J), q(T, J)) \in D_c$ then the solution can be continued forward by jumping. If $(x(T, J), q(T, J)) \in C_c$ and ξ cannot flow forward in time, then, since the flow map is continuous on C_c , $(x(T, J), q(T, J))$ is either in the boundary of C_c^a and not in C_c^b or is in the boundary of C_c^b and not in C_c^a . If $(x(T, J), q(T, J))$ is in the boundary of C_c^a and not in C_c^b then, by construction of D_c , $(x(T, J), q(T, J)) \in D_c$ and the solution can be continued forward by jumping. If $(x(T, J), q(T, J))$ is in the boundary of C_c^b and not in C_c^a then, since by construction of C_c and D_c we have $(O \times Q) \setminus C_c^a \subset D_c$, then $(x(T, J), q(T, J)) \in D_c$ and the solution can also be continued forward by jumping. Hence, every solution to \mathcal{H}_{cl} from $O \times Q$ is complete.

Asymptotic stability of $\mathcal{A} \times Q$ is shown by establishing uniform convergence to and forward invariance of $\mathcal{A} \times Q$. By the definition of D_c , every $(x, q) \in D_c$ is such that

$$V_q(x) \geq (\mu - \lambda) \min_{p \in Q} V_p(x) .$$

By construction of Q_c

$$V_q(x) \geq (\mu - \lambda) V_{q'}(x) \quad \forall q' \in Q_c(x, q), (x, q) \in D_c .$$

Let $\gamma' := (\mu - \lambda)^{-1}$, $\gamma' \in (0, 1)$. Then

$$V_{q'}(x) \leq \gamma' V_q(x) \quad \forall q' \in Q_c(x, q), \forall (x, q) \in D_c . \quad (\text{B.39})$$

Moreover, from (6.5) we have

$$\langle \nabla V_q(x), f_p(x, \kappa_q(x)) \rangle \leq -\rho(V_q(x)) \quad \forall (x, q) \in C_c . \quad (\text{B.40})$$

Let $W(x, q) := V_q(x)$. Given any compact set $K \subset O$ and $\varepsilon > 0$, define

$$M := \max_{z \in K} \alpha_1^{-1} \circ \alpha_2(\omega(z)), \quad m := \min_{z \in \Omega(\varepsilon, M)} \alpha_1(\omega(z))$$

where $\Omega(\varepsilon, M) := \{x \in O \mid \varepsilon \leq \omega(x) \leq M\}$. Note that $m, M > 0$. Let $x^0 \in K$ and $(x(t, j), q(t, j))$ be a solution to \mathcal{H}_{cl} with $x(0, 0) = x^0$ and $q(0, 0) \in Q$. Let $t(j)$ denote the least time t such that $(t, j) \in \text{dom}(x, q)$, and $j(t)$ denote the least index j such that $(t, j) \in \text{dom}(x, q)$. Then

$$W((x, q)(t, j)) - W((x, q)(0, 0)) = \int_0^t \frac{d}{d\tau} W((x, q)(\tau, j(\tau))) d\tau + \sum_{i=1}^j [W((x, q)(t(i), i)) - W((x, q)(t(i), i-1))]$$

where the shorthand notation $(x, q)(t, j) = (x(t, j), q(t, j))$ was used. Combining (B.39), (B.40), and the lower bound in (6.4) yields

$$W((x, q)(t, j)) - W((x, q)(0, 0)) \leq - \int_0^t \rho \circ \alpha_1(\omega(x(\tau, j(\tau)))) d\tau - \sum_{i=1}^j (1 - \gamma') \alpha_1(\omega(x(t(i), i-1))) . \quad (\text{B.41})$$

Since the right-hand side of this expression is nonpositive, W does not increase along solutions. Then, solutions starting from K stay in $\Omega(0, M)$ for all time. For every $(t, j) \in \text{dom}(x, q)$ such that $x(t, j) \in \Omega(\varepsilon, M)$, $\alpha_1(|x(t, j)|) \geq m$. Then, from (B.41),

$$\begin{aligned} W(x(t, j), q(t, j)) &\leq -\rho(m)t - m(1 - \gamma')j + W(x(0, 0), q(0, 0)) \\ &\leq -\varepsilon'(t + j) + \alpha_1(M) \end{aligned} \quad (\text{B.42})$$

where $\varepsilon' = \min\{\rho(m), m(1 - \gamma')\} > 0$. Then, $n = \frac{\alpha_1(M) - \alpha_1(\varepsilon)}{\varepsilon'}$ is such that for every solution x from K we have $\omega(x(t, j)) \leq \varepsilon$ for all $t + j \geq n$, $(t, j) \in \text{dom}(x, q)$. This follows since, with the choice of n , from (B.42) and (6.4) we have that

$$\omega(x(t, j)) \leq -\varepsilon'n + \alpha_1(M) = \varepsilon \quad \forall t + j \geq n, (t, j) \in \text{dom}(x, q).$$

Then, $\mathcal{A} \times Q$ is uniformly attractive from $K \times Q$.

To show that $\mathcal{A} \times Q$ is forward invariant, suppose $(x', q') \in \mathcal{A} \times Q$. First note that, from (6.4), for every $(x', q') \in \mathcal{A} \times Q$, $\min_{p \in Q} V_p(x') = 0$. Suppose $V_{q'}(x') = 0$. Then, using (B.39) and (B.40), along each solution (x, q) with $(x(0, 0), q(0, 0)) = (x', q')$, W remains identically zero. Then, using (6.4)

$$\alpha_1(\omega(x(t, j))) \leq \min_{p \in Q} V_p(x(t, j)) \leq W(x(t, j), q(t, j)) = 0 \quad (\text{B.43})$$

for all $(t, j) \in \text{dom}(x, q)$. This implies that the x component of the solution remains in \mathcal{A} . Next, suppose $V_{q'}(x') > 0$. It follows that $(x', q') \notin C_c^a$ since $\min_{p \in Q} V_p(x') = 0$. Moreover, with Assumption 6.9, $(x', q') \notin C_c^b$. It follows that $(x', q') \in D_c$. Then, solutions from $(x', q') \in \mathcal{A} \times Q$ with $V_{q'}(x') > 0$ jump at $(0, 0)$. Let $q'' \in Q$ be the value of the logic state after the jump. Since $(x', q'') \in \mathcal{A} \times Q$, if $V_{q''}(x') = 0$ then it follows, as above, that the trajectory remains in $\mathcal{A} \times Q$. If $V_{q''}(x') > 0$ then it follows again that $(x', q'') \notin C_c^a$ (respectively, $(x', q'') \notin C_c^b$). By repeating this argument we conclude that no trajectory can leave $\mathcal{A} \times Q$.

Then, since $\mathcal{A} \times Q$ is forward invariant and uniformly attractive from compact sets of $O \times Q$, asymptotic stability with basin of attraction $O \times Q$ follows from [39, Proposition 6.1].

B.4.4 Proof of Theorem 6.12

The following lemma together with the properties of the data of \mathcal{H}_{cl} in Lemma 6.10 guarantee existence of solutions from every point in $C \cup D$ for small enough perturbation. Note that since $\mu - \lambda < \mu$, the sets C_c and D_c have a nonzero overlap which can be adjusted by the parameter λ . The construction of these sets guarantees that for small enough measurement noise, solutions to the closed-loop system \mathcal{H}_{cl} exist since, as stated below, it can be shown that for every point in $(x, q) \in O \times Q$, points (y, q) nearby are either in C_c or D_c . (When existence of solutions is not a concern, like in the case of sample-and-hold implementation, one can take $\lambda = 0$.)

Lemma B.21 (existence of solutions under perturbations) *For each compact set $K \subset O \times Q$, there exists $\delta > 0$ such that for each (x, q) in K either $(\{x\} + \delta\mathbb{B}) \times \{q\} \subset C_c$ or $(\{x\} + \delta\mathbb{B}) \times \{q\} \subset D_c$.*

Proof. For a given compact set $K \subset O$, let $K_1, K_2 \subset O$ be compact sets such that $K = K_1 \cup K_2$, $K_1 \subset O \setminus \mathcal{A}$, and $\mathcal{A} \subset K_2 \subset O$. It is shown first that there exists $\delta > 0$ such that for each $(x, q) \in K_1 \times Q$, either $(x + \delta\mathbb{B}) \times \{q\} \subset C_c^a$ or $(x + \delta\mathbb{B}) \times \{q\} \subset D_c$. To this end, note that if $V_q(x)$ is not finite, then $(x, q) \in D_c$ since by definition of V_q and O for some $q' \in Q$, $V_{q'}(x) < \infty$. Then $x \in O_{q'}$ and since $O_{q'}$ is open, there exists $\delta > 0$ so that $(x + \delta\mathbb{B}) \times \{q\} \subset D_c$. We now consider the case that $V_q(x)$ is finite. We consider the following two cases:

$$V_q(x) \leq (\mu - \lambda/2) \min_{p \in Q} V_p(x) \quad (\text{B.44})$$

and

$$V_q(x) \geq (\mu - \lambda/2) \min_{p \in Q} V_{q'}(x) . \quad (\text{B.45})$$

If (B.44) holds, then, by continuity of V , for every $\varepsilon' > 0$ there exists $\delta > 0$ such that for each $z \in x + \delta\mathbb{B}$

$$V_q(z) \leq V_q(x) + \varepsilon' . \quad (\text{B.46})$$

Then

$$V_q(z) \leq \mu \min_{p \in Q} V_p(z) + \varepsilon' \quad (\text{B.47})$$

$$\leq \mu \min_{p \in Q} V_p(z) + (1 + \mu - \frac{\lambda}{2})\varepsilon' - \frac{\lambda}{2} \min_{p \in Q} V_{q'}(z) \quad (\text{B.48})$$

for every $z \in x + \delta\mathbb{B}$. Let $M = \max_{x \in K_1} \omega(x)$. Using the upper bound in (6.4) and choosing $\varepsilon' \leq \frac{\alpha_2(M)\lambda/2}{1+\mu-\lambda/2}$, we have

$$V_q(z) \leq \mu \min_{p \in Q} V_p(z) \quad (\text{B.49})$$

for every $z \in x + \delta\mathbb{B}$. Then, $(x + \delta\mathbb{B}) \times \{q\} \subset C_c^a$.

Proceeding similarly, if (B.45) holds, then, by continuity of V , we have

$$V_q(z) \geq (\mu - \lambda) \min_{p \in Q} V_p(z) - (1 + \mu - \frac{\lambda}{2})\varepsilon' + \frac{\lambda}{2} \min_{p \in Q} V_p(z) \quad (\text{B.50})$$

and, for small ε' gives

$$V_q(z) \geq (\mu - \lambda) \min_{p \in Q} V_p(z) \quad (\text{B.51})$$

for every $z \in x + \delta\mathbb{B}$. Then, $(x + \delta\mathbb{B}) \times \{q\} \subset D_c$.

It is shown now that there exists $\delta > 0$ such that for each $(x, q) \in K_2 \times Q$ either $(x + \delta\mathbb{B}) \times \{q\} \subset C_c$ or $(x + \delta\mathbb{B}) \times \{q\} \subset D_c$. If $V_q(x) \leq \frac{\rho}{2}$, by continuity of V there exists $\delta > 0$ so that $V_q(z) \leq \rho$ for all $z \in x + \delta\mathbb{B}$ which implies that $(x + \delta\mathbb{B}) \times \{q\} \subset C_c^b$. Suppose now that $V_q(x) \geq \frac{\rho}{2}$. If $(x, q) \in \mathcal{A} \times Q$ then $\min_{p \in Q} V_p(x) = 0$ and by continuity of V there exists $\delta > 0$ such that $(x + \delta\mathbb{B}) \times \{q\} \subset D_c$, while if $(x, q) \in \mathcal{A} \times Q$ the analysis above for K_1 applies. \square

From Theorem 6.11, the closed-loop system \mathcal{H}_{cl} has the set $\mathcal{A} \times Q$ nominally asymptotically stable with basin of attraction $\mathcal{B}_A = O \times Q = C_c \cup D_c$. Let $U = O \times \mathbb{R}$ and for each $(x, q) \in U$, $\tilde{\omega}(x, q) := \omega(x) + |q|_Q$ where ω is the proper indicator of $\mathcal{A} \times Q$ with respect to O in Section 6.1.3. Then, $\tilde{\omega}$ is a proper indicator of $\mathcal{A} \times Q$ with respect to U . Then, by Theorem 6.5 [39], there exists $\beta \in \mathcal{K}\mathcal{L}\mathcal{L}$ such that, for all solutions (x, q) to \mathcal{H}_{cl} starting in \mathcal{B}_A ,

$$\tilde{\omega}(x(t, j), q(t, j)) \leq \beta(\tilde{\omega}(x(0, 0), q(0, 0)), t, j) \quad (\text{B.52})$$

for all $(t, j) \in \text{dom}(x, q)$.

Let $\delta' > 0$, which is a function of μ and λ , be given by Lemma B.21. Let $\delta < \delta'$ and assume that the measurements y of the state x satisfy $y \in x + \delta\mathbb{B}$. Then, the hybrid closed-loop system can be written as the family of hybrid systems \mathcal{H}_{cl}^δ with parameter δ :

$$\left. \begin{array}{l} \dot{x} \in F_\delta(x, q) \\ \dot{q} = 0 \end{array} \right\} \quad (x, q) \in C_\delta$$

$$\left. \begin{array}{l} x^+ = x \\ q^+ \in Q_\delta(x, q) \end{array} \right\} \quad (x, q) \in D_\delta$$

where, for each $(x, q) \in O \times \mathbb{R}$

$$\bullet F_\delta(x, q) := \begin{cases} f_p(x, \kappa(z, q)) & (z, q) \in ((x + \delta\overline{\mathbb{B}}) \times \{q\}) \cap C_c \\ \emptyset & \text{otherwise ;} \end{cases}$$

- $Q_\delta(x, q) := \begin{cases} Q_c(z, q) & (z, q) \in ((x + \delta\overline{\mathbb{B}}) \times \{q\}) \cap D_c \\ \emptyset & \text{otherwise ;} \end{cases}$

and

- $C_\delta = \{(x, q) \in O \times Q \mid ((x + \delta\overline{\mathbb{B}}) \times \{q\}) \cap C_c \neq \emptyset\};$
- $D_\delta = \{(x, q) \in O \times Q \mid ((x + \delta\overline{\mathbb{B}}) \times \{q\}) \cap D_c \neq \emptyset\}.$

Following Example 5.3 in [39], the convergence property (CP) in [39, Section 5] is satisfied by \mathcal{H}_{cl}^δ . Then, by Theorem 6.6 [39], given the compact set $K \subset O$ and $\varepsilon > 0$ there exists $\delta^* > 0$ such that for each $\delta \in (0, \delta^*]$, the solutions (x_δ, q_δ) to \mathcal{H}_{cl}^δ from $K \times Q$ satisfy, for all $(t, j) \in \text{dom}(x_\delta, q_\delta)$

$$\tilde{\omega}(x_\delta(t, j), q_\delta(t, j)) \leq \beta(\tilde{\omega}(x_\delta(0, 0)), t, j) + \varepsilon. \quad (\text{B.53})$$

To finish the proof, note that by Lemma B.21 and Proposition 2.4 in [39], there exist nontrivial solutions from every point in $C_c \cup D_c$. Completeness of solutions from $K \times Q$ follows with a similar argument to the one in the proof of Theorem 6.11.

B.4.5 Proof of Theorem 6.14

The construction of the hybrid controller is such that, the following holds.

For each $(i, j) \in L^t$:

- 1) The flow set $C_{i,j}^t$ and the jump set $D_{i,j}^t$ satisfy $\mathbb{R}^n \setminus C_{i,j}^t \subset D_{i,j}^t \subset S_{i,j}$;
- 2) The flow set $C_{i,j}^c$ and the jump set $D_{i,j}^c$ satisfy $E_{i,j} \subset \mathbb{R}^n \setminus C_{i,j}^c \subset D_{i,j}^c \subset \mathcal{B}_{\mathcal{A}_{i+1,j}}$.

Moreover, for every $(i, j) \in \cup_{k \in P}((Q_k^t \setminus \{1\}) \times \{k\})$:

- 3) For every $(i, j) \in \cup_{k \in P}(Q_k^c \times \{k\})$, the jump set $D_{|i|-1,j}^c$ satisfies

$$\text{reach}_{i,j}(D_{|i|-1,j}^c) \subset \mathbb{R}^n \setminus D_{i,j}^r \subset C_{i,j}^r;$$

- 4) For every $(i, j) \in L^t$, the flow set $C_{i,j}^t$ is such that $C_{i,j}^t \neq \emptyset$, $C_{i,j}^t \cap \mathcal{A}_{i,j} \neq \emptyset$.

From 1) and the definition of g_{c2} , for each $(i, j) \in L^t$, jumps to “throw” mode occur only when $x \in S_{i,j}$. By definition of κ , the control law $\alpha_{(i,j) \rightarrow (i+1,j)}$ is only applied when $x \in S_{i,j}$. By the properties of $\alpha_{(i,j) \rightarrow (i+1,j)}$ in Assumption 6.13 and 2), after a throw with $(i, j) \in L^t$, the trajectories reach $E_{i,j} \subset \mathcal{B}_{\mathcal{A}_{i+1,j}}$. Since from 2), $D_{i,j}^c \subset \mathcal{B}_{\mathcal{A}_{i+1,j}}$, jumps to catch mode are only possible when in the basin of attraction of $\mathcal{A}_{i+1,j}$.

From 3), for each $(i, j) \in \cup_{k \in P}(Q_k^c \times \{k\})$, every solution to $\dot{x} = f(x, \kappa_{i,j}(x))$ starting from $D_{|i|-1,j}^c$ stays in $C_{i,j}^r$. Using the fact from 2) stating that $D_{|i|-1,j}^c \subset \mathcal{B}_{\mathcal{A}_{i,j}}$ and the stabilizing properties of $\kappa_{i,j}$ in Assumption 6.13, it follows from 4) that every solution to $\dot{x} = f(x, \kappa_{i,j}(x))$ starting from $D_{|i|-1,j}^c$ reaches in finite time $\mathbb{R}^n \setminus C_{i,j}^t$. Note that by 1) we have $\mathbb{R}^n \setminus C_{i,j}^t \subset S_{i,j}$. By the definition of g_{c1} , this implies that after jumps to “catch mode”, the state is in $S_{q,p}$, $(q, p) \in \cup_{k \in P}((Q_k^t \setminus \{1\}) \times \{k\})$.

Jumps to “recovery” mode occur when the closed-loop state is in D_{c3} . By the properties of the “bootstrap” controller κ_0 in Assumption 6.13.4, solutions reach one of the jump sets $D_{i,j}^t$ or $D_{i,j}^c$ for some (i, j) .

Combining the arguments above, solutions follow a “throw”-“catch” sequence, potentially after being in “recovery” mode, that steers them to $D_{q,p}^c$, for some $(q,p) \in (\cup_{k \in P} \{-q_{\max}^k\} \times \{k\})$, and by the properties of the local stabilizer $\kappa_{q,p}$, their x component converge to $\mathcal{A}_{q,p} = \mathcal{A}$. Then, every solution starting from

$$(x^0, q^0, p^0, \tau^0) \in \mathbb{R}^n \times L \times \mathbb{R}$$

converges to $\mathcal{A} \times \{q_{\max}^p\} \times \{p\} \times [0, \bar{\tau}]$, for some $p \in P$. Finally, stability follows from the properties of the local stabilizer for \mathcal{A} .

B.4.6 Proof of Theorem 6.15

By the construction of the flow and jump sets since, for each $(i,j) \in L^t$, we have

$$C_{i,j}^t = \overline{\mathbb{R}^n \setminus D_{i,j}^t} + \frac{\delta_{i,j}^t}{2} \mathbb{B}, \quad C_{i,j}^c = \overline{\mathbb{R}^n \setminus D_{i,j}^c} + \frac{\delta_{i,j}^c}{2} \mathbb{B},$$

and, for each $(i,j) \in \cup_{k \in P} (Q_k^c \times \{k\})$,

$$D_{i,j}^r = \overline{\mathbb{R}^n \setminus C_{i,j}^r} + \frac{\delta_{i,j}^r}{2} \mathbb{B},$$

and

$$C_{0,0}^r = \mathbb{R}^n \setminus D_{0,0}^r + \frac{\delta_{0,0}^r}{2}.$$

Existence of solutions to \mathcal{H}_{cl} follows from the fact that for each compact set $K \subset \mathbb{R}^n$, there exists $\delta' > 0$ such that for each x in K either $(\{x\} + \delta' \mathbb{B}) \times \{q\} \subset C_c$ or $(\{x\} + \delta' \mathbb{B}) \times \{q\} \subset D_c$. In fact, it holds for each $\delta' > 0$, $\delta' \in [0, \delta^*]$, where

$$\delta^* := \frac{1}{2} \min \left\{ \min_{(i,j) \in L^t} \delta_{i,j}^t, \min_{(i,j) \in L^t} \delta_{i,j}^c, \min_{(i,j) \in \cup_{p \in P} Q_k^c \times \{k\}} \delta_{i,j}^r, \delta_{0,0}^r \right\}. \quad (\text{B.54})$$

By Theorem 6.14, $\tilde{\mathcal{A}} = \mathcal{A} \times (\cup_{j \in P} (\{q_{\max}^j\} \times \{j\})) \times [0, \bar{\tau}]$ is asymptotically stable with basin of attraction $\mathcal{B}_{\tilde{\mathcal{A}}} = C_c \cup D_c$. Let U be any open set such that $C_c \cup D_c \subset U$. By Theorem B.14, for each proper indicator $\tilde{\omega} : U \rightarrow \mathbb{R}_{\geq 0}$ of $\tilde{\mathcal{A}}$ with respect to U , there exists $\beta \in \mathcal{KLL}$ such that for all solutions ξ to \mathcal{H}_{cl} starting in $\mathcal{B}_{\tilde{\mathcal{A}}}$, for all $(t,j) \in \text{dom } \xi$, satisfy

$$\tilde{\omega}(\xi(t,j)) \leq \beta(\tilde{\omega}(\xi(0,0)), t, j).$$

The closed-loop system \mathcal{H}_{cl} with measurement noise in the state x is given by

$$\left. \begin{aligned} \dot{x} &= f(x, \kappa_c(x + e, q, p, \tau)) \\ (\dot{q}, \dot{p}) &= (0, 0) \\ \dot{\tau} &= 1 \end{aligned} \right\} (x + e, q, p, \tau) \in C_c$$

$$\left. \begin{aligned} x^+ &= x \\ (q, p)^+ &\in g_c(x + e, q, p, \tau) \\ \tau^+ &= 0 \end{aligned} \right\} (x + e, q, p, \tau) \in D_c,$$

Let $\delta > 0$ and $e : \mathbb{R}_{\geq 0} \rightarrow \delta\overline{\mathbb{B}}$. The closed-loop system \mathcal{H}_{cl} with measurement noise can be written as

$$\begin{aligned} \dot{\xi} &\in F_\delta(\xi) & \xi &\in C_\delta \\ \xi^+ &\in G_\delta(\xi) & \xi &\in D_\delta \end{aligned}$$

where

$$\begin{aligned} F_\delta(\xi) &:= \overline{\text{co}}f(x, \kappa_c(x + \delta\overline{\mathbb{B}}, q, p, \tau)) \\ G_\delta(\xi) &:= g_c(x + \delta\overline{\mathbb{B}}, q, p, \tau) \\ C_\delta &:= \{\xi \in O_c \mid (x + \delta\overline{\mathbb{B}}, q, p, \tau) \cap C_c \neq \emptyset\} \\ D_\delta &:= \{\xi \in O_c \mid (x + \delta\overline{\mathbb{B}}, q, p, \tau) \cap D_c \neq \emptyset\} \end{aligned}$$

which we denote as \mathcal{H}_δ . This hybrid system corresponds to an outer perturbation of \mathcal{H}_{cl} and satisfies (C1), (C2), (C3), and (C4) in [39] by the properties of f , κ_c , and g_c (see Example 5.3 in [39] for more details).

It follows by Theorem B.15 that for each compact set $\tilde{K} \subset \mathcal{B}_{\tilde{\mathcal{A}}}$ and each $\varepsilon > 0$ there exists $\delta^* > 0$ such that for each $\delta \in (0, \delta^*]$, every solution ξ_δ to \mathcal{H}_δ from \tilde{K} satisfies, for all $(t, j) \in \text{dom } \xi_\delta$,

$$\tilde{\omega}(\xi_\delta(t, j)) \leq \beta(\tilde{\omega}(\xi_\delta(0, 0)), t, j) + \varepsilon.$$

The claim follows with compact set K such that $\tilde{K} = K \times K'$ and proper indicator $\tilde{\omega}$ given by $|\cdot|_{\mathcal{A}}$.

Bibliography

- [1] P.-A. Absil and R. Sepulchre. A hybrid control scheme for swing up acrobatics. In *European Conference on Control ECC*, 2001.
- [2] R. Alur, T. Dang, J. Esposito, Y. Hur, F. Ivancic, V. Kumar, I. Lee, P. Mishra, G. J. Pappas, and O. Sokolsky. Hierarchical modeling and analysis of embedded systems. *Proc. of the IEEE*, 91:11–28, 2003.
- [3] F. Ancona and A. Bressan. Patchy vector fields and asymptotic stabilization. *ESAIM-COCV*, 4:445–471, 1999.
- [4] P.J. Antsaklis, J.A. Stiver, and M.D. Lemmon. Hybrid systems modeling and autonomous control systems. In R. L. Grossman, A. Nerode, A. P. Ravn, and H. Rishel, editors, *Hybrid Systems*, volume 736. Lecture Notes in Computer Science, 1993.
- [5] U. M. Ascher and L. R. Petzold. *Computer Methods for Ordinary Differential Equations and Differential-Algebraic Equations*. SIAM, 1998.
- [6] K. J. Astrom and K. Furuta. Swinging up a pendulum by energy control. *Automatica*, 36:287–295, 2000.
- [7] J.-P. Aubin, J. Lygeros, M. Quincampoix, S. S. Sastry, and N. Seube. Impulse differential inclusions: a viability approach to hybrid systems. *IEEE Trans. Aut. Control*, 47(1):2–20, 2002.
- [8] A. Bacciotti and F. Ceragioli. Nonsmooth Lyapunov functions and discontinuous Carathéodory systems. In *Proc. NOLCOS*, 2004.
- [9] A. Bacciotti and F. Ceragioli. Nonpathological Lyapunov functions and discontinuous Carathéodory systems. *Automatica*, 42:453–458, 2006.
- [10] A. Bacciotti and L. Mazzi. An invariance principle for nonlinear switched systems. *Sys. & Cont. Lett.*, 54:1109–1119, 2005.
- [11] D. D. Bainov and P.S. Simeonov. *Systems with Impulse Effect: Stability, Theory, and Applications*. Ellis Horwood Limited, 1989.
- [12] O. Beker, C.V. Hollot, Y. Chait, and H. Han. Fundamental properties of reset control systems. *Automatica*, 40(6):905–915, 2004.
- [13] M. Boccadoro, Y. Wardi, M. Egerstedt, and E. Verriest. Optimal control of switching surfaces in hybrid dynamical systems. *Discrete Event Dynamic Systems-Theory and Applications*, 15(4):433–448, 2005.
- [14] M. S. Branicky. Multiple Lyapunov functions and other analysis tools for switched and hybrid systems. *IEEE Trans. Aut. Control*, 43:1679–1684, 1998.
- [15] M.S. Branicky, V. S. Borkar, and S. K. Mitter. A unified framework for hybrid control: Model and optimal control theory. *IEEE Trans. Aut. Control*, 43(1):31–45, 1998.

- [16] B. Brogliato. *Nonsmooth Mechanics Models, Dynamics and Control*. Springer, 1996.
- [17] B. Brogliato and A. Zavala-Rio. On the control of complementary-slackness juggling mechanical systems. *IEEE Trans. Aut. Control*, 45(2):235–246, Feb. 2000.
- [18] M. Broucke and A. Arapostathis. Continuous selections of trajectories of hybrid systems. *Systems & Control Lett.*, 47:149–157, 2002.
- [19] M. Buehler, D.E. Koditschek, and P.J. Kindlmann. Planning and control of robotic juggling and catching tasks. *The International Journal of Robotics Research*, 13(2):101–118, 1994.
- [20] C.I. Byrnes and C.F. Martin. An integral-invariance principle for nonlinear systems. *IEEE Trans. Aut. Control*, 40(6):983–994, 1995.
- [21] C. Cai, A. R. Teel, and R. Goebel. Results on relaxation theorems for hybrid systems. In *Proc. 45th IEEE Conference on Decision and Control*, pages 276 – 281, 2006.
- [22] C. Cai, A. R. Teel, and R. Goebel. Smooth Lyapunov functions for hybrid systems – Part II: Pre-asymptotically stable compact sets. *To appear in IEEE Trans. Aut. Cont.*, 2007. Available at <http://www.ccec.ece.ucsb.edu/~cai/part2.pdf>.
- [23] C. Cai, A.R. Teel, and R. Goebel. Converse Lyapunov theorems and robust asymptotic stability for hybrid systems. In *Proc. 24th American Control Conference*, pages 12–17, 2005.
- [24] R. Carloni, R. G. Sanfelice, A. R. Teel, and C. Melchiorri. A hybrid control strategy for robust contact detection and force regulation. In *Proc. 26th American Control Conference*, pages 1461–1466, 2007.
- [25] V. Chellaboina, S.P. Bhat, and W.H. Haddad. An invariance principle for nonlinear hybrid and impulsive dynamical systems. *Nonlin. Anal.*, 53:527–550, 2003.
- [26] C. Chung and J. Hauser. Nonlinear control of a swinging pendulum. *Automatica*, 31:851–862, 1995.
- [27] F.H. Clarke. *Optimization and Nonsmooth Analysis*. SIAM’s Classic in Applied Mathematics, 1990.
- [28] F.H. Clarke, Yu. S. Ledyaev, L. Rifford, and R.J. Stern. Feedback stabilization and Lyapunov functions. *SIAM J. Control Optimization*, 39(1):25–48, 2000.
- [29] J. C. Clegg. A nonlinear integrator for servomechanisms. *Transactions A.I.E.E.*, 77 (Part II):41–42, 1958.
- [30] P. Collins. A trajectory-space approach to hybrid systems. In *Proc. 16th MTNS*, 2004.
- [31] J-M. Coron and L. Rosier. A relation between continuous time-varying and discontinuous feedback stabilization. *Journal of Math. Sys., Est., and Control*, 4(1):67–84, 1994.
- [32] R.A. DeCarlo, M.S. Branicky, S. Pettersson, and B. Lennartson. Perspectives and results on the stability and stabilizability of hybrid systems. *Proc. of IEEE*, 88(7):1069–1082, 2000.
- [33] A. Dontchev and F. Lempio. Difference methods for differential inclusions: A survey. *SIAM Review*, 34:263–294, 1992.
- [34] H. Elmqvist, S.E. Mattsson, and M. Otter. Modelica: The new object-oriented modeling language. In *Proc. of 12th European Simulation Multiconference*, 1998.
- [35] I. Fantoni, R. Lozano, and M. W. Spong. Energy based control of the pendubot. *IEEE Trans. Aut. Control*, 45:725–729, 2000.
- [36] A.F. Filippov. Differential equations with discontinuous right-hand sides (english). *Matemat. Sbornik.*, 51(93):99–128, 1960.

- [37] M. Garavello and B. Piccoli. Hybrid necessary principle. *SIAM J. Control Optim.*, 43(5):1867–1887, 2005.
- [38] R. Goebel, J.P. Hespanha, A.R. Teel, C. Cai, and R.G. Sanfelice. Hybrid systems: generalized solutions and robust stability. In *Proc. 6th IFAC Symposium in Nonlinear Control Systems*, pages 1–12, 2004.
- [39] R. Goebel and A.R. Teel. Solutions to hybrid inclusions via set and graphical convergence with stability theory applications. *Automatica*, 42(4):573–587, 2006.
- [40] Wassim M. Haddad, VijaySekhar Chellaboina, and Sergey G. Nersesov. *Impulsive and Hybrid Dynamical Systems: Stability, Dissipativity, and Control*. Princeton University, 2006.
- [41] E. Hairer and G. Wanner. Algebraically stable and implementable Runge-Kutta methods of high order. *SIAM J. Numer. Anal.*, 18:1098–1108, 1981.
- [42] O. Håjek. Discontinuous differential equations I. *Journal of Diff. Eqn.*, 32:149–170, 1979.
- [43] T. A. Henzinger. The theory of hybrid automata. In *Proc. of the 11th Annual Symp. on Logic in Comp. Science*, pages 278–292. IEEE CS Press, 1996.
- [44] H. Hermes. Discontinuous vector fields and feedback control. In J.K. Hale and J.P. LaSalle, editors, *Differential Equations and Dynamical Systems*, pages 155–165. Academic Press, New York, 1967.
- [45] F. Herrman and M. Seitz. How does the ball-chain work? *American Association of Physics Teachers*, 50(11):977–981, 1982.
- [46] J.P. Hespanha. Uniform stability of switched linear systems: Extensions of LaSalle’s invariance principle. *IEEE Trans. Aut. Control*, 49(4):470–482, 2004.
- [47] J.P. Hespanha. A model for stochastic hybrid systems with application to communication networks. *Nonlinear Analysis, Special Issue on Hybrid Systems*, 62:1353–1383, 2005.
- [48] J.P. Hespanha, D. Liberzon, and A.R. Teel. On input-to-state stability of impulsive systems. In *Proc. 44th IEEE Conference on Decision and Control and European Control Conference*, pages 3992–3997, 2005.
- [49] J.P. Hespanha and A.S. Morse. Stabilization of nonholonomic integrators via logic-based switching. *Automatica*, 35(3):385–393, 1999.
- [50] A.R. Humphries and A. M. Stuart. Runge-Kutta methods for dissipative and gradient dynamical systems. *SIAM J. Numer. Anal.*, 31:1452–1485, 1994.
- [51] J.Rubi, A.Rubio, and A.Avello. Swing-up control problem for a self-erecting double inverted pendulum. *IEE Proc.- Control Theory Applications*, 149:169–175, 2002.
- [52] C. M. Kellet and A. R. Teel. Smooth Lyapunov functions and robustness of stability for differential inclusions. *Systems & Control Lett.*, 52:395–405, 2004.
- [53] C.M. Kellett, H. Shim, and A.R. Teel. Further results on robustness of (possibly discontinuous) sample and hold feedback. *IEEE Trans. Aut. Control*, 49(7), 2004.
- [54] N.N. Krasovskii. *Problems of the Theory of Stability of Motion*. Stanford Univ. Press, 1963. Trans. of Russian edition, Moscow, 1959.
- [55] N.N. Krasovskii. *Game-Theoretic Problems of Capture*. Nauka, Moscow, 1970.
- [56] K.R. Krishnan and I.M. Horowitz. Synthesis of a non-linear feedback system with significant plant-ignorance for prescribed system tolerances. *International Journal of Control*, 19:689–706, 1974.

- [57] Y. Kuwata and J. How. Receding horizon implementation of MILP for vehicle guidance. In *Proc. American Control Conference*, pages 2684–2685, Portland, Oregon, USA, June 2005.
- [58] T. Lapp and L. Singh. Model predictive control based trajectory optimization for nap-of-the-earth (noe) flight including obstacle avoidance. In *Proc. American Control Conference*, pages 891–896, Boston, Massachusetts, June/July 2004.
- [59] J. P. LaSalle. Some extensions of Liapunov’s second method. *IRE Trans. Circuit Theory*, 7(4):520–527, 1960.
- [60] J.P. LaSalle. *The Stability of Dynamical Systems*. SIAM’s Regional Conference Series in Applied Mathematics, 1976.
- [61] E. A. Lee and H. Zheng. Operational semantics for hybrid systems. In *Hybrid Systems: Computation and Control: 8th International Workshop*, pages 25–53, 2005.
- [62] T. Lee and B. Chen. A general stability criterion for time-varying systems using a modified detectability condition. *IEEE Trans. Aut. Control*, 47(5):797–802, May 2002.
- [63] J. Liu and E. A. Lee. A component-based approach to modeling and simulating mixed-signal and hybrid systems. *ACM Transactions on Modeling and Computer Simulation*, 12(4):343–368, 2002.
- [64] J. Liu, X. Liu, T. J. Koo, B. Sinopoli, S.Sastry, and E. A. Lee. A hierarchical hybrid system model and its simulation. In *Proc. 38th IEEE Conference on Decision and Control*, volume 4, pages 3508 – 3513, 1999.
- [65] H. Logemann and E.P. Ryan. Asymptotic behaviour of nonlinear systems. *Amer. Math. Month.*, 111:864–889, 2004.
- [66] J. Lygeros, K.H. Johansson, S. S. Sastry, and M. Egerstedt. On the existence of executions of hybrid automata. In *Proc. 41st Conference on Decision and Control*, pages 2249–2254, 1999.
- [67] J. Lygeros, K.H. Johansson, S.N. Simić, J. Zhang, and S. S. Sastry. Dynamical properties of hybrid automata. *IEEE Trans. Aut. Control*, 48(1):2–17, 2003.
- [68] C. G. Mayhew, R. G. Sanfelice, and A. R. Teel. Robust source seeking hybrid controllers for autonomous vehicles. In *Proc. 26th American Control Conference*, pages 1185–1190, 2007.
- [69] A. N. Michel, L. Wang, and B. Hu. *Qualitative Theory of Dynamical Systems*. Dekker, 2001.
- [70] A.N. Michel. Recent trends in the stability analysis of hybrid dynamical systems. *IEEE Trans. Circuits Syst. – I. Fund. Theory Appl.*, 45(1):120–134, 1999.
- [71] J. J. Moreau. *Non-Smooth Mechanics and Applications*, chapter Unilateral contact and dry friction in finite freedom dynamics, pages 1–82. Springer, 1988.
- [72] J.J. Moreau. *Topics in Nonsmooth Mechanics*, chapter Bounded variation in time, pages 1–74. Birkhäuser Verlag, 1988.
- [73] P.J. Mosterman and G. Biswas. A hybrid modeling and simulation methodology for dynamic physical systems. *Simulation*, 78:5–17, 2002.
- [74] A. Nerode and W. Kohn. Models for hybrid systems: Automata, topologies, stability. In *Hybrid Systems volume 736 of Lecture Notes in Computer Science*, pages 317–356, 1993.
- [75] D. Nesic and A.R. Teel. A framework for stabilization of nonlinear sampled-data systems based on their approximate discrete-time models. *IEEE Trans. Aut. Control*, 49:1103 – 1122, 2004.

- [76] C. Prieur and A. Astolfi. Robust stabilization of chained systems via hybrid control. *IEEE Trans. Aut. Control*, 48(10):1768–1772, October 2003.
- [77] C. Prieur, R. Goebel, and A. R. Teel. Results on robust stabilization of asymptotically controllable systems by hybrid feedback. In *Proc. 44th IEEE Conference on Decision and Control and European Control Conference*, pages 2598–2603, 2005.
- [78] R. Sepulchre R. Ronsse, P. Lefevre. Sensorless stabilization of bounce juggling. *IEEE Transactions on Robotics*, 22(1):147–59, 2006.
- [79] R.T. Rockafellar and R. J-B Wets. *Variational Analysis*. Springer, 1998.
- [80] R. Ronsse and R. Sepulchre. Feedback control of impact dynamics: the bouncing ball revisited. In *Proc. of the 45th IEEE Conference on Decision and Control*, pages 4807–4812, 2006.
- [81] E.P. Ryan. An integral invariance principle for differential inclusions with applications in adaptive control. *SIAM’s Journal of Control and Optimization*, 36(3):960–980, 1998.
- [82] R. G. Sanfelice, M. J. Messina, S. E. Tuna, and A. R. Teel. Robust hybrid controllers for continuous-time systems with applications to obstacle avoidance and regulation to disconnected set of points. In *Proc. 26th American Control Conference*, pages 3352–3357, 2006.
- [83] R. G. Sanfelice and A. R. Teel. Lyapunov analysis of sample-and-hold hybrid feedbacks. In *Proc. 45th IEEE Conference on Decision and Control*, pages 4879–4884, 2006.
- [84] R. G. Sanfelice and A. R. Teel. On the continuity of asymptotically stable compact sets for simulations of hybrid systems. In *Proc. 45th IEEE Conference on Decision and Control*, pages 270–275, 2006.
- [85] R. G. Sanfelice and A. R. Teel. A “throw-and-catch” hybrid control strategy for robust global stabilization of nonlinear systems. In *Proc. 26th American Control Conference*, pages 3470–3475, 2007.
- [86] R. G. Sanfelice, A. R. Teel, R. Goebel, and C. Prieur. On the robustness to measurement noise and unmodeled dynamics of stability in hybrid systems. In *Proc. 25th American Control Conference*, pages 4061–4066, 2006.
- [87] R.G. Sanfelice, R. Goebel, and A.R. Teel. Results on convergence in hybrid systems via detectability and an invariance principle. In *Proc. 24th American Control Conference*, pages 551–556, 2005.
- [88] R.G. Sanfelice, R. Goebel, and A.R. Teel. A feedback control motivation for generalized solutions to hybrid systems. *Hybrid Systems: Computation and Control, Lecture Notes in Computer Science 3927*, pages 522–536, 2006.
- [89] R.G. Sanfelice, R. Goebel, and A.R. Teel. Invariance principles for hybrid systems with connections to detectability and asymptotic stability. *IEEE Transactions on Automatic Control*, 52(12):2282–2297, December 2007. See also [87].
- [90] R.G. Sanfelice, R. Goebel, and A.R. Teel. Generalized solutions to hybrid dynamical systems. *To appear in ESAIM: Control, Optimisation and Calculus of Variations*, 2008. See also [88].
- [91] R.G. Sanfelice, A. R. Teel, and R. Sepulchre. A hybrid systems approach to trajectory tracking control for juggling systems. In *Proc. 46th IEEE Conference on Decision and Control*, pages 5282–5287, 2007.
- [92] R.G. Sanfelice and A.R. Teel. On hybrid controllers that induce input-to-state stability with respect to measurement noise. In *Proc. 44th IEEE Conference on Decision and Control and European Control Conference*, pages 4891–4896, 2005.

- [93] S. Schaal and C. G. Atkeson. Open loop stable control strategies for robot juggling. In *IEEE International Conference on Robotics and Automation*, volume 3, pages 913–918, 1993.
- [94] R. Sepulchre and M. Gerard. Stabilization of periodic orbits in a wedge billiard. In *Proc. 42nd IEEE Conference on Decision and Control*, pages 1568–1573, 2003.
- [95] E.D. Sontag. Clocks and insensitivity to small measurement errors. *ESAIM-COCV*, 4:537–557, 1999.
- [96] A. M. Stuart and A.R. Humphries. *Dynamical Systems and Numerical Analysis*. Cambridge University Press, 1996.
- [97] L. Tavernini. Differential automata and their discrete simulators. *Nonlin. Anal.*, 11(6):665–683, 1987.
- [98] L. Tavernini. Generic properties of impulsive hybrid systems. *Dynamic Systems & Applications*, 13:533–551, 2004.
- [99] A. R. Teel. A nonlinear small gain theorem for the analysis of control systems with saturation. *IEEE Trans. Aut. Control*, 41(9):1256–1270, September 1996.
- [100] F.D. Torrisi and A. Bemporad. HYSDEL - A tool for generating computational hybrid models for analysis and synthesis problems. *IEEE Trans. Control Systems Technology*, 12:235–249, 2004.
- [101] S. E. Tuna, R. G. Sanfelice, M. J. Messina, and A. R. Teel. Hybrid MPC: Open-minded but not easily swayed. *Assessment and Future Directions of Nonlinear Model Predictive Control*, Lecture Notes in Control and Information Sciences 358:17–34, 2007.
- [102] M. Uchida and K. Nakano. Swing up control of an inverted pendulum. *ICECS*, 20:992–995, 1997.
- [103] A. van der Schaft and H. Schumacher. *An Introduction to Hybrid Dynamical Systems*. Lecture Notes in Control and Information Sciences, Springer, 2000.
- [104] T.L. Vincent. Controlling a ball to bounce at a fixed height. In *Proceedings of the American Control Conference*, volume 1, pages 842–846, 1995.
- [105] H. S. Witsenhausen. A class of hybrid-state continuous-time dynamic systems. *IEEE Trans. Aut. Control*, 11(2):161–167, 1966.
- [106] L. Zaccarian, D. Nesic, and A.R. Teel. First order reset elements and the Clegg integrator revisited. In *Proc. 24th American Control Conference*, pages 563–568, 2005.
- [107] A. Zavala-Rio and B. Brogliato. On the control of a one degree-of-freedom juggling robot. *Dynamics and Control*, 9:67–90, 1999.